A THESIS ENTITLED

EXPRESSION AND INTERACTIONS OF CYTOSKELETAL ELEMENTS AND SPHINGOLIPIDS IN THE DIFFERENTIATION OF MYELIN-FORMING CELLS IN THE VERTEBRATE NERVOUS SYSTEM

PRESENTED FOR THE DEGREE OF DOCTOR OF PHILOSOPHY IN BIOCHEMISTRY

IN THE

DEPARTMENT OF BIOLOGICAL AND MOLECULAR SCIENCES

UNIVERSITY OF STIRLING

BY

DEMETRIUS ANASTASIOU VOUYIOUKLIS B.Sc. (STIRLING)

SEPTEMBER 1992

DEDICATION

To Karen, Gary and Simon

Abbreviations used in this thesis

AMP	Adenosine 2´-monophosphate
ATP	Adenosine 5´-triphosphate
BFA	Brefeldin A
bFGF	Basic fibroblast growth factor
BHT	2,6-Di-tert-butyl-p-cresol
BODIPY	Boron dipyrremethene difluoride
BSA	Bovine serum albumin
C_5-DMB-Cer	N-[5(5,7-dimethyl borondipyrromethene difluoride)-1-pentanoyl] D-erythro sphingosine
C_6-NBD-Cer	N-[7-(4nitrobenzo-2-oxa-1,3-diazole)]-6-aminocaproyl-D-erythro sphingosine
cAMP	Adenosine 3´,5´-cyclic monophosphate
Cb	Cerebroside
Cer	Ceramide
CHL	Chinese hamster lung
CHO	Chinese hamster ovary
CMP	Cytidine 5´-monophosphate
CNP	2´,3´-Cyclic nucleotide 3´-phosphohyrolase
CNS	Central nervous system
CSK	Cytoskeleton
DAB	3,3´-Diaminobenzidine
DF-BSA	Defatted bovine serum albumin
DMA	Dimethylacetal
DMB	5,7-dimethyl boron dipyrromethene difluoride
DMEM	Dulbecco's modified Eagle's medium
DMPG	Dimyristoylphosphatidylglycerol
DMSO	Dimethyl sulphoxide
DTAF	Dichlorotriazinylamino fluorescein

DTT	Dithiothreitol
E...	Embryonic day ...
EDTA	Ethylenediaminetetraacetic acid
EGF	Epidermal growth factor
EGTA	Ethylene glycol-bis(ß-aminoethyl ether) N´,N,´N´N´- tetraacetic acid
ER	Endoplasmic reticulum
F-actin	Filamentous actin
FA	Fatty acid
FACS	Fluorescent activated cell sorting
FCS	Foetal calf serum
FITC	Fluorescein isothiocyanate
G_7	Sialogalactosylceramide
GalC	Galactocerebroside
GFAP	Glial fibrilary acidic protein
G_{M1}	Monosialogalactosylceramide
G_{M4}	Sialogalactosylceramide
GMP	Guanosine 5´-monophosphate
GPI	Glycophosphatidyl inositol
GTP	Guanosine 5´-triphosphate
HBSS	Hank's balanced salt solution
HEPES	N-2-hydroxyethylpiperazine- N´-2-ethanesulphonic acid
HPTLC	High performance thin layer chromatography
HUVEC	Human umbilical vein endothelial cell
IHU	Immunoglobulin homology unit
INA	5-[^{125}I] Iodonaphthyl-1-azide
jp	Jimpy
jp^{msd}	Myelin synthesis deficient
LacC	Lactosylcerebroside
L_{M1}	Sialosyl-lactotetraosylceramide
mAb	Monoclonal antibody

MAG	Myelin-associated glycoprotein
Man II	Mannosidase II
MAP	Microtubule-associated protein
MBP	Myelin basic protein
MDCK	Madin Darby canine kidney
MTOC	Microtubule organizing centre
MVB	Multivesicular body
NAD	Nicotinamide adenine dinucleotide
NBD	4-chloro-7-nitrobenz-1,3-diazole
NCAM	Neural cell adhesion molecule
NFM	Neurofilament
NP-A	Niemann-Pick Type A
O-2A	Oligodendrocyte-type 2 astrocyte
P...	Postnatal day...
PBS	Phosphate buffered saline
PC	Phosphatidylcholine
PCR	Polymerase chain reaction
PDGF	Platelet derived growth factor
PDMP	1-phenyl-2-(decanoylamino)-3-morpholino-1-propanol
PE	Phosphatidylethanolamine
PI	Phosphatidylinositol
PIPES	Piperazine-N´,N´,-bis[ethanesulphonic acid]
PLAP	Placental alkaline phosphatase
PLP	Proteolipid protein
PMSF	Phenylmethylsulphonyl fluoride
PNS	Peripheral nervous system
PS	Phosphatidylserine
PtK_1	Rat kangaroo kidney
PUFA	Polyunsaturated fatty acid
qk	Quaking

RER	Rough endoplasmic reticulum
rsh	Rumpshaker
SAT	Sialyltranferase
SDS PAGE	Sodium dodecyl sulphate polyacrylamide gel electrophoresis
shi	Shiverer
SM	Sphingomyelin
SRP	Signal recognition particle
Tf	Transferrin
TGN	*trans*- Golgi network
TLC	Thin layer chromatography
TLCK	Tosyl lysyl chloromethyl ketone (Na-p-tosyl-L-lysine methyl ester)
TPPase	Thiamine pyrophosphatase
tr	Trembler
TRITC	Tetramethylrhodamine B isothiocyanate
tw	Twitcher
UDP	Uridine 5´-diphosphate
UMP	Uridine 5´-monophosphate
UV	Ultraviolet
WGA	Wheat germ agglutinin
wt	Wild type

ABSTRACT

A tissue culture system was developed and characterized, which permitted the biochemical and immunocytochemical analysis of the differentiation of oligodendrocytes from their progenitors. Three facets of this differentiation process were investigated.

1. The microtubule-associated protein MAP1B was shown to be expressed immediately before terminal differentiation. Since inhibition of MAP1B synthesis caused the thinning and retraction of oligodendrocyte processes, MAP1B appears to stabilize the extension of myelin processes during myelination.

2. Galactocerebroside (GalC) is a characteristic lipid of differentiated oligodendrocytes and is abundant in the myelin membrane; therefore the biosynthesis and trafficking of GalC was studied using fluorescently-labeled ceramides and brefeldin A (BFA). The metabolic fate of labeled ceramides was related to their sites of accumulation in the Golgi network and was shown to be influenced by the reorganization of the secretory pathway in response to BFA.

3. The possible role of sphingolipid and protein interaction with the cytoskeleton in myelination during development was investigated in cultured cells and purified myelin. Sphingolipids are enriched in cytoskeletons copurifying with CNS and PNS myelin and GalC codistributes with oligodendrocyte cytoskeletal proteins during development. Incubations with fluorescent sphingolipids confirmed the ability of sphingolipids to interact with the cytoskeleton, but suggested that association probably depends on acyl chain composition. The importance of sphingolipids in myelin assembly was emphasized by their marked reduction in the hypomyelinating mutant rumpshaker (*rsh*).

Myelin-associated glycoprotein (MAG) associates with mature oligodendrocyte cytoskeletons, colocalizing with microtubules. MAG interacts with microtubules and early isoforms of myelin basic protein (MBP) in the myelin cytoskeleton at early stages of myelination; microfilaments and 2',3'-cyclic nucleotide 3' phosphohydrolase (CNP) become associated with the cytoskeleton as myelination proceeds. Cytoskeletal myelin proteins (except CNP2) are underphosphorylated compared to detergent-soluble forms, indicating that cytoskeletal association may either restrain phosphorylation or characterize specific subsets of myelin proteins.

CONTENTS

Introduction

1.1 MYELIN

I. Historical aspects

The presence of a sheath surrounding nerve fibres in the vertebrate nervous system was initially reported by Virchow (1854). Following the advent of improved histological techniques and polarization microscopy, Ranvier (1871) showed that the myelin sheath was segmented and he established the involvement of the segmented junctions of this membrane (nodes of Ranvier) in saltatory conduction, which is the specialized form of impulse conduction found in myelinating axons.

Most of the early myelin work was performed on peripheral nervous system (PNS) tissue due to its experimental accessibility when compared to the central nervous system (CNS). The observations of Schmitt and co-workers (1935) and Schmitt and Bear (1939) established that myelin is a concentric, layered structure consisting of a single repeating unit. Using electron microscopy Sjöstrand (1949) and Fernandez-Moran (1950) confirmed the multilamellar nature of myelin and Geren and Smitt (1954) showed that the formation of myelin was due to the spiraling of the membrane around the neuronal axon to form the compact sheath. The configuration of CNS myelin was subsequently shown to be similar to that of PNS myelin (Maturana, 1960; Peters, 1960).

II. CNS myelin

Myelination in the CNS commences when the diameter of axons has reached approximately 1μm, which is somewhat later than in the PNS (Raine, 1984). Bunge et al., (1961) showed that an oligodendrocyte can myelinate multiple axonal segments by extending many shovel-shaped myelin processes (Fig. 1). When studied by electron microscopy, CNS myelin is initially to be seen wrapped loosely around an axonal segment when it forms a loose cup, one lip of which (the future "inner tongue") will work its way underneath the other. The multilamellar structure is formed by further rotation of the inner tongue around the axon and at the same time the cytoplasm between layers is compressed to a continuous thin strip

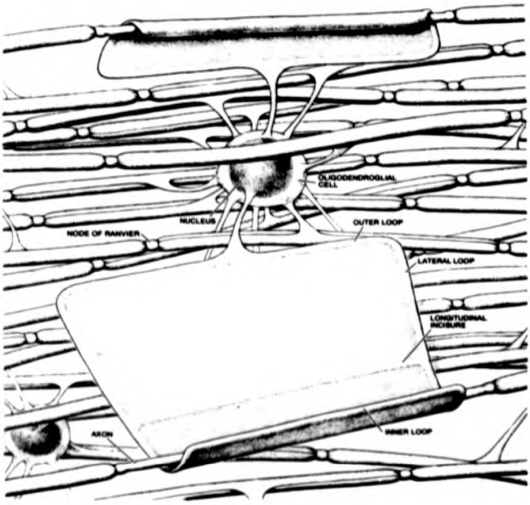

Fig. 1 A diagramatic representation of myelinating oligodendrocytes

Oligodendroglial soma attached to numerous myelin sheaths unfolded to varying degrees to demonstrate the enormous surface area they occupy. Note also the displacement of oligodendrocyte cytoplasm to narrow ridges in the flattened sheath of myelin. (From Raine, 1984).

(Schmidt-Lanterman incisures), which marks the initiation of compaction. When compaction is complete the layers appear fused, forming a single major dense line between the cytoplasmic surfaces of the membrane and an intraperiod line resulting from the close apposition of the outer leaflets. The major morphological features of a myelinated axon are shown in Fig. 2.

III. PNS myelin

Schwann cells are responsible for myelination in the PNS. Although CNS and PNS myelin differ in their origins, timing of appearance and ultrastructure, they function similarly. Early work on the lipid composition revealed differences only in proportions but not in species and it seemed possible that this would also be true for the protein constituents. The advent of SDS-PAGE revealed that although CNS and PNS myelin have many proteins in common, the relative proportions of the proteins vary and PNS myelin has at least one additional major protein.

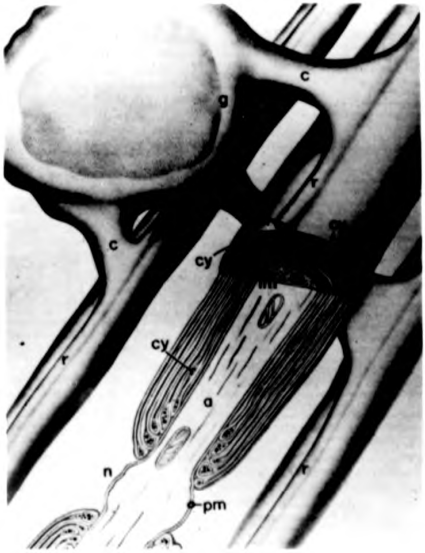

Fig. 2 Diagram of CNS myelination

An oligodendrocyte cell body is attached to three internodes of myelin, one of which is seen in section to demonstrate the lamellar arrangement of the myelin sheath.

a, axon; n, node; pm, plasma membrane; im, inner mesaxon; cy, cytoplasm; ol, outer loop; r, ridge formed by outer loop; c, connection to oligodendroglial cell body (g).

After Bunge, (1961).

1.2 MYELIN-FORMING CELLS IN THE CNS

In the past, most studies on myelin-forming glia were carried out *in vivo* (reviewed by Wood and Bunge, 1984). However the study of cell lineage and development *in vitro* has been facilitated by the production of highly specific monoclonal antibodies reacting with molecules characteristic of each developmental stage, better methods for the isolation and culturing of highly purified glial cell populations, the purification of polypeptide growth factors and the cloning and characterization of the genes especially expressed in glial cells. These studies led to the discovery of the oligodendrocyte-type 2 astrocyte (O-2A) bipotential progenitor cell which can, under appropriate conditions, give rise to either oligodendrocytes or Type-2 astrocytes *in vitro* (Raff et al., 1983). The other major glial cell type in the CNS is the Type-1 astrocyte, which is believed to be derived from a different progenitor (Raff, 1989).

I. Antibody markers

Several monoclonal antibodies (mAbs) that can recognize oligodendrocytes and their progenitors have been described. The mAb A2B5 binds a tetraganglioside present in O-2A progenitors and neurons (Eisenbarth et al., 1979) as well as Type-2 astrocytes (Raff, 1989), therefore labeling of cells from areas other than the optic nerve, which contains glial cells only, is difficult to assign. Antibodies recognising the intermediate filament protein vimentin stain O-2A progenitors from the optic nerve intracellularly (Raff et al., 1983). NSP4 recognizes a family of glycoproteins on the surface of O-2A cells (ffrench-Constant et al., 1986; Behar et al., 1988) and antibodies to G_{D3} ganglioside label O-2A progenitors both *in vivo* and *in vitro* (Levine and Goldman, 1988a; Norton and Farooq, 1989).

O4 (Sommer and Schachner, 1981; Schachner et al., 1981) recognizes sulfatide (galactocerebroside-3-sulfate), seminolipids and an unknown antigen in rodent CNS (Bansal et al., 1989; Godfraind et al., 1989) and labels a more advanced developmental stage of proliferating O-2A progenitors. 007, another rat monoclonal antibody reacting strongly with sulfatide, is also thought to recognize developmentally advanced proliferating O-2A progenitors (Benjamins et al., 1987).

Differentiating O-2A progenitors express myelin-specific lipids and proteins. The most widely used antibodies against galactocerebroside (GalC), a lipid characteristic of oligodendrocytes and myelin in the CNS, are O1 (Sommer and Schachner, 1981; Schachner et al., 1981) and R-mAb (Rancht et al., 1982). O1 and R-mAb not only recognize GalC but another two and four lipid antigens, respectively, however R-mAb recognizes an additional unknown antigen (Bansal et al., 1990). Therefore, O1 may be a better antibody against GalC, as the other two lipids that it recognizes (monogalactosyldiglyceride and psychosine) are normally minor components in oligodendrocytes.

Several antibodies against myelin-specific proteins have been described.

Most of the antibodies used for studying cells of the O-2A lineage in the CNS, with the exception of A2B5, have also been used with Schwann cells in the PNS (Jessen and Mirsky, 1991).

II. In vitro studies

a) A2B5$^+$ O4$^-$ cells (O-2A progenitors)

Time-lapse microcinematography studies suggest that A2B5$^+$ O4$^-$ cells are migratory. At embryonic day 16 (E16) O-2A progenitors are found in cultures from brain but not from optic nerve, which suggests that these cells move into the optic nerve during later life (for review see Raff, 1989). Although O-2A progenitors from brain have been isolated to high purity and characterized by several laboratories (McKinnon et al., 1990; Levi et al., 1991, Louis et al., 1992), most of the recent knowledge about O-2A progenitors has originated from studies on optic nerve.

Wolswijk and Noble (1989) have identified two distinct precursor populations, the O-2A^{perinatal} and O2-A^{adult} progenitors in young and mature optic nerve cultures, respectively. O-2A^{perinatal} and O2-A^{adult} progenitor cells differ in morphology (bipolar versus multipolar), average cell cycle time (18h versus 66h), average rate of migration (21mm h^{-1} versus 4mm h^{-1}), time course of differentiation (3d versus 7d) and antigenic phenotype (O4$^-$ vimentin$^+$ versus O4$^+$ vimentin$^-$). Further characterization of O2-A^{adult} progenitor cells (Wren et al., 1992) showed that they behave like a population of stem cells and are derived from a sub-population of O-2A^{perinatal} progenitors.

b) O4$^+$ GalC$^-$ cells (Preoligodendrocytes)

Cells in cultures from early postnatal mouse cerebellum were labeled with the O1 antibody and subjected to complement-dependent immunocytolysis (Sommer and Schachner, 1982); the remaining (viable) cells could be immunolabeled with the O4 antibody and differentiated to GalC$^+$ oligodendrocytes. In similar cultures, cells with several processes that were stained with the 007 monoclonal antibody were GalC$^-$; these cells were actively proliferating committed oligodendrocyte progenitors (Skoff and Knapp, 1991). These studies showed that in culture, developmentally advanced progenitors with the potential to differentiate to oligodendrocytes co-exist with oligodendrocytes.

The O4$^+$ progenitor cell defines a transitional intermediate between the O-2A cell and the GalC$^+$ oligodendrocyte and is the earliest cell type in the cortical oligodendrocyte cell lineage (Gard and Pfeiffer, 1989, 1990). Therefore, O4 is the earliest surface marker restricted to cells destined to become oligodendrocytes in the CNS and these cells are also known as preoligodendrocytes.

Gard and Pfeiffer (1989), who termed the O4$^+$ GalC$^-$ cells proligodendrocytes, showed that in their culture system only 80% of the preoligodendrocyte population differentiated to O4$^+$ GalC$^+$ cells and there always existed a quiescent population of O4$^+$ GalC$^-$ cells. When this is considered in combination with the findings of Wren et al., (1992) it raises the possibility that in adult CNS populations of O-2A^{adult} progenitors and O4$^+$ GalC$^-$ preoligodendrocytes may co-exist with mature oligodendrocytes; these two types of progenitors may have roles in cell replenishment, myelin repair and remyelination.

Preoligodendrocytes retain a high developmental plasticity and under appropriate culture conditions can either differentiate to oligodendrocytes or de-differentiate to O-2A progenitors and further divide, or become astrocytes (Aloisi et al., 1988; Trotter and Schachner, 1989). Gard and Pfeiffer, (1990) using bromodeoxyuridine incorporation into newly synthesized DNA, showed that in rat brain the A2B5$^+$ O4$^+$, O4$^+$ GalC$^-$ and O4$^+$ GalC$^+$ cell phenotypes emerge in sequence and only the first two are proliferative. The emergence of GalC at the cell surface in oligodendrocytes may mark their withdrawal from the cell cycle.

c) O4$^+$ GalC$^+$ cells (Oligodendrocytes)

In the absence of foetal calf serum (FCS) most cells in an optic nerve culture system develop to oligodendrocytes (Raff et al., 1983). Miller et al., (1985) used an *in vitro* system that totally excluded neurons and showed that in the rat optic nerve the three types of macroglial cells develop in a strict sequence: Type-1 astrocytes appear first at E18, oligodendrocytes at birth and Type-2 astrocytes between P7 and P10; they further demonstrated that O-2A progenitors give rise to either oligodendrocytes or Type-2 astrocytes (see further), whereas a totally different progenitor cell gives rise to Type-1 astrocytes.

The almost simultaneous appearance of GalC (Raff et al., 1978), and 2',3'-cyclic nucleotide 3'-phosphohydrolase (CNP) (Bansal and Pfeiffer, 1985) and eventual loss of A2B5 by cultured O4$^+$ GalC$^-$ cells correspond to the second phase of oligodendrocyte maturation for cells cultured from cerebral cortex. Morphologically, these differentiating cells are characterized by increases in cell size and in the number and diameter of their processes. It is not yet known for certain whether the appearance of CNP and GalC coincides with the cessation of proliferative activity for preoligodendrocytes in culture (Gard and Pfeiffer, 1989) or whether these cells can, under appropriate conditions, de-differentiate and, following cell division, produce new myelinating oligodendrocytes (Wood and Bunge 1991). However, various *in situ* studies using postnatal rodent brain and optic nerve have suggested that oligodendrocytes containing GalC and sulfatide are proliferative (for review see Skoff and Knapp, 1991).

Dubois-Dalcq et al., (1986) have characterized the maturation stages for cultured oligodendrocytes derived from either brain or optic nerve on the basis of the sequential appearance and translocation of myelin-associated glycoprotein (MAG), proteolipid protein (PLP) and myelin basic protein (MBP) from the cell body to the processes. MAG appears first and its transport to the processes is an early event; PLP remains associated with the cell body for some time, while MBP is transported to the cell processes after MAG but before PLP.

A summary diagram of the known routes of O-2A progenitor cell differentiation *in vitro* is presented in Fig. 3.

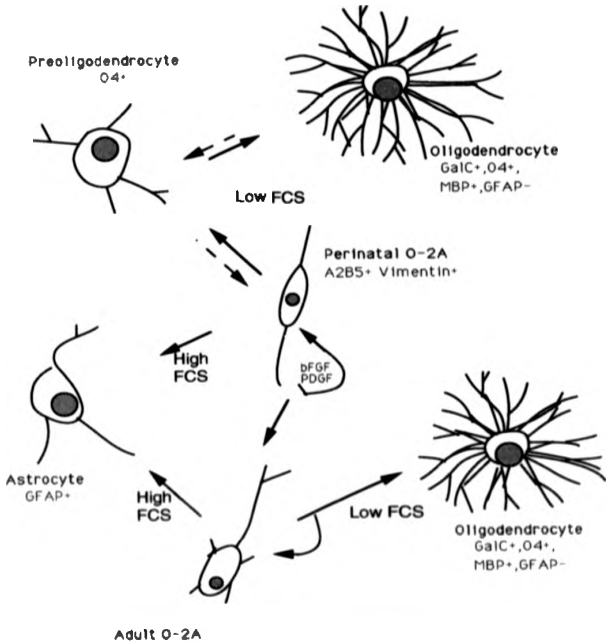

Fig. 3 Current views on the differentiation of cells of the O-2A lineage

Cells of the O-2A lineage arise as tripotential progenitors that may divide in the presence of basic Fibroblast Growth Factor (bFGF) or Platelet Derived Growth Factor (PDGF) or differentiate to either oligodendrocytes or astrocytes, depending on the concentration of foetal calf serum (FCS). Perinatal O-2A progenitors destined to become oligodendrocytes in the presence of low concentrations of FCS undergo a limited number of divisions, acquire an intermediate phenotype called the O4+ preoligodendrocyte and finally differentiate to oligodendrocytes. O-2A progenitors in adult animals are derived from perinatal O-2A progenitors and divide asymetrically, giving rise to their own progeny and oligodendrocytes. Under appropriate conditions, oligodendrocytes may be able to de-differentiate by following the differentiation pathway in reverse (dashed arrows).

III. Factors involved in proliferation and development

Although in vivo studies are of use in providing information regarding the loci, general timetable of differentiation and descriptive aspects of development and function of oligodendrocytes, until the last decade little was known about the different factors that influence the expansion of the progenitor cell population and oligodendrocyte differentiation. Developments in cell culture techniques allowed the growth of oligodendrocytes (Mc Carthy and de Vellis, 1980; Lisak et al., 1981) and their progenitors from either brain or optic nerve (McKinnon et al., 1990; Wolswijk et al., 1991 and others) in high purity. These techniques have yielded considerable information concerning the factors controlling O-2A progenitor proliferation, differentiation and development. O-2A development appears very complex as it is under the control of multiple growth and differentiation factors, the effects of which are only beginning to emerge.

O-2A proliferation in vitro is affected by a growth factor produced by the type of glial fibrilary acidic protein positive ($GFAP^+$) astrocytes not expressing gangliosides recognized by A2B5 (Type-1 astrocytes, Raff, 1989). Wolswijk et al., (1991) demonstrated that platelet derived growth factor (PDGF) was secreted by Type 1 astrocytes and was mitogenic for both $O\text{-}2A^{perinatal}$ and $O\text{-}2A^{adult}$ progenitors; furthermore, when either of these O-2A progenitors were treated with PDGF, they retained their respective phenotypes and other characteristics. Bögler et al., (1990) showed that cooperation between two mitogens, basic fibroblast growth factor (bFGF) and PDGF was able to promote continuous self renewal and inhibit differentiation of O-2A progenitor cells from optic nerve to oligodendrocytes. McKinnon et al., (1990) demonstrated that bFGF stimulated the proliferation of brain-derived O-2A progenitors and modulated the PDGF-driven pathway of oligodendrocyte development by inducing PDGF receptors on the cell surface.

Insulin and insulin growth factors appear to influence oligodendrocyte development by promoting cell proliferation and by influencing the differentiation choice of uncommitted progenitors to the oligodendrocytic phenotype. By acting in this manner, these regulatory peptides and cyclic AMP (cAMP) increase the overall synthesis and accumulation of myelin, although cAMP does not affect lineage decisions (reviewed by McMorris et al., 1990).

Neuronally derived factors may act in concert with other growth factors to expand the population of O-2A progenitors (Levine, 1989) and appear to be particularly mitogenic for O4$^+$ GalC$^-$ preoligodendrocytes (Gard and Pfeiffer, 1990). Preferential differentiation of brain O-2A cells to oligodendrocytes is achieved by growth to high densities and is unrelated to the total number of cultured cells, whereas O-2A progenitors seeded at low densities differentiate to Type-2 astrocytes (Levi et al., 1991). Additionally, medium conditioned by high-density subcultures of O-2A cells contains high-molecular weight (>30 kDa) non-mitogenic factor(s), which are capable of inducing differentiation of O-2A cells to oligodendrocytes, with preferential differentiation of O-2A progenitors to oligodendrocytes occurring for cells seeded at either high or low densities. Differentiation to oligodendrocytes may therefore be triggered by direct homotypic interactions and be additionally dependent on the secretion of short range autocrine or parsorine factors by O-2A progenitors.

iv. In vivo studies

a) O-2A progenitors

Beginning at around E16, O-2A progenitor cells were first detected with anti-G_{D3} in the subventricular zone (Levine and Goldman, 1988a).

There is circumstantial evidence to suggest that the O-2A progenitors do not develop from the neuroepithelial cells of the optic stalk but instead migrate into the developing optic nerve from the brain. In support of this proposed migratory behavior, O-2A cells have been shown to be able to journey substantial distances into normal CNS tissue either from CNS transplants *in vivo* or CNS explants *in vitro* (for reviews see Raff, 1989; Dubois-Dalcq and Armstrong, 1991). As they migrate into white matter, G_{D3}^+ cells lose G_{D3} and start to express GalC, CNP and MBP within two days; interestingly Type-2 astrocytes (G_{D3}^+ GFAP$^+$) could not be identified *in situ* in cerebrum or cerebellum, while this cell type was readily identified *in vitro* (Curtis et al., 1988).

Isolated cortical O-2A progenitors differentiate on a time schedule *in vitro* that approximates the time schedule of myelinogenic activity observed *in vivo* (Gard and Pfeiffer, 1989). Although O-2A^{perinatal} progenitors were not found in optic nerve after one month, O-2A^{adult} progenitors persisted for up to a year *in vivo* and it was proposed that O-2A^{adult}

progenitors may be able to support the generation of both differentiated progeny cells as well as their own continued replenishment through adult life (Wren et al., 1992)

Although cultured O-2A cells from optic nerve (Raff et al.,1983) and brain (McKinnon et al., 1990; Hardy and Reynolds, 1991) have the potential to generate either oligodendrocytes in the absence of FCS or Type-2 astrocytes in the presence of 10-20% FCS (Raff, 1989), it is still unclear whether these progenitors become other than oligodendrocytes in vivo (Skoff, 1992). What is also unknown is whether the O-2A lineage represents the only route for the generation of oligodendrocytes in the neonatal CNS. Williams et al., (1991) using a retroviral vector (Price, 1987) identified a bipotential progenitor with the ability to generate both neurons and oligodendrocytes in the cerebral cortex. This suggests that neurons and glia of the O-2A lineage probably arise from the same progenitor cell in the CNS, as was previously suggested by others (for review see Cameron and Pakic, 1991).

b) Oligodendrocytes

Robertson (1899), experimenting with silver impregnation of CNS tissue, provided the first demonstration of oligodendrocytes by describing "small branching cells of very characteristic aspect distributed throughout the white matter of brain". Ramon y Cayal (1913) described "a third element" in addition to astrocytes and neurons in CNS cells and another Spanish histologist, del Rio Hortega (1919) showed that this third element comprised oligodendroglia and microglia, which originated from the neuroectoderm and mesoderm, respectively. The genesis of oligodendrocytes in vivo was initially studied morphologically by the use of electron microscopy. These studies were coupled with others where dividing cells were labeled with [^{3}H]-thymidine and their developmental fate was followed by autoradiography (reviewed by Polak et al., 1982).

Oligodendrocytes mainly develop during postnatal life and this is related to myelination in the different parts of the CNS. Cells from the subventricular layer, a CNS area consisting of immature cells, migrate to various locations in the brain prior to differentiation (Sturrock, 1982; Paterson, 1983). The in vivo sequence of oligodendrocyte differentiation is in the following order: subventricular cells, glioblasts, oligodendroblasts, light oligodendrocytes, medium oligodendrocytes and finally dark oligodendrocytes. The formation of light

oligodendrocytes corresponds to the period of rapid myelination; these cells are the largest in the developmental series, with cytoplasm rich in organelles and microtubules, suggestive of high metabolic activity (Federoff, 1985). Maturation into medium and dark oligodendrocytes takes a further one and three weeks, respectively, and the dark cells have dense nuclei and cytoplasm and are less metabolically active than their light and medium counterparts.

As mature oligodendrocytes are in intimate contact with myelinated axons, their replacement must involve considerable disturbance to the glial-axon spatial arrangement and it would be reasonable to expect that the turnover in the population of dark oligodendrocytes in the CNS is rather slow (Sturrock, 1985). Indeed, autoradiographic data indicate that in adult mice the oligodendroglial turnover time is between one and two years (Imamoto et al., 1978; Kaplan and Hinds, 1980), which is considerably slower than that of astrocytes (Paterson, 1983).

Due to the high degree of heterogeneity of differentiating O-2A cells in the CNS that probably results in different rates of myelination in different areas, it is still unclear to what extent cultured oligodendrocytes resemble their in vivo counterparts. Although oligodendrocyte cultures from the optic nerve have the advantages of high purity and approximately synchronous differentiation, they are not thought to be representative of the situation in brain, where myelination proceeds along a caudorostral gradient, occurring at different times and rates among, and within, tracts and cortical areas (Skoff et al., 1976); on the other hand, well characterized cultures from cerebral hemispheres may represent more realistic models of O-2A progenitor differentiation and metabolic activity in vivo. Long-term survival and synthesis of myelin-like membrane by cultured oligodendrocytes from rat cortex was achieved by growing highly purified cell populations on a substratum derived from lysed glia, FCS and high concentrations of transferrin (Rome et al., 1986). Under these conditions, a myelin-like membrane was produced following a similar developmental pattern to that observed in vivo and the membrane had the structural characteristics of loosely compacted CNS myelin.

The proliferative and differentiation routes for CNS glial cells are rather complex, as spatial and topographic considerations must be taken into account in addition to the variety of growth and differentiation factors present in CNS tissue (reviewed by Dubois-Dalcq and

Armstrong, 1991). Comparative in vivo and in vitro studies of cells cutured from specific CNS areas may be the way to further clarify O-2A lineage and development in the medium term.

1.3 MYELIN PROTEINS

The oligodendrocyte-specific proteins PLP, MBP, CNP and the MAG make up approximately 80% of the total CNS myelin protein (Eylar, 1972). CNP, MBP and MAG are present in both CNS and PNS myelin, although MBPs is found at a lower level of expression in PNS myelin. Po is unique to PNS myelin and PLP and DM20 were once thought to be unique to CNS myelin until Pucket et al., (1987) showed that Schwann cells express PLP at very low levels and Agrawal and Agrawal, (1991) further demonstrated that PLP as well as DM20 are present in Schwann cells and PNS myelin, albeit at much reduced levels compared with CNS myelin. The putative disposition of the major myelin proteins within the sheath is shown in Fig. 4 and the main structural features of these proteins will be discussed.

I. PLP and DM20

PLP is the major integral protein of the CNS myelin sheath and in some species it represents as much as 50% of the total myelin protein. Folch and Lees (1951) coined the term proteolipid to describe proteins which were soluble in organic solvents but insoluble in water, even when devoid of their non-covalently associated complex lipid. PLP was the only myelin protein found in chloroform-methanol extracts of bovine brain white matter (Cambi et al.,1983).

a) Structure

PLP is extremely hydrophobic and models constructed on the basis of sequencing data suggest that this protein may form three transmembrane segments traversing the bilayer, with a highly charged domain on the extracellular side and random loops in the intracellular space (Laursen et al., 1984; Fig. 4). However, on the basis of immunocytochemical labeling of oligodendrocytes by residue-specific antibodies, Hudson et al., (1989) have suggested a very different model, postulating only two transmembrane domains, with the remainder of the molecule exposed at the extracellular face. PLP is highly conserved across species; rat and

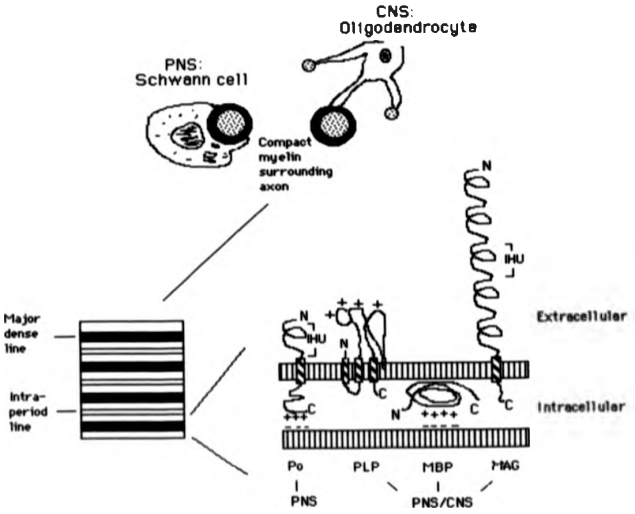

Fig 4: Molecular organization of myelin

A schematic cross-section of myelinated axons in the CNS and the PNS (upper centre). The myelin sheath is amplified to illustrate the detailed structure of compacted layers (lower left) and how the CNs and PNS polypeptides are inserted in the putative membrane (lower right).

N and C: amino and carboxy termini, respectively. IHU: immunoglobulin homology unit. Note the presence of a single IHU in Po and five IHUs in MAG.

(From Lemke, 1988).

human PLP (each 276 amino acids) are identical and such strong conservation implies that the structure of PLP is very important for its function (Lemke, 1988).

b) Biosynthesis

Transcription of the single rat PLP gene begins postnatally coincident with the onset of myelination; the MW of the mature polypeptide as determined from the amino acid sequence of cDNA clones is 30.0 kDa (Milner et al., 1985; Naismith et al., 1985).

DM20, a protein with a MW of 26.5 kDa, is a product of the same gene as PLP but is found in smaller quantities in CNS myelin (Lees and Brostoff,1984). DM20 is expressed prior to PLP in various species (Gardiner and Macklin, 1988; Van Dorsselaer, 1987; Kronquist et al., 1987) but as development proceeds, PLP becomes the most abundant of the two. DM20 is the product of an alternatively spliced mRNA which lacks the coding region for residues 116-151 (Nave et al., 1987); a secondary splice site within the third exon of the PLP gene is utilized for DM20 synthesis, which is a much less common mechanism than the widespread process of independent exon splicing (Diehl et al., 1986).

Le Vine et al., (1990) have established that in rat, PLP and DM20 mRNAs have essentially identical developmental profiles postnatally, although the DM20 mRNA is expressed at lower levels than the PLP mRNA. This may mean that the mechanism responsible for altering the PLP/DM20 protein ratio during development occurs posttranscriptionally.

PLP is not synthesized as a precursor, since the primary translation product is the same size as the mature protein (Colman et al., 1982). In vitro experiments suggest that PLP is synthesized on bound polysomes, inserts into the rough endoplasmic reticulum (RER) in a signal recognition particle (SRP)-dependent manner and is subsequently transported through the Golgi apparatus to the plasma membrane (Colman et al., 1982).

Recent evidence (Timsit et al., 1992) showing that the DM20 mRNA is present in 10 d old rat embryos at specific areas of the developing brain, suggests that some of the products of the PLP/DM20 gene may have additional roles during the compartmentalization and differentiation of the neural tube. Another report (Ikenaka et al., 1992) suggests that since DM20 mRNA was detected by the polymerase chain reaction (PCR) in mouse brain at E11, DM20 cannot be a product of oligodendrocytes alone; indeed, DM20 mRNA was produced

by all the cells of the nervous system, including glia, and in peripheral sciatic nerve.

c) Posttranslational modifications

PLP is posttranslationally acylated on at least one residue (198) and acquires two molecules of palmitate per polypeptide chain. Bizzozero and Lees (1986) have identified palmitoyl-CoA as the lipid donor in purified myelin. It is now known that fatty acylation is widespread amongst membrane proteins (Schmidt, 1983). Shlesinger, (1992) has proposed that such covalent attachment may ensure that the appropriate fatty acid is located in the correct position adjacent to the transmembrane segment of the protein in the bilayer. Attached lipid may be necessary for maintaining the lipid-protein interactions which, for a structure as specialized as CNS myelin, must be of paramount importance. Interestingly, PLP (and DM20) are not acylated in Schwann cells or PNS myelin (Agrawal and Agrawal, 1991).

II. The MBPs

This protein family consists of highly charged extrinsic membrane proteins localized on the cytoplasmic face of the myelin membrane, where they form the major dense line of compact myelin (Fig. 4). The MBPs constitute approximately 30 and 10% of the total CNS and PNS myelin protein, respectively.

In rodents four MBPs sharing common amino acid sequence with MWs of 21.5, 18.5, 17.0 and 14.0 kDa were initially identified (Barbarese et al., 1977). The 21.5 and 17.0 kDa species are the least abundant in mature myelin. Newman et al., (1987) identified a fifth MBP (17.0 kDa) by the use of cDNA cloning; this variant is expressed at a much lower level than the 17.0 kDa MBP mentioned above. It has also been suggested that rat brain may contain a 23.0 kDa MBP which appears to be translated from a mRNA not coding for any of the other forms of MBP (Agrawal et al., 1986).

a) Structure

Although the MBPs are not as highly conserved as PLP and DM20, there nevertheless

appears to be considerable sequence homology between the MBPs from different species; for instance, there is 90% conservation between the bovine and rat MBPs. Sequence examination via the available cDNA and genomic clones (de Ferra et al., 1985) showed that there are no cysteinyl residues in MBPs, therefore these proteins have no capacity to form intramolecular disulfide bridges. However, although the MBPs essentially form random coils in solution, there do exist regions of localized structure; MBP assumes highly ordered conformations in organic solvent mixtures and upon binding to lipid bilayers (Stoner,1984). Most of the ordered conformation of the MBPs is in the form of overlapping ß-turns forming a pleated sheet and Stoner (1984) proposed that the folding of MBP arises from a hairpin structure.

The isoelectric points of the MBPs are >10. In MBP, 12 lysyl and 19 arginyl residues are randomly distributed along the polypeptide chain (Lees and Brostoff, 1984) and are oriented in a way that favors interaction with the phospholipids of the cytoplasmic face of myelin. In this respect, the MBPs may primarily function in compressing the cytoplasmic space to form compact myelin.

A portion of the MBP molecule may be partially embedded in the membrane via the covalent linking of Ser-54 with polyphosphoinositide (Chang et al., 1986); the last notion however has been challenged when shown that the 4 mol% stoichiometry of inositol with MBP rules out a covalent lipid linkage as a general mechanism for attachment of this protein to membrane. Sankaram et al., (1989a) utilized chemical binding assays and spin-label electron spin resonance spectroscopy to show that the electrostatic interaction of MBP with membrane bilayers formed by the acidic lipid dimyristoylphosphatidylglycerol (DMPG) was obligatory for binding and that MBP could partially penetrate the bilayer. The same workers also showed that when MBP is incubated with different lipid mixtures, phosphatidylserine, one of the two major negatively charged lipids of myelin, is bound by MBP with high specificity.

MBP contains a single Trp residue, which is thought to serve as the focal point for the known encephalitogenic properties of this protein. Sankaram et al., (1989b) cleaved the MBP molecule at the Trp residue and studied the interactions of the 12.6 kDa (N-terminal) and 5.6 kDa (C-terminal) fragments with bilayers of DMPG. Their results suggested that the

principal sites of interaction of the MBP molecule with the lipid bilayer were at least partly located in the 12.6 kDa fragment and that the Trp residue must be important for the structural and functional properties of intact MBP.

b) Biosynthesis

In rodents the 32kb MBP gene is made up of seven exons, alternate splicing of which gives rise to each individual polypeptide. Mentaberry et al., (1988) have shown that this gene is also reponsible for the expression of the (same) MBPs in PNS myelin.

Transcription of the MBP gene begins during the first postnatal week in the CNS and PNS (Roussel and Nussbaum, 1981, Jessen and Mirsky, 1991). Zeller et al., (1985) used purified oligodendrocytes from different regions of the CNS and showed that cells from the spinal cord expressed MBP prior to those from mid-brain or brain hemispheres, thus correlating the *in vitro* expression of MBP to that observed *in vivo*.

There is evidence for control of MBP synthesis at the level of transcription. Thyroid hormone (T_3) was shown to increase MBP mRNA levels by an unknown mechanism (Shanker et al., 1987) and Bologa et al., (1986) showed that the production of MBP is controlled by a soluble neuronal factor. Further support for the influence of neurons on myelin protein synthesis in the CNS has been provided by Macklin et al., (1986) who demonstrated that MBP and PLP mRNA levels increase fourfold when oligodendrocytes are co-cultured with spinal cord neurons. In contrast to oligodendrocytes, where the presence of neurons is not essential for the initiation of transcription of myelin proteins, neuron-Schwann cell interactions are essential for the activation of myelin protein synthesis in Schwann cells (Jessen and Mirsky, 1991).

The levels of the 21.5 and 17.0 kDa MBP polypeptides decrease relative to the levels of the 18.5 and 14.0 kDa species between P15 and P60 in rat (Barbarese et al., 1978). Carson et al., (1983) have proposed that the 21.5 and 17.0 kDa MBPs may play a more important role in the early stages of myelin wrapping, since they are relatively abundant at that time.

In situ hybridisation has shown that MBP mRNAs are segregated within the peripheral regions of the oligodendrocyte and close to the sites of myelin assembly (Trapp et al., 1988). When oligodendrocytes are grown in culture, MBP can initially be detected at the cell body

but when the cell matures MBP is also found in the thick processes and membrane sheets, where it is in close association with microtubules (Wilson and Brophy, 1989). Colman et al., (1982) were the first to show conclusively that the MBPs are synthesized on free polysomes, by isolating rat brain RNA from free or bound polysomes and using it to program a wheatgerm translation system. These authors suggested that segregation of MBP mRNAs into the peripheral myelinating regions of the oligodendrocyte prevents the highly charged MBPs from associating non-specifically with intracellular membranes. Gillespie et al., (1990a) demonstrated that in oligodendrocytes from rabbit spinal cord, MBP is also synthesized on free polysomes.

c) Posttranslational modifications

A number of enzymes found in compact myelin use MBP as substrate and the products of these reactions are highly modified MBP molecules. The posttranslational modifications of MBP include acetylation, methylation and phosphorylation (Moscarello, 1990) which gives rise to charge heterogeneity.

MBP was shown to be acetylated on the N-terminal alanine in all species examined so far. Methylation on Arg-106 increases during active myelination (Crang and Jackobsen, 1983) and decreases as the animal matures (Chandekar et al., 1986), suggesting that MBP methylation may have a role during myelination.

The microheterogeneity of MBP was first demonstrated by Martenson et al., (1969) who resolved MBP into multiple bands on urea gels pH 10.6. The source of charge microheterogeneity was ascribed to deamidation, phosphorylation and loss of C-terminal arginine. Continuous *in vivo* alteration in the structure of the MBP molecule through microheterogeneity generated *in situ* is a possibility which may influence the structure of myelin.

The *in vivo* phosphorylation of MBP is a very rapid event with a turnover rate of minutes (Des Jardins and Morell, 1983), but only a small percentage of the total MBP is found in the phosphorylated form *in vivo* (Martenson et al., 1983). MBP phosphorylation has also been demonstrated *in vitro* (Kobayashi, 1984). Although the exact role of MBP phosphorylation is unknown, it has been proposed that when MBP is in a phosphorylated form compact myelin

may be transiently destabilized, causing a reversible separation of the apposed cytoplasmic faces (the major dense line) at specific areas (Turner et al.,1984). This would suggest a possible regulatory role for endogenous myelin phosphatases such as PL2, which was discovered by Yang et al., (1987). The regulation of MBP phosphorylation/dephosphorylation events in vivo may create flexibility in the structure of myelin and make this membrane a more dynamic structure.

III. The CNPs

CNPs (EC 3.1.4.37), once referred to as the Wolfgram (Wolfgram and Kotorii, 1968) doublet from SDS-PAGE studies (Waenheldt and Malotka, 1980) are not unique to the nervous system. CNPs were initially reported in spleen, pancreas, thymus and brain and they have since been found in lymphoid tissue (Sprinkle et al., 1985), adrenal medulla (Tirell and Coffee, 1986) and circulating blood lymphocytes (Bernier et al., 1987). CNP activity is highest in the corpus callosum, an area of the brain characterized by its high myelin content (Kurihara and Takahashi, 1973). Although the association of CNP with myelin was known for some time, purification required drastic solubilisation procedures such as detergent pre-treatment steps (Wells and Sprinkle, 1981) in order to release this enzyme from its strong binding to the membrane.

CNP is expressed exclusively by oligodendroglia in the CNS and is not present in compact myelin, but is concentrated within specific regions of the oligodendrocyte and myelin internode (Trapp et al., 1988). Recent in vitro evidence suggests that CNP may have an active role during oligodendroglial process extension via its strong interaction with filamentous actin (F-actin), as CNP and F-actin disappear concomitantly from the cell extremities upon maturation (Wilson and Brophy, 1989).

Two CNP polypeptides are found in myelin, CNP1 and CNP2. Cloning of CNP1 from rat brain (Bernier et al., 1987) and CNP2 from bovine brain (Vogel and Thompson, 1987) has yielded MWs of 44875 and 45592 Da, respectively. Kinetic studies (Matthiew et al., 1980) did not reveal any significant differences between the CNPs from the CNS and PNS, but a monoclonal antibody raised by Fujishiro et al., (1986) recognized CNP in the CNS only,

indicating that the molecular differences between the CNPs from CNS and PNS do not significantly affect its catalytic site. The relative amounts of myelin CNP1 and CNP2 vary between species, but CNP1 is in greatest abundance in the myelin of all animals studied with the exception of bovine myelin. Electrophoresis of the native enzyme under non-denaturing conditions places the M_r of CNP at approximately 100 kDa, suggesting a dimeric structure (Sprinkle et al., 1980). Kurihara et al., (1968) were able to detect a third form of CNP with an apparent SDS-PAGE M_r of 45.0 kDa.

a) Enzymic reactions

CNP catalyses the hydrolysis of 2',3'-cyclic nucleotides to form 2'-nucleotides and Sheedlo et al., (1984) have shown that only the 2'-isomer is formed. CNP from CNS myelin has a very high specific activity when hydrolyzing 2',3'-cyclic AMP (approximately 1,000-4,400 µmoles / min / mg protein) as well as 2',3'-cyclic-GMP, -CMP and -UMP whereas CNP from sciatic nerve is far less active (Kurihara and Tsukada, 1967).

The in vivo substrate(s) and physiological role(s) of CNP are not known. 2', 3'-cyclic nucleotides are enzymatic RNA breakdown products that do not accumulate in cells (Olafson et al., 1969) and although their hydrolysis is by no means confined to CNP, this is the only CNS and PNS enzyme with the capacity to produce 2'-nucleotides. Takahashi, (1961) proposed the hydrolysis of 2'-nucleotides by a nucleotide phosphomonoesterase and Nakamura et al., (1979) as well as Vogel and Thompson, (1988) have purified this enzyme from brain.

CNP may be involved in RNA metabolism (Sprinkle et al., 1987), as this enzyme has been shown to have an additional 5'-polynucleotide kinase activity. Therefore, CNP displays two of the three known activities of RNA ligases: 5'-polynucleotide kinase, 2',3'-cyclic phosphodiesterase and ligase (Pick and Hurwitz, 1986; Phizicky and Abelson 1986). Nevertheless, at the present time CNP is an enigmatic, if abundant, enzyme of myelin and oligodendrocytes.

b) Biosynthesis

Bernier et al., (1987) have shown that in rat thymus a single mRNA species codes for both

forms of CNP and Kurihara et al., (1988) demonstrated that alternative splicing of exon 1 of the CNP gene results in the generation of a second mRNA from the gene in mouse brain, which accounts for CNP1 and CNP2.

Karin and Waehneldt, (1985) had suggested that CNP is synthesized on free polysomes because labeled CNP was found to accumulate rapidly in rat optic nerve myelin after its synthesis; monensin, a drug that stops transport from the Golgi apparatus to the plasma membrane, had no effect on the appearance of CNP in myelin. Gillespie et al., (1990b) investigated the site of synthesis of CNP in rat brain and their combined data on the rapid kinetics of incorporation of CNPs into the oligodendroglial plasma membrane and in vitro translation of RNA isolated from free and bound polysomes, suggested that synthesis of CNP must occur on free polysomes as was previously shown for MBP (Colman et al., 1982; Gillespie et al., 1990a). Gillespie et al., (1990b) also showed that in contrast to MBP mRNAs which are enriched in actively myelinating processes, CNP mRNAs are not enriched in the myelin-associated pool of RNA and suggested that the CNPs probably associate with the cytoplasmic surface of the oligodendrocyte plasma membrane through interactions with membrane-bound receptors.

c) Posttranslational modifications

Most of the acidic amino acids of CNPs are amidated, giving these enzymes isoelectric points of 8.5-9.0. CNP2 in CNS myelin only is the only myelin protein known to be phosphorylated in a cAMP-dependent manner by an endogenous myelin kinase (Bradbury and Thompson, 1984) and Ser-74, Ser-177 and Ser-305 have been proposed as possible phosphorylation sites (Vogel and Thompson, 1987). Bernier et al., (1987) have identified a CNP sequence that is homologous to cyclic nucleotide binding sites from other proteins. The rate of CNP phosphorylation in vivo is rapid, suggesting that reversible CNP phosphorylation may have a physiological role in myelin (Bradbury et al., 1984). CNP can be palmitoylated in vitro, but the extent to which this occurs in vivo and the contribution of this modification to the binding properties of CNP remain unknown (Agrawal et al., 1990a). CNP is isoprenylated by a mevalonic acid derivative in cultured C_6 glioma cells (Braun et al., 1991) and isoprenylation as well as palmitoylation may explain why although >80% of the CNP is synthesized on free

polysomes in oligodendrocytes (Gillespie et al., 1990) and CNP has no apparent transmembrane or other strongly hydrophobic domains (Bernier et al., 1987). CNP associates readily with membranes.

iv. The MAG polypeptides

MAG is a relatively minor component of CNS myelin, comprising approximately 1% of the total sheath protein (Quarles et al., 1972); this protein can be detected at the earliest stages of myelination, before any of the major myelin proteins are detectably expressed (Trapp et al., 1981). Lectin binding, periodate-Schiff staining and fucose incorporation have revealed multiple CNS myelin glycoproteins (Poduslo and Brown, 1975) but MAG is the most abundant and best characterized.

Glycoproteins related to the immunoglobulin gene superfamily mediate cell surface adhesion among neural cell types and are thought to play a key role in the development of the CNS (Cunningham, 1987). MAG is member of this gene superfamily (Poltorak, 1987) and is expressed on the surface of oligodendrocytes in the CNS. Additionally, MAG has considerable sequence homology with well characterized cell adhesion molecules such as the neural cell adhesion molecule (NCAM), L1 and I-CAM (Edelman, 1984; Williams, 1988).

a) Structure

Two MAG polypeptides designated large (L-MAG) and small (S-MAG) have been identified (Lai et al., 1987; Salzer et al., 1987) but as MAG consists of approximately 30% N-linked carbohydrate, the two polypeptides comigrate as a wide band with an approximate M_r of 100.0 kDa in SDS-PAGE. Deglycosylated L-MAG and S-MAG have MWs of 66.9 and 64.0 KDa, respectively (Quarles et al., 1983). An analysis of the deduced MAG amino acid sequences has suggested potential structure-function correlates (Salzer et al., 1987). Both MAG isoforms are predicted to have in common a large, extracellularly disposed amino-terminal segment and a single transmembrane segment (Fig. 4) but they differ in their carboxy-terminal, presumptive cytoplasmic sequences. The extracellular segment contains five immunoglobulin homology units (IHUs, a term coined by Hunkapiller and Hood in 1986)

and this portion of MAG is believed to mediate binding to the axon.

Also present in the ectodomain of MAG is the tripeptide recognition sequence Arg-Gly-Asp, which is a frequent determinant of the binding of cell recognition and extracellular matrix molecules. Such molecules are known to bind integrins, a family of heterodimeric surface receptors (Johnson et al., 1989) and it is possible that MAG may bind to axons in a similar fashion, thus linking myelin and the neuronal surface.

The role of MAG in axon-Schwann cell interactions leading to myelination has been further elucidated by experiments in which cultured Schwann cells were initially infected with recombinant viruses expressing MAG sense or antisense RNA and subsequently induced to myelinate by coculturing with neurons (Owens and Bunge, 1991). Electron microscopy revealed that the cells expressing RNA in the antisense orientation to MAG mRNA failed to segregate large axons and initiate a myelin spiral, despite having formed the basal lamina that normally triggers Schwann cell differentiation; cells expressing RNA in the sense orientation myelinated normally. These observations suggested that MAG may be the critical Schwann cell component induced by neural interaction which initiates peripheral myelination.

b) Biosynthesis

cDNAs for both MAG isoforms have been isolated and characterized, the MAG mRNAs are encoded by a single gene whose primary transcript is alternatively spliced (Lai et al., 1987; Salzer et al., 1987). Frail and Brown, (1984) showed that the mRNA for each MAG polypeptide is developmentally regulated. L-MAG mRNA appears before S-MAG mRNA and remains the dominant mRNA species during active myelination but as the rate of myelination decreases, S-MAG mRNA becomes the dominant species. It has been consistently observed that in rats, glycosylated MAG in immature myelin has a higher apparent molecular mass than in mature myelin and this developmental shift has also been observed in gerbils, and hamsters, but not in mice (Campagnoni, 1988). However, as it has never been shown that the MAG apoprotein ratios change during development, the possibility exists that posttranscriptional and posttranslational regulation may determine the levels of L- and S-MAG in vivo.

In cultured oligodendrocytes MBP and MAG appear 5-7 days postnatally followed by PLP

1-2 days later (Dubois-Dalcq et al., 1986). MAG appears in oligodendroglial processes well before MBP, suggesting that early MAG transport to the cell periphery may be important for myelin-axon interactions, as was previously proposed (Trapp et al., 1984; Bunge, 1991). The MAG polypeptides are type 1 integral membrane proteins and their precursors have identifiable signal peptidase cleavage sites.

c) Posttranslational modifications

The sugar moieties present in MAG are N-acetylglucosamine, mannose, galactose, N-acetylneuraminic (sialic) acid and fucose (34, 23, 20, 18 and 5% respectively) (Quarles et al., 1983). MAG is sulfated, most probably on the sugar residues.

The IHUs in MAG are linked by disulfide bridges and a cysteine within the lipid bilayer in MAG is posttranslationally palmitylated (Pedzara et al., 1990).

cDNA sequencing showed that there are four potential sites for L-MAG phosphorylation: one by calcium/calmodulin dependent protein kinases, two by protein kinase C and one by tyrosine kinase (Salzer et al., 1987; Lai et al., 1987), but only the calcium/calmodulin dependent protein kinase site is available in S-MAG. Edwards et al., (1989) had stated that in the CNS only the cytoplasmic domain of L-MAG was phosphorylated both in vivo and in vitro. A later report by Afar et al., (1990) showed that although L-MAG phosphorylation occurs on serine, threonine and tyrosine residues, CNS S-MAG is also phosphorylated in vivo but only on serine residues. The in vivo phosphorylation of the main PNS myelin MAG species (S-MAG) was shown to occur on a serine residue (Agrawal et al., 1990a). This supports the findings of Afar et al., (1990) and suggests that S-MAG may be phosphorylated by similar mechanisms in both CNS and PNS myelin.

v. P_o

P_o accounts for approximately 50% of the total PNS myelin protein. Po is a transmembrane glycoprotein and the deglycosylated polypeptide has a MW of 24.9 kDa (D'Urso et al., 1990) while the glycosylated form has a MW of 28.5 kDa.

a) Structure

P_o is highly conserved (Saavedra et al., 1989) and its distribution is restricted to compact myelin layers. X-Ray diffraction studies have led to the belief that P_o acts as a "structural cement" in order to bring in close apposition both the cytoplasmic and the extracellular faces of PNS myelin (Lemke and Axel, 1985). Transfection of HeLa cells (not normally expressing P_o) with P_o cDNA showed that transfectants made substantial contact with their non-transfected counterparts (D'Urso et al., 1990), strengthening the notion that P_o is an adhesion molecule. Filbin et al., (1990) also transfected Chinese hamster ovary cells with a plasmid containing Po cDNA and examined the aggregation properties of transfectants in suspension; such cells formed desmosomes and aggregated via homophilic interactions of the extracellular domains of P_o, whereas non-transfected cells did not. These experiments led to the hypothesis that the extracellular leaflets of PNS myelin may be held together by homophilic interactions of Po molecules, involving this protein in myelin compaction.

As in the MBPs, the cytoplasmic domain of Po is extremely basic. MBPs in PNS myelin constitute only 5-15% of the total protein and the basic portion of Po has been proposed to replace the function of MBP in at least one MBP mutant (see further).

b) Biosynthesis

Analysis of the intron-exon organization of P_o shows that this protein resembles a primordial cell-cell adhesion molecule that must have arisen very early in metazoan evolution and given rise to the immunoglobulin gene superfamily (Williams, 1987). In the Po gene, the sequence encoding the extracellular immunoglobulin-related domains is split into two exons of similar structure and length (Lemke et al., 1988); this gene is highly conserved and its structure conforms to predictions made for members of the immunoglobulin gene superfamily (Amzel and Poljack, 1979).

Po inserts into the RER in a SRP-dependent manner and is transported through Golgi to the plasma membrane, as is PLP. The cleaved amino-terminal signal sequence in Po is followed by a relatively hydrophobic extracellular domain, a single membrane-spanning domain and a very basic intracellular domain (Lemke and Axel, 1985; D'Urso et al., 1990; Fig. 4).

c) Posttranslational modifications

The posttranslational modifications of P_0 include glycosylation, phosphorylation, acylation and sulfation (Everly et al., 1973; Wiggins and Morell, 1980; Matthieu et al., 1975). Suzuki et al. (1990) have suggested that phosphorylation of P_0, which is mainly via calcium/calmodulin-dependent protein kinase II, may be important for the maintenance of the major dense line in PNS myelin. All the phosphorylation sites of P_0 are present at the cytoplasmic surface.

1.4 MYELIN LIPID METABOLISM AND MEMBRANE TRAFFIC

I. Myelin lipids

Myelin is a very unusual biological membrane in that it has a very high lipid to protein ratio. It comprises approximately 25% of the dry weight of brain in mature rat (35% in human) and 40% of total brain lipid. In order of abundance, the main lipids of myelin are cholesterol, GalC and ethanolamine plasmalogen. GalC and sulfatide are not myelin-specific lipids but are much more abundant in myelin than in other membranes.

CNS and PNS myelin differ less in their lipid compositions (Table 1) than their protein compositions. The main quantitative differences between CNS and PNS myelin lipids are in the sphingolipids. PNS myelin from different species contains less galactolipid and considerably more of the phospholipid sphingomyelin (SM) than CNS myelin (Norton and Cammer, 1984). In contrast to CNS myelin, the amounts of SM and phosphatidylethanolamine (PE) are similar in PNS tissue.

Myelin sphingolipids

All sphingolipids possess the long chain amino alcohol sphingosine backbone and, after phosphoglycerides, are the second major class of lipids in animal membranes. In rat CNS myelin, the concentration of sphingolipids is directly proportional to the amount of myelin present (Norton and Cammer, 1984).

Sphingomyelin

Sphingomyelin (SM) is synthesized by direct transfer of the phosphorylcholine headgroup from phosphatidylcholine (PC) to ceramide (Cer) by the enzyme ceramide phosphatidylcholine phosphocholinetransferase (sphingomyelin synthase; Kishimoto, 1983). Studies using highly purified brain and liver membrane fractions (Malgat, 1986; Maurice, 1989) have revealed a second pathway of SM biosynthesis in these tissues. This involves the transfer of phosphorylethanolamine from PE to Cer, followed by methylation; although this second pathway is minor, it may be of high importance in brain that has a high PE content. As SM does not flip-flop due to its highly polar head group (van Meer et al., 1987), its exclusive localization on the exoplasmic leaflet must be established during biosynthesis.

Table 1. The lipid compositions of mature human CNS and PNS myelin.
Individual lipid classes are expressed as percentages of total phospholipid.
*: Primary ethanolamine plasmalogen. #: included with phosphatidylserine
(From Norton and Cammer, 1984).

Component	CNS	PNS
	% of dry weight	
Protein	30.0	28.7
Lipid	70.0	71.3
	% of lipid weight	
Cholesterol	28.4	23.0
Tot. Galactolipid	27.8	22.1
Tot. Phospholipid	43.8	54.9
Ethanolamine*	43.2	35.0
Choline	26.0	15.0
Serine	11.1	17.0
Inositol	1.4	#
Sphingomyelin	18.3	33.0

Myelin phospholipids are enriched in long chain fatty acids. SM contains large amounts of 24:1, 18:0 and 24:0, which are synthesized by chain elongation of fatty acids such as palmitic acid (16:0) and oleic acid (18:1) (Boyer, 1983). However, the function of long chain fatty acids in myelin is not clear (also see under The Secretory Pathway).

Galactocerebroside

Myelin GalC is synthesized from UDP-Gal and Cer by the action of the enzyme UDP-galactose galactosyltransferase. Sulfatide is formed from GalC by cerebroside sulfotransferase by transfer of sulfate from phosphoadenosine phosphosulfate to GalC, and both enzymes require "boundary lipids" (mainly phospholipids) for activation (Boyer, 1983). The work of Brammer, (1984) showed that brain GalC is formed from UDP-Glu and Cer following the epimerisation of UDP-Glu to UDP-Gal (via the action of UDP-galactose-4'-epimerase), rather than by synthesis of UDP-Gal from Gal-1-P and UDP-Glu. The interconversion of the two UDP-hexoses requires nicotinamide adenine dinucleotide (NAD) and proceeds via a 4-keto intermediate.

Myelin galactolipids are also enriched in long-chain saturated and monoenoic fatty acids, mainly C_{18}-C_{26}. The presence of long chain fatty acids in myelin lipids is thought to be important in membrane compaction and maintenance. Brain Cer can be divided into those with α-hydroxy fatty acids and those with non-hydroxy fatty acids. Brain hydroxy fatty acids are derived directly from their corresponding non-hydroxy counterparts and it is thought that microsomal enzymes are responsible for supplying the fatty acid moieties to sphingolipids.

The structures of typical myelin Cer, GalC and SM are shown in Fig. 5.

Gangliosides

Myelin also contains small (0.2%) but significant amounts of gangliosides. Monosialogalactosylceramide (G_{M1}), which was shown to be the functional receptor of the cholera toxin by direct activation of adenylate cyclase in murine neuroblastoma cells (Gonatas et al., 1983), is found amongst many species and is enriched in myelin. Myelin and the oligodendrocytes of higher primates and birds uniquely contain sialogalactosylceramide (G_{M4} or G_7). Gangliosides are believed to have functions in cell-cell recognition, communication and growth in vitro (Bremer et al., 1984) and it is possible

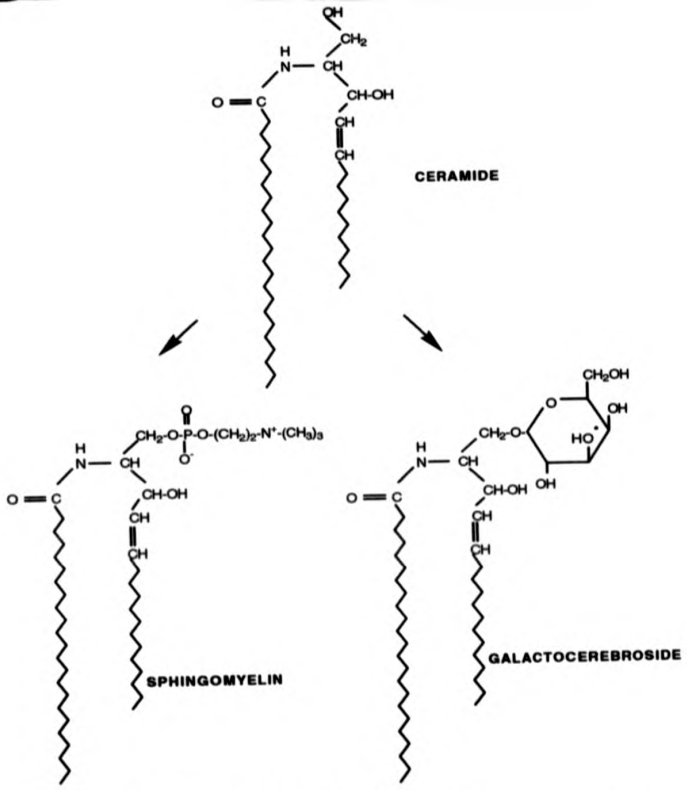

Fig. 5 The structure of the major sphingolipids of myelin-forming cells

Ceramide is the precursor of sphingomyelin and galactocerebroside and these sphingolipids are formed via different metabolic pathways. Galactocerebroside can be further converted to sulfatide by the addition of $-SO_3^-$ at the -OH of galactose that is marked by the asterisk.

that these sphingolipids may have specific functions in myelin in vivo (Wiegandt, 1982). Sung et al., (1991) have shown that exogenous G_{M3} ganglioside stimulates process formation and glycoprotein release by cultured bovine oligodendrocytes. PNS myelin also contains gangliosides (Ledeen et al., 1975) but at less than half the total concentration present in CNS myelin. Sialosyl-lactotetraosylceramide (L_{M1}) is a characteristic PNS myelin component in some species.

Sphingolipid biosynthesis in myelinating cells shares many common characteristics with sphingolipid biosynthesis in other cell types and the biosynthesis of sphingolipids is linked with intracellular transport through the secretory pathway.

II. The secretory pathway

Discovered by Camillo Golgi in 1898, the Golgi apparatus has long fascinated cytologists because of its distinct morphology, comprising flat cisternae which form characteristic 'stacks' that are interconnected by cisternal and tubulo-reticular bridges. In addition, numerous small membraneous vesicles are usually found associated with this organelle. At least four Golgi subcompartments, the *cis*-, *medial*-, *trans*-Golgi and the *trans*- Golgi network (TGN), an extensive tubulovesicular structure, can be identified by electron microscopy. The *cis*-compartments are situated closest to the nucleus and the *trans*-elements are the most distant.

The Golgi appparatus is currently attracting a lot of attention because of its central role in directing protein traffic within cells (Rothman and Orci, 1990; Hopkins, 1992; Lobel et al., 1989). The general pathway for the transport of secretory proteins from their site of synthesis to the cell surface involves at least three crucial sorting and translocation steps (for review see Hopkins, 1992): initially, proteins are inserted into the lumen of the ER via the signal peptide/SRP/receptor system (Blobel and Dobberstein, 1975). The second step from the ER to the Golgi is far less understood but it is known to be highly regulated. Finally, the TGN is the site where proteins are sorted to the plasma membrane or lysosomes (Snider and Rogers, 1985; Sossin et al., 1990).

Work in several laboratories has suggested that sphingolipids may be sorted coordinately

with proteins through the Golgi (Simons and van Meer, 1988; Simons and Wandinger-Ness 1990; Rosenwald et al., 1992). A recent report (Bertho et al., 1991) suggests that in leek seedlings, where transport of newly synthesized lipids and fatty acids from the ER is via bulk transport (without sorting), phospholipids containing fatty acids with chain length of more than 18 carbon atoms are transported preferentially through the Golgi apparatus. This result, together with the inability of the plasma membrane to synthesize long-chain fatty acids, leads to the hypothesis of a sorting function of the Golgi, based on fatty acid chain length. It is then possible that myelin proteins and sphingolipids that contain long chain fatty acids (such as sphingomyelin) may be cotransported and sorted through the Golgi en route to myelin.

Fig. 6 shows a model depicting traffic through the different Golgi compartments. The TGN also participates in retrieval and re-utilization of plasma membrane components internalized by endocytosis, such as mannose-6-phosphate and transferrin receptors (Duncan and Kornfeld, 1988) and probably also sphingolipids (Kok et al., 1989).

III. The use of Brefeldin A in studies of cellular metabolism and traffic

Metabolic inhibitors permit the detailed study of key metabolic events via the disruption of particular steps in the pathway. For example, the ionophore monensin has multiple intracellular effects but is most remarkable for blocking the intracellular transport of secretory glycoproteins, acting somewhere between the proximal and distal regions of the Golgi (Tartakoff, 1983).

The formation and localization of the Golgi complex appears to involve the direct or indirect interaction of this organelle with microtubules. Indeed, Golgi organization is lost during mitosis, when the depolymerisation of microtubules causes the breakdown of this complex into small, dispersed clusters (Lucocq and Warren, 1987). Understanding how Golgi structure is determined and maintained and how this structure relates to function is a fundamental problem in cell biology. Pharmacologic perturbation has provided a lot of information regarding Golgi structure / function correlates. Drugs such as colchicine and nocodazole that disrupt microtubule organization, result in the fragmentation and dispersion

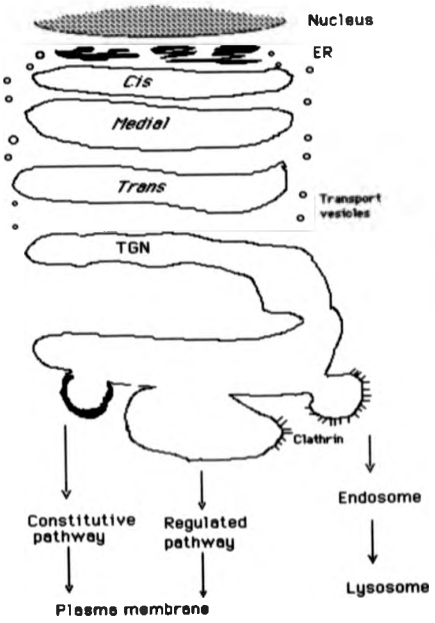

Fig. 6. Model for protein synthesis at the endoplasmic reticulum (ER) and sorting at the *trans*-Golgi network (TGN). (Adapted from Griffiths and Simons, 1986).

of the Golgi apparatus (Kreis, 1990). Although microtubule-perturbing agents fragment the Golgi, they do not abrogate the identity of this organelle as a distinct entity (Ho et al., 1989), nor do they affect its function (Rogalski et al., 1984). In contrast, the ability of Brefeldin A (BFA) to cause loss of the Golgi complex as an identifiable entity has added a new dimension to our ability to perturb this organelle.

BFA is a heterocyclic lactone produced by several fungi (Harri et al., 1963; Fig. 7a) which dramatically alters Golgi structure (Fujiwara et al., 1988). BFA effectively stops secretion from the ER and causes the redistribution of Golgi proteins into the ER (Misumi et al., 1986; Lippincott-Schwartz et al., 1989a; Dome et al, 1989). Morphological changes in the Golgi apparatus are seen within minutes after the addition of BFA in vivo and in vitro; initially the cisternal structure is lost and is replaced by swollen vacuoles that give rise to long tubulovesicular extensions, throughout which Golgi membrane and content are delivered to the ER. With continued BFA treatment no recognizable Golgi structures are seen in the cell (Lippincott-Schwartz et al., 1990). Disruption of the Golgi is accompanied by cessation of anterograde transport from the ER / Golgi fused system to more peripheral organelles.

The earliest known effect of BFA is the dissociation of the 110 kDa cytoplasmically oriented coat protein ß-cop from the Golgi peripheral membrane within 30s (Donaldson et al., 1990). The effect of BFA on the formation of a continuous tubular network between these two organelles might be explained if the role of ß-cop is to prevent fusion of Golgi and ER membranes (Orci, et al., 1991). Pelham, (1991) proposed that formation of long tubular structures emanating from the Golgi and fusing with the ER can probably be explained by the effect of BFA in unmasking the microtubule motor attachment sites that are normally covered by coat proteins such as ß-cop. In this scenario, microtubule-linked motors would carry uncoated Golgi tubules in a retrograde direction (i.e. from the Golgi to the ER) and due to the absence of coating proteins, vesicles would fail to pinch in and participate in anterograde transport, causing the eventual fusion of the ER with the Golgi. The formation of the TGN/endosomal system is also thought to occur by the extension of tubular structures that emanate from the TGN and proceed along microtubules to fuse with lysosomes (Wood et al., 1991). However, the detyrosynated microtubule network, comprising stable microtubules colocalizing with the Golgi in several cell lines, may be unaffected (Burgess et al., 1990).

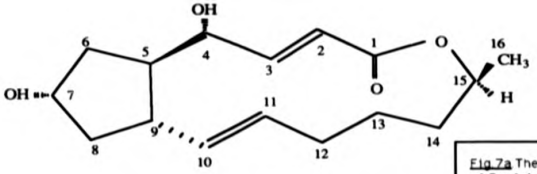

Fig 7a The structure of Brefeldin A (BFA)

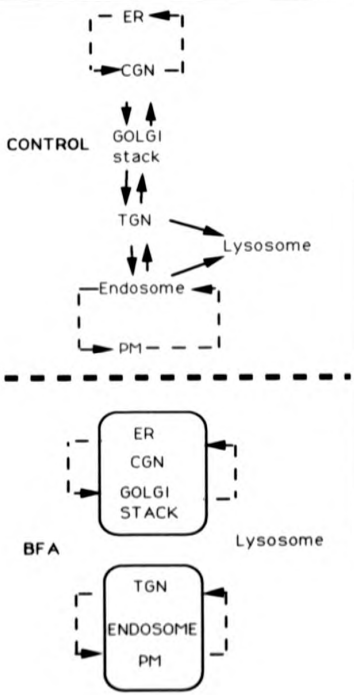

Figure 7b. Proposed model for the effect of BFA on organelle pathways of the central vacuolar system
BFA causes the formation of tubular processes mediating membrane transport Gross mixing of membrane does not occur, rather, organellar components seem to fuse and mix with distinct 'homotypic' membrane systems Thus, as shown in the bottom panel, Golgi stacks appear to fuse and mix with the recycling ER/cis-Golgi network (CGN) tubule system, while the *trans*- Golgi network (TGN) appears to fuse and mix with the recycling endosomal tubule system in BFA-treated cells Lysosomes apparently remain apart from these two mutually exclusive homotypic membrane systems Thus, according to this model, BFA interferes with the heterotypic membrane transport pathways (see top panel) that in control cells connect homotypic membrane systems to each other (After Lippincott-Schwartz et al., 1991a)

It is now known that BFA effects not only fusion of the *cis*-, *medial*- and *trans*-Golgi complex with the ER, but also of the endosomal system with the TGN. When the endosomal system of Madin Darby canine kidney (MDCK) cells was perturbed by BFA, early endosomes formed a tubular network and endocytosis, recycling of receptors to the cell surface and degradation of endocytosed material continued as before. In rat cells treated with BFA the endosome-TGN system collapsed into the centrosome region, probably driven by the motors that mediate the normal movement of endosomal material to the vicinity of the Golgi apparatus. A summary of the known effects of BFA is presented in Fig. 7b. BFA action is species- and probably cell-specific and in rat and bovine cells both the TGN/endosomal and ER/*cis*-, *medial*- and *trans*-Golgi systems are affected, while in canine (MDCK) and rat kangaroo kidney (PtK_1) cells the Golgi/ER system is BFA-resistant while the TGN/endosomal system remains sensitive (Wood et al., 1991; Lippincott-Schwartz et al., 1991b; Hunziker et al., 1991). This means that BFA has at least one more site of action than was originally thought and shows that each cell type must be investigated for its particular response to BFA.

As the effects of BFA are reversible (Pelham, 1991) cellular recovery and organelle reformation following BFA treatment may also yield important insights regarding the forces that drive organelle specific component re-assembly and the molecular relationships involved in these processes. An example of a process that may be further understood by experiments involving BFA is cytokinesis, which involves the reassembly of organelles such as the Golgi following mitosis.

iv. Fluorescent lipid probes

A difficult problem in membrane biology has been to define the pathways and study the molecular mechanisms by which the many lipid species move from one organelle to another after their biosynthesis, mainly because techniques for studying lipid traffic within cells have not been available. These problems are currently being addressed by the use of a series of fluorescent lipid analogues in which one of the naturally occurring fatty acids has been replaced by a fluorescent molecule. Drugs that disrupt membrane traffic also have the

potential to contribute significantly to these studies.

a) 4-chloro-7-nitrobenz-1,3-diazole (NBD) lipids

Ghosh and Whitehouse, (1968) first described 4-chloro-7-nitrobenz-1,3-diazole (NBD-chloride), a reagent which reacts with amino and thiol groups to form stable, highly fluorescent derivatives (Birkett et al., 1970; Price et al., 1975). NBD-chloride and NBD-fluoride have had multiple applications in the analysis of protein structure and conformational changes, in the chromatographic detection of amino acids and in the labeling of colcemid to study its interactions with the cytoskeleton (Chattopadhyay,1990).

Another important application of the NBD group is its increasing use to monitor the properties of biological and model membranes. Various synthetic lipids have been prepared by attaching NBD to the polar head or the non-polar fatty acid chain of the lipid precursor and using this probe as an analogue of the native lipid molecule. The processes studied with NBD lipids include spontaneous and protein-mediated transfer of lipids between vesicles or between vesicles and cell membranes (Nicols and Pagano, 1981; Nicols and Pagano, 1982; Arvinte and Hildenbrand, 1984; Nicols, 1985; Schroit and Madsen, 1983), membrane fusion, aggregation and lateral phase separation by resonance energy transfer and related methods (Uster and Deamer, 1981; Hoekstra, 1982), intracellular lipid transport and metabolism in living cells (Tanaka and Schroit, 1983; Lipsky and Pagano, 1985a; Sleight and Pagano, 1985), the study of lipid monolayers (Balakrishnan et al., 1982) and the study of the Golgi complex (Lipsky and Pagano, 1985b; Pagano, 1989; Pagano and Martin, 1988).

The most widely used NBD glycerolipids and sphingolipids for studying lipid metabolism and intracellular translocation in living cells are ones in which one of the naturally occurring fatty acids has been replaced with N-[7-NBD]-6-aminocaproic acid (C_6-NBD fatty acid, Lipsky and Pagano, 1983). Amongst the C_6-NBD-lipids that Pagano has studied over the last decade, C_6-NBD-ceramide (C_6-NBD-Cer, Fig. 8) has had the greatest impact in cell biology studies as it is both a vital Golgi marker and a good substrate for the enzymes of at least two metabolic pathways. Clearly, an important question is how accurately C_6-NBD-lipids mimic their normal intracellular counterparts; the following points (1-4, Pagano and

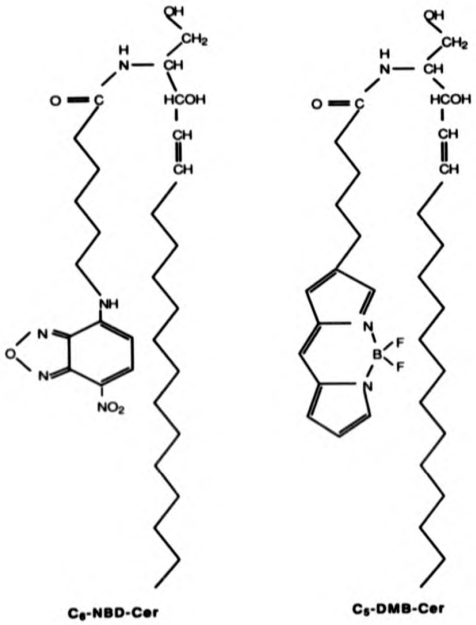

Fig. 8 The structures of N-[7-(4-nitrobenzo-2-oxa-1,3 diazole)]-6-aminocaproyl-D-erythro-sphingosine (C6-NBD-Cer) and N-[5-(5,7-dimethyl boron dipyrromethene difluoride)-1-pentanoyl]-D-erythro-sphingosine (C5-DMB-Cer).

Sleight, 1985a) suggest that C_6-NBD-lipids are good analogs

1) Various C_6-NBD lipids are metabolized to products that classical biochemical pathways predict and during co-incubation with their non-fluorescent radioactive counterparts there is no preferred substrate. 90 mol% of C_6-NBD-Cer fed to cellular monolayers grown in vitro can be converted to C_6-NBD-glucocerebroside (C_6-NBD-GlcC) and C_6-NBD-sphingomyelin (C_6-NBD-SM) within two hours of incubation at 37°C (Lipsky and Pagano, 1983). C_6-NBD-Cer is also metabolized in vivo and in experiments where this lipid analogue was dissolved in saline and injected in rat brain, the main metabolic products were fluorescent cerebrosides (Cbs), sulfatides and SM (Di Biase et al., 1991).

2) The time required for the translocation of newly synthesized fluorescent SM and Cb to the plasma membrane is consistent with the time required for newly synthesized isotopically labeled neuronal ganglioside, which is delivered in a similar fashion to SM and Cb, to appear at the plasma membrane.

3) Monensin inhibits the appearance of both isotopically labeled glycosphingolipids and C_6-NBD-Cb to the cell surface, showing that C_6-NBD-lipid and glucosphingolipid transport is subject to similar constraints.

4) Both C_6-NBD-PE and radioactivelly labeled PE which is synthesized de-novo appear to undergo transbilayer movement at the plasma membrane.

The NBD moiety is not charged at neutral pH (Chattopadhay and London,1986). This means that the actual charge on C_6-NBD-lipids labeled in their acyl chains will be the same as the corresponding endogenous lipids under physiological conditions. However, as detected by differential spin label quenching and other studies (Chattopadhyay and London, 1987, 1988) the NBD group is polar and loops back to the polar region of the membrane (Pagano et al., 1991). Therefore, if the acyl chain conformation is important, these lipids should be used with caution. A further possible disadvantage of NBD is that it is very susceptible to photochemical decomposition (bleaching).

b) 5,7-dimethyl boron dipyrromethene difluoride (DMB) lipids

Although much useful information has been obtained using NBD-labeled analogues, chemists have tried to design similar but more photostable molecules. In the case of

fluorescent lipids, membrane insertion in a manner resembling natural lipids was an additional goal. Boron dipyrromethene difluoride (BODIPY) is a novel fluorophore (Moore et al., 1988; Kang et al., 1988), long chain BODIPY fatty acids show rapid incorporation into most lipids (Kasurinen and Somerharju, 1992) and Pagano et al., (1991) were the first to synthesize and describe the use of a DMB ceramide, N-[5(5,7-dimethyl BODIPY)-1-pentanoyl] ceramide (C_5-DMB-Cer, Fig. 8). C_5-DMB-Cer is a vital Golgi stain (in addition to C_6-NBD-Cer), can be metabolized to C_5-DMB-SM and C_5-DMB-GlcC and has approximately two- to three-fold higher fluorescent yield and photostability than C_6-NBD-Cer (Pagano et al., 1991). Studies on the spectral properties of C_5-DMB-Cer revealed that the fluorescence emission maximum was strongly dependent upon the concentration of the probe in the membrane; this fluorophore exhibits a shift in its emission maximum from green (~515nm) to red (~620 nm) wavelengths with increasing concentrations. Therefore, C_5-DMB-lipids can be detected in regions where they are most concentrated by means of appropriate selection of filters in a fluorescence microscope.

v. Sphingolipid biosynthesis and traffic

Most cellular lipids are synthesized at the ER (Allan and Walkin, 1988), yet the membranes of the various organelles possess unique lipid compositions. Thus mechanisms must exist that allow lipid sorting. Although a lot of information is available about the role of the Golgi in protein processing and transport, the function of this organelle in lipid metabolism and trafficking is only beginning to emerge.

Simons and colleagues (Simons and van Meer, 1988; Simons and Wandinger-Ness, 1990) proposed that in the Golgi of MDCK cells, apical membrane proteins may be sorted coordinately with glucosphingolipids; Rosenwald et al., (1992) found that in the presence of 1-phenyl-2-(decanoylamino)-3-morpholino-1-propanol (PDMP), an inhibitor of sphingolipid biosynthesis, retardation of transport for secretory proteins also occurred, suggesting that transport of proteins and sphingolipids through the secretory pathway may be coupled to sphingolipid biosynthesis.

The general pathways of sphingolipid biosynthesis are probably common to all tissues,

including myelinating systems. Fig. 9 shows the main biosynthetic routes for sphingolipids and the enzymes responsible for each consecutive conversion. With the exception of the biosynthesis of Cer at the ER (Schwarzmann and Sandhoff, 1990), the various steps in sphingolipid assembly are believed to take place in the various cisternae of the Golgi in many non-glial cell types (Miller-Prodzars and Fishman, 1984; Lipsky and Pagano, 1985b; Rosenwald et al., 1992).

Although much is known about the metabolism and the various pathways by which sphingolipids traffic within cells, a single unifying model for intracellular transport cannot account for all of the existing data on sphingolipid movement within cells. Multiple pathways of intracellular lipid transport appear to depend on sphingolipid type, molecular species, cell type and the membranes under consideration (Koval and Pagano, 1990). Further investigations are needed in order to establish the exact routes of intracellular traffic and exact sites of biosynthesis of sphingolipids. This is particularly important in view of the regulation of glucosphingolipid biosynthesis through the effects of their concentration and composition of intracellular membranes and the cell surface. Myelinating cells should serve as good models for such investigations, as they are enriched in sphingolipids. Additionally, investigations into sphingolipid biosynthesis and traffic are important as it is becoming increasingly apparent that such lipids may have functional as well as structural roles (Gonatas et al., 1983; Bremer et al., 1984; Sung et al., 1991).

a) Ceramides

Radioactive and truncated ceramides

When radioactive-Cer was injected into rat brains it was metabolized to radioactive-GalC, -sulfatide and -SM (Kishimoto and Kawamura, 1979). Lipid analysis showed that at 30 min post-injection and at all subsequent times radioactive-GalC was the main lipid found in myelin, suggesting that GalC is the main sphingolipid that may either be synthesized in myelin and/or be transported to myelin and that association of GalC with myelin probably occurs shortly after GalC biosynthesis.

C_8C_8-Cer is a water-soluble, amphiphilic Cer analogue truncated in both hydrophobic regions (Karrenbauer et al., 1990), permitting this molecule to diffuse through

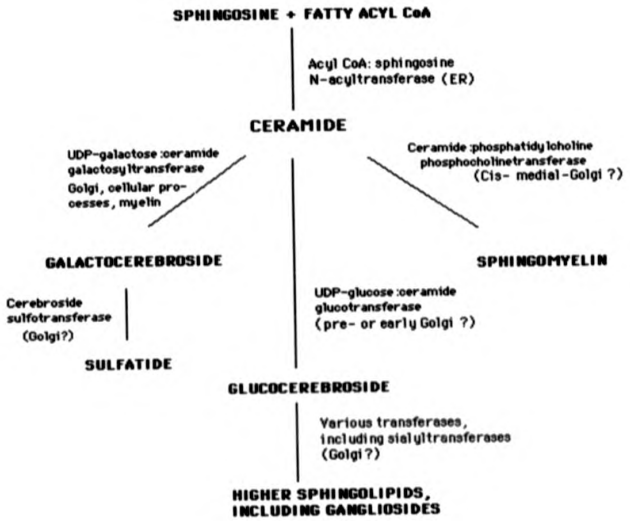

Fig. 9 The pathways, enzymes and possible locations of sphingolipid biosynthesis in mammalian cells.

lipid bilayers and get trapped in organelle(s) after the transfer of the hydrophilic head group. When C_8C_8-Cer was incubated with Chinese hamster ovary (CHO) cells in the presence of BFA, the overall synthesis of C_8C_8-SM increased and the synthesis of C_8C_8-GlcC remained unaffected (Brüning et al., 1992). The authors suggested that the increase in C_8C_8-SM synthesis in the presence of BFA probably reflected the translocation of sphingomyelin synthase from the Golgi apparatus to a mixed ER/Golgi organelle, where a pool of Cer larger than in the Golgi alone was available. However, as GlcC biosynthesis is thought to take place in a light, smooth vesicle fraction that could be a pre- (Futerman and Pagano, 1991) or early-Golgi (Jeckel et al., 1992) compartment, the apparent lack of change in C_8C_8-GlcC biosynthesis in the presence of BFA is not clear, as the intermixing of the Golgi with the ER would also provide a larger pool of Cer for the biosynthesis of C_8C_8-GlcC. A BFA-induced decrease in cellular SM levels that was accompanied by the induction of differentiation in HL-60 leukemia cells has also been reported (Linardic et al., 1992).

Fluorescent ceramides

After initial localization into the Golgi, C_6-NBD-Cer and its fluorescent metabolic products traffic through the intracellular compartments of cultured cells (Lipsky and Pagano, 1983). The intracellular transport of C_6-NBD-Cer and its metabolites can be followed by the use of fluorescence microscopy and lipid analysis can provide insights regarding their localization at given incubation times. Using these techniques Lipsky and Pagano, (1985a) showed that when monolayers of Chinese hamster lung (CHL) fibroblasts were incubated with C_6-NBD-Cer at 2°C, initial fluorescent labeling of the mitochondria, ER and nuclear envelope occurred; upon warming to 37°C, the Golgi apparatus and later the plasma membrane became intensely fluorescent. The experimental evidence suggested that both fluorescent SM and GlcC were transported to the cell surface via the Golgi.

When fixed cells were treated with C_6-NBD-Cer and photobleached in the presence of 3,3'-diaminobenzidine (DAB) (Sandel and Mashland, 1988), photo-oxidation caused polymerization of DAB at the site of the fluorescent label and the dark product was specifically localized at the Golgi apparatus (Pagano et al., 1989). C_6-NBD-Cer was shown to specifically label the *trans*-Golgi cisternae, as in experiments where thiamine

pyrophosphatase (TPPase, an enzymic marker of the *trans*- Golgi) had been labeled with Pb, DAB product did not accumulate. C_6-NBD-Cer accumulated in the *trans*-Golgi of cells fixed in a variety of ways, but accumulation was inhibited when either fixation protocols that extracted or modified cellular lipid or post-fixation permeabilization with detergent had been used. These observations suggested that the trapping of C_6-NBD-Cer at the *trans*-Golgi was due to interaction with the Golgi lipid.

Intraventricular administration of C_6-NBD-Cer into the brains of adult rats followed by isolation of myelin and microsomal fractions showed that unmetabolized C_6-NBD-Cer was located in a microsomal fraction; fluorescent Cb accumulated 2 h post inoculation, then decreased with the concomitant accumulation of fluorescent sulfatide (Di Biase et al., 1991). By contrast, fluorescent Cb and SM were present in myelin 30 min post-inoculation and then at all times studied. Fluorescence microscopy revealed that at 30 min post-inoculation fluorescence was only located in the cells lining the ventricles, while after 24 h fluorescence was also present in the paraventricular areas. This study demonstrated that when C_6-NBD-Cer is metabolized in the CNS in vivo, fluorescent Cbs are transported in brain and accumulate in myelin, as was previously found for radioactive Cer and GalC, respectively (Kishimoto and Kawamura, 1979). In brain at least, C_6-NBD-Cer and radioactive Cer appear to have the same metabolic fates, which indicates that these Cers may perhaps be used interchangeably for studies in vivo. It is also significant that fluorescent as well as radioactive Cbs are transported to myelin in preference to other sphingolipids, suggesting that specific mechanisms for Cb delivery to myelin may exist and that Cbs may have an important role in this membrane.

When C_5-DMB-Cer was used to label a variety of living cells, membranes containing high concentrations of C_5-DMB-Cer and its metabolites (the corresponding analogues of -SM and -GlcC) could be differentiated from other regions of the cell where smaller amounts of the probe were present, as concentrated DMB displayed its characteristic fluorescent shift (Pagano et al., 1991). Using this approach, prominent red fluorescent labeling of the Golgi apparatus, Golgi-associated tubulovesicular processes and putative Golgi-derived vesicles were seen in a variety of cell types and the concentration of C_5-DMB-lipids in the Golgi was calculated to be 5-10 mol% of the total Golgi lipid. C_5-DMB-Cer was mainly metabolized to

C_5-DMB-SM and only a small amount of C_5-DMB-GlcC was formed, in contrast to the metabolism of C_6-NBD-Cer where the ratio of C_6-NBD-SM/GlcC was ~1.31 under similar incubation conditions. The authors speculated that either only small amounts of C_5-DMB-Cer could reach the intracellular compartment(s) where the majority of GlcC synthesis occurs or that C_5-DMB-Cer is a poor substrate for glucocerebroside synthase because of the nature of the DMB fatty acid. In apparent support of the second hypothesis, Stein et al., (1989) have shown that the metabolic fates of Cers are critically dependent upon their fatty acyl chain compositions.

Back exchange is a technique that employs defatted bovine serum albumin (DF-BSA) in culture medium in order to remove fluorescent lipid from the plasma membrane of fixed cells, and back-exchange was previously used in order to remove and quantify C_6-NBD-Cer and its metabolites (van Meer et al., 1987; Pagano et al, 1989). Back-exchange could not deplete the surface of cells treated with C_5-DMB-Cer (Pagano et al., 1991) and it may be that strong interactions between C_5-DMB-lipids and other cellular lipids and / or proteins hinder the re-association of C_5-DMB-lipids with DF-BSA. While the inability to back-exchange C_5-DMB-lipids is an apparent limitation, their spectral properties can alternatively be used for quantitation.

b) Products of ceramide metabolism

Sphingomyelin

The precise site(s) of SM biosynthesis are not clearly defined; the suggestion that SM biosynthesis occurs in the *cis-* and *medial*-Golgi and that SM is subsequently delivered to the plasma membrane (Futerman et al., 1990; Jeckel et al., 1990) has been challenged by reports suggesting that although the main site of SM biosynthesis is the Golgi, some SM is also synthesized at the plasma membrane (reviewed by Koval and Pagano, 1991). Di Biase et al., (1991) speculated that SM is probably synthesized in the plasma membrane as well as in the Golgi of brain cells *in vivo* and then rapidly incorporated in myelin and in other cellular components such as microsomes, on the basis that similar amounts of C_6-NBD-SM were found in myelin and in microsomes at 30 min post-intraventricular injection with C_6-NBD-Cer.

The insensitivity of C_6-NBD-SM biosynthesis to treatment of intact Golgi membranes with

pronase (Jeckel et al., 1992) or trypsin (Futerman et al., 1990) coupled with the inability of SM to undergo transbilayer movement, suggested that SM is probably synthesized at the lumenal surface of the Golgi.

C_6-NBD-SM inserted into the exoplasmic leaflet of fibroblasts was sequentially endocytosed into early, peripheral and perinuclear endosomes and the $t_{1/2}$ for a complete round of recycling was approximately 40 min (Pagano and Sleight, 1985a; Koval and Pagano, 1989). Comparison of C_6-NBD-SM transport and metabolism in normal and (lysosomal) acid-sphingomyelinase-deficient Niemann-Pick Type A (NP-A) fibroblasts indicated that the rate of C_6-NBD-SM transport along the degradative pathway was approximately 18-fold slower when compared to the rate of recycling, supporting the notion that most endocytosed membrane lipid is recycled to the plasma membrane. Experiments that compared the recycling of C_6-NBD-SM and transferrin (the latter of which is known to be involved in receptor-mediated endocytosis) in a variety of cell types, demonstrated that internalized plasma membrane C_6-NBD-SM cycles very similarly to transferrin. The authors concluded that during endocytosis, C_6-NBD-SM recycles through sorting endosomes and/or the Golgi (from which recycling to the plasma membrane can also occur) (Stoorvogel et al., 1988) in a cell-specific manner.

The mechanism of transport of SM through the Golgi stacks is not understood, but the TGN is believed to be the site of sorting for exocytic C_6-NBD-SM (van Meer, 1989). Cholesterol is also transported along the exocytic pathway and as cholesterol interacts preferentially with SM rather than with other phospholipids (Gardam et al., 1989), van Meer, (1989) suggested that SM and cholesterol may be cotransported. As the SM content of intracellular membranes can be correlated to their content in cholesterol (Patton, 1970), it is possible that endogenous sphingomyelinase may be involved in the maintenance of membrane cholesterol levels by regulating intracellular SM levels (Koval and Pagano, 1991).

Lipsky and Pagano, (1985) showed that when monolayers of Chinese hamster lung fibroblasts had been incubated with C_6-NBD-Cer in the presence of monensin the fluorescent label accumulated in an enlarged Golgi apparatus, whereas in the absence of monensin the Golgi as well as the plasma membrane were labeled. These experiments suggested that newly synthesized C_6-NBD-GlcC and C_6-NBD-SM are transported through

the Golgi and probably arrive at the plasma membrane in vesicles originating from the TGN. Monensin also increased the total amount of fluorescent SM without affecting the amount of fluorescent GlcC found in those cells and the mechanism of this is unclear, although another apparent effect of monensin is to block the glycosylation of Cer (Saito et al., 1984; Miller-Prodzara and Fishman, 1984).

Although the metabolism, biosynthesis and traffic of SM have been under intensive investigation, it is not yet understood how metabolism and transport are coordinated to maintain the content of this lipid in each organelle, whether SM recycles through the Golgi and the exact role of the strong interaction between SM and cholesterol.

Cerebrosides

Subfractionation of rat liver and incubation with radioactive and fluorescent Cer analogues suggested that GlcC is probably synthesized in a pre- or early-Golgi compartment (Futerman and Pagano, 1991) and significant amounts of GlcC are probably synthesized at the cytosolic face (Jeckel et al., 1992; van Echten and Sandhoff, 1989; van Meer, 1989; Pagano et al., 1991). When radiolabeled glucosphingolipid precursors were fed to cultured murine BFA-treated cells, GlcC and lactosylcerebroside (LacC) radioactivity accumulated; this was taken to mean that BFA selectively disrupts the further metabolism of these lipids and that the GlcC and LacC synthases are probably localized at the proximal Golgi (van Echten et al., 1990). Newly synthesized C_6-NBD-GlcC appears to transit through the Golgi and has the energy-dependent vesicular transport characteristics of C_6-NBD-SM (van Meer, 1989).

Sorting of C_6-NBD-GlcC was shown to occur in the TGN of polarized (MDCK) cells (Simons and van Meer, 1988; van Meer, 1989). The combined use of C_6-NBD-GlcC and transferrin (Kok et al., 1989), showed that C_6-NBD-GlcC recycles between intracellular compartments and the plasma membrane in a manner similar to C_6-NBD-SM (Koval and Pagano, 1989).

Developmental studies where radiolabeled precursors of Cer and sulfatide were injected in brain *in vivo* suggested that the amount of label incorporation coincided with the onset, progress and decline of active myelination. The rates of galactosylation of Cer and sulfation of GalC *in vitro* closely resembled those measured *in vivo*, with peak enzyme activities

corresponding to peak rates of myelin accumulation (for review see Morell et al., 1989).

In cultured oligodendrocytes, gradual progressive hypoxia or the depletion of ATP specifically inhibited the synthesis of [^{3}H]GalC from [^{3}H]Cer, with [^{3}H]Cer accumulating in the ER. This showed that the site of synthesis of GalC is probably in a compartment separate from the ER and that GalC synthesis may be coupled to energy dependent transport (Kendler and Dawson, 1992).

The galactosyltransferase that catalyzes the formation of galactosylhydroxycerebrosides, the major brain galactolipids, has been extensively studied (Morell and Radin, 1969; Warren et al., 1976) and activity is found in a brain microsomal (mainly Golgi) fraction (Omanand et al., 1988), although a significant amount of activity is also associated with the myelin membrane fraction (Nescovic et al., 1973; Constantino-Ceccarini and Suzuki, 1975; Koul and Jungalwala, 1981). The specific activity of this enzyme increases during active myelination (Koul and Jungalwala, 1986) and reaches a maximum at P16 in myelin and at P20 in microsomes. In P16 animals the specific activity of UDP-galasctose:ceramide galactosyltransferase is 3-4 times higher in myelin than in microsomes (Koul et al., 1980) and Constantino-Ceccarini and Suzuki, (1978) have isolated a heat stable factor that appears to control the activity of this enzyme in brain.

There appears to be a precursor-product relationship between GalC in oligodendrocyte microsomes and perikarya and GalC in myelin (Sato et al., 1986) supporting the view that newly synthesized GalC from either intracellular compartments or the plasma membrane may be transported to myelin. Immunocytochemistry showed that in oligodendrocytes, UDP-galactose:ceramide galactosyltransferase is located in the cytoplasm, the cellular processes and in loosely wrapped myelin membranes (Roussel et al., 1987).

Sato et al., (1986) studied the in vitro effects of colchicine and monensin upon sulfatide delivery from microsomes and perikarya of oligodendroglial cells and the further incorporation of sulfatide into myelin. They showed that although the total amount of newly synthesized sulfatide was not depressed, delivery into myelin was inhibited by 50%, consistent with a possible involvement of the Golgi complex and cytoplasmic microtubules in the transport of sulfatide towards myelin. Using similar experimental conditions, Townsend et al., (1984) found that although the synthesis of GalC and sulfatide was normal in the

presence of either colchicine or monensin, the entry of these sphingolipids into the myelin sheath was greatly inhibited.

These results indicate that GalC (and perhaps also sulfatide) biosynthesis in oligodendrocytes probably takes place in the plasma membrane and in intracellular compartments, and that the entry of these lipids into myelin may be dependent on vesicular transport through the secretory pathway. This differs from GlcC biosynthesis, which is apparently restricted to a pre-or early Golgi compartment, as well as GlcC transport in other cell types and may reflect the specialization of oligodendrocytes as myelinating cells and the need for the delivery of galactolipids over considerable distances during active myelination and perhaps also in compact myelin.

Gangliosides

Gangliosides also transit through the Golgi (Klein et al., 1988; van Meer, 1989). Many enzymes of ganglioside biosynthesis reside in the Golgi (Keenan et al., 1974); the glycosphingolipid sialyltranferases SAT-1 and SAT-4 reside in the *cis*- and *trans*-cisternae, respectively (Trinchera and Ghidoni, 1989).

van Echten et al., (1990) showed that the biosynthesis of G_{M1}, G_{D1a}, G_{T1b} and G_{D3} was inhibited in BFA-treated cells and in similar experiments Young et al., (1990) showed that G_{A2} / G_{M2} and G_{D2} synthases were *trans* to the BFA block.

Cellular gangliosides that were initially detected in endosomes did not appear to reach the lysosome efficiently and their half-lives were of the order of 10-50 h (Miller-Prodzara and Fishman, 1984); when this is considered with the recycling of C_6-NBD-SM and -Cb through endosomal compartments, it strengthens the notion that endosomes may also be involved in lipid sorting.

1.6 THE CYTOSKELETON

The cytoskeleton of eukaryotic cells comprises microfilaments, microtubules, intermediate filaments and associated molecules. The cellular cytoskeleton has been implicated in processes as diverse as cell division, migration, shape change, cell adhesion, cell-cell interaction and possibly the transfer of information from the plasma membrane to the nucleus, thereby affecting gene expression (Ben-Ze'-ev, 1986; Watt, 1986). An operational and experimental description of the cytoskeleton is "the insoluble residue remaining after extraction with nonionic detergent" (Brown et al., 1976). Although the best characterized cellular cytoskeleton is that of the erythrocyte (Birchmeier, 1984), considerable progress has also been made in characterizing the cytoskeletons of myelin and myelinating cells (Gillespie et al., 1989; Pereyra et al., 1988; Wilson and Brophy, 1989).

i. Cytoskeletal components in non-myelin forming cells

a) Proteins

Microtubules and associated proteins

Microtubules are 25 nm tubular filaments composed of heterodimers of α- and β-tubulins, which are 55.0 and 54.0 kDa subunits, respectively. These structures disassemble and reassemble around a spindle during mitosis (Brenner and Brinkley, 1981) and are involved in cellular processes such as the movement of cilia and flagella by the microtubule-associated ATPase dynein (Warner and Mitchell, 1980) and others. Polymerization and stabilization of microtubules is believed to be influenced by microtubule-associated proteins (MAPs), which include the large polypeptides MAP1B and MAP2 with M_rs >250.0 kDa, and tau-proteins with M_rs of 60-70.0 kDa (Connolly and Kalnins, 1980). MAPs may also be involved in the association of microtubules with microfilaments (Griffith and Pollard, 1982) and / or neurofilaments (Letterier et al., 1982).

Microfilaments

Microfilaments are composed of actin in linear homopolymers approximately 7nm in diameter. In living cells filamentous actin (F-actin) exists in diverse polymeric forms which are in equilibrium with monomeric G-actin and with associated forms of actin which cannot be readily defined as either F- nor G-actin (Koffer et al., 1983). Actin binding proteins which cap, sever, stabilize and crosslink microfilaments control the various actin structures in the living cell (for review see Niggli and Burger, 1987).

Intermediate filaments

Intermediate filaments are 10 nm diameter fibers that are both more stable and more diverse than microfilaments. Six major classes of intermediate filaments have been described, based on their cell of origin and the nature of their subunits. These include GFAP, with a 50.0 kDa subunit in astroglial and non-myelinating Schwann cells and vimentin, with a 53 kDa subunit in mesenchymal cells, O-2A progenitors (Raff, 1983), myelinating and non-myelinating Schwann cells both in vivo and in vitro (Jessen and Mirsky, 1991) and in other cultured cells. Although neurofilaments with 70, 140 and 200.0 kDa subunits were once thought to be specific to neuronal tissue, the 140 kDa subunit neurofilament NFM is also found in cultured Schwann cells (Kelly et al., 1992).

b) Lipids

Burn and Burger, (1985) first observed the presence of specific lipids in the cytoskeletons of platelets. They found that the Triton-X-100 insoluble frameworks of thrombin-activated platelets previously incubated with [^{3}H]-palmitate contained significantly increased amounts of labeled lipids when compared to resting platelets. Palmitate, diacylglycerol and some phospholipids were particularly enriched in the cytoskeleton and these lipids interacted strongly with α-actinin, a protein occurring in the general contact area between F-actin and the membrane.

Many GPI-anchored proteins were found to be insoluble in Triton X-100, leading to speculation that they may associate with the cytoskeleton (reviewed by Low, 1992). Brown and Rose, (1992) have shown that human placental alkaline phosphatase (PLAP) which

contains a GPI-anchor, becomes Triton X-100-insoluble together with glycosphingolipids only after it has been transported through the Golgi, supporting the model of Simon and co-workers (Simons and van Meer 1988; Simons and Wandinger-Ness, 1990) for sorting of certain membrane proteins to the apical cell surface after intracellular association with glycosphingolipids. Although PLAP is mostly insoluble in Triton X-100 and -114, >95% of the protein is solubilized by octyl glucoside, suggesting that lipid association with the cytoskeleton may be a function of selective detergent insolubility. A recent report (Moss and White, 1992) suggests that in the neuronal cell adhesion molecule GP130 (contactin) contains a GPI-anchor group which is necessary for the interaction of this protein with the actin Nonidet P-40-insoluble cytoskeleton. The authors speculated that the GPI-anchor of GP130 may interact directly with cytoskeletal actin-binding phospholipids and that non-ionic detergents may preferentially solubilize some membrane lipids only.

Sphingolipids display strong affinity for cytoskeletons. Sakakibara et al., (1981) reported that antibodies against GalC produced a microtubule-like staining pattern in several epithelial cell lines and that this pattern was abiated by treatment of the cells with colchicine, a drug that prevents microtubule polymerization. Ceramides co-purify with the Triton X-100 insoluble residue of platelets (Packham et al., 1991) and globoside, the most abundant neutral glucosphingolipid of human umbilical vein endothelial cells (HUVEC), as well as G_{M3} were found associated with intermediate filaments in these cells (Gillard et al., 1991). Globoside colocalizes with vimentin, desmin, keratin and GFAP in a variety of cell types, with a preference for vimentin in cells that contain both vimentin and keratin networks (Gillard et al., 1992).

The transport of lipid vesicles by microtubules has been extensively studied (Mateoni and Kreis, 1987; Vale and Hotani, 1988) and it is also possible that intermediate filament proteins may constitute a distinct transport system for intracellular vesicles with or without association with microtubules (Steinert and Roop, 1988). Lipid-cytoskeletal protein interactions must therefore be a prerequisite for vesicular transport. Furthermore, lipid-protein interactions in the cytoskeleton may play dynamic and/or regulatory roles during development. Cells of the oligodendrocyte lineage should be good models for studying cytoskeletal lipid-protein interactions, as extension of long myelin-like processes during their development to

oligodendrocytes must involve dramatic rearrangements in the cellular cytoskeleton.

II. The membrane-associated cytoskeleton of CNS myelin

Tubulin copurifies with CNS myelin (de Nechaud et al., 1983). In an attempt to account for the presence of tubulin in myelin, Modesti and Barra, (1986) showed that MBP can interact with tubulin in solution, thus inhibiting the activity of tubulin carboxypeptidase. When Gillespie et al., (1989) incubated rat CNS myelin with a buffer containing Triton X-100 that had been specifically designed to preserve intact microtubules, all the PLP and DM20 were extracted and the insoluble cytoskeletal residue contained all the tubulin and half the actin. The 21.5 kDa MBP and CNP2 were totally associated with the cytoskeleton whereas only half the 18.5, 17.0 and 14.0 kDa MBPs and CNP1 were extracted by Triton X-100. Although both CNPs are palmitoylated in vitro (Agrawal et al., 1990a), isoprenylation of CNP1 but not CNP2 (Braun et al., 1991) may explain why CNP1 is more readily extracted by detergent. Isoprenylation is characteristic of proteins involved in the regulation of the cell cycle and signal transduction, such as ras and ras-like proteins, heterotrimeric GTP-binding proteins (Malleze, 1990) and nuclear lamins (intermediate filament proteins lining the inner face of the nuclear membrane) (Kitten and Nigg, 1991) where isoprenylation may be important in the association with the nuclear membrane (Suzan et al., 1992). CNP may therefore be involved in aspects of the cell cycle and/or signal transduction and this could involve the cytoskeleton.

Gillespie et al., (1989) also showed that a distinct subset of myelin lipids, particularly enriched in the myelin-specific lipids GalC and SM, is strongly bound to the cytoskeleton of CNS myelin (Table 2). The strength of lipid-protein interactions in the cytoskeletal fraction was exemplified by the comigration of macromolecular lipid-protein complexes during sucrose density-gradient centrifugation.

III. The oligodendrocytic cytoskeleton

Oligodendrocytes in vivo possess an extensive cytoskeletal network composed entirely of microtubules (Wood and Bunge, 1984). The extension of multiple myelin lamellae followed by their enwrapment around axonal segments is analogous to cellular processes where the cytoskeleton has been implicated in controlling shape and motility (Niggli and Burger, 1987).

Table 2 Lipid composition of the Triton X-100-insoluble cytoskeleton residue compared with that of myelin.

Lipids were extracted from whole myelin and from the detergent-insoluble residue and the values were the means of measurements made on at least three different preparations. The standard deviations never exceeded 15% of each mean value.

Abbreviations: PE: Phosphatidylethanolamine, PC: Phosphatidylcholine, PS: Phosphatidylserine, PI: Phosphatidylinositol, SM: Sphingomyelin. H, NH: Hydroxy, non-hydroxy. ND: not detected. (From Gillespie et al., 1989).

Component	Myelin	TX-100--insol.residue
	COMPOSITION	
Total lipid (μmol/mg protein)	2.46	0.73
Cholesterol (mol% tot. lipid)	39.8	38.4
Cerebroside (mol% tot. lipid)	11.4	35.6
Cerebroside-NH (mol% cerebroside)	32	23
Cerebroside-H (mol% cerebroside)	68	77
Sulfatide (mol% tot. lipid)	5.3	1.4
Phospholipid (mol% tot. lipid)	43.5	19.5
PE (mol% phospholipid)	45	13
PC(mol% phospholipid)	32	39
PS(mol% phospholipid)	13	ND
PI (mol% phospholipid)	4	ND
SM (mol% phospholipid)	6	48

There is growing evidence that myelin-specific proteins interact with the oligodendrocytic cytoskeleton and such interactions may be involved in directing myelin extension, enwrapment around axonal segments and stabilization of the sheath in vivo. Wilson and Brophy, (1989) used indirect immunocytochemistry and Western blotting to show that when rat oligodendrocytes are grown in vitro, CNP associates with microfilaments early in development and is eventually lost from the cell periphery, whereas MBP remains associated with the thick tubulin processes of the cytoskeleton upon cellular maturation. Dyer and Benjamins, (1989a) showed that in cultured oligodendrocytes F-actin, tubulin and CNP probably interact, as the association between these proteins is breached with the F-actin disrupting drug cytochalasin B. The authors suggested that the oligodendrocyte cell surface lipid GalC may be linked to microtubules via MBP, as treatment with anti-GalC antibodies causes GalC patching over MBP domains, which is accompanied by the disruption of microtubules in membrane sheets and resembles the disruptive effects of colchicine.

Recent reports (Diaz and Avila, 1989; Fischer et al., 1990) have indicated that the microtubule-associated protein MAP1B is present in glia including oligodendrocytes but nothing is known about the function of MAP1B in these cells. Oligodendroglia and neurons are believed to arise from a common progenitor cell in the cerebral cortex (Price, 1987; Cameron and Rakic, 1991) and MAPs have been strongly implicated in the development of neuronal polarity (Matus, 1988, 1990). In neurons, MAP1B is found in association with microtubules at very early stages of process extension, presumably crosslinking microtubules (Noble et al., 1989; Sato-Yoshitake et al., 1989). This has led to the proposal that MAP1B has an important role in neurite extension (Tucker et al., 1988a, b; Tucker and Matus, 1988) and this view is supported by the fact that MAP1B is down-regulated in all mature neurons in the adult rat nervous system, with the exception of cells that retain the ability to reinnervate such as neurons of the olfactory system (Viereck et al., 1989).

1.6 The RUMPSHAKER (*rsh*) MOUSE

A considerable number of mutations affecting the process of myelin deposition have been identified in the CNS. Mutant animals have been very useful in attempting to unravel the complexity of cellular interactions and the roles of the various molecules in myelination. Initially the jimpy (*jp*), quaking (*qk*) and myelin synthesis deficient (jp^{msd}) mouse mutants were described and more recently the shiverer (*shi*), twitcher (*tw*) trembler (*tr*) and other mouse mutations have also been recognized (Hogan and Greenfield, 1984). Most of these mutants have ephemeral oligodendrocytes and limited life spans, but differ in the morphology and biochemistry of their respective CNS myelin sheaths and in their clinical effects.

An almost universal feature amongst CNS myelin mutants is the drastic reduction in the total myelin membrane, which is reflected in both myelin specific proteins and lipids. PLP and the MBPs are reduced in *jp* (Nussbaum and Mandel, 1973; Lerner et al., 1974) and *qk* (Nussbaum and Mandel, 1973) and at least PLP is reduced in jp^{msd} (Hogan and Greenfield, 1984). In these animals GalC, sulfatide and cholesterol are the main lipids reduced in myelin (Galli and Galli, 1968; Meir and MacPike, 1970; Bird et al., 1978).

Specific defects have been recognized in the expression of individual myelin protein genes and in some cases the genomic defect has been defined (Lemke, 1986,1988; Sutcliffe, 1987). In *shi* the MBP gene is defective and although in homozygotes this results in CNS demyelination, PNS myelin is unaffected, this led to the belief that in PNS myelin the basic (intracellular) portion of Po may be able to replace the function of the MBPs (Ganser and Kirshner, 1980).

In *jp* a specific point mutation in the PLP gene results in deletion of exon 5 (Nave et al., 1987) and in the shaking pup proline is substituted for histidine in exon 2; these mutations are inherited in an X-linked manner, consistent with the localization of the PLP gene on the X-chromosome (Willard and Riordan, 1985). These myelin mutants are characterized by development of tremors in hemizygous males at P10-15 and seizures are common in the rodent; both *jp* mouse and the shaking pup have short life spans by comparison with their wild type counterparts.

A new myelin mutant was recently recognized at the MRC Radiobiology Unit, Didcot,

Oxford U. K. A small stock of mice displayed tremors which were found to be associated with hypomyelination in the CNS; genetic analysis indicated an X-linked inheritance and immunochemical studies suggested a defect in PLP expression. This mutation was given the name rumpshaker (*rsh*) and was found to be quite different to *jp* (mouse) and the shaking pup.

In brain, *rsh* myelination commences appropriately but the majority of sheaths fail to develop normally. Oligodendrocytes are increased in number and have prominent Golgi apparatus, RER and free ribosomes, degenerative changes are not observed and cell death is not common. Immunostaining demonstrated a major defect in the expression of PLP and DM20, and site-specific antisera against portions of the PLP/DM20 molecule placed the major defect on PLP, where very few myelin sheaths were positive. Although genetic analysis indicated a locus at or close to the PLP *jp* locus, *rsh* is quite different from *jp* in that the former display normal longevity and breeding, produce substantially more myelin and have increased numbers of oligodendrocytes in brain (Griffiths et al., 1990)

A study of heterozygous *rsh* females showed that although major CNS hypomyelinated/amyelinated areas do not exist, hypomyelinated fibers are found in some areas and particularly in the spinal cord (Fanarraga et al., 1991). This resembles the situation in *rsh* hemizygous males and homozygous females but is considerably different from other X-linked PLP mutation heterozygotes, which are noted for more severe lesions and failure to recover with age.

A comparison between the optic nerve and spinal cord in *rsh* showed that the optic nerve contains varying numbers of myelinated and amyelinated fibers and that the majority of the sheath is of normal thickness; it was therefore thought that the disproportionately thin myelin sheaths in the spinal cord may be related to the difference in axon diameter between optic nerve and spinal cord, as axons in the spinal cord have proportionately large diameters that require more myelin per axon (Fannarraga et al., 1992). Although oligodendrocyte numbers are slightly increased in the optic nerve in young animals, the numbers in mature animals fall below those in wild type (wt) controls; by contrast, the number of oligodendrocytes in the spinal cord is consistently increased after P15. Immunostaining intensity in the optic nerve as well as the spinal cord is reduced for MBP and PLP and increased for GFAP.

The continued study of mutants such as *rsh* will be useful in trying to identify the cause(s) of demyelination and these animals also represent good model systems for remyelination experiments.

1.7 AIMS OF THIS STUDY

One of the major problems for investigators of CNS glia is establishing culture systems of homogeneous oligodendrocyte populations that can closely mimic the events associated with myelinogenesis in vivo, although some considerable progress has been recently made in this front. Some tissue culture systems, such as the one for O-2A cells from optic nerve, have been characterized very well but cell yields are rather low and this makes biochemical investigations problematic.

My goal was to prepare and characterize a primary culture system where highly purified cells of the O-2A lineage could divide and differentiate preferentially to oligodendrocytes. This model system would have to be highly reproducible, relatively easy for others to follow and repeat and should provide high cell numbers from few experimental animals, thereby permitting simultaneous immunochemical and biochemical examination of cells of the oligodendrocyte lineage at specific developmental stages.

An initial objective was to examine the developmental appearance of cytoskeletal and cytoskeletally-associated proteins and lipids in culture, as they may be of importance in myelination. I also intended to investigate the developmental pattern of sphingolipid metabolism in vitro by the use of fluorescent Cer analogues and determine whether such analogues associate with the cellular cytoskeleton. I decided to examine the effects of BFA on organelle structure and attempt to relate this to lipid traffic in oligodendrocytes.

A parallel goal was to characterize CNS myelin further, by establishing the degree of association of myelin-specific proteins with the cytoskeleton during development.

As phosphorylation is a major regulatory mechanism in biological membranes, it was important to assess the effect(s) of phosphorylation on the association of myelin-specific proteins with the cytoskeleton and whether cytoskeletally-associated proteins constitute a distinct pool of myelin proteins, distinguished by their phosphorylation status.

I had hoped that by comparing the cytoskeletal protein and lipid compositions of a known myelin mutant with its wild type counterpart, I might gain insights regarding the importance of the different components in intact myelin.

I also undertook to extend any interesting findings from the CNS investigations to PNS

myelin and Schwann cells.

Materials and Methods

2.1 Antibodies

I. Sources and dilutions

The antibody concentrations that follow were the ones used for immunocytochemistry. For a given antibody, concentrations for Western blotting were, as a general rule, 1/10th of these concentrations.

Mouse hybridomas that produce the A2B5, O4 and O1 IgM mAbs were generous gifts from Dr I. Sommer, Institute of Neurology, University of Glasgow; each was used as the crude hybridoma supernatant diluted 1:10, 1:10 and 1:20, respectively. The production of monoclonal antibody from hybridomas will be described.

A mouse anti-MAP1B mAb of the IgG1 subclass was obtained from Sigma (anti-MAP5, cat no M-4528, Huber and Matus, 1984) and was used at 1:200.

Rabbit anti-MBP was used at 1:200 (1:50 for immunoelectron microscopy). This antibody was raised against a synthetic peptide comprising the N-terminal seven amino acid sequence of rat MBP exon 1 and was a generous gift from Dr N. Groome, Department of Biology, Oxford Polytechnic. This peptide is common to all known forms of rat MBP and was coupled to Keyhole Limpet hemocyanin for antiserum production by standard techniques. Similarly an antibody was produced against the N-terminal fifteen amino acid sequence of mouse MAP1B (Noble et al., 1989) and was used at 1:100.

A rabbit anti-tubulin (cat no.65-095-1, ICN Israel), a mouse anti-tubulin (cat no. MCA78A, Serotec, U. K.) and a rabbit anti-γ-actin (a gift from Dr C. Bulinsky Dept. of Anatomy and Cell Biology, Columbia University, U.S.A) were used at 1:100.

Affinity-purified rabbit anti-MAG (1:100), anti-CNP (1:100) and anti-PLP/DM20 (1:100) were from Dr D. Colman, Department of Anatomy and Cell Biology, Columbia University. Rabbit anti-bovine GFAP (1:500) was from Dr E. Bock, University of Copenhagen. Rabbit anti-TGN38 (1:1000 for immunofluorescence and 1:500 for immunoelectron microscopy), which specifically recognizes a resident protein of the TGN, was from Dr P. Luzio, Department of Clinical Biochemistry, University of Cambridge (Luzio et al., 1990). Tissue culture supernatant containing the antibody 53FC3 which recognizes mannosidase II, a *cis*- and *medial*- Golgi component (Burke and Warren, 1984) was the kind gift of Dr. G. Warren and

for our purposes had to be concentrated 10-fold by overnight precipitation in 50% ammonium sulfate pH 7.4, resuspension in PBS and 24h dialysis versus three changes of PBS at 4°C; this concentrate was used undiluted.

Wheat germ agglutinin (WGA) coupled to tetramethylrhodamine B isothiocyanate (TRITC), which recognizes N-acetyl-β,D-glucosamine was purchased from SIGMA and was used at 1,1000.

Fluoresecent second antibodies conjugated to fluorescein isothiocyanate (FITC), (TRITC) or dichlorotriazinylamino fluorescein (DTAF) were used at a concentration of 1:100. Type-specific goat anti-mouse IgM (FITC) and goat anti-mouse IgG (TRITC) which we confirmed to be specific for mouse IgM and IgG1 respectively, were from Southern Biotechnology Associates (U.K.). Donkey anti-mouse IgG (DTAF) and donkey anti-rabbit IgG (TRITC) were from Jackson ImmunoResearch Labs., USA. Phalloidin-TRITC (SIGMA), specifically recognising F-actin, was used at 1:100.

Goat anti-rabbit IgG (Scottish Antibody Production Unit, SAPU) and goat anti-mouse IgG (Jackson Immunoresearch) conjugated to horseradish peroxidase were diluted 1:2,000 and 1:500 respectively for Western blotting and the former was diluted 1:200 for immunoelectron microscopy.

Goat anti-mouse IgG and IgM conjugated to 5 nm gold and goat anti-rabbit IgG conjugated to 10nm gold were from Amersham and were used for immunoelectron microscopy at a dilution of 1:20.

II. Monoclonal antibodies from hybridoma cell lines

Hybridoma cells were either pelleted at 200*g* for 10 min at room temperature or thawed directly from liquid nitrogen storage into a 37°C water bath, suspended into Optimem I (Gibco BRL), 10% FCS, penicillin (100 IU/ml), streptomycin (100 µg/ml) to a density of 10^4 cells ml^{-1} and incubated in sealed flasks at 37°C to a density of 10^5 cells ml^{-1}. The cells were then either diluted to the initial density or induced to produce high titre antibody by (only) adding fresh penicillin and streptomycin every three days, until a density of 10^6 cells ml^{-1} was reached. The hybridomas were pelleted, resuspended to 10^7 cells ml^{-1} in 90% FCS / 10% dimethylsulphoxide (DMSO) and cooled sequentially to +4, -20, -70 and -176°C

by allowing two hours between each cooling step.

The tissue culture supernatant was dot-blot tested for anti-mouse antibody content by diluting in PBS, spotting 1 µl aliquots on nitrocellulose strips, air drying, blocking for 3 h in 0.2% (w/v) pig skin gelatin / 0.1% (v/v) Triton X-100 in PBS, pH 7.4 and following the protocol for Western blotting (see further) from the point immediately after primary antibody incubation. Suitable concentrations were determined using immunofluorescence, by comparison with previously isolated antibody; in the case of A2B5, half the dilution used for immunofluorescence was suitable during reverse panning of O-2A progenitors.

2.2 Cell cultures

I. Isolation of O-2A progenitors and differentiation to oligodendrocytes

Wistar rats of both sexes aged 1-2 day old were decapitated and the heads were swabbed with 70% ethanol. Meninges and blood vessels were removed from the cerebral hemispheres on 3MM chromatography paper (Whatman) pre-soaked in Hank's balanced salt solution without Ca^{2+} or Mg^{2+} (HBSS-Ca,Mg). The tissue was dissociated into single cells by chopping the cerebral hemispheres in 1.5 ml of HBSS-Ca,Mg per brain; the segments were then passed gently 3-4 times through a 16 gauge needle and forced slowly and sequentially through 136 µm and 30 µm nylon mesh (Nybolt, Plastock Assoc., Birkenhead, U.K.). Cells were harvested at 500*g* for 5 min and resuspended to 2 m/telencephalon in Dulbecco's modified Eagle's medium (DMEM) containing 10% FCS (Flow, U.K.), penicillin (100 IU/ml) and streptomycin (100 µg/ml). The suspension was adjusted to 2.5×10^6 cells ml^{-1} and seeded at 3.3×10^5 cells cm^{-2} in 75cm^2 flasks, which had been pre-coated with 0.2 mg/ml poly-D-lysine hydrobromide (30-70,000 M_r, SIGMA) for 30 min. Poly-lysine was prepared by suspension in Milli-Q water followed by autoclaving and was stored at -20°C. The cultures were maintained at 37°C in a water-saturated atmosphere with 5% CO_2 (Wilson and Brophy, 1989) and the medium was replaced once after 3 d. After 6-7 d in culture when a clearly defined bilayer of cells had formed, the top layer consisting of phase-dark cells with few or no processes was harvested together with non-adherent microglia at 37°C by sealing and shaking the flasks at 100 rpm for 18 h followed by 180 rpm for 1 h in a Gallenkamp orbital incubator (McCarthy and DeVellis, 1980). The A2B5 mAb (Eisenbarth et al., 1979)

was added at a 1:10 concentration directly to the growth medium (Behar et al., 1988). The flasks were sealed, gently shaken for 15 min at room temperature, inverted and incubated at 37°C for 20 min. The non-adherent O-2A progenitors were harvested at 1000*g* for 10 min at room temperature and plated on glass coverslips (washed overnight in 5% w/v chromic acid in concentrated H_2SO_4, rinsed extensively with water, autoclaved and coated with poly-D-lysine) at a density of $5x10^3$ cells per 13mm coverslip (No1 thickness, BDH, UK) or seeded directly in 75 cm^2 flasks at 3 x 10^6 cells per flask. The O-2A cells were stimulated to divide with 1 ng/ml of bovine bFGF (British Biotechnology Ltd, Oxford, U.K.) in a defined, serum-free medium consisting of DMEM with the following supplements: transferrin (50 µg/ml), insulin (5 µg/ml), sodium selenite (20 nM), triiodo-L-thyronine (30 nM), D-biotin (10 ng/ml), penicillin (100 IU/ml), streptomycin (100 µg/ml). Half the medium was replenished and fresh bFGF was added daily for the first 4 d of culture. The medium was then removed, the cells were washed twice with pre-warmed DMEM and FCS (1%) was added to defined medium in order to induce progenitors to differentiate into oligodendrocytes. This medium was replenished every 3 d for up to 9 d. A diagrammatic representation of this procedure is shown in Fig. 10.

II. Schwann Cell Cultures

These cultures were prepared and experimentally handled throughout by Dr. Bernadette Kelly. Ten 4 d old rat pups were killed by decapitation and swabbed in ethanol. The sciatic nerves were dissected, washed into 1 ml L-15 medium (Gibco BRL) and cut into small pieces in 1 ml of medium (Brockes et al., 1979). Collagenase (Lorne Diagnostics, UK) was added to 0.078% (w/v) and the tissue was incubated at 37°C for 37 min; trypsin (Flow, UK) to 0.15% (w/v) was added for a further 15 min and the reaction was stopped with 1ml of FCS. The tissue was triturated gently using a 21g needle followed by a 25g needle. Five mls of Optimem I and 1ml of FCS were added and the suspension was centrifuged for 5 mins at 1000*g*. The pellet was resuspended in Optimem I / 10% FCS and the cells were incubated at 37°C overnight.

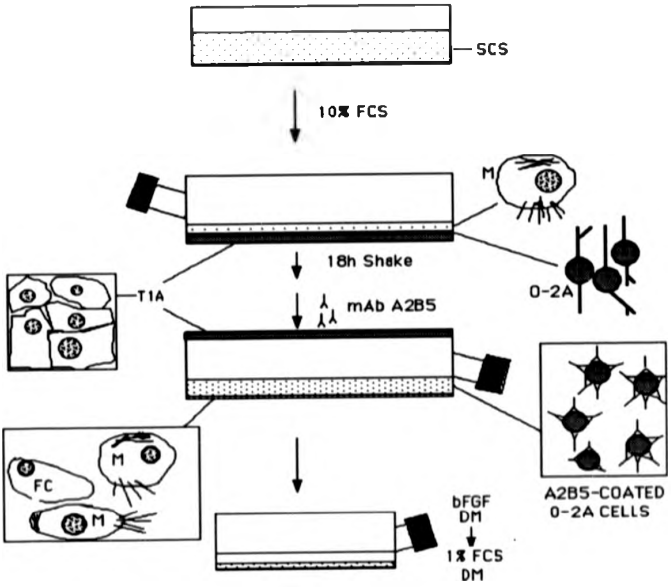

Fig. 10 The isolation of O-2A progenitors from mixed glial cultures and differentiation to the oligodendrocytic phenotype.

Cerebral hemispheres from neonatal rats were dissociated to single cells and plated in poly-D-lysine coated flasks in DMEM / 10% foetal calf serum (FCS). After 6-8d the base of the dish was covered by a layer of Type-1 astrocytes (T1A) and flat cells (FC), which were overlayed by process-bearing O-2A progenitors. Macrophages (M) did not adhere to the bilayer. Following overnight shaking, the O-2A cells had retracted their processes and detached. The mAb A2B5 was added to the medium and the flasks were inverted and incubated at 37°C for 20 min. FC and M adhered to the plastic while the A2B5-coated O-2As remained non-adherent. The O-2As were plated in defined medium containing basic fibroblast growth factor (bFGF). After four days the bFGF was replaced with 1% FCS.

2.3 Batch screening of foetal calf serum (FCS)

FCS from at least four different sources was screened at any one time. Two well characterized hybridoma cell lines with different growth characteristics (such as A2B5 and O1) were grown in parallel and the chosen sera were further tested with mixed and enriched glial cultures.

Sera were diluted to 10% (v/v) in Optimem-1, penicillin (100 IU/ml), streptomycin (100 µg/ml) and 100 µl aliquots were dispensed with a multiwell pipettor in 96-well tissue culture dishes. In order to adjust the pH, the dishes were placed in a 37°C incubator maintaining a 5% CO_2 humid atmosphere for 1 h.

The hybridomas were centrifuged at 200*g* for 10 min at room temperature, resuspended in medium minus serum, washed twice and resuspended in medium to a concentration of 10^5 cells ml^{-1}. 100 µl aliquots of the cell suspensions were added in each of the eight left hand side wells of the 96-well tissue culture dish, one cell line per duplicate plate. The cells were suspended to homogeneity, 100 µl aliquots were placed in the next set of wells and this was repeated, thus enabling 1:2 serial dilutions across the plate. The dilutions were confirmed by light microscopy and cell growth was assessed after 7, 10 and 14 days. Undiluted cells always grew vigorously whereas growth in wells with smaller cell numbers varied, presumably depending on the ability of the individual batch of serum to support it. Sera were initially chosen according to their ability to support as few as 20-100 cells per well and the final choice depended on the growth of mixed glial and enriched differentiating O-2A cell cultures.

2.4 Indirect immunofluorescence

All procedures took place at room temperature. In order to detect surface antigens antibodies were diluted in PBS pH7.4 containing 2% (v/v) goat serum (SAPU) and applied to living cells by inverting the coverslip on 30µl of antibody for 30 min in a humid chamber. For detection of cytoskeletal antigens the cells were extracted for 3 min by mild shaking in a buffer containing 10 mM Pipes pH 6.9, 50 mM KCl, 2 mM EGTA, 1 mM $MgCl_2$, 2 M glycerol, 10 µg/ml leupeptin, 10 µg/ml antipain and 0.5% (v/v) Triton X-100 (Wilson and Brophy, 1989).

Cells and cell cytoskeletons were fixed with 4% (w/v) paraformaldehyde (Sigma) in PBS for 20 min at room temperature, quenched with 0.1 M Glycine in PBS for 2x10 min and non-extracted cells were permeabilized with 0.1% (v/v) Triton X-100 in PBS for 5 min. Non-specific binding was blocked with 0.2% (w/v) pig skin gelatin (BDH) in PBS for an hour.

The cells were incubated with primary antibodies in PBS/gelatin / 2% goat or donkey serum (depending on the source of the secondary antibodies) for 30 min. After washing several times over 20 min with blocking buffer, the antigens were stained for 30 min with appropriate secondary fluorescent antibody conjugates (FITC, TRITC or DTAF) in PBS/10% goat or donkey serum in darkness. The coverslips were washed several times with blocking buffer and finally with PBS and then mounted on glass slides in either 90% glycerol, 10% PBS, 0.1% 1,4-phenylenediamine (Aldrich) or anti-fade 1 (AF1, Citifluor Ltd, UK). Fluorescence was viewed using x40 or x63 objectives on a Zeiss Universal microscope equipped with phase-contrast and epifluorescence optics and Kodak T-Max (400 ASA) film was used for all photomicrography.

2.5 Incubations with antisense oligonucleotides

O-2A progenitors were permitted to differentiate for 6 d after which the coverslips were placed in 24 x 16mm well tissue culture dishes and washed twice with DMEM prewarmed to 37°C. Sense or antisense oligonucleotides were added to the cultures at a final concentration of 50 µM in DMEM without FCS and control cultures were incubated in medium without oligonucleotides. Two HPLC-purified oligonucleotides (5'-TGA AGA GAG TCC GAA CTC-3' and 5'-ACC ACC ACG GTC GCC ATC CT-3') which are complementary to murine MAP1B mRNA (Noble, et al., 1989) at nucleotide positions -31 to -14 and -3 to +17 respectively as well as their corresponding sense oligonucleotides were purchased from the Oswel DNA Service, Department of Chemistry, University of Edinburgh. The coverslips were processed for immunofluorescence after 5 h of incubation with the sense or antisense oligonucleotides.

2.6 Fluorescent lipids

I. Preparation of C_6-NBD-Cer and C_5-DMB-Cer / BSA complexes

A modification of the method of Pagano & Martin (1988) was used. Preparation of lipid-protein complexes and all subsequent procedures took place in complete darkness. A 50 nmol aliquot of C_6-NBD- or C_5-DMB-Cer (Molecular Probes Inc. Eugene, USA) in chloroform / methanol 1:1 (v/v) was dried with N_2 followed by at least 2 h of desiccation. The lipid was dissolved in 200 µl ethanol and injected into 10 ml of Optimem I, defatted bovine serum albumin (DF-BSA, 3.4 mg/l) and sodium bicarbonate (2g/l) while vortexing. This solution was dialyzed overnight at 4°C against DMEM, 4mM HEPES, pH 7.4, aliquoted into eppendorf tubes and stored at -20°C for up to three months. The resultant C_6-NBD- or C_5-DMB-Cer / BSA complexes had a final concentration of 5 µM both in fluorescent lipid and DF-BSA. Fluorescent lipid was extracted every four to five weeks and was compared against non-complexed standards by thin layer chromatography (TLC, see under Lipid analysis).

II. Incubations with C_6-NBD- or C_5-DMB-Cer / BSA complexes

a) Live cells

Cells grown on coverslips in 35mm dishes were washed with pre-warmed DMEM and incubated at 37°C with 1 ml of 5µM C_6-NBD- or C_5-DMB-Cer/BSA complexes for 15 min. The cells were washed and either fixed and quenched immediately or further incubated for various periods of time and subsequently fixed and quenched (see Immunofluorescence). BFA (Epicentre Technologies, Madison, WI, USA or SIGMA) was prepared as a 10,000x stock solution in either methanol or ethanol and used at 1 µg/ml (3.6 nM) final concentration. Methyl(5(2-thienylcarbonyl)-1H-benzimidazol-2-yl)carbamate (nocodazole, SIGMA), was dissolved in DMSO and was used at 10 µg/ml (33mM) final concentration. Controls for BFA and nocodazole experiments included samples incubated in medium as well as samples incubated in medium containing the same volumes of methanol, ethanol or DMSO as BFA- or nocodazole- treated cells.

When an intracellular antibody was to be used in conjunction with fluorescent-lipid labeled cells, fixed cells were inverted on a drop of medium or PBS, viewed and photographed. Lipid was then extracted with methanol pre-cooled to -20°C for 10s and indirect

immunofluorescence was as for permeabilized cells.

We discovered that the fluorescent properties of NBD-lipids permitted initial labeling of cellular compartments, followed by surface labeling with an antibody recognising surface antigens of oligodendroglia (such as GalC) and anti-GalC-TRITC. After NBD-lipid incubation at 37°C, the cells were lightly fixed with paraformaldehyde for 7 min, quenched, washed with PBS and surface labeled in the usual fashion. This fluorescent lipid analogue / antibody double labeling technique is of potential use for the detection of intracellular compartments in cell types which can be identified unambiguously via their expression of specific surface antigens; however, DMB-lipids cannot be used, as the latter fluoresce strongly in both green and red channels.

b) Fixed cells

Cells were fixed in 0.5% (v/v) glutaraldehyde / 10% (w/v) sucrose / 100mM PIPES, pH7 for 30 min at room temperature, quenched 3x5 min with 0.5 mg/ml freshly prepared $NaBH_4$ in ice-cold PBS, pH 7.4 and rinsed several times over 10 min in cold PBS. The cells were subsequently incubated with 5μM C_6-NBD-Cer or C_5-DMB-Cer/BSA complexes for 30 min at 2°C, washed with DMEM and back-exchanged with 5μM DF-BSA in Optimem-I for 4x30 min at room temperature, in order to remove fluorescent sphingolipids from the lumenal leaflet of the plasma membrane (Lipsky and Pagano, 1985; van Meer et al., 1987). The cells were finally washed with PBS and mounted in the usual fashion.

2.7 Iodination of transferrin and measurement of exocytosis in oligodendrocytes

Transferrin (Tf) was radioiodinated by a modification of the method described by Woodman and Warren (1989): 20μl of a 0.5mg/ml solution of 1,3,4,6-tetrachloro-3α,6α-diphenylglycoluril (Iodogen, Pierce Chemical Co., Rockford, IL, USA) in chloroform was evaporated slowly in a glass tube using nitrogen, ensuring that the glassware was evenly coated. Twenty ml of a 2.5mg/ml solution of human holotransferrin (SIGMA) in 100mM sodium phosphate, pH 7.4 and 1 mCi (20μl) $Na^{125}I$ (16 mCi/μg) were added sequentially and the mixture was incubated on ice for 15 min. The reaction was stopped by diluting with 200μl of the phosphate buffer and the protein was separated from free iodine on a 10ml Sephadex G-50 column run in phosphate buffer. The peak (which was approximately

equivalent to the void volume) was dialyzed overnight against 200 volumes of PBS at 4°C and the specific radioactivity was measured in a Packard gamma-counter and was approximately $6x10^6$ dpm/µg of Tf.

Oligodendrocytes grown in 35mm dishes and permitted to differentiate for six days after the removal of bFGF were washed 2x with Tf-free RPMI (Gibco, BRL) and incubated in RPMI ± 1µg/ml BFA at 37°C for 2 h. The cells were washed and incubated in RPMI (± BFA) in the presence of 3.5µg ^{125}I-Tf for 1 h. In order to demonstrate that the binding of ^{125}I-Tf to receptors was specific, a 100-fold excess of non-iodinated Tf was added in control cells. The oligodendrocytes were washed with RPMI at 4°C and warmed to 37°C for specific times. The cells were finally washed in PBS, solubilized in 1M NaOH and the radioactivity was counted as before.

2.8 Preparation of 6nm gold / BSA complexes

All procedures took place in a darkened room. A colloidal gold suspension with mean particle size of approximately 6nm was prepared by heating 150µl tannic acid (10mg/ml) / 4.0 ml sodium citrate (10mg/ml) / 15.9 ml Milli-Q water in a 50 ml beaker and 200µl of $HAuCl_4$ (50mg / ml of Milli-Q water) / 80 ml Milli-Q water in a 250 ml beaker to 60°C for 15 min. The two solutions were combined with stirring and the suspension was allowed to cool slowly.

Seven ml of 0.2M sodium phosphate, pH 6.1 were added in a bolus to 63 ml of the colloidal gold solution at 4°C. Sixty-five ml of this suspension were added to 0.5 ml of 1mg/ml BSA in 0.1M sodium phosphate, pH 6.1. The mixture was centrifuged at 50,000*g* for 45 min at 4°C and the pellet was resuspended in 2 ml of PBS. A 1/20 dilution of the sample in PBS yielded an A_{520} of 0.15.

2.9 Electron microscopy

O-2A progenitors were seeded on poly-D-lysine coated 1cm^2 aclar squares (Allied Chem. Corp.) in 35mm dishes and allowed to differentiate to oligodendrocytes for six d following the removal of bFGF. Protocols a) and b) were subsequently carried out by Ms. Diane Sherman, who also prepared and examined the sections from cells in procedure c). All solutions were prepared using Milli-Q water, the experiments were performed at room temperature and

washes were for 5 min unless otherwise specified.

I. Localization of MBP and MAP1B in oligodendrocytes.

The cells were fixed for 1.5 h in 4% (w/v) paraformaldehyde, 0.1% (v/v) glutaraldehyde, 0.5 mM $CaCl_2$ in 0.1 M sodium phosphate pH 7.4 (all from Sigma). After washing the cells several times in the same buffer with 3.5% sucrose in the absence of fixatives (Buffer A), the aldehydes were quenched with 50 mM NH_4Cl in Buffer A and rinsed again in several changes of Buffer A. The squares were washed in 0.1 M sodium maleate pH 6.5 containing 3.5% sucrose (Buffer B) and post-fixed for 1 h at 4°C with 2% uranyl acetate in Buffer B adjusted to pH 6.0. The cells were dehydrated through a graded series of ethanol and infiltrated overnight at 4°C with a 1:1 ratio of LR White (Agar Scientific, UK) and ethanol, followed by two changes of LR White over 2-4 h. The cells were embedded by inverting the square on a well (made by punching out the center of a second square) filled with fresh LR White and polymerized in a N_2 atmosphere at 52°C for 24 h. Sections on formvar- and carbon-coated nickel grids were blocked with 1% BSA, 0.5% fish gelatin, 0.1% Triton X-100 in Buffer C (20 mM Tris, 200 mM NaCl, 3 mM NaN_3, pH 7.4) for 1 h and incubated with mouse anti-MAP1B and rabbit anti-MBP in Buffer D (which comprised Buffer C with 0.2% BSA, 0.5% fish gelatin and 0.1% Triton X-100) for 3 h. Grids were washed three times with Buffer D then incubated for 3 h with goat anti-mouse IgG and IgM conjugated to 5 nm gold together with goat anti-rabbit IgG conjugated to 10nm gold in Buffer D. After washing with Milli-Q water the sections were fixed in 2.5% glutaraldehyde for 5 min, rinsed in distilled water, dried and stained with 5% uranyl acetate and lead citrate. Sections were examined on a Jeol 100 CX transmission electron microscope.

II. Immunoperoxidase staining of the TGN

Cells were washed briefly with DMEM / 1% FCS and fixed with 4% (w/v) paraformaldehyde and 0.1% (v/v) glutaraldehyde in 0.1 M sodium phosphate buffer, pH 7.4 for 1 h. The cultures were briefly washed twice in 0.1 M phosphate buffer, quenched 3x10 min with 50 mM NH_4Cl in sodium phosphate and washed in PBS. The cells were then permeabilized by incubating with 0.05% (w/v) saponin in PBS for 5 min and non-specific antibody binding was

blocked by incubating in 1% (w/v) BSA and 0.05 (w/v) saponin in PBS (Buffer A) for 20 min. The cells were incubated with anti-TGN38 in Buffer B (i.e. Buffer A in which the concentration of BSA was decreased to 0.3%) for 2 h by inverting the aclar square on 100µl of antibody. The squares were washed three times in buffer B and the cells were incubated with goat anti-rabbit IgG peroxidase conjugate in buffer B for 1.5 hours, washed twice in buffer B and twice in PBS. The tissue was fixed in 1.5% (v/v) glutaraldehyde, 5% (w/v) sucrose, 0.1 M sodium cacodylate, pH 7.4 (Buffer C) for 30 min, washed three times in Buffer D (i.e. Buffer C containing 7.5% sucrose) and rinsed three times in 7.5% (w/v) sucrose, 50 mMTris/HCl pH 7.4 (Buffer E). DAB pH 7.4 (0.2% w/v in Buffer E) was filter sterilized with a 20 µl Millipore filter and added at 1 ml per petri dish for 1 min; 1 µl volumes of 3% (v/v) H_2O_2 were added sequentially to this solution over a five minute period and this was repeated three times. The reaction was stopped after 15 min by washing twice in buffer E. The cells were rinsed in Buffer C minus sucrose (Buffer F) and postfixed in 1% (v/v) OsO_4, 1% (w/v) potassium ferrocyanide in buffer F for an hour at 4°C. The discs were dehydrated in absolute ethanol, infiltrated and embedded in Epon 812 (Taab). Sections were examined on a JEOL 100 CX electron microscope.

III. Detection of fluorescent lipids.

Oligodendrocytes were washed with DMEM prewarmed to 37°C and after adding 1ml of 5 µM C_6-NBD-Cer or 5 µM C_5-DMB-Cer / DF-BSA complexes the cells were incubated at 37°C for several periods of time. On some occasions, control cultures and cells treated with BFA were incubated (in the continued presence of BFA) for 5 min with a 1/20 dilution of 8nm gold / BSA complexes in DMEM with supplements, washed and incubated for 15 min with C_6-NBD-Cer / DF-BSA complexes.

The cells were fixed in 1% (v/v) glutaraldehyde in 0.1M sodium phosphate, pH 7.4 for 30 min and washed with 0.1M Tris, pH 8.2 at 4°C. The cells were then warmed to room temperature while incubating with DAB (1.5 mg/ml in Tris, pH 8.2) for 10 min and the DAB solution was replenished and volume adjusted to 1 ml. Small areas on the aclar square were irradiated by focusing the blue beam (λ_{ex}.470nm) of either a Zeiss universal microscope through a 16x (numerical apperture 0.4) lens for 50 min or the 20x (numerical apperture 0.7)

lens of an Olympus BH-2 microscope for 30 min at room temperature. Although some of these procedures were modifications of the method used by Pagano et al., (1989) they differed in principle in that in our experiments the cellular compartments of live cells had been labeled with fluorescent lipid pre-fixation. The cells were washed with 0.1M sodium cacodylate, pH7.4, post-fixed with 1% (w/v) OsO_4, 0.1M sodium cacodylate, 1% (w/v) potassium ferrocyanide for 1 h and washed extensively with sodium cacodylate buffer. The cells were successively dehydrated for 10 min periods in 50, 70 and 90% (v/v) ethanol / water and for 2x10 min in absolute ethanol. Infiltration in epoxy resin (Taab) was by shaking mildly with resin / absolute ethanol 1:1 (v/v) for 1 h followed by two changes of undiluted resin for half hour. Following removal of excess resin the aclar squares were inverted on 100 µl of embedding medium and polymerized at 60°C for 18 h. Sections were examined as before.

2.10 Protein estimation

Protein content was routinely determined by a modification of the method of Lowry et al., (1951) and included SDS to solubilize membrane proteins. All tests were carried out in duplicate. 250µl of 1M NaOH, 0.25% (w/v) SDS was added to samples made up to 200 µl with distilled water as well as standards containing 10-120 µg of BSA (Fraction V, Sigma) and these were incubated at 60°C for 15 min. Then, 0.5 ml of 2% (w/v) Na,K Tartarate, 0.5 ml of 1% (w/v) $CuSO_4$ and 0.5 ml of 2% (w/v) Na_2CO_3 were added sequentially and with mixing and the samples were incubated for 15 min at room temperature. Folin-Ciacolteau reagent (BDH) was freshly diluted 1:1 with double distilled water, 250 µl were added to the samples and the OD_{750} was measured after a 45 min incubation.

2.11 Myelin

I. Isolation

This procedure is a modification of the method of Norton and Poduslo (1973) and takes advantage of the low buoyant density of myelin. Brains or peripheral nerve (sciatic or trigeminal) were removed from 3-4 week old Wistar rats of both sexes that had been killed by asphyxiation followed by decapitation. Brains from hemizygous males and homozygous

females from rumpshaker (*rsh*)and wild type (of the same genetic background as *rsh*) mice were prepared similarly. The tissue was frozen in liquid N_2 and was either used immediately or stored for up to six months at -80°C.

All subsequent procedures were performed under sterile conditions at 4°C. The brains were homogenized to 5% (w/v) final concentration in 0.85 M sucrose, 10 mM N-2-hydroxyethylpiperazine- N'-2-ethanesulphonic acid (Hepes), pH 7.4, 3 mM dithiothreitol (DTT), 1 mM tosyl-lysyl-chloromethyl-ketone (TLCK) using a Potter-Elvehjem glass homogeniser (Orme Scientific, Man. U.K.). PNS tissue was initially ground to a fine powder in a mortar in liquid N_2 and was homogenised in a fashion similar to CNS tissue with the exception that the 0.85M solution was further supplemented with 0.5 mg/ml phenylmethylsulphonyl fluoride (PMSF), 0.01 mg/ml leupeptin, 0.01 mg/ml chymostatin, 0.01 mg/ml antipain, 0.01 mg/ml pepstatin-A, 10 mM benzamidine, 1 mM ethylenediaminetetraacetic acid (EDTA) pH 8.0, 1 mM ethylene glycol-bis (β-aminoethyl ether) N',N,N'N'-tetraacetic acid (EGTA), pH7.4 and 0.01% (w/v) NaN_3.

The CNS tissue homogenate was adjusted to 40 ml in polycarbonate tubes and overlaid with 10 ml of 0.25 M sucrose, 10 mM Hepes, pH7.4, 3 mM DTT and 1 mM TLCK; PNS homogenate was overlaid with this solution which additionally contained protease inhibitors to concentrations identical to the 0.85M sucrose PNS homogenisation buffer. Density-gradient centrifugation was at 70,000*g* for 90 min in an MSE 3x70 swing-out rotor.

The membrane was removed from the 0.85 / 0.25M sucrose interface and subjected to hypo-osmotic shock by either resuspending in 10 vol Milli-Q water, 1mM TLCK (CNS myelin) or shocking solution further supplemented with the protease inhibitors of the 0.85M PNS homogenisation buffer to one tenth final concentration (PNS myelin).

The membrane was recovered by centrifugation at 23,000*g* for 30 min at 4°C in a Sorvall SA600 rotor. The shock procedure was repeated at least twice or until the supernatant was clear. Purified myelin was resuspended in a small volume of Milli-Q water and used immediately or aliquoted and stored at -40°C.

II. Protein phosphorylation

Myelin proteins were analyzed for cAMP-dependent and -independent phosphorylation by a

modification of the method of Bradbury et al., (1984). Thirty µg of myelin protein were diluted in 1mM $MgCl_2$, 0.02% (v/v) Triton X-100, 60µM ATP, 10µM of 0.5-3.0 Ci/mmol γ-^{32}P-ATP (Amersham, U.K), 45mM Tris/HCl, pH7.4 in a total volume of 55 µl by initially preparing a cocktail of $MgCl_2$, Tris/HCl and Triton X-100 to which the ATPs were added. The procedure was carried out in a hood suitably adapted for the use and disposal of radioactive isotopes and the mixture was allowed to equilibrate at room temperature for 1 min. The reaction was started by adding myelin and vortexing and was carried out at 37°C for 8 min in the presence or absence of 7µM cAMP. The reaction mixture was centrifuged at 4°C for 20 min and the supernatant was removed by aspiration. Phosphorylated myelin samples or Triton X-100-soluble and -insoluble fractions prepared after phosphorylation were subjected to SDS-PAGE. The gels were either stained with PAGE blue and dried under vacuum or electrotransferred to nitrocellulose for Western blotting.

iii. Protein deglycosylation

Myelin (30 µg protein) or the equivalent Triton X-100-soluble and -insoluble fractions were made up to 20 µl in 1% (w/v) SDS, 1 % (v/v) β-mercaptoethanol and boiled for 2.5 min. The samples were allowed to cool and diluted to a final volume of 98 µl in 2mM EDTA, 1% (v/v) Nonidet P40 and 0.1% (w/v) sodium phosphate, pH 6.3. Endoglycosidase-F (0.05 units, 1unit of activity per 20 µl) (Boehringer Manheim) was added and the samples were vortexed and incubated for 5 h at room temperature. Another 0.05 units endoglycosidase-F were added and the samples were incubated for a further 18 h.

iv. Extraction with non-ionic detergent

Myelin was aliquoted in eppendorf tubes and centrifuged at 13,000*g* for 30 min at 4°C in an MSE-Microcentaur microfuge. The water was removed by aspiration and the pellet was resuspended in filter-sterilized cytoskeleton (CSK) buffer (Gillespie et al., 1989) to a concentration of 1 mg/ml. This buffer was similar to the cell extraction buffer (previously mentioned under Indirect Immunofluorescence) with the exception that for myelin extraction the concentration of KCl was 100mM instead of 50mM.

Following a 5 min incubation at room temperature, the sample was centrifuged, the

supernatant (soluble fraction) was retained and the procedure was repeated. The pellet was resuspended in Milli-Q water to the same volume of the combined soluble fractions. The Triton X-100-soluble and -insoluble fractions were either used immediately or aliquoted and frozen at -20°C.

2.12 Protein detection

I. Sodium dodecyl sulphate polyacrylamide gel electrophoresis (SDS-PAGE)

Proteins were separated by SDS-PAGE on 5-17% slab gels using the discontinuous system of Laemmli (1970). Samples were boiled for 2.5 min in a buffer containing 2.5% (w/v) SDS, 125 mM DTT, 0.001% (w/v) bromophenol blue and 20% (v/v) glycerol. Electrophoresis was for 16-18 hours at 5 mA in a running buffer consisting of 0.03% (w/v) Tris[hydroxymethyl]aminomethane, 0.12% (w/v) glycine. Proteins separated according to size could be visualized by immersing the whole gel or a strip in 0.001% (w/v) PAGE blue (BDH) in 20% (v/v) methanol, 10% acetic acid (v/v) for 2-3 h.

II. Western blotting

Proteins separated by SDS-PAGE were electrotransferred to 0.45µm pore nitrocellulose paper (Schleicher and Schuell, Anderman Ltd) at 0.25A for 3 hours by the method of Towbin et al., (1979) in a Transblot apparatus (Biorad Laboratories, U. K.). The efficiency of transfer was assessed by staining nitrocellulose strips with 0.2% (w/v) Amido Black in 25% (v/v) methanol, 10% (v/v) acetic acid for 10 s and rinsing with solvent. Residual protein on the gels was visualized by staining with PAGE blue.

For immunoblotting all incubations were at room temperature and washes were for 5 min with mild shaking. Non-specific binding to nitrocellulose was blocked by incubating with 0.2% (w/v) pig skin gelatin, 0.1% (v/v) Triton X-100 in PBS, pH 7.4 (Buffer I) for 3 h and the blots were further incubated in Buffer I containing the appropriate dilution of primary antibody for 1 h. The blots were rinsed several times over 30 min with Buffer I and incubated with either goat anti-rabbit IgG or goat anti-mouse IgG (depending on the source of the primary antibody) conjugated to horseradish peroxidase for 1 h. After washing several times in Buffer I, twice in Buffer I minus Triton X-100 and once in PBS, immunostained proteins were

detected using 0.5 mg/ml DAB in Tris/HCl, pH 7.6 and 1µl of 30% (v/v) H_2O_2 per ml of DAB solution as substrates. The reaction was terminated with 2% SDS and the DAB solution was neutralized with bleach prior to disposal.

2.13 LIPID ANALYSIS

I. Lipid extraction

Lipid was extracted in glass stoppered tubes by the method of Bligh and Dyer (1959). Five ml of chloroform / methanol / β-hydroxytoluene (BHT) (2:1:0.05, v/v/w) were added to each mg of protein (myelin, Triton X-100-insoluble pellet or cell protein) suspended in 200 µl distilled water. The sample was vortexed, extracted for 10 min at room temperature and 0.2 volumes of 0.1M KCl were added with vigorous vortexing. The suspension was centrifuged at 1000*g* for 10 min at room temperature and the lower phase was carefully removed with a Pasteur pipette and placed in a conical glass tube with an equal vol. of 0.1M KCl / CH_3OH 1:1 (v/v). The suspension was vortexed and centrifuged as before, the lower layer was uptaken and passed through 3MM filter paper (Whatman) in pre-weighed glass storage conical vials and the solvent was evaporated with N_2 and immersion in warm water. The lipid was desiccated in darkness overnight, weighed and resuspended in chloroform / methanol 1:1 (v/v) containing BHT, gassed with N_2 and stored at -20°C in darkness for up to six months.

II. Lipid class analysis

a) Phospholipid

The Eng and Noble (1968) method was used to measure total phospholipid as well as phospholipid classes. This method takes advantage of the reaction of inorganic phosphate with ammonium molybdate to form phosphomolybdic acid which is reduced and the product is determined spectrophotometrically.

Individual phospholipid classes were separated by streaking 500-1,000 nmoles phospholipid on 20 cm^2 60 Kieselgel high performance TLC (HPTLC) plates (Merck, W. Germany) which had been pre-developed with chloroform / methanol, (1:1, v/v), air dried,

pre-developed with hexane / diethyl ether / acetic acid (85:15:1.5, v/v) and activated at 100°C for 15 min. The plates were developed in methyl acetate / propan-2-ol / chloroform / methanol / 0.025% w/v KCl (25:25:25:10:9) and individual phospholipid classes were identified by their co-migration with commercially purchased standards (Sigma) and with the components of a well characterized rat myelin lipid standard (Gillespie et al., 1989). Total myelin lipid, phospholipids scraped together with silica from HPTLC plates and standards (0-400 nmoles KH_2PO_4) were pipetted in thick-walled test tubes which had been washed by overnight immersion in chromic acid. The organic solvents were evaporated at 100° C in a fume hood; 0.65ml of 70% (v/v) perchloric acid was added and the tubes were stoppered with glass marbles and heated to 180° C for at least 3 h until the samples were clear of color. The volumes were made up to 3.3 ml with distilled water before adding 0.5 ml of 2% (w/v) ammonium molybdate and 0.5 ml of freshly made 10% (w/v) ascorbic acid and the samples were mixed by vortexing. The tubes were heated for 5 min in a boiling water bath, allowed to cool and, after the silica had been pelleted at 1,000*g* for 10 min, the A_{800} was measured. The graph slope was linear and 400nm phosphate yielded an average A_{800}~1.9.

b) Sulfatides

The method of Kean (1968) was employed, this exploits the ability of lipid sulfates to form colored azure A complexes that are extractable into chloroform/methanol solutions. Samples and commercially purchased standards ranging from 0-35 nmoles were placed in stoppered glass tubes. After evaporating to dryness by heating at 100°C, 5 ml chloroform/methanol (1:1, v/v), 5 ml of 25µM H_2SO_4 and 5ml Azure-A dye solution (0.004% w/v Azure-A in 2.5µM H_2SO_4, stored at room temperature in darkness for up to a week) were added. The tubes were stoppered, shaken for 30 s, centrifuged at 1000*g* for 5 min at room temperature and the A_{645} was measured; 25 nmoles of sulfatide yielded an A_{645}~0.65.

c) Cerebrosides

The method of Macala et al. (1983) was employed. Samples, hydroxy and non-hydroxy cerebroside standards (0-6 nmoles) were spotted over 0.5 cm on pre-washed HPTLC plates. Development was in methyl acetate / propan-2-ol / chloroform / methanol / 0.2% (w/v) KCl (25:25:25:10:9, v/v/v/v/v) until the solvent front reached the upper limit of the plate. After evaporating the solvents by vacuum desiccation over 3 h, the plates were sprayed with 3%

(w/v) cupric acetate and 8% (w/v) phosphoric acid. The plates were then air dried and charred by baking at 160°C for 15 min. Cerebrosides were quantified by densitometry using a Shimadzu CS-9000 dual wavelength flying spot TLC scanner and a DR-13 recording integrator. This method could also be adapted for the quantification of other lipid classes.

d) Cholesterol

The chemical method of Sperry & Brand (1943) which is based on the Liebermann-Burchard reaction was employed. Five ml of acid-free chloroform was added to dried lipid samples or standards (0-700 nmoles) in glass stoppered tubes. The tubes were equilibrated in a water bath at 24°C and, following the addition of 2 ml of cold acetic anhydride reagent (20 ml acetic anhydride and 1 ml of concentrated H_2SO_4 incubated on ice for 9 min) were shaken vigorously and incubated for a further 20 min in darkness. The A_{640} was read, the graph slope was linear and 700 nmoles cholesterol yielded an A_{640}~0.18.

III. Fatty acid analysis

Total lipid or lipid classes that had been separated by TLC using methyl acetate, propan-2-ol / chloroform / methanol / 0.2% (w/v) KCl (25:25:25:10:9 v/v/v/v/v) were subjected to acid-catalyzed transmethylation (Christie, 1982). Polar lipid classes identified against commercial standards by lightly spraying the TLC plate with 2',2'-dichlorofluorescein (DCF) were scraped off and transmethylated directly on silica. One ml of hexane and 2.5 ml of methanol containing 1% (v/v) concentrated H_2SO_4 were added to a maximum of 1 mg of dried lipid in a glass stoppered tube. The mixture was vortexed, gassed with N_2 and, by ventilating the stopper with a small piece of paper, heated at 50°C overnight.

Methyl esters were extracted from the transmethylation mixture by adding 5ml hexane/diethyl ether 1:1 (v/v) and 2.5 ml distilled water, vortexing, centrifuging at 1000*g* for 5 min at room temperature and taking the upper layer into a clean tube. This was repeated and the extracts were pooled. After addition of 2.5 ml of 2% (w/v) $KHCO_3$ the tubes were vortexed, centrifuged and the upper layer was dried with N_2 and resuspended in hexane. The methyl esters were further purified by TLC using hexane / diethyl ether / concentrated acetic acid (90:10:1, v/v/v) as the developing solvent. They were then redissolved in hexane containing 0.05% (w/v) BHT and analysed on a Packard 436 gas chromatography by using

on-column injection. The carrier gas was H_2 and the thermal gradient ranged from 50-235°C. Individual methyl esters were identified by comparison with well characterized fish oil methyl ester standards (Bell et al., 1983).

iv. Fluorescent lipid analysis

Cells of the O-2A lineage were grown in plastic 25cm^2 or 75 cm^2 flasks to developmental stages that had been previously characterized in terms of morphology and the time of appearance of myelin-specific antigens. The cells were washed twice with pre-warmed defined medium (see Cell Culture) without FCS and incubated with 5mM C_6-NBD- or C_5-DMB-Cer / BSA complexes (3ml fluorescent lipid/BSA complex solution per 75cm^2 flask containing approximately 10^7 cells or one ml per 25cm^2 flask containing $3.3x10^6$ cells) for 15 min at 37° C. The cells were washed twice with warm medium and incubated in medium without fluorescent lipid precursors for a total of 2 h. The cells were removed from the flasks using a rubber policeman, pelleted at 10,000*g* for 10 min and total lipid was extracted. Equal amounts of fluorescence were applied to HPTLC plates and these were developed with methyl acetate / propan-2-ol / chloroform / methanol / 0.25% w/v KCl (25:25:25:10:9, v/v) (solvent 1).

The fluorescent lipid metabolites C_6-NBD-SM, C_5-DMB-SM, C_6-NBD-GlcCer, C_6-NBD-GalCer and C_5-DMB-GlcCer were identified by comparison with authentic standards, which were the generous gifts of Dr Richard Pagano. Fluorescent spots were scraped from the TLC plates, dissolved in chloroform:methanol 2:1 (v/v) and quantified by spectrofluorimetry with a Perkin Elmer LS50 luminescence spectrometer equipped with Fluorescence Data Manager software in the Scan mode, using λ_{ex}470nm and λ_{em}530nm, slit width of 10nm and integration time of 10s. For quantitative measurements, known molar quantities of standards were treated identically to metabolized lipid.

Total fluorescent cerebrosides were resolved in the gluco- and galacto-forms on borate-treated HPTLC plates. These plates were pre-washed in the usual manner (see under phospholipid), immersed in 1.2% (w/v) analar quality boric acid (BDH) in Milli-Q water / ethanol (1:1, v/v) overnight, air dried and activated for 10 min at 100°C. The plates were developed in chloroform / methanol / water / ammonia (72:48:9:2, v/v) (solvent 2) and the

fluorescent cerebrosides were quantitated as before.

Since no standard was available for C_5-DMB-GalCer, this minor metabolite was tentatively identified by its R_f value (smaller than the R_f value of C_5-DMB-GlcCer), by either spraying plates with orcinol / sulfuric acid which recognizes carbohydrates, or periodate-Schiff's reagent which identifies vicinal diols (Christie, 1973). Developed borate-treated TLC plates were lightly sprayed with orcinol (2 mg/ml) in 75% sulfuric acid and heated for 15 min at 100°C. Carbohydrate-containing lipids appeared as blue-violet spots. Alternatively, the plates were sprayed with 2% (w/v) sodium periodate and dried at 55°C, then sprayed with 2% (w/v) sodium bisulfate and dried; the last step was repeated until the iodine stain had disappeared, when the plate was cooled and sprayed with Schiff's reagent (pararosaniline chloride 1% w/v, sodium bisulfite 4% w/v in 0.25 M HCl) (Sigma). The plate was allowed to dry and developed at room temperature for at least six hours, after which sugar-containing lipids appeared as purple spots. The lipid identified as C_5-DMB-GalCer only reacted in tests that detected glycolipids; it was negative in the various other colorimetric tests for polar and non-polar lipids. The Rf values for the various sphingolipids are given in Table 3.

Table 3 The R_f values of various sphingolipids

R_f value	Endogenous lipid	C_6-NBD-lipid	C_5-DMB-lipid
a) Solvent 1			
Cer	0.88	0.84	0.88
GalC		0.80	0.84
Non-OH	0.85		
OH	0.78		
Glc	0.91	0.77	0.82*
SM1		0.07	0.07
SM2		0.05	
SM-A	0.13		
SM-B	0.11		
Solvent 2			
GlcC	0.76	0.73	0.76
GalC		0.53	0.64*
Non-OH	0.70		
OH	0.50		

Solvent 1, Solvent 2: see Text

*: Tentative identification

SM1, SM2 and SM-A, SM-B: Sphingomyelin with either N-acyl sphingosine (SM1, SM-A) or dihydrosphingosine (sphinganine) (SM2, SM-B) backbone. The R_f values of SM1 and SM2 corresponded to those of stereoisomers of C_5-DMB-SM. These idendtifications were also tentative.

Establishment and characterization of a primary culture system for glia of the O-2A lineage derived from brain

3.1 Introduction

The analysis of cell lineage during development in the mammalian CNS has been facilitated by methods that identify, isolate and manipulate specific cell types under defined culture conditions. Such approaches were initially used to isolate and characterize the O-2A progenitor cell that can, under appropriate conditions, give rise to oligodendrocytes or Type-2 astrocytes (for review see Raff, 1989). A ligand produced by Type-1 astrocytes and identified as the A-chain of PDGF (Richardson et al., 1988) is mitogenic for optic nerve O-2A progenitor cells (Noble et al., 1988). Raff et al., (1988) have proposed that PDGF drives a "clock" that counts cell divisions and regulates the timing of oligodendrocyte development in culture.

Several other polypeptide growth factors have been shown to influence oligodendroglial development in culture, including insulin-like growth factor (McMorris and Dubois-Dalcq, 1988), epidermal growth factor (EGF) (Sheng et al., 1989) and bFGF (Besnard et al., 1989). Since bFGF is present in brain during development (Gonzalez et al., 1990), it is possible that this polypeptide may have a role in gliogenesis. The continued presence of bFGF can maintain a high rate of mitosis and block differentiation in O-2A progenitors grown in culture and this mitogen also increases the sensitivity of O-2A cells to PDGF by maintaining a high level of expression of PDGF α-receptors (McKinnon et al., 1990). Louis et al., (1992) have recently shown that the combined use of bFGF and PDGF can stimulate prolonged division of O-2A cells from cerebral cortex, as had previously been shown for O-2A progenitors from optic nerve (Bögler et al., 1990).

Preferential differentiation of O-2A cells to oligodendrocytes was achieved for cells grown to high densities and was unrelated to the total number of cultured cells, whereas O-2A cells seeded at low densities differentiated to Type-2 astrocytes (Levi et al., 1991). Additionally, medium conditioned by high-density subcultures of O-2A cells contained high MW (>30 kDa) non-mitogenic factor(s) that were capable of inducing differentiation of O-2A cells to oligodendrocytes. Preferential differentiation of O-2A progenitors to oligodendrocytes occurred for cells seeded at either high or low densities. Such differentiation may be triggered by direct homotypic interactions and could be additionally dependent on the secretion of short range autocrine or paracrine factors by O-2A progenitors.

An enriched oligodendrocyte culture system with at least 60% purity had been previously characterized in our laboratory. Although this system had been useful for both immunocytochemical and biochemical analyses (Wilson and Brophy, 1989), an improved method was deemed necessary in order to:

a) increase the cell purity and yield

b) partially synchronize the cell population that is isolated during the initial enrichment from mixed glial cultures to the O-2A progenitor cell stage and

c) permit O-2A cell differentiation to oligodendrocytes in a sequential manner and characterize this progression by counting the cells that express well known markers of glial cell differentiation.

Although increased cell purity was desirable, high cell yields were essential considering that the proposed investigations included the use of a lipid analogue with low fluorescence yield (C_6-NBD-Cer) as well as analysis of oligodendroglial cytoskeletal lipid, which was expected to be a small proportion of the total cellular lipid. In the case of CNS myelin which, by comparison with oligodendrocytes, can be isolated at relatively high abundance, the lipid isolating with the cytoskeleton is approximately 12 mol% of the total membrane lipid (Gillespie et al., 1989).

The primary cell culture system that was eventually developed (see Materials and Methods) combined elements from the system of Wilson and Brophy, (1989) with more recent knowledge regarding the specifics of O-2A progenitor cell development in culture. Cells of the O-2A lineage were permitted to differentiate to oligodendrocytes and were characterized at specific developmental stages by indirect immunofluorescence using stage-specific antibodies. The successive morphologies of differentiating O-2A cells were used as rough guides prior to performing biochemical and immunocytochemical analyses and at least one previously characterized antigen of development was used as a control at all times.

3.2 Results

Isolation of O-2A progenitors and differentiation to oligodendrocytes

Dissociated cells from neonatal rat cortex were cultured in DMEM/10% FCS for 6-8 d as described in the Methods and Methods section and formed a bilayer consisting of small, phase-dark cells adhering to a basement of flat, lighter cells (Fig. *11A*). The dark cells were released by shaking the cultures overnight, the mAb A2B5 was introduced in the culture medium and O-2A progenitors (Fig. *11B*) were isolated by reverse panning and induced to divide with bFGF in defined, serum-free medium. O-2A progenitors from brain typically have a bi- or multi-polar morphology, which was also described by others (McKinnon et al., 1990; Louis et al., 1992). After four days in mitogen, the O-2A progenitors were allowed to differentiate in fresh medium where bFGF had been replaced by 1% FCS. Prooligodendrocytes ($O4^+$ $GalC^-$ cells) are larger than O-2A progenitors with wider, more extensive processes and the highest proportion of prooligodendrocytes was found 1-2 d after the removal of bFGF (Fig. *11C*). For most O-2A progenitors, terminal differentiation to oligodendrocytes ($GalC^+$ MBP^+ cells) required culturing for 6 d subsequent to the removal of bFGF. Oligodendrocytes have larger cell bodies than prooligodendrocytes and the thick, branching extensions of the former terminate in a meshwork of finer processes (Fig. *11D*).

The layer resulting after the removal of phase-dark cells (Fig. *11E*) consisted mainly Type-1 astrocytes (65±4% $A2B5^-$ $GFAP^+$) and unidentified cells (<1% $O4^+$ $GalC^+$ MBP^+). Cells adhering on plastic during reverse panning were incubated in DMEM / 1% FCS for 2 h (Fig. *11F*). Some of these cells were Type-2 astrocytes (14±2% $A2B5^+$ $GFAP^+$) and the rest were not identified (<1% $O4^+$ $GalC^+$ MBP^+).

O-2A progenitors differentiate to oligodendrocytes within 6 d in culture

Non-adherent (A2B5-coated) cells that were recovered by reverse panning were incubated in defined medium/1% FCS for 4 h, immunostained for the different antigens that mark the differentiation of O-2A progenitor cells to the oligodendrocytic phenotype and positive cells were counted. These cells were approximately 63% $A2B5^+$, 28% $O4^+$, 17% $O1^+$, 2% MBP^+ and 10% $GFAP^+$, i. e. mainly O-2A progenitors ($A2B5^+$ $GFAP^-$) with some prooligodendrocytes ($O4^+$ $GalC^-$), oligodendrocytes ($O4^+$ $GalC^+$) and astrocytes ($GFAP^+$).

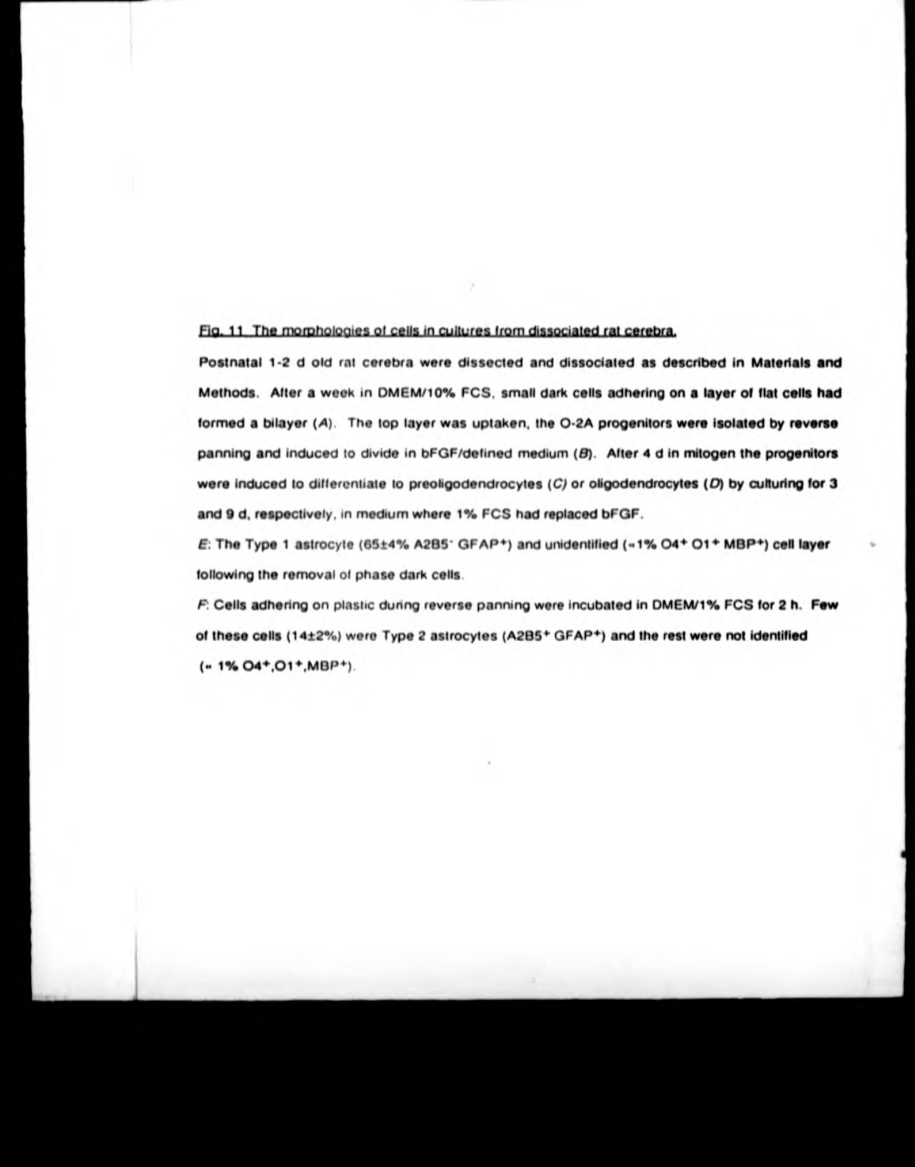

Fig. 11. The morphologies of cells in cultures from dissociated rat cerebra.

Postnatal 1-2 d old rat cerebra were dissected and dissociated as described in Materials and Methods. After a week in DMEM/10% FCS, small dark cells adhering on a layer of flat cells had formed a bilayer (*A*). The top layer was uptaken, the O-2A progenitors were isolated by reverse panning and induced to divide in bFGF/defined medium (*B*). After 4 d in mitogen the progenitors were induced to differentiate to preoligodendrocytes (*C*) or oligodendrocytes (*D*) by culturing for 3 and 9 d, respectively, in medium where 1% FCS had replaced bFGF.

E: The Type 1 astrocyte (65±4% $A2B5^-$ $GFAP^+$) and unidentified (≈1% $O4^+$ $O1^+$ MBP^+) cell layer following the removal of phase dark cells.

F: Cells adhering on plastic during reverse panning were incubated in DMEM/1% FCS for 2 h. Few of these cells (14±2%) were Type 2 astrocytes ($A2B5^+$ $GFAP^+$) and the rest were not identified (≈ 1% $O4^+$,$O1^+$,MBP^+).

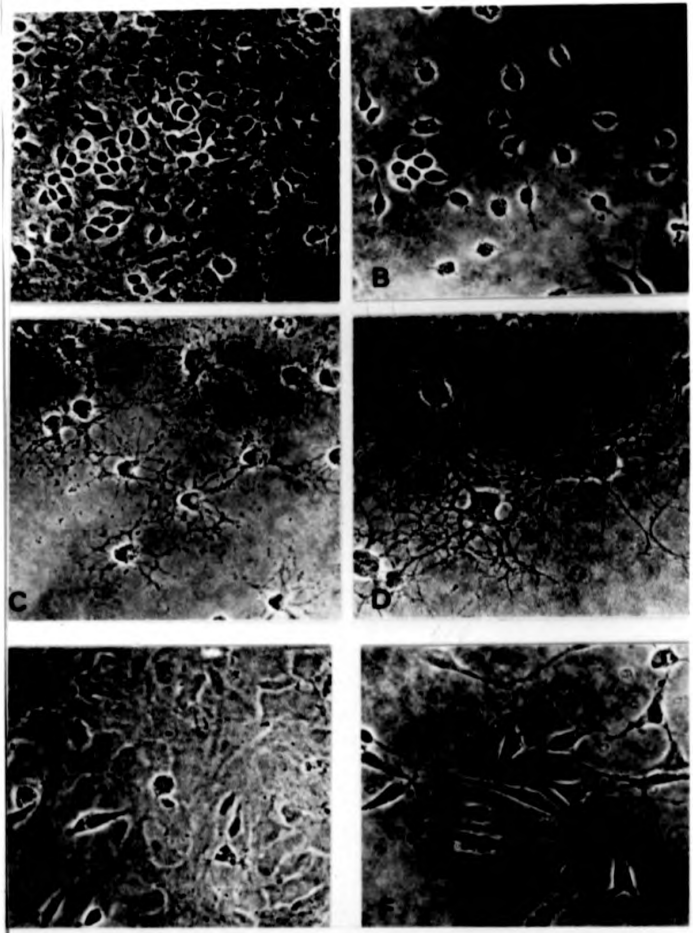
B
C
D

When the cell population resulting from reverse panning was incubated for 4 d in defined medium/bFGF followed by 1 d in defined medium/1% FCS (1 d post-bFGF, Fig. 12), O-2A progenitors dominated the culture (>80% A2B5$^+$ GFAP$^-$) and only 10% of the cells were Type 2 astrocytes (A2B5$^+$ GFAP$^+$). The total cell number had increased approximately 10-fold, as was determined by counting cells before and after bFGF in a number of similar fields. The effect of bFGF was identical at concentrations between 1-10ng/ml and daily renewal was necessary for the differentiation block and division to occur, as had been previously found by McKinnon et al., (1990). At 2 d post-bFGF a large proportion (~40%) of the O-2A progenitor cell population had differentiated to O4$^+$GalC$^-$ prooligodendrocytes and there was a sharp rise in the numbers of oligodendrocytes (O4$^+$ GalC$^+$) between 2 and 3 d. Although the number of MBP$^+$ cells also rose substantially during 2 and 3 d, GalC$^+$ MBP$^+$ oligodendrocytes remained fewer than their GalC$^+$ MBP$^-$ counterparts until 6 d post-induction, when the GalC$^+$ MBP$^+$ oligodendrocytes represented approximately 80% of the total cells in culture.

In experiments where the 4 d of incubation in bFGF had been omitted, the O-2A progenitors differentiated to oligodendrocytes within 36-48 h, yields and purity were low and the cells were approximately 60% O4$^+$ GalC$^+$ MBP$^+$ oligodendrocytes / 40% A2B5$^+$ GFAP$^+$ Type-2 astrocytes at 6 d after reverse panning. Control cultures treated with bFGF gave substantial yields of high purity cells, which differentiated sequentially and over a period of several days. O-2A progenitors that were seeded at low densities (<4x10^5 cells cm^{-2}) differentiated to approximately 60-70% A2B5$^+$ GFAP$^+$ Type-2 astrocytes in the presence of either bFGF or 1% FCS and the total cell yields were low.

Since Type-1 astrocytes secrete PDGF <u>in vitro</u> (Raff et al., 1988), an attempt was made to produce conditioned medium containing PDGF (or PDGF-like) activity by incubating Type-1 astrocyte layers (resulting after O-2A removal, Fig. *11E*) with defined medium containing 0, 1 or 10% FCS for 24-48 h. This "conditioned" medium failed to stimulate the proliferation of O-2A progenitor cells in the absence of bFGF, but incubation of O-2A cells in the presence of "conditioned" medium containing bFGF for 4 d, followed by incubation in "conditioned" medium/1% FCS, resulted in the proliferation of O-2A cells and their differentiation to oligodendrocytes, a result similar to that obtained with defined medium.

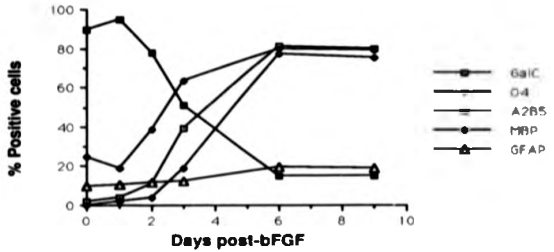

Fig. 12 Developmental markers of O-2A progenitor differentiation in culture.

O-2A progenitors were grown for 4 d in defined medium containing 1 ng/ml bFGF then switched to medium containing 1% FCS without bFGF (0 d of differentiation). The numbers of cells expressing A2B5, O4, GalC, MBP and GFAP were determined by indirect immunofluorescence. A minimum total of 700 cells per duplicate coverslip were counted in at least ten randomly selected optical fields in three different experiments; SEMs were ≤10% of each mean value. Cultures that had been allowed to differentiate for 6 d consisted primarily of oligodendrocytes (80% GalC$^+$, MBP$^+$ cells) with some Type-2 astrocytes (A2B5$^+$ GFAP$^+$), few oligodendrocytes that had not yet fully differentiated and a very small number of flat fibroblast-like cells.

3.3 Discussion

Fibroblast growth factors (FGFs) are a family of seven structurally related polypeptides which are highly mitogenic for cells derived from mesoderm and neuroectoderm (for review see Vlodansky et al., 1991). The effect of bFGF on O-2A progenitors from rat brain has been studied by McKinnon et al., (1990) and this polypeptide was shown to be mitogenic for O-2A progenitors cultured in defined medium / 0.5% FCS for at least four days.

These experiments confirmed the findings of McKinnon et al., (1990), 2x their yield was achieved and it was additionally found that when seeding progenitors at high densities division could take place in the total absence of FCS. The O-2A cells were predominantly multipolar and such a morphology is an apparent function of high seeding density (Louis et al., 1992).

$O\text{-}2A^{perinatal}$ progenitors from the optic nerve have an average cell cycle time of 18 h (Wolswijk and Noble, 1989); in the present experiments, the total number of cells increased approximately 10-fold after 4 d in bFGF, when the cells were mostly O-2A progenitors. Such proliferation was consistent with a cell cycle time of 18 h, when considering that the starting cell population (i. e. cells prepared by reverse panning) was not homogeneous in O-2A progenitors.

O-2A cells could differentiate to approximately 80% pure oligodendrocytes in the presence of low (1%) concentrations of FCS and later experiments also showed that the O-2A progenitors could differentiate to oligodendrocytes in the total absence of FCS (results not shown). These experiments suggested that high cell density during the initial seeding of O-2A progenitors may be very important for differentiation to the oligodendrocytic phenotype (consistent with the findings of Levi et al., 1991) and that high cell density may also promote proliferation. Low concentrations of FCS may have a supportive role for cells seeded at low densities only and it is possible that autocrine and / or paracrine short-range factors produced by O-2A progenitor cells may promote their own survival, proliferation and differentiation to oligodendrocytes.

It is not understood why Type-1 astrocyte "conditioned" medium failed to stimulate the proliferation of O-2A progenitors. One possible explanation is that in astrocytes remaining after the removal of the top layer of phase-dark cells, PDGF biosynthesis may be down-

regulated or PDGF secretion inhibited if the production of a certain number of O-2A progenitors has already occurred. No conclusions can therefore be drawn from the experiments involving conditioned medium and future work will either require commercially purchased PDGF or preparation of conditioned medium from Type-1 astrocyte layers grown specifically for PDGF production, such as the ones described by Wolswijk et al., (1991) and Louis et al., (1992).

These experiments suggested that cultured O-2A progenitor cells differentiate to oligodendrocytes in a sequential manner. Cell counts indicated that three stages of O-2A progenitor cell development emerged in sequence and could be identified on the basis of antigenic phenotype. O-2A progenitors ($A2B5^+$ $GFAP^-$) predominated 1-3 d after bFGF removal. $O4^+$ $GalC^-$ prolligodendrocytes appeared transiently (2-3 d) and terminally differentiated oligodendrocytes ($GalC^+$ MBP^+) were the main cells in the cultures from 6 d onwards. Such a sequence in appearance of antigenic phenotypes has been observed by others (Gard and Pfeiffer, 1990; Dubois-Dalcq et al., 1986) both in vivo and in vitro.

This primary cell culture system appeared to fulfill the following criteria:

a) establishment of the cultures was easy and reproducible

b) O-2A progenitors and oligodendrocytes were present at a relatively high purity

c) high cell yields were possible, thus enabling future immunocytochemical and biochemical experiments with cells from the same preparation to be carried out in parallel.

d) The stages of O-2A development had been characterized with a variety of well established antigenic markers, thereby investigations at key points of development were possible.

Since the criteria for a primary cell culture system had been largely met, it was decided to proceed with developmental, metabolic and trafficking investigations and perhaps develop the culture system further at a later date

Microtubule-associated protein MAP1B: Role in stabilizing the morphology of differentiated oligodendrocytes

4.1 Introduction

During the most active phase of myelination in the mammalian CNS, oligodendrocytes extend numerous myelinating processes that are responsible for ensheathing many nerve fibres simultaneously (Wood and Bunge, 1984). In culture, oligodendrocytes extend a complex system of processes from the cell body coincident with their terminal differentiation from progenitor cells (Gard and Pfeiffer, 1989). Although much has been discovered about the factors that influence oligodendrocyte progenitor development (for a review see Raff, 1989), the factors that regulate the formation and extension of myelinating processes are unknown. The study of the cytoskeleton of myelin-forming cells and their progenitors might help in understanding how their morphology is determined during differentiation (Gillespie et al., 1989; Wilson and Brophy, 1989; Kelly et al., 1992). Unlike their progenitors, oligodendrocytes do not contain any known intermediate filaments (Raff et al., 1984), consequently they must rely on microtubules and microfilaments for the morphological reorganization required for the formation, extension and stabilization of myelin processes.

Microtubule-associated protein MAP1B, which may function as a microtubule crosslinker (Noble et al., 1989; Sato-Yoshitake et al., 1989), is found associated with neurites during the early stages of process extension, where it is probably involved in neuronal growth (Tucker et al., 1988a; Tucker et al., 1988b; Tucker and Matus, 1988) and the development of polarity (Matus, 1988; Matus, 1990). Since MAP1B is also present in glia (Diaz and Avila, 1989) including oligodendrocytes (Fischer et al., 1990) but its function in these cells has not been investigated, this study undertook to quantify the amount of MAP1B expression in cultured glia, the point at which MAP1B first appears during the differentiation of O-2A progenitors, and assess the possible role of MAP1B in oligodendrocytes. The amount of expression and the developmental appearance of MAP1B was investigated by double label immunofluorescence using anti-MAP1B and antibodies that either characterize the development of O-2A progenitors to oligodendrocytes (A2B5, O4, O1 and MBP) or recognize astrocytes (GFAP). The possible role of MAP1B in oligodendrocytes was examined by inhibiting its synthesis with antisense oligonucleotides.

4.2 Results

MAP1B expression in oligodendrocytes and astrocytes

Surface expression of the sphingolipid GalC marks differentiated oligodendrocytes upon their development from progenitors and these cells possess MAP1B (Fig. 13, *A* and *B*). In addition to oligodendrocytes, these cultures contain some astrocytes and a small number (<1%) of fibroblasts. In contrast to oligodendrocytes, GFAP$^+$ astrocytes have little detectable MAP1B except for perhaps in some regions of their fibrous processes (Fig. 13, *C* and *D*). Adjacent to the astrocyte in Fig. 13 *C* is shown a rare flat fibroblast-like cell that does possess MAP1B, although at a reduced level of expression in comparison with oligodendrocytes in the same cultures.

Immunoblotting shows that the MAP1B detected immunocytochemically in oligodendrocyte cultures comigrates with brain MAP1B in SDS gels (Fig. 14, Panel *A*), therefore the oligodendrocyte protein is probably identical to the well-characterized MAP1B of neurons (Noble et al., 1989) as suggested by Fischer et al., (1990). Since it is believed that MAP1B interacts only weakly with microtubules in neurons (Matus, 1988), the strength of MAP1B interaction with the cytoskeletons of oligodendrocytes was assessed by fractionating the cells into a detergent-soluble fraction and a detergent-insoluble cytoskeleton (Wilson and Brophy, 1989). Immunoblotting shows that most of the MAP1B does not remain associated with the cytoskeleton but is rather soluble in detergent (Fig. 14, Panel *B*). The presence of significant amounts of tubulin in the cytoskeleton fraction suggests that the extraction procedure does not unduly disrupt microtubules (Wilson and Brophy, 1989). In spite of their apparently weak interaction, tubulin and MAP1B colocalize in intact oligodendrocytes (Fig. 15, *A*, *B* and *E*) as demonstrated previously by Fischer et al. (1990), furthermore MAP1B can be detected in association with microtubules in the oligodendrocyte cytoskeleton (Fig. 15, *C* and *D*).

MAP1B expression precedes the terminal differentiation of O-2A progenitors into complex process bearing oligodendrocytes

Preliminary experiments showed that MAP1B could not be detected immunocytochemically in oligodendrocyte progenitors, despite the abundance of MAP1B in oligodendrocytes, which

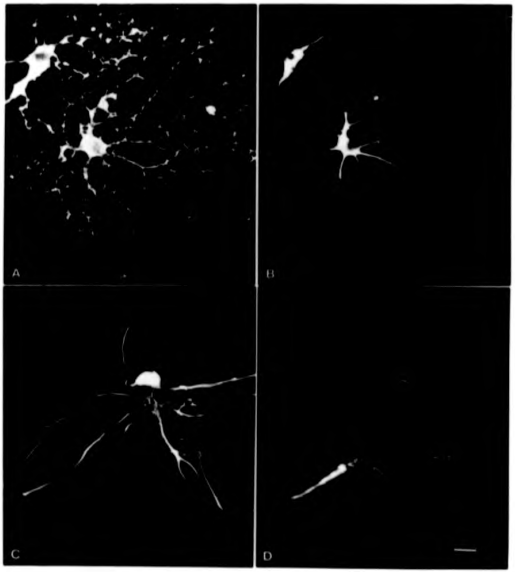

Fig. 13 MAP1B is abundantly expressed in the cell body and major processes of mature oligodendrocytes.

O-2A progenitors were stimulated to divide in the presence of bFGF and then allowed to differentiate to oligodendrocytes in medium containing 1% FCS without bFGF. After six days in culture oligodendrocytes with complex, well developed processes appear, which are strongly GalC$^+$(FITC) (*A*); these cells express MAP1B (TRITC) in their cell bodies and major processes (*B*). There are small numbers of astrocytes which express GFAP (FITC) (*C*), however only faint MAP1B staining is detectable in some of their processes (arrows in *C* and *D*). Very rare (<1%) flat fibroblast-like cells which are GFAP$^-$ (*C*) also express MAP1B (*D*, arrowhead). Bar, 5 μm.

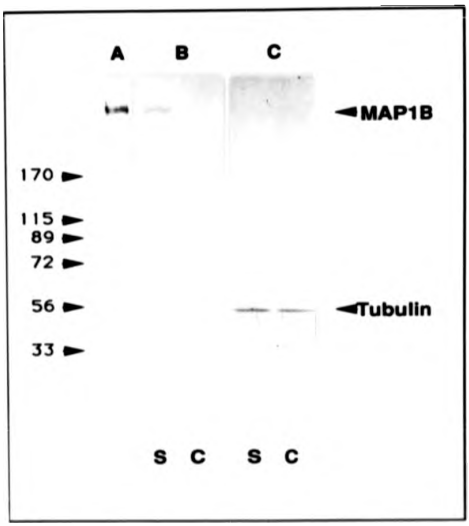

Fig. 14. MAP1B interacts weakly with the oligodendrocyte cytoskeleton.

MAP1B was detected by Western blot analysis in a brain homogenate from postnatal day 5 (P5) rats (Panel *A*) and in oligodendrocytes that had been allowed to differentiate for 5 d in culture (Panels *B* and *C*). Soluble (S) and cytoskeleton (C) fractions of oligodendrocytes were prepared by extraction with a buffer containing 0.5% (v/v) Triton X-100 (see Methods section). After SDS-PAGE in 5-17% slab gels, the proteins were transferred to nitrocellulose and immunostained with antibodies against MAP1B (Panels *A* and *B*) and tubulin (Panel *C*). Oligodendrocyte MAP1B was predominantly in the soluble fraction (Panel *B*) and had an identical M_r to that of brain protein (Panel *A*). Panel *C* shows that approximately half of the tubulin in these cultures remains assembled in microtubules, which indicates that the microtubules remained relatively intact under these conditions of extraction (Wilson and Brophy, 1989).

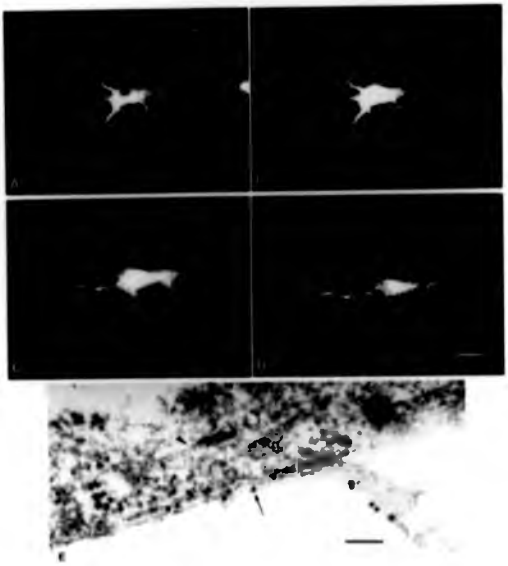

Fig. 15 MAP1B colocalizes with tubulin and associates with microtubules in the oligodendrocyte cytoskeleton.

Progenitors were allowed to differentiate for 6 d and either fixed and permeabilized (*A* and *B*) or detergent-extracted and then fixed (*C* and *D*). Cells were analyzed by double label immunofluorescence for MAP1B (DTAF) (*A* and *C*) and tubulin (TRITC) (*B* and *D*). MAP1B colocalizes with tubulin in intact cells (*A* and *B*) and codistributes with microtubules in oligodendroglial cytoskeletons (*C* and *D*). Hence some MAP1B remains associated with microtubules. Bar, 5 μm. Close interaction of microtubules and MAP1B is also demonstrated by immunogold electron microscopy in Panel *E*. An oligodendrocyte labeled with antibodies against MBP (10 nm gold, arrow) possesses a microtubule decorated with MAP1B as detected by anti-MAP1B and secondary antibodies coupled to 5 nm gold (arrowhead). Bar, 0.1 μm.

prompted an investigation into the stage of MAP1B is expression during oligodendrocyte development by comparison with the well-defined differentiation markers A2B5, O4 and GalC together with the myelin membrane proteins MBPs.

By 2 d of differentiation there is a large number of A2B5$^+$ cells (78%), a substantial population of cells bearing the early marker O4 (39%) and a small but significant number of O4$^+$,GalC$^+$ oligodendrocytes (11%) (see Section 3, Fig. 12). This was thought to be an appropriate developmental stage to identify the phenotypes of MAP1B$^+$ cells during early oligodendrocyte differentiation, when the cells are undergoing the transition from multipolar preoligodendrocyte to complex, process-bearing oligodendrocyte. Therefore, cultures at 2 d of differentiation were double-labeled with antibodies against MAP1B and three of the markers that had been used to define oligodendrocyte differentiation (A2B5, O4 and GalC).

Fig. 16 illustrates the phenotypes of MAP1B$^+$ cells at a time when these cells are becoming preoligodendrocytes and beginning to lose A2B5. An A2B5$^+$,MAP1B$^+$ cell that is in such a transitional stage is shown by the arrowhead alongside two A2B5$^+$ progenitor cells that have yet to acquire MAP1B (Fig. 16, *A* and *B*). Another cell that no longer expresses A2B5 has the type of small, intensely-labeled MAP1B$^+$ cell body that one observes in strongly O4$^+$ cells (Fig. 16, *C* and *D*). Preoligodendrocytes at an early stage of acquiring O4 (Fig. 16, *C* and *D*, small arrows) do not express MAP1B and have yet to develop an extensive system of processes. As preoligodendrocytes mature to oligodendrocytes, their major processes increase in diameter and terminate in a myriad of fine processes (Fig. 16, *E* and *F*). This morphological transition is initiated before the expression of GalC and coincides with the movement of MAP1B to the major outgrowths from the cell body. Subsequently, MAP1B is consolidated in the major processes of GalC$^+$ oligodendrocytes (Fig. 16, *E* and *F*). A MAP1B$^+$,GalC$^-$ preoligodendrocyte (Fig. 16 *F*, arrow) in which MAP1B is now present in the processes has a transitional morphology between the MAP1B$^+$,O4$^+$ cells (Fig. 16, *C* and *D*) and more mature GalC$^+$ oligodendrocytes (Fig. 16, *E* and *F*).

The data in Fig. 16 suggested that MAP1B is expressed by preoligodendrocytes before they acquire the terminal differentiation marker GalC. This view was confirmed by double label immunofluorescence and by measuring the number of MAP1B$^+$ and GalC$^+$ cells in cultures at different stages of development. From 0 d to 4 d of differentiation there

Fig. 16. MAP1B is first expressed by preoligodendrocytes during O-2A cell differentiation.

O-2A progenitors were allowed to differentiate for 2 d (*A* and *B*), 4 d (*C* and *D*) and 6 d (*E* and *F*) in culture and the developmental appearance of antigens was followed by indirect immunofluorescence. Cells were surface-labeled with IgM mAbs against A2B5 (*A*), O4 (*C*) or GalC (*E*), then fixed, permeabilized and stained with anti-IgM (FITC) followed by anti-MAP1B (*B*, *D* and *F*) and anti-IgG1 (TRITC). Two adjacent A2B5$^+$ cells are visible, one of which is weakly MAP1B$^+$ (*A*, *B*, arrowhead) whereas the other is MAP1B$^-$; an A2B5$^-$ cell in the same field is strongly MAP1B$^+$ (*B*, arrow). Early O4$^+$ cells are MAP1B$^-$ (*C* and *D*, arrows) and, when expressed at this stage of development, MAP1B is confined to the cell body (*D*). Some cells that are not yet fully differentiated (i.e. GalC$^-$ cells) express MAP1B strongly in their cell bodies and major processes (*F*, arrow) but GalC$^+$ oligodendrocytes are always MAP1B$^+$. In contrast, the phenotypes A2B5$^-$,MAP1B$^+$ and O4$^-$,MAP1B$^+$, GalC$^+$,MAP1B$^-$ are not observed. Bar, 10 μm.

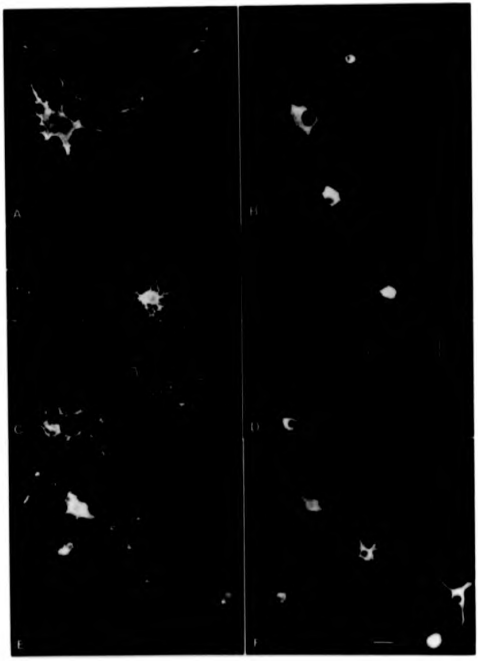
A
B
C
D
E
F

are always more MAP1B$^+$ than GalC$^+$ cells (Fig. 17), and at all stages of oligodendrocyte differentiation the GalC$^+$ cells are MAP1B$^+$. By 4 d of differentiation, 80% of the cells express MAP1B, which corresponds to the number of MBP$^+$ oligodendrocytes that ultimately develop in these cultures (Section 3, Fig. 12). These observations show that MAP1B expression precedes terminal differentiation and, since MAP1B is not a component of the purified myelin membrane (data not shown), its synthesis appears to be fundamentally related to the morphological reorganization of the oligodendrocyte.

Effect of reduced MAP1B levels on oligodendrocyte morphology and localization of tubulin

In order to investigate the role of MAP1B in oligodendrocyte differentiation, it was attempted to inhibit MAP1B synthesis by treating oligodendrocytes with antisense oligonucleotides and their respective sense congeners. Of two antisense oligonucleotides tested, one that was complementary to the region of the MAP1B mRNA flanking the initiation codon (nucleotides −3 to +17 of the mouse MAP1B cDNA sequence, Noble et al., 1989) was effective in inhibiting MAP1B expression in oligodendrocytes (Fig. 18, *B* and *E*). The other antisense oligonucleotide might have been ineffective because the 5′-sequence of rat MAP1B mRNA may differ from the equivalent region in mouse. The nucleotide sequences corresponding to the N-terminal regions of the rat protein are probably similar, because an antibody raised against the N-terminal 15 amino acid peptide of mouse MAP1B (see Materials and Methods) cross-reacts strongly with rat MAP1B. The expression of MAP1B and tubulin in sense controls was identical to untreated cells. Decreased levels of MAP1B caused the thinning and retraction of processes (Fig. 18, *A* and *D*) accompanied by the concentration of tubulin in the cell body (Fig. 18, *C* and *F*). The effects of the antisense oligonucleotide were fully reversible. These data suggest that reduced levels of MAP1B might influence the morphology of the oligodendrocyte by an effect on microtubule stability in the myelinating processes.

The specificity of the antisense oligonucleotide in inhibiting MAP1B synthesis is demonstrated in Fig. 19*a*, where the intensity of immunofluorescence staining with antibodies against MBP and MAP1B is compared in cells treated with sense and antisense oligonucleotides. Although the levels of MAP1B were drastically reduced, the MBPs were

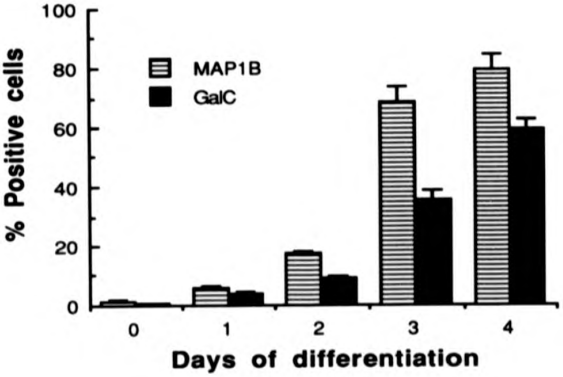

Fig. 17 Developmental expression of MAP1B in differentiating oligodendrocytes. Oligodendrocyte progenitors were allowed to differentiate and the developmental appearance of MAP1B and GalC was followed by indirect immunofluorescence using anti-IgG1-TRITC (specific for anti-MAP1B) and anti-IgM-FITC (specific for anti-GalC) secondary antibodies. Cell counts were from ten randomly selected fields of approximately 700 cells per duplicate coverslip in three different experiments, data are means ± SEM. All $GalC^+$ oligodendrocytes were $MAP1B^+$.

Fig.18 Inhibition of MAP1B synthesis by antisense oligonucleotide changes the morphology of oligodendrocyte processes.

O-2A cells that had differentiated for 5 d in culture were treated with sense (*A*, *B* and *C*) or antisense (*D*, *E* and *F*) oligonucleotides and MAP1B (*B* and *E*) and tubulin (*C* and *F*) were viewed by double label indirect immunofluorescence (DTAF and TRITC, respectively). Thinning and partial retraction of the processes in response to antisense oligonucleotide was evident by phase contrast microscopy (*A* and *D*, arrow and arrowhead) and was accompanied by the down-regulation of MAP1B (*E*) and withdrawal of tubulin (*F*) to the cell body. Bar, 10 mm.

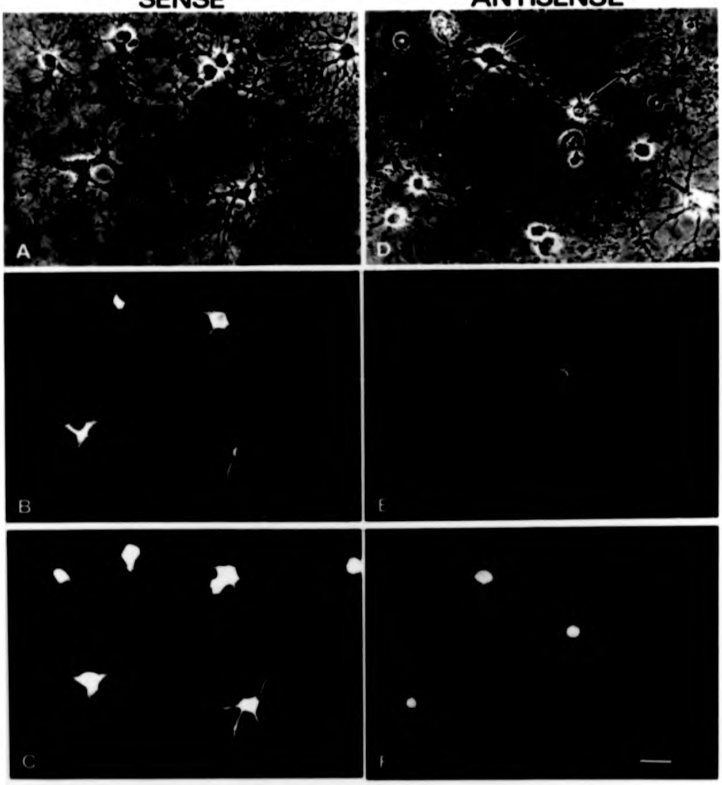
SENSE
ANTISENSE
A
D
B
E
C
F

Fig 19 Inhibition of MAP1B synthesis does not affect the expression of the myelin basic proteins (MBPs).

a: Oligodendrocytes that had differentiated for 5 d were treated for 5 h with sense (*A* and *B*) or antisense oligonucleotide to MAP1B (*C* and *D*) and stained for MBP (TRITC) (*A* and *C*) and MAP1B (DTAF) (*B* and *D*). Antisense-treated cells had reduced MAP1B by comparison with sense controls whereas MBP was unaffected. Bar, 5 mm.

b The amounts of MAP1B and MBP in 300 and 100 mg respectively of total protein were estimated by immunoblotting oligodendrocytes treated with sense (S) or antisense (A) oligonucleotide to MAP1B. MAP1B was reduced in antisense-treated cells, whereas identical amounts of the four major MBP isoforms (21.5, 18.5, 17 and 14 kD respectively) were detected in sense and antisense-treated cells.

a

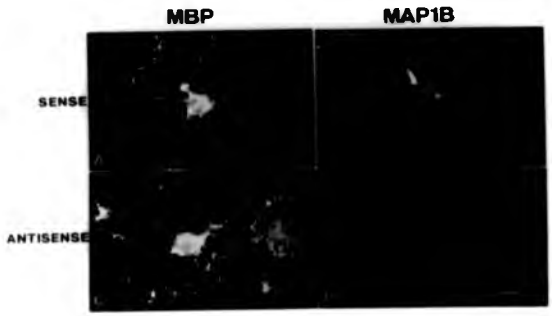

b

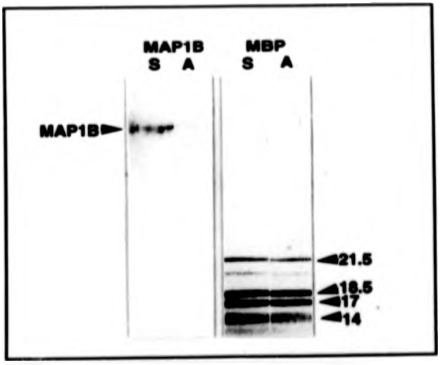

unaffected in antisense-treated cells. The proteolipid protein, another major protein of differentiated oligodendrocytes was also unaffected in antisense-treated cells (data not shown). Western blotting confirmed the reduction in MAP1B expression caused by antisense oligonucleotide, whereas MBP polypeptides were expressed at control levels (Fig. 19b). Scanning densitometry showed that the amount of MAP1B in antisense-treated cells was reduced by 62% compared to control cells.

4.3 Discussion

It seems likely that cytoskeletal reorganization might play a fundamental role in preparing the myelin-forming cell for the extraordinary changes in shape necessitated by the extension of myelinating processes and the envelopment of axons. Indeed, recent studies have revealed that the cytoskeleton of Schwann cells, the myelin-forming cells of the PNS, are remodeled during differentiation (Kelly et al., 1992). In this study we present two distinct arguments to support the view that the microtubule-associated protein MAP1B plays a central role in the formation and stabilization of myelinating processes in the differentiation of oligodendrocytes. First, we show that in differentiated cells MAP1B colocalizes and interacts with microtubules and that developing oligodendrocytes express MAP1B immediately before assuming the process-bearing morphology required for myelination. Secondly, oligodendrocytes with decreased levels of MAP1B as a result of treatment with antisense oligonucleotide have thinned and retracted processes, and their microtubules are withdrawn to the cell body. Down-regulation of MAP1B by antisense oligonucleotide is specific because neither the localization nor the amounts of the four MBP isoforms are affected, each of which is encoded by a unique mRNA (de Ferra et al., 1985).

Direct evidence for the role of MAPs in the development of neuronal morphology has been adduced from experiments in which the expression of MAP tau and MAP2 in neurons has been attenuated by the introduction of antisense oligonucleotides and antisense RNA respectively (Caceres and Kosik, 1990; Dinsmore and Solomon, 1991). Microtubules and their MAPs are likely to have a similar vital function in the development of the characteristic process-bearing phenotype of oligodendrocytes since the induction of MAP1B expression coincides with the preoligodendrocyte stage of O-2A cell development, immediately prior to terminal differentiation. MAP1B can form cross-bridges between microtubules (Sato-Yoshitake et al., 1989) thus it could provide the structural support necessary for the stabilization of large complex outgrowths from the oligodendrocyte's cell body. Nevertheless, only a small fraction of the total MAP1B in oligodendrocytes remains associated with the cytoskeleton after detergent-extraction, which is consistent with the fact that MAP1B cycles very inefficiently with brain microtubules and that most MAP1B does not associate with the cytoskeleton in HeLa cells transfected with MAP1B cDNA (Bloom et al., 1985; Noble et al.,

1989). This work suggests that similar weak interactions between MAP1B and microtubules must occur in oligodendrocytes; however, in contrast to the cytoskeletons of transfected HeLa cells, a fraction of MAP1B is detectable by immunofluorescence bound to the oligodendrocyte cytoskeleton. Both *a*-tubulin and MAP1B are susceptible to extensive post-translational modification, which might be responsible for modulating the strength of interaction between microtubules and MAP1B and thereby help to explain cell type-specific differences in the strength of microtubule-MAP1B interactions. For example, phosphorylated forms of MAP1B are known to be particularly abundant in growing axons (Sato-Yoshitake et al., 1989), and *a*-tubulin is predominantly tyrosinated in the labile dynamic microtubules of axons, whereas stable nucleating microtubules are rich in detyrosinated and acetylated *a*-tubulin (Baas and Black, 1990).

Metabolism and traffic of fluorescent sphingolipids in oligodendrocytes

5.1 Introduction

During the most active period of myelination, oligodendrocytes synthesize more than three times their own weight of myelin membrane per day (Norton, 1981). Since myelin is 70-80% lipid, these cells should be excellent models for studying the metabolism and traffic of membrane lipids.

Cer is the backbone structure of the sphingolipids SM, GlcC, GalC and sulfatide, the last two of which are characteristic of myelin in the nervous system. Although a considerable volume of information exists about the metabolism and transport of SM and GlcC (for reviews see Koval and Pagano, 1991; van Meer, 1989; Schwarzmann and Sandhoff, 1990), relatively little is known about the metabolism and transport of GalC and sulfatide; this may be because until recently it was not possible to culture sufficient numbers of oligodendrocytes for biochemical investigations. These problems have now been mostly overcome and it is possible to obtain sufficient, relatively homogeneous oligodendrocyte lineage cells at different developmental stages (McKinnon et al., 1990).

UDP-galactose ceramide galactosyltransferase (UDP-galactose:2 hydroxyacyl sphingosine galactosyltransferase, E.C.2.4.1.45) catalyzes the transfer of galactose from UDP-gal to Cer and is the terminal enzyme in the biosynthesis of GalC, the main sphingolipid in brain. Roussel et al., (1987) showed that in oligodendrocytes this enzyme may have a very wide distribution, since it is found in the Golgi, the cellular processes and in loosely wrapped myelin. By contrast, UDP-glucose ceramide glucosyltransferase which is responsible for the synthesis of GlcC, is probably restricted to a pre-Golgi compartment and/or in the *cis*-Golgi in various non-glial cells (Futerman and Pagano, 1991; van Meer et al., 1989; van Echten and Sandhoff, 1989). In such cells, most SM biosynthesis is believed to occur in the *cis*- and *medial*-Golgi (Futerman et al., 1990; Jeckel et al., 1990), although some may also take place at the plasma membrane (Koval and Pagano, 1991). It has been recently suggested that oligodendrocytes may be unusual in that equal amounts of SM may be synthesized in the plasma membrane and the Golgi (Di Biase et al., 1991).

In order to study sphingolipid biosynthesis and traffic in cultured oligodendrocytes, it was important to define an active stage of GalC biosynthesis during development. Therefore, the

relative extent of conversion of C_6-NBD-Cer to C_6-NBD-GalC and C_5-DMB-Cer to C_5-DMB-GalC were studied at different stages of oligodendrocyte differentiation in culture. A suitable time point was identified that coincided with the expression of oligodendrocyte differentiation markers, and cells at this stage were used to study the initial localizations of C_6-NBD-Cer and C_5-DMB-Cer in specific intracellular compartments and their subsequent transport and metabolism. These investigations were carried out at the light and ultrastructural levels and the localizations of fluorescent sphingolipids were compared with those of specific markers of organelles that are involved in lipid metabolism and traffic.

Sphingolipids and proteins are probably cotransported along the secretory and recycling pathways (Simons and van Meer, 1988; Simons and Wandinger-Ness, 1990; Rosenwald et al., 1992; Kok et al., 1989) and BFA has been shown to be an extremely useful tool in the analysis of such pathways (for reviews see Pelham, 1991; Klausner et al., 1992). Sphingolipid traffic is considered to be intimately linked with metabolism (Miller-Prodzara and Fishman, 1984; Lipsky and Pagano, 1985b; Rosenwald et al., 1992; Koval and Pagano, 1991), therefore it was of great interest to attempt to determine the influence of disrupting the secretory pathway with BFA on sphingolipid metabolism and traffic. The effects of BFA would also indicate whether oligodendrocytes belong to the group of cells in which BFA causes the TGN to fuse with the rest of the Golgi and the ER (Alcade et al., 1991), or to those in which the TGN/plasma membrane/endosomes and the *cis-/medial-/trans*-Golgi/ER constitute two separate compartments (Reaves and Banting, 1992; Lippincott-Schwartz, et al., 1991b; Wood et al., 1991), or to a third class where the TGN/plasma membrane/endosomal system is formed but the *cis-/medial-/trans*-Golgi/ER fusion does not occur (Lippincott-Schwartz, et al., 1991b). This analysis would therefore permit a detailed comparison between the organization of the secretory and recycling pathways of oligodendrocytes with those in other cell types and might provide information about the biosynthesis and transport of myelin-specific lipids.

Microtubules are involved in many BFA-enhanced (such as retrograde transport) or BFA-inhibited (such as anterograde transport from the *cis-*, *medial-*, *trans*-Golgi and the TGN, Klausner et al., 1992; Wood et al., 1991) cellular functions, as well as functions that remain unaffected such as the movement of endocytosed material (Pelham, 1991; Lippincott-

Schwartz et al., 1991a). Microtubules also play an important role in the structural integrity and location of the Golgi apparatus (for reviews see Thyberg and Moskalewski, 1985; Kreis, 1990), and in several cell lines a set of stable (detyrosinated) microtubules that are apparently unaffected by BFA colocalize with the Golgi (Burgess et al., 1991). Mature oligodendrocytes contain microtubules both in vivo and in vitro (Wood and Bunge, 1984; Wilson and Brophy, 1989), but these cells are quite unusual in that they do not contain any known forms of intermediate filaments and microfilaments appear to be predominantly in the cell periphery. Oligodendrocytes should therefore represent unique models for studying the effects of BFA on microtubules.

Removal of BFA leads to cell recovery via the reformation of organelles of the secretory pathway (Pelham, 1991; Alcade et al., 1992), therefore the study of recovery should yield information about the sequence of molecular, metabolic and transport events that lead to the restructuring of cellular organelles. Such studies may serve as models for understanding the formation and maintenance of cellular architecture involving the cytoskeleton. Considering the intimate link between the Golgi and microtubules, it was decided to study the reformation of this organelle with respect to tubulin in oligodendrocytes recovering from BFA.

5.2 Results

Cells of the oligodendrocyte lineage: changes in sphingolipid metabolism during development

Initial time course experiments using oligodendrocytes at 6 d of differentiation indicated that during incubation at 37°C, little or no conversion of C_6-NBD- and C_5-DMB-Cer occurs before 15 min. Maximum conversion to fluorescent Cbs and SM takes place after approximately 2 h and these products persist for up to 5 h, however the ratios of fluorescent Cbs/SM and GalC/GlcC remain constant (data not shown). As a consequence, a 2 h incubation period was used in all the metabolic experiments involving fluorescent Cer analogues.

Both C_6-NBD-Cer and C_5-DMB-Cer are metabolized to their respective SM and Cb analogues by oligodendrocytes and considerably more fluorescent Cb is produced from C_6-NBD-Cer than from C_5-DMB-Cer at all times during development (Fig. 20). Similar observations were made by Pagano et al., (1991) who compared the in vitro metabolism of C_6-NBD-Cer and C_5-DMB-Cer in human skin fibroblasts and found that the ratio of C_6-NBD-Cb/SM was ~0.77 while the ratio of C_5-DMB-Cb/SM was ~0.06 (recalculated data). The percent conversion of C_6-NBD-Cer to C_6-NBD-Cbs increases with a concomitant decrease in the biosynthesis of C_6-NBD-SM during differentiation (Fig. 21). The increase in Cb biosynthesis is the result of elevated production of C_6-NBD-GalC at the expense of GlcC between 6 and 9 d of development. The increase in C_6-NBD-GalC synthesis is accompanied by the conversion of O-2A progenitors into $GalC^+$,MBP^+ oligodendrocytes during development (see Fig. 12, Section 3).

GlcC biosynthesis in the brain predominates before the onset of myelination, whereas GalC becomes the main Cb during myelination (Koul et al., 1988). Similarly, the present in vitro data suggest that O-2A progenitors and perhaps preoligodendrocytes predominantly convert C_6-NBD-Cer to C_6-NBD-GlcC, while oligodendrocytes at 6 d and 9 d of differentiation produce considerable amounts of C_6-NBD-GalC. Although C_5-DMB-Cer is mainly converted to C_5-DMB-SM (Fig. 20) and the main C_5-DMB-Cb is C_5-DMB-GlcC, the relative amount of C_5-DMB-GalC also increases during development (not shown).

It is noteworthy that some C_6-NBD-GalC and C_5-DMB-GalC are formed at 0 d of differentiation, when cells in equivalent cultures are at least 80% O-2A progenitors, 25% $O4^+$

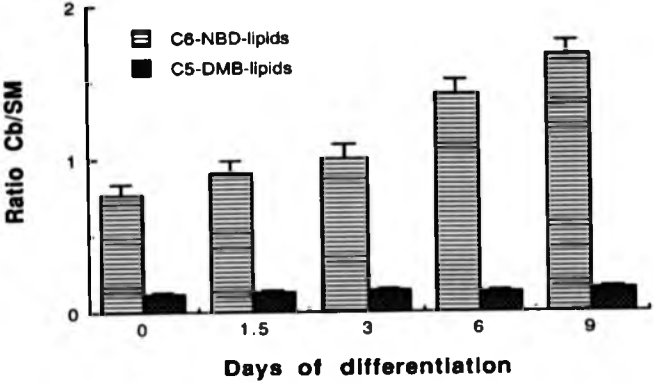

Fig. 20. Comparison of the metabolism of C_6-NBD-Cer and C_5-DMB-Cer to fluorescent-Cbs and -SM by differentiating O-2A progenitors.

O-2A progenitors were permitted to differentiate for 0, 1.5, 3, 6 and 9 d, when they were incubated for 2 h with C_6-NBD-Cer/DF-BSA or C_5-DMB-Cer/DF-BSA complexes. Fluorescent lipids were identified with authentic standards and quantified as described in Materials and Methods. The ratio of C_6-NBD-Cb/SM increased during differentiation; C_6-NBD-SM was the main metabolic product in O-2A progenitors (0 d of differentiation) and C_6-NBD-Cbs predominated in terminally differentiated oligodendrocytes (9 d of differentiation). By contrast, C_5-DMB-Cer was mainly metabolized to C_5-DMB-SM and the ratio of C_5-DMB-Cbs/SM was very similar throughout development.

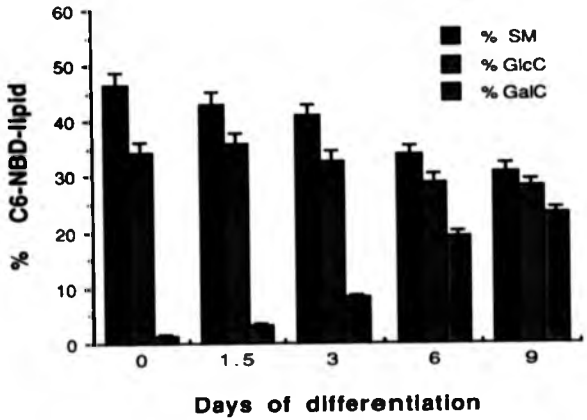

Fig. 21. Biosynthesis of C_6-NBD-GalC from C_6-NBD-Cer during oligodendrocyte development

O-2A progenitors were permitted to differentiate for 0, 1.5, 3, 6 and 9 d, then incubated with C_6-NBD-Cer/DF-BSA complexes for 2 h. C_6-NBD-SM, -GlcC and -GalC were identified and quantified as described in Materials and Methods. C_6-NBD-SM and -GlcC were the main metabolic products in O-2A progenitors (0 d) but with the onset (1.5 and 3 d) and progress (6 and 9 d) of differentiation, more C_6-NBD-GalC and less C_6-NBD-SM was produced. At 6 d and 9 d the relative amount of C_6-NBD-Cbs exceeded that of C_6-NBD-SM. The proportion of C_6-NBD-GlcC was constant at 0, 1.5 and 3 d of differentiation and somewhat reduced at 6 and 9 d of differentiation.

cells (preoligodendrocytes) and ~1% terminally differentiated oligodendrocytes (see Section 3). It therefore appears that O-2A progenitors and/or preoligodendrocytes may have a basal level of UDP-galactose-4'-epimerase and UDP-galactose:ceramide galactosyltransferase activities. In these cultures the formation of C_6-NBD-GalC and C_5-DMB-GalC is specific to oligodendrocyte lineage cells, because only GlcC and SM derivatives are formed when Type-1 or -2 astrocyte monolayers are incubated with either C_6-NBD-Cer or C_5-DMB-Cer (data not shown).

The conversion of C_6-NBD-Cer and C_5-DMB-Cer to either C_6-NBD-GalC or C_5-DMB-GalC by differentiating O-2A cells is probably underestimated at later stages of differentiation, when up to 20% of the cells in the cultures are Type-2 astrocytes. However, the high levels of C_6-NBD-GlcC and even higher levels of C_5-DMB-GlcC at all developmental stages may reflect the propensity of C_6-NBD-Cer and C_5-DMB-Cer to be preferentially converted to the GlcC analogue. The small amounts of fluorescent GalC may also be caused by the inability of cultured oligodendrocytes to produce only large amounts of GalC (Poduslo et al., 1990).

Two forms of C_5-DMB-SM were identified, SM1 and SM2, whose R_f values correspond to stereoisomers of C_5-DMB-SM. However, in biological systems one stereoisomer is usually formed (the L-isomer) therefore SM1 (R_f 0.07) and SM2 (R_f 0.05) are probably not stereoisomers but instead correspond to SMs with sphinganine and N-acyl sphingosine backbones, respectively. SM2 predominates over SM1 at 0 d of differentiation (mol% SM2/SM1~7.3) but when the majority of the cells have differentiated to oligodendrocytes (i.e. at 9 d of differentiation), the relative amount of SM2 is almost equal to SM1 (SM2/SM1~1.2). The significance of this is not understood, but when the lipids from mature rat CNS myelin are separated by TLC two bands of SM in approximately similar amounts are detected (data not shown), indicating that SM in myelin may contain sphinganine and sphingosine backbones. Almost equal amounts of SM1 and SM2 may therefore signify that as oligodendrocytes mature they tend to synthesize myelin-specific SM; however, two bands of SM in myelin may arise due to the presence of fatty acids with different chain lengths.

By 6 d of differentiation the cultures are approximately 80% pure in oligodendrocytes ($GalC^+$,MBP^+) and at this point oligodendrocytes are able to convert C_6-NBD-Cer to sphingolipids that include considerable amounts of C_6-NBD-GalC. These results suggested

that in the present culture system, 6 d of differentiation probably represent a good stage at which to study sphingolipid metabolism and transport in oligodendrocytes.

Characterization of the Golgi in oligodendrocytes

Cultured oligodendrocytes have small cell bodies, multiple branching processes and express GalC on the cell surface (Fig. 22, Panel *a*). Since the Golgi is thought to be the site of sphingolipid biosynthesis and transport (Simons and van Meer, 1988; Simons and Wandinger-Ness, 1990), this organelle was initially characterized in oligodendrocytes at 6 d of differentiation at the light level by utilizing a range of Golgi markers. C_6-NBD-Cer (*b*), C_5-DMB-Cer (*d*) and TGN38, a marker for the trans-Golgi network, (Luzio et al., 1990) (*c* and *e*) label perinuclear locations, whereas WGA-TRITC labels a perinuclear location as well as the cell surface (*f*). C_6-NBD-Cer and C_5-DMB-Cer were previously shown to be vital markers for the Golgi apparatus (Lipsky and Pagano, 1983; Pagano et al., 1991) and in fixed human skin fibroblasts C_6-NBD-Cer and C_5-DMB-Cer labels the *trans*-Golgi and multiple Golgi stacks, respectively (Pagano et al., 1989; Pagano et al., 1991). WGA binds N-acetyl-glucosamine and sialic acid residues (for review see Geuze and Morré, 1991), therefore WGA-TRITC probably labels the *trans*-Golgi, the TGN, secretory vesicles and the plasma membrane in oligodendrocytes. Another fluorescent lectin, *Ricinus communis* Agglutinin-I-TRITC which binds β-gal residues, labels oligodendrocytes in a similar way to WGA-TRITC (data not shown). These observations suggested that C_6-NBD-Cer and C_5-DMB-Cer concentrate in the Golgi of oligodendrocytes.

Incubation with C_6-NBD-Cer indicates that at the light level, the Golgi of live oligodendrocytes has a different morphology from that of astrocytes and fibroblasts (Fig. 23). The Golgi appears thin and elongated in fibroblasts, extensive and tubulovesicular in astrocytes and relatively compact in oligodendrocytes.

These initial experiments indicated that in cultured oligodendrocytes different Golgi markers may label similar but not identical Golgi compartments. Additionally, the Golgi of oligodendrocytes appears different from that of other cells in these cultures at the light level.

Fig.22 C_6-NBD-Cer and C_5-DMB-Cer colocalize with Golgi markers in oligodendrocytes

O-2A progenitors were permitted to differentiate to oligodendrocytes for 6 d in defined medium/1% FCS. Live cells were incubated with C_6-NBD-Cer/DF-BSA for 15 min at 37°C (*b*), surface-labeled with anti-GalC followed by indirect immunofluorescence with secondary antibodies coupled to TRITC (*a*). Alternatively, live cells were incubated with C_5-DMB-Cer/DF-BSA, fixed and photographed (*d*), then extracted with methanol and labeled with TGN38 (DTAF) (*c*). Oligodendrocytes were labeled with TGN38 (DTAF) (*e*) and WGA-TRITC (*f*). C_6-NBD-Cer, C_5-DMB-Cer and TGN38 labeled perinuclear locations; by contrast, WGA-TRITC labeled the plasma membrane as well as a perinuclear location.

Bars: 10μm.

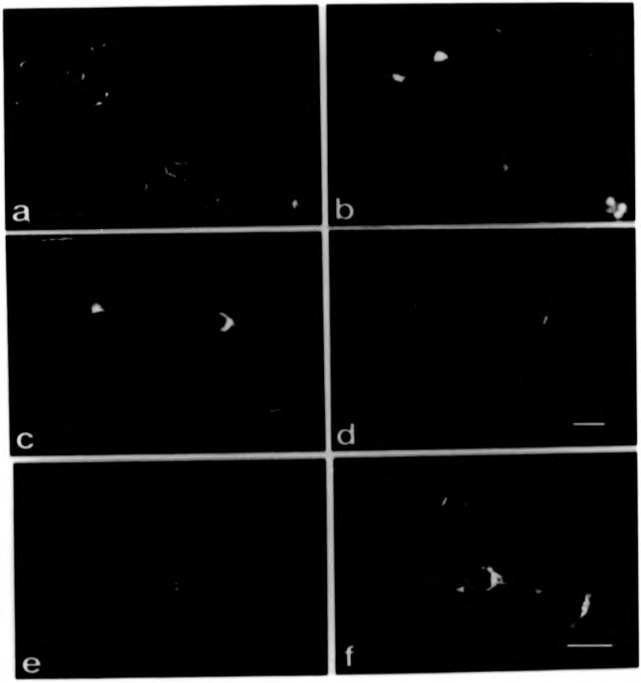
a
b
c
d
e
f

Fig. 23. The Golgi of oligodendrocytes labeled with C_6-NBD-Cer has a different morphology to Golgi of other brain cells.

Mixed glial cultures were seeded in 35mm dishes and grown in DMEM/10% FCS for one week and in defined medium/1% FCS for a further 6 d. The cells were incubated with C_6-NBD-Cer/DF-BSA for 15 min at 37°C, fixed and examined by fluorescence microscopy. Although oligodendrocytes (arrowhead), fibroblasts (large arrow) and astrocytes (small arrow) were all labeled in a perinuclear location, their patterns of labeling were strikingly different at the light level. Bar: 10µm.

Since I intended to study the intracellular transport of C_6-NBD- and C_5-DMB-lipids in oligodendrocytes in order to relate it to metabolism, it was important that light level observations at key metabolic points should be further examined at the ultrastructural level. Fig. 24 demonstrates that in oligodendrocytes, C_6-NBD-lipid labels the *trans*-Golgi and the TGN while C_5-DMB-lipid is distributed throughout the Golgi excluding the TGN. At this point little or no metabolism of C_6-NBD-Cer and C_5-DMB-Cer would have occurred, therefore it appears that in oligodendrocytes C_6-NBD-Cer labels the *trans*-Golgi and the TGN, while C_5-DMB-Cer labels the rest of the Golgi, excluding the TGN. Pagano et al., (1989) have shown that C_6-NBD-Cer targets organelle-specific lipids and they speculated that the lipid composition of the *trans*-Golgi apparatus may be unique. However, the exact lipid compositions of the various Golgi subcompartments are not known, although Brasitus et al., (1988) have shown that in order of abundance, the principal lipids of the Golgi in rat proximal small intestinal cells are PC, cholesterol, PE and SM. The Golgi probably exchanges lipids with other organelles continuously, through its involvement not only in secretion but also in the intracellular routing of molecules during endocytosis and the recycling pathways from the plasma membrane (for a review see Geuze and Morré, 1991), therefore it must possess mechanisms for lipid sorting in order to maintain a constant lipid composition.

The products of C_6-NBD-Cer and C_5-DMB-Cer metabolism traffic through different intracellular compartments

Fluorescence analysis indicates that after 2 and 5 h of incubation at 37°C, C_6-NBD-Cer and C_5-DMB-Cer metabolites of probably distribute in different intracellular compartments (Fig. 25). However, although the patterns of fluorescence are different at 2 and 5 h, the same major fluorescent metabolic products are found at these time points of incubation and it was therefore assumed that the fluorescence at 2 h and at 5 h originates from the same sets of C_6-NBD- or C_5-DMB-lipids. Electron microscopy (Fig. 26) indicates that after 2 h of incubation C_6-NBD-Cb and -SM are in structures resembling TGN-derived vesicles and early endosomes, whereas C_5-DMB-lipids (comprising 72% C_5-DMB-SM) are in structures resembling ER and in the plasma membrane. After 5 h of incubation C_6-NBD-lipids are in endosomes or lysosomes and C_5-DMB-lipids are in the Golgi and Golgi-associated vesicles.

Fig. 24 C_6-NBD-Cer and C_5-DMB-Cer label different Golgi compartments in oligodendrocytes

Oligodendrocytes at 6 d of differentiation were fixed, peroxidase-labeled with TGN38 and processed for electron microscopy (*a*). Alternatively, live cells were incubated for 15 min at 37°C with either C_6-NBD-Cer/DF-BSA (*b*) or C_5-DMB-Cer/DF-BSA (*c*), fixed, photobleached in the presence of DAB and processed for electron microscopy. C_6-NBD-Cer and TGN38 specifically labeled the *trans*-Golgi and the *trans*-Golgi network (TGN); by contrast, C_5-DMB-Cer did not label the TGN but was distributed throughout the rest of the Golgi stacks. Bar: 500nm.

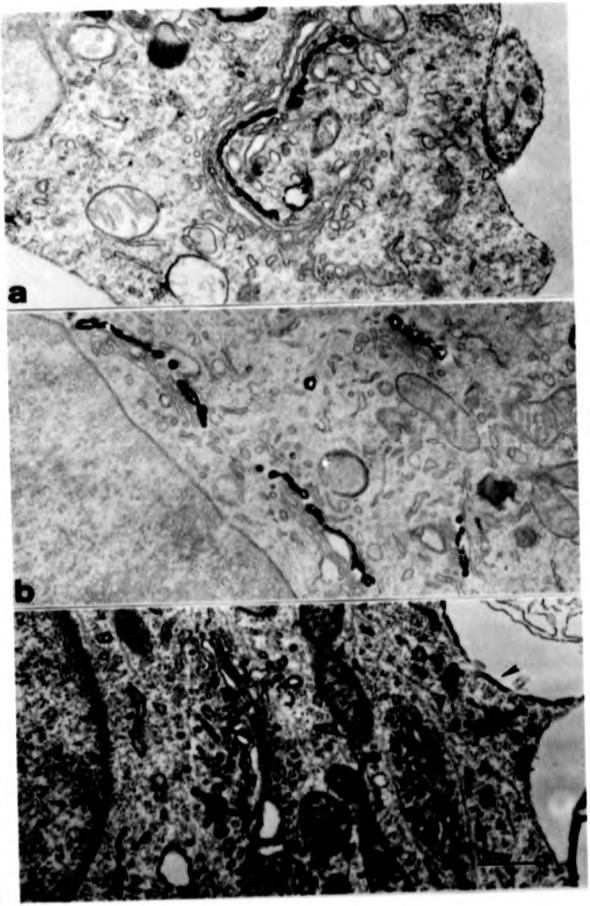
a
b

Fig. 2F. The metabolism of C_6-NBD-Cer and C_6-DMB-Cer have different fates

Oligodendrocytes were incubated for 15 min at 37°C with either C_6-NBD-Cer/DF-BSA (*a* and *c*) or C_6-DMB-Cer/DF-BSA (*b* and *d*), washed and incubated up to 2 h (*a* and *b*) or 5 h (*c* and *d*). The cells were fixed and photographed in the green and red microscope channels for NBD- and DMB-fluorescence, respectively. At 2, h C_6-NBD-lipids labeled perinuclear compartments whereas C_6-DMB-lipids were present in the cell body and in the processes. At 5 h the fluorescence from both C_6-NBD- and C_6-DMB-lipids was mainly restricted to the cell body. Bar: 10μm

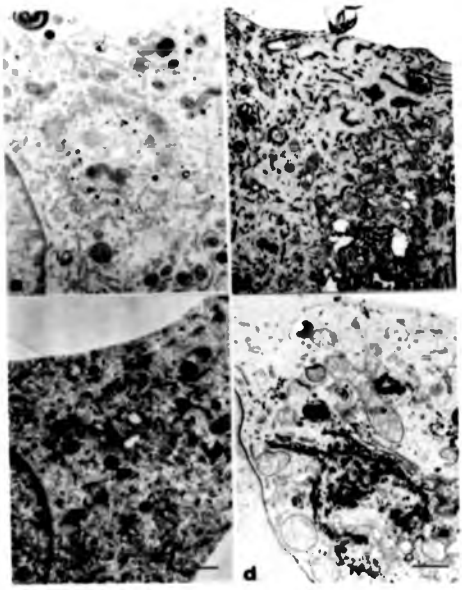

Fig. 2a. C_6-NBD- and C_5-DMB-metabolites are transported to different intracellular compartments.

Oligodendrocytes at 6 d of differentiation were incubated for 15 min at 37°C with either C_6-NBD-Cer/DF-BSA (*a* and *c*) or C_5-DMB-Cer/DF-BSA (*b* and *d*), washed, incubated up to 2 h (*a* and *b*) or 5 h (*c* and *d*), fixed, photobleached in the presence of DAB and processed for electron microscopy. At 2 h the metabolic products of C_6-NBD-Cer were in structures resembling the TGN, TGN-derived vesicles and early endosomes (*a*), whereas C_5-DMB-lipids were located in the ER and at the plasma membrane (*b*). At 5 h C_6-NBD-Cbs and -SM were found in endosomes (*c*), whereas C_5-DMB-SM was mainly in the Golgi (*d*). Bars: 500nm.

These observations suggest that at 37°C, C_6-NBD-Cer localizes in the *trans*-Golgi and the TGN by 15 min, the products of its metabolism distribute between TGN-derived vesicles and early endosomal compartments by 2 h and in late endosomes and lysosomes by 5 h. By contrast, C_5-DMB-Cer initially localizes in various Golgi compartments excluding the TGN. C_5-DMB-SM is in the ER and the plasma membrane at 2 h and in the Golgi and Golgi-derived vesicles at 5 h. Lipsky and Pagano, (1983) showed that when Chinese hamster fibroblasts are incubated with C_6-NBD-Cer, cytoplasmic structures, the Golgi and the plasma membrane are sequentially labeled; significant metabolism of C_6-NBD-Cer to C_6-NBD-Cb and C_6-NBD-SM occurs within 15 min and by 1 h approximately similar amounts of C_6-NBD-Cb and C_6-NBD-SM are produced and remain at the same levels by 2 h. In this culture system the ratio of C_6-NBD-Cb/SM alters through development and similar amounts of C_6-NBD-Cb and C_6-NBD-SM are obtained at 2 and 3 d of differentiation (Figs. 20 and 21).

Although C_6-NBD-Cer is apparently a vital stain for the *trans*-Golgi in human skin fibroblasts (Pagano et al., 1989), in oligodendrocytes C_6-NBD-Cer labels the *trans*-Golgi and the TGN. The finding that C_5-DMB-Cer initially labels multiple Golgi stacks is in agreement with the obeervations of Pagano et al., (1991) and in oligodendrocytes these stacks may represent Golgi compartments earlier than the TGN, i.e. *cis*-, *medial*- and perhaps *trans*-Golgi. In any event, C_5-DMB-Cer is initially localized to a more proximal location than C_6-NBD-Cer in the Golgi stack. C_5-DMB-Cer is also metabolized much slower by oligodendrocytes than human skin fibroblasts (Pagano et al., 1991) and in both cell types is mainly converted to C_5-DMB-SM.

These results indicate that in oligodendrocytes C_6-NBD-Cer and C_5-DMB-Cer initially concentrate in different intracellular loci, probably as a result of interactions between Golgi lipid and the C_6-NBD and C_5-DMB fluorophores; indeed, Pagano et al., (1991) have suggested this possibility for C_5-DMB-Cer. Subsequent metabolism and intracellular transport of these lipids may be determined by the localization and specificities of the enzymes involved in sphingolipid metabolism and transport mechanisms, either at the *trans*-Golgi and the TGN in the case of C_6-NBD-Cer or at the early Golgi in the case of C_5-DMB-Cer. In order to test this hypothesis, we utilized BFA which is known to either fuse the *cis*-, *medial*- and *trans*-Golgi in some cells and/or the TGN with endosomes in others (Reeves and

Banting, 1992; Wood et al., 1991; Lippincott-Schwartz et al., 1991a; Hunziker et al., 1991), thus physically separating the TGN from the rest of the Golgi. Therefore it was of great interest to determine if disrupting the organization of the secretory membrane system, and perhaps causing the coalescence of organelles that are normally physically separated might affect the manner in which sphingolipids are metabolized in oligodendrocytes. Thereby, it was hoped that insights would be gained into the roles of different compartments of the secretory pathway and sphingolipid traffic.

The TGN of BFA-treated oligodendrocytes disorganizes more slowly and recovers faster than the *cis*- and *medial*-Golgi.

Before analyzing the effects of BFA on lipid metabolism and traffic, it was important to establish how BFA affected the organelles of the secretory pathway in oligodendrocytes. The TGN and the *cis*- and *medial*-Golgi of oligodendrocytes are in similar but not identical locations (Fig. 27, *a* and *b*), as shown by TGN38, a marker of the *trans*-Golgi network and anti-Man II, a marker of the *cis*- and *medial*-Golgi (Luzio et al., 1990; Burke and Warren, 1984). BFA affects the whole Golgi (Fig. 27, *c* and *d*); after 0.5 h in BFA, TGN38 is present in a MTOC-like location but anti-Man II fluorescence is weak and dissipated (Fig. 27, *c* and *d*), as was also observed in BFA-treated NRK cells (Reaves and Banting, 1992; Alcade et al., 1992; Wood et al., 1991). Weak Man II fluorescence is seen in an ER-like pattern after 1 h in BFA, when the TGN is probably distributed with the recycling endosomal system (Fig. 27, *e* and *f*). At 3 and 4 h in BFA, TGN38 is seen intracellularly and at the plasma membrane and Man II is distributed in an ER-like pattern (Fig. 27, *g*, *h*, *i* and *j*). Wood et al., (1991) showed that when the TGN/endosomal network was formed in response to BFA, there was a >5-fold increase in mannose-6-phosphate receptors (M6PRs) to the cell surface, consistent with this redistribution, considerable amounts of TGN38 are found at the cell surface of cells treated with BFA for 3 h (Fig. 27; Lippincott-Schwartz et al., 1991a).

These results support the idea that in oligodendrocytes BFA causes the *cis*-and *medial*-Golgi to fuse with the ER while the TGN distributes with the recycling endosomal system; this was also seen in other cell types (Lippincott-Schwartz et al., 1991b; Reaves and Banting, 1992; Wood et al., 1991).

Fig. 27 The effects of BFA on the *cis*- and *medial*-Golgi and the TGN.

Oligodendrocytes were incubated for 0 h (*a* and *b*), 0.5 h (*c* and *d*), 1 h (*e* and *f*), 3 h (*g* and *h*), and 4 h (*i* and *j*) at 37°C in the presence of BFA , fixed and processed for double indirect immunofluorescence using TGN38 (DTAF) (*a, c, e, g, i*) and the *cis*- and *medial*-Golgi marker anti-Man II (TRITC) (*b, d, f, h* and *j*). In control cells, TGN38 and anti-Man II labeled similar but not identical compartments (*a* and *b*). After 0.5 h in BFA, TGN38 fluorescence was reduced and concentrated in a MTOC-like location, whereas anti-Man II fluorescence was extremely weak (*c* and *d*). The fluorescence from TGN38 was very weak and dispersed after 1 h in BFA when a faint, ER-type staining was detected with anti-Man II (*e* and *f*). TGN38 fluorescence reappeared at the cell body after 3 h in BFA and Man II was distributed in a punctate pattern resembling the ER (*g* and *h*). At 4 h, TGN38 fluorescence was increased in the cell body whereas Man II retained the ER-like distribution that was seen at 3 h. Bar: 10μm.

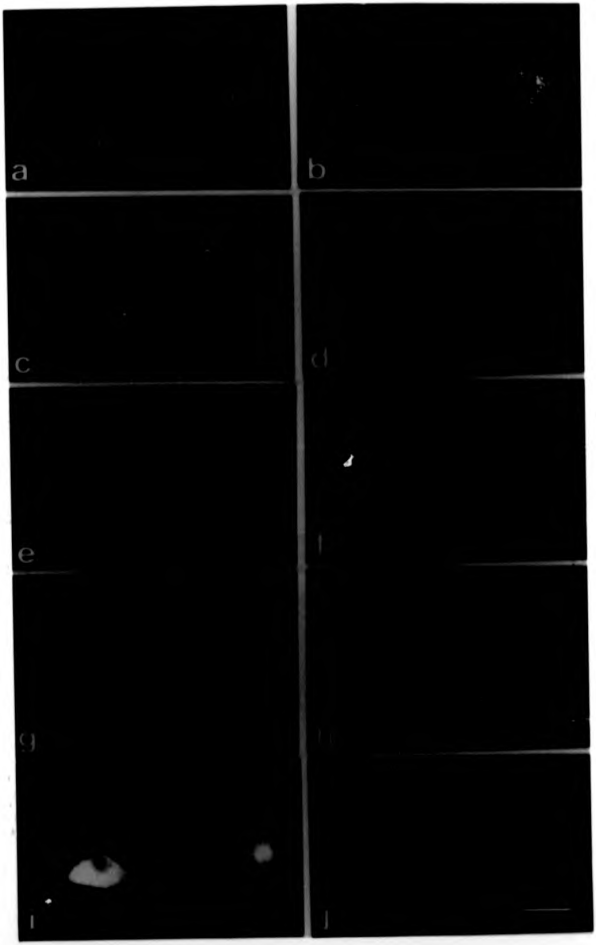
a
b
c
d
e
f
g
h
i
j

During recovery from BFA, TGN-derived structures re-form much faster than those from the *cis*- and *medial*-Golgi (Fig. 28). After 0.5 h of recovery, TGN38 plasma membrane fluorescence is reduced and vesicular structures begin to appear, but only weak Man II fluorescence can be seen (Fig. 28, *a* and *b*). This stage is somewhat similar to that of 0.5 h of incubation in the presence of BFA (Fig. 27, *c* and *d*), suggesting that during recovery from BFA the TGN may reform prior to the *cis*- and *medial*-Golgi. In contrast, Alcade et al., (1992) showed that during the recovery of NRK cells from BFA the *cis*- and *medial*-Golgi reform before the TGN and suggested that the *cis*-/*medial*-/*trans*-Golgi as well as the TGN may fuse with the ER. However, it should be pointed out that when others (Wood et al., 1991; Lippincott-Schwartz et al., 1991) treated NRK cells with BFA, they observed fusion of the TGN with the recycling plasma membrane/endosomal system and the *cis*- and *medial*-Golgi with the ER, as was seen in oligodendrocytes (Fig 27), although they did not examine recovery. The relative rates of recovery from BFA for the different Golgi compartments may therefore depend on cell subtype and whether reassembly originates at the ER and/or the endosomal system.

BFA causes redistribution of tubulin and the TGN in oligodendrocytes

Since the changes caused by BFA are believed to be mediated by microtubules (Alcade et al., 1992; Lippincott-Schwartz et al., 1991a; Wood et al., 1991; Pelham, 1991; Klausner et al., 1992), oligodendrocytes were incubated with BFA and the intracellular distribution of the TGN was assessed in relation to tubulin.

The TGN of BFA-treated oligodendrocytes undergoes a dramatic change in morphology (Fig. 29, *b*, *d*, *f*, *h* and *j*) that has also been described by others (Lippincott-Schwartz et al., 1990; Reaves and Banting, 1992; Alcade et al., 1992). After 4 h in BFA, bright plasma membrane labeling as well as labeling at the extremities of the cellular processes is seen with TGN38 (Fig. 29, *j*); this indicates that TGN38 has cycled to the plasma membrane and that during this cycling, TGN38 was transported to cellular loci as distant as the extremities of the cellular processes (see also Fig. 27).

The initial collapse of the TGN in an area resembling the MTOC and its eventual relocation at the cell surface in the presence of BFA is accompanied by the redistribution of

Fig.2B The asynchronous recoveries of the TGN and the *cis*- and *medial*-Golgi following incubation with BFA

Oligodendrocytes were incubated for 2 h at 37°C in the presence of BFA, washed and incubated in medium minus BFA for 0.5 h (*a* and *b*), 1 h (*c* and *d*), 2 h (*e* and *f*), 4 h (*g* and *h*) or overnight (*i* and *j*). The cells were fixed and labeled for indirect immunofluorescence with TGN38 (DTAF) (*a*, *c*, *e*, *g* and *i*) and anti-Man II (TRITC) (*b*, *d*, *f*, *h* and *j*). After 0.5 h of recovery, TGN38 was seen in a perinuclear location, appearing punctate/tubulovesicular in some cells or decorating the plasma membrane and a MTOC-like location in others (*a*); by contrast, only weak, diffuse Man II fluorescence could be observed at that time (*b*). The localization of TGN38 at 1 h of recovery resembled that at 0.5 h (*c* and *a*) and Man II was distributed in a punctate/vesicular pattern (*d*). TGN38 and Man II were in juxtanuclear, Golgi-like tubulovesicular processes at 2 h (*e* and *f*) and at 4 h most of the TGN and Man II had accumulated in a perinuclear location (*g* and *h*). Both the TGN and the *cis*- and *medial*-Golgi were totally recovered after overnight incubation (*i* and *j*). Bar: 10μm

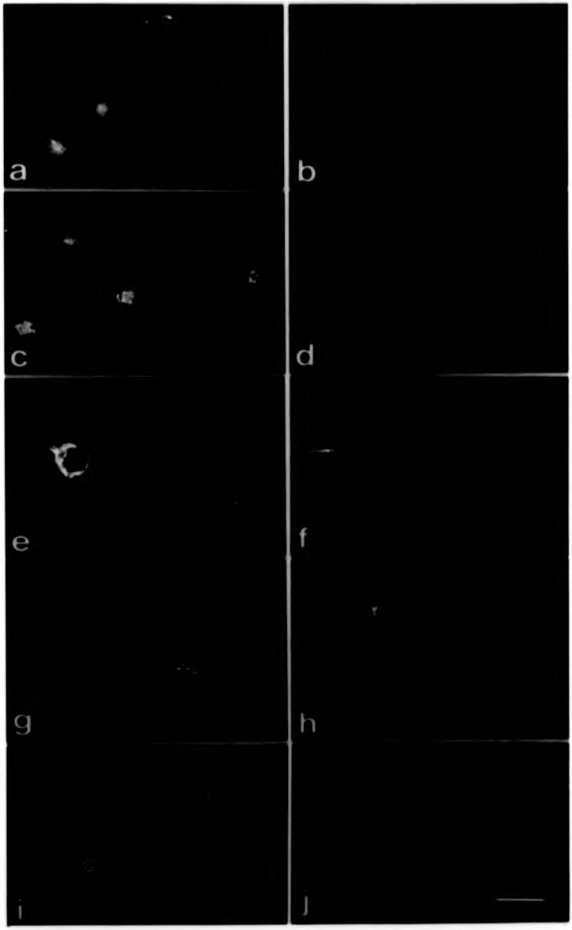
a
b
c
d
e
f
g
h
i
j

Fig. 29 The effects of BFA on tubulin and the TGN.

Oligodendrocytes were incubated for periods of 0 h (*a* and *b*), 0.5 h (*c* and *d*), 1 h (*e* and *f*), 3 h (*g* and *h*) and 4 h (*i* and *j*) at 37°C in the presence of BFA. The cells were fixed and labeled for double indirect immunofluorescence with anti-tubulin (TRITC) (*a*, *c*, *e*, *g* and *i*) and TGN38 (DTAF) (*b*, *d*, *f*, *h* and *j*). Tubulin was found in the cell body and the major processes of control cells (*a*). After 0.5 h and 1 h of incubation in the presence of BFA, tubulin appeared progressively withdrawn to the cell body (*c* and *e*), then reappeared at the processes at 3 h (*g*); by 4 h tubulin was present again in the cell body and major processes (*i*). After 0.5 h in BFA, the fluorescence from TGN38 was reduced by comparison with the control and was mainly seen in a MTOC-like location (*b* and *d*). TGN38-derived fluorescence was very weak and dispersed throughout the cell body at 1 h (*f*), whereas at 3 h it was seen in a perinuclear location, the plasma membrane and dispersed throughout the cell body (*h*). After 4 h in BFA, the fluorescence from TGN38 was approximately as strong as in control cells; however, instead of marking a single perinuclear location, TGN38 decorated the cell body and the extremities of the cellular processes (*j*). Bar: 10μm.

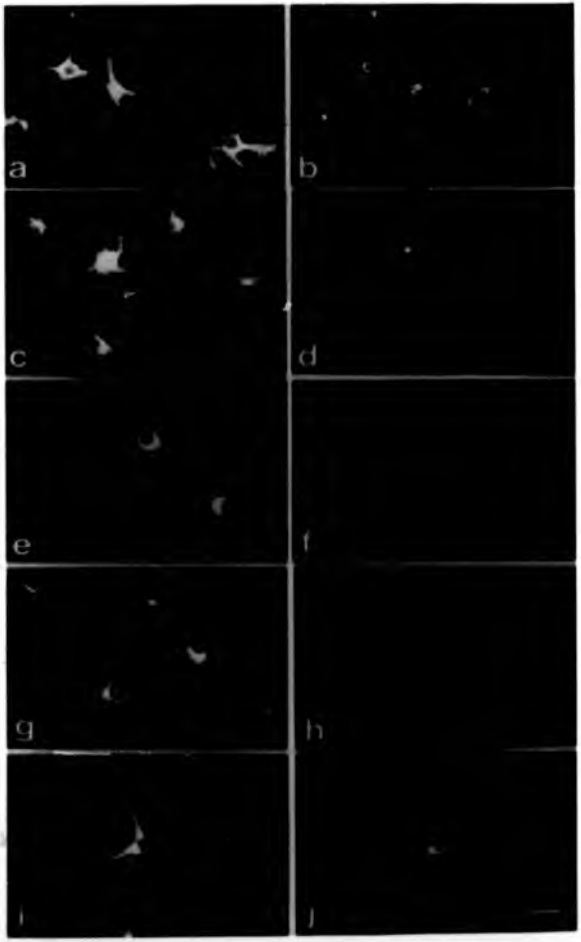
a
b
c
d
e
f
g
h
i
j

cellular tubulin. Tubulin is partly withdrawn from the cell processes after 0.5 h in BFA (Fig. 29, *c*), is mainly present in the cell body after 1 h in BFA (Fig. 29, *e*), reappears at the processes after 3 h in BFA (Fig. 29, *g*) and is present in processes to the same extent as control cells by 4 h in BFA (Fig. 29, *i*).

Phase contrast optics indicate that the changes in tubulin distribution are accompanied by an increase in the size of the cell body, coupled with an initial thinning and eventual re-thickening of the cellular processes (data not shown). It therefore appears that in the presence of BFA, tubulin re-acquires its normal distribution once the recycling endosomal-plasma membrane-TGN system has formed. To our knowledge, no such redistribution of tubulin upon BFA treatment was shown in other cell types. BFA may either affect microtubules directly since microfilaments and intermediate filaments that could support microtubules in other cell types are absent from oligodendrocytes, or indirectly via MAPs and/or associated lipids.

When oligodendrocytes are recovering after 2 h of incubation in the presence of BFA (i.e. before the complete formation of the recycling endosomal/plasma membrane/TGN system), punctate tubulin staining is seen in some areas of the cellular processes and TGN38 decorates a perinuclear location and tubulovesicular structures at 2 h of recovery (Fig. 30, *a* and *b*). At 4 h of recovery, tubulin is distributed sparsely throughout the cellular processes while TGN38 is still present in a perinuclear location in and tubulovesicular processes (Fig. 30, *c* and *d*). It therefore appears that tubulin localizes in similar but not identical compartments during incubation with and recovery from BFA. Abundant tubulin at the cellular processes with completely recovered TGN is only seen after overnight recovery (Fig. 30, *e* and *f*). In cells that are incubated with BFA for longer than 2 h, recovery of tubulin and the TGN requires at least 24 h (results not shown).

Fluorescent ceramide labeling of BFA-treated cells.

C_6-NBD-Cer and C_5-DMB-Cer label the Golgi in a variety of cell types (Lipsky and Pagano, 1983; Pagano et al., 1989; Pagano et al., 1991), most probably by interacting with Golgi compartment-specific lipids (Pagano et al., 1989). Therefore, oligodendrocytes were incubated with BFA, fixed and incubated with either C_6-NBD-Cer or C_5-DMB-Cer in order to

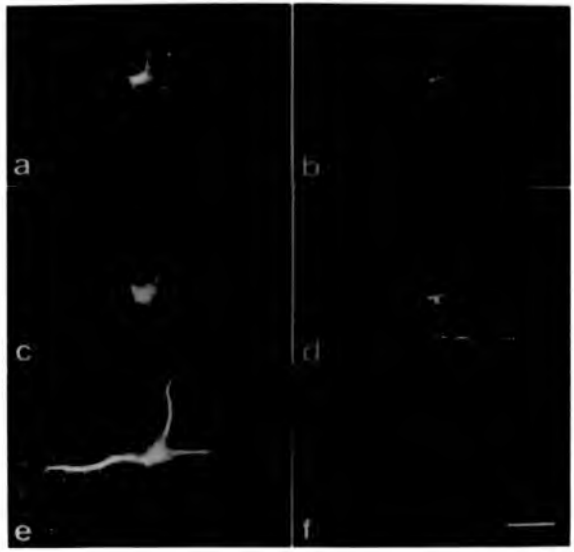

Fig. 30 The distribution of tubulin and the TGN in oligodendrocytes recovering from BFA

Oligodendrocytes were incubated in the presence of BFA for 2 h at 37°C, washed and permitted to recover in the absence of BFA for 2 h (*a* and *b*), 4 h (*c* and *d*) or overnight (*e* and *f*). The cells were fixed and labeled for indirect immunofluorescence with anti-tubulin (TRITC) (*a*, *c* and *e*) and TGN38 (DTAF) (*b*, *d* and *f*). At 2 h of recovery, tubulin was seen in the cell body as well as in the origins and at discrete areas along the major process (*a*), at which time TGN38 labeled tubulovesicular processes emanating from a perinuclear location (*b*). After 4 h of recovery, tubulin accumulated in a perinuclear location reminiscent of the MTOC and thin strands of tubulin were present in the major processes (*c*), when TGN38 fluorescence was seen in a perinuclear location and in associated tubulovesicular processes (*d*). Tubulin and the TGN assumed their normal distributions after overnight recovery (*e* and *f*). Bar: 10μm.

assess the BFA-induced redistribution of Golgi-specific lipids.

Golgi labeling is seen in non-BFA-treated controls (Fig. 31, *c* and *d*). In BFA-treated oligodendrocytes C_6-NBD-Cer is distributed throughout the cytoplasm (Fig. 31, *g*), while C_5-DMB-Cer labeling is seen throughout the cell body and at the sites where the major processes exit from the cell body (Fig. 31, *h*). C_6-NBD-Cer labeled intracellular compartments and the plasma membrane of BFA-treated oligodendrocytes at the light level, since substantial amounts of fluorescence were found in the back-exchange medium by comparison with controls. However, since back-exchange could not remove plasma membrane-associated C_5-DMB-Cer (also see Pagano et al., 1991), it was not possible to tell whether more compartments than the plasma membrane had been labeled with C_5-DMB-Cer in BFA-treated oligodendrocytes.

In order to determine the structures in which the *trans*-Golgi and TGN lipids reside in BFA-treated oligodendrocytes, live cells were incubated with BSA-colloidal gold and C_6-NBD-Cer. In control cells BSA-colloidal gold labels endosomes and C_6-NBD-Cer the *trans*-Golgi and the TGN (Fig. 32, *a*). By contrast, in BFA-treated oligodendrocytes BSA-gold and C_6-NBD-Cer accumulate in tubulovesicular processes such as those observed by Lippincott-Schwartz et al., (1991a) and in endosomes (Fig. 32, *b* and *c*). This probably means that in BFA treated oligodendrocytes C_6-NBD-Cer accumulates in a fused plasma membrane/endosomal/TGN compartment, physically separated from the *cis-/medial-/trans*-Golgi/ER compartment (see Fig. 27).

Since the accumulation of C_6-NBD-Cer in the Golgi is probably via recognition of Golgi-specific lipids, the present data further suggest that after 3 h in BFA endogenous TGN lipids as well as proteins (such as the one recognized by TGN38, Lippincott-Schwartz et al., 1991a and M6PRs, Wood et al., 1991) also redistribute to the recycling plasma membrane/endosomal/TGN compartment (Fig. 27, *g*).

The recycling of transferrin is unaffected by BFA in oligodendrocytes

Cultured oligodendrocytes possess high affinity transferrin (Tf) receptors, but the number of Tf receptors in these cells is at least two orders of magnitude lower than in most other cell types (Espinosa and Foucaud, 1987). In order to examine the function of the distal regions

Fig. 31. C_6-NBD-Cer and C_5-DMB-Cer labeling of BFA-treated, fixed oligodendrocytes.

Oligodendrocytes were incubated for 3 h at 37°C in the absence (*a*, *b*, *c* and *d*) or presence (*e*, *f*, *g* and *h*) of BFA, fixed, labeled with C_6-NBD-Cer (*c* and *g*) or C_5-DMB-Cer (*d* and *h*) and back-exchanged with DF-BSA. In oligodendrocytes not previously treated with BFA, C_6-NBD-Cer and C_5-DMB-Cer labeled Golgi compartments (*c* and *d*). By contrast, in BFA-treated cells C_6-NBD-Cer labeled the plasma membrane, cytoplasm and a perinuclear location (*g*), while C_5-DMB-Cer labeled the cell body, plasma membrane and beginnings of the branching processes (*h*). Plasma membrane-associated fluorescence could be back-exchanged from cells incubated with C_6-NBD-Cer but not C_5-DMB-Cer. Bar: 10μm.

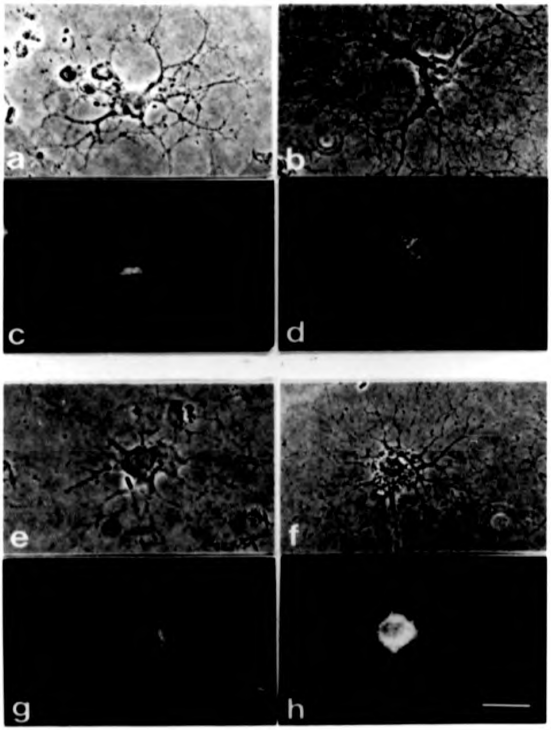
a
b
c
d
e
f
g
h

Fig. 32 BSA-colloidal gold and C_6-NBD-Cer colocalize in BFA-treated cells.

Oligodendrocytes on aclar squares were incubated for 2 h 40 min at 37°C in the absence (*a*) or presence (*b* and *c*) of BFA, then incubated with BSA-colloidal gold for 5 min, followed by C_6-NBD-Cer/DF-BSA for 15 min, in the continued absence (*a*) or presence (*b* and *c*) of BFA. The cells were fixed, incubated with DAB and photobleached, then processed for electron microscopy. Cells not previously incubated with BFA accumulated C_6-NBD-Cer in the TGN and BSA-gold in endosomes (*a*, arrow). By contrast, in BFA-treated cells C_6-NBD-Cer and BSA-gold colocalized in long, tubulovesicular processes (*b*, arrow) and endosomes (*c*, arrow). Bar: 500nm.

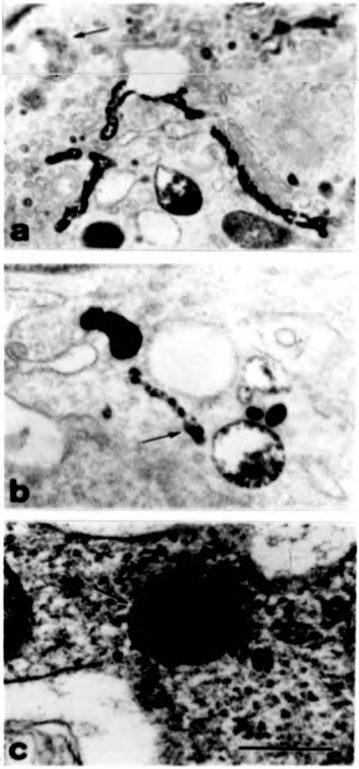
a
b
c

of the secretory pathway in BFA-treated oligodendrocytes, cells at 6 d of differentiation were incubated for 2 h in the presence of BFA, loaded with [^{125}I]Tf for 1 h and the amounts of cell-associated [^{125}I]Tf were determined at different time points (Fig. 33). The uptake of [^{125}I]Tf was specific, since incubation with a 100-fold excess of unlabeled Tf caused a 3-4 fold decrease in the amount of cell-associated radioactivity.

Quantitative measurements showed that 50% of the cell bound radioactivity was released in approximately 3.5 min and that the rate of efflux of cell-associated Tf was the same as in controls, indicating that BFA does not affect receptor-mediated recycling in oligodendrocytes. In an analogous experiment, Lippincott-Schwartz et al., (1991a) loaded NRK cells with [^{125}I]Tf in the absence of BFA and measured the cell-associated radioactivity during subsequent incubation in the presence of BFA. They also found that BFA did not affect the cycling of Tf, but by comparison to oligodendrocytes NRK cells released 50% of the cell bound radioactivity in approximately 7 min. Therefore BFA appears not to impair vesicular traffic between the plasma membrane and the TGN/endosomal network in oligodendrocytes.

BFA alters the metabolism of C_6-NBD-Cer

In order to determine whether the BFA-induced redistribution of the secretory pathway in oligodendrocytes is accompanied by changes in sphingolipid metabolism, the cells were fed with fluorescent Cer analogues in the presence of BFA. Although control and BFA-treated oligodendrocytes metabolize C_6-NBD-Cer to the same extent, the C_6-NBD-Cb/SM ratio is increased in BFA treated cells, although the C_6-NBD-GalC/GlcC ratio is unaffected (Fig. 34). This change in the metabolism of C_6-NBD-Cer in BFA-treted oligodendrocytes is only noted after the first 3 h of incubation and becomes more pronounced with increased time in BFA. This might mean that the change in the metabolism of C_6-NBD-Cer in BFA-treated oligodendrocytes occurs after the fusion of the TGN/endosomal/plasma membrane and the *cis-/medial-/trans*-Golgi/ER systems (see Fig. 27, *g* and *h*). The increases in the C_6-NBD-Cb/SM ratios persist, even after 2 h of recovery and/or the presence of nocodazole, a drug that disrupts microtubule organization and disperses the Golgi (Kreis, 1990). These experiments show that once the BFA-dependent change in the metabolism of C_6-NBD-Cer

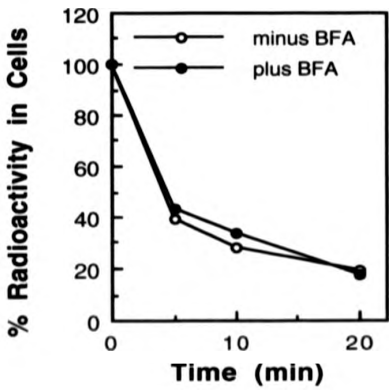

Fig.33 The release of transferrin (Tf) by BFA-treated oligodendrocytes

Oligodendrocytes were washed with RPMI and incubated in RPMI (± BFA) for 2 h at 37°C. The cells were washed, incubated with [^{125}I]Tf in RPMI for 1 h at 37°C, then washed several times at 4° C. The cells were warmed to 37°C for the indicated times, solubilized in 1M NaOH and scraped into vials, when the cell-associated radioactivity was measured.

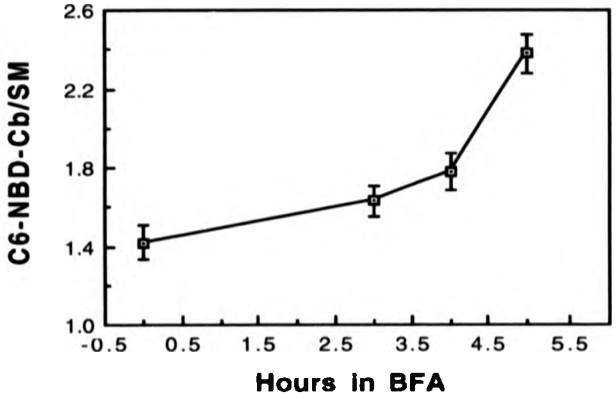

Fig. 34 The metabolism of C_6-NBD-Cer in BFA-treated oligodendrocytes

Oligodendrocytes were incubated at 37°C in medium containing BFA for the indicated times. The cells were then incubated for 2 h at 37°C with C_6-NBD-Cer in the continuous presence of BFA and the fluorescent lipids were identified and quantitated as described in Materials and Methods. Although the amounts of metabolized C_6-NBD-Cer/mg cellular protein were identical in BFA-treated and control cells, the ratio of C_6-NBD-Cb/SM increased in BFA-treated cells, whereas the C_6-NBD-GalC/GlcC ratio was unchanged.

has occurred in oligodendrocytes, it persists during the (slow) restructuring of the secretory pathway and is independent of the precise structure of the Golgi and the microtubule cytoskeleton. Therefore BFA may cause extensive alterations in the enzymic machinery involved in sphingolipid metabolism in oligodendrocytes.

The relative amounts of metabolized C_6-DMB-Cer and the C_5-DMB-Cb/SM and C_5-DMB-GalC/GlcC ratios were identical in BFA-treated cells and controls, indicating that metabolism of C_5-DMB-Cer is unaffected by BFA-induced changes. Additionally, the change in the C_6-NBD-Cb/SM ratio was not observed in BFA-treated Type-1 astrocytes, although it was not examined whether in Type-1 astrocytes BFA has the same effects on organelles of the secretory pathway as in oligodendrocytes. Therefore, the change in Cb/SM ratio may only take place in oligodendrocytes in these cultures and depend on the use of a Cer analogue that recognizes lipids of the recycling TGN/plasma membrane/endosomal system. The finding that BFA affects the metabolism of C_6-NBD-Cer in oligodendrocytes but not astrocytes was not too surprising, since several other effects of BFA are cell-type specific (for review see Pelham, 1991) and BFA is known to cause changes in sphingolipid metabolism. When different cell types were fed with radiolabeled sphingolipid precursors in the presence of BFA, radiolabeled Cbs accumulated (van Echten et al., 1990; Young et al., 1990). Linardic et al., (1992a, b) reported a BFA dose-dependent decrease in cellular SM levels in HL-60 leukemia cells and attributed it to BFA acting to bring pools of SM in contact with sphingomyelinase. In contrast, Brüning et al., (1992) found an increase in C_8C_8-SM but not C_8C_8-GlcC when C_8C_8-Cer was fed to BFA-treated CHO cells; they proposed that the Golgi/ER fusion may make more substrate available to ceramide:phosphatidylcholine phosphocholinetransferase thought to reside in the *cis*- and *medial*-Golgi, thus favoring SM biosynthesis. However, it is not clear why the relative amount of C_8C_8-GlcC was not increased, since the intermixing of the Golgi with the ER should also favor GlcC biosynthesis by making more Cer available to UDP-glucose:glucotransferase, which is located in a pre- and the *cis*-Golgi compartments (Futerman and Pagano, 1991). Since these other workers did not examine the BFA-induced redistributions of the secretory pathway in each cell type by immunocytochemistry, absolute comparisons with oligodendrocytes are not possible.

It therefore appears that BFA-induced changes in sphingolipid metabolism may be cell-

type specific, therefore the exact effects of BFA must be determined for a particular cell type with respect to rearrangements in the secretory pathway. The present data also suggest that the sphingolipid analogue one uses is important, since the structure of the Cer analogue may determine the site(s) of intracellular metabolism and transport by preferentially associating with different Golgi subcompartments through recognition of specific lipids.

5.3 Discussion

Since little or no metabolism of fluorescent Cers occurred at the time these lipids are in the Golgi, Cer metabolism may be a prequisite for exit from the Golgi. Cells of the oligodendrocyte lineage could convert C_6-NBD-Cer to increasingly higher proportions of C_6-NBD-GalC and smaller proportions of C_6-NBD-SM as a function of differentiation to the oligodendrocytic phenotype. This finding was in agreement with the conversion of C_6-NBD-Cer to C_6-NBD-GalC and -SM (Di Biase et al., 1991) and with GalC marking differentiation (Raff et al., 1978; Bansal and Pfeiffer, 1985; Gard and Pfeiffer, 1989; Wood and Bunge, 1984). It was puzzling however that little C_5-DMB-Cb was produced from C_5-DMB-Cer throughout development, although Pagano et al., (1991) have shown that C_5-DMB-Cer is predominantly converted to C_5-DMB-SM in various non-myelinating cell types. These data suggested that C_6-NBD-Cer and C_5-DMB-Cer are metabolized in different ways and prompted me to investigate the intracellular sites of their metabolism and traffic in oligodendrocytes.

C_6-NBD-Cer and C_5-DMB-Cer localized in different Golgi subcompartments prior to metabolism, suggesting that localization might be determined by the interaction of their fluorescent FA chains with compartment-specific lipids. Moreover, the subsequent metabolism and transport of C_6-NBD- and C_5-DMB-lipids appeared to depend on the specific Golgi subcompartment which was originally targeted. Accordingly, the initial localization of C_6-NBD-Cer to the *trans*-Golgi and the TGN and C_5-DMB-Cer to Golgi stacks proximal to the TGN in oligodendrocytes may determine the metabolism and transport of these lipids and their products.

Biosynthesis of GalC in oligodendrocytes is thought to take place in the Golgi and at the plasma membrane (including myelin), both in vivo and in vitro (Roussel et al., 1987; Nescovic et al., 1973; Constantino-Ceccarini and Suzuki, 1975; Koul and Jungalwala, 1981). The same might be true for SM (Di Biase et al., 1991). The possible site(s) of GlcC biosynthesis have not been determined in cells of the oligodendrocyte lineage, although a pre- or early-Golgi compartment have been implicated in other cell types (Futerman and Pagano, 1991). C_6-NBD-Cer is converted to C_6-NBD-Cbs and -SM in cells of the oligodendrocyte lineage, and -GlcC and -SM in non-myelinating cells (Lipsky and Pagano, 1983). However, only

small amounts of C_5-DMB-Cer may reach the sites of Cb biosynthesis in oligodendrocytes, because (as in other cells, Pagano et al., 1991) C_5-DMB-Cer was predominantly converted to C_5-DMB-SM. Stein et al., (1989) showed that the metabolic fate of Cers is critically dependent upon the acyl chain composition of the sphingolipid precursor, which these results suggest could be a due to the initial localization of Cers to different Golgi subcompartments. This possibility was tested with the use of BFA, a fungal metabolite that can potentially disconnect the TGN from other Golgi compartments (Klausner et al., 1992; Pelham, 1991).

BFA caused the formation of two separate compartments in oligodendrocytes, the TGN/plasma membrane/endosomal and *cis-/medial-/trans*-Golgi/ER compartments. BFA also caused changes in the metabolism of C_6-NBD-Cer, in that the C_6-NBD-Cb/SM ratio was increased although the extent of C_6-NBD-Cer metabolism was unaffected. However, BFA did not influence the metabolism of C_5-DMB-Cer. The increased C_6-NBD-GalC/SM ratio in BFA-treated oligodendrocytes may be due to C_6-NBD-Cer targeting TGN-specific lipids in the fused TGN/plasma membrane/endosomal system and being metabolized by resident enzymes. The C_6-NBD-Cer metabolites will not diffuse once they have acquired a polar head group and will probably remain trapped in this system, which is physically separated from other Golgi and ER membranes. The fused TGN/plasma membrane/endosomal system must therefore have an increased GalC and decreased SM biosynthetic capacity. In support of this argument, the specific activity of UDP-galactose ceramide galactosyltransferase is much higher in the plasma membrane of oligodendrocytes than in the Golgi during active myelination (Koul and Jungalwala, 1986). Since SM biosynthesis probably occurs at the Golgi and at the plasma membrane (Koval and Pagano, 1991; Di Biase et al., 1991), in BFA-treated cells C_6-NBD-Cer would be more available for (more active) GalC biosynthesis at the fused TGN/plasma membrane/endosomal system only. Concurrently, C_6-NBD-SM biosynthesis may be reduced by only occurring in the fused TGN/plasma membrane/endosomal system and not in the proximal Golgi, and might be further decreased by the action of acid and perhaps neutral (Linardic et al., 1992a, b) sphingomyelinases. The reason why the C_6-NBD-GlcC/SM ratio increases in the presence of BFA is not clear, but may be caused by BFA selectively disrupting the further metabolism of GlcC and C_6-NBD-GlcC accumulating, as was shown when radioactive glucosphingolipid precursors were fed to

cultured murine cells (Young et al., 1989; van Echten et al., 1990). The intracellular compartments of C_6-NBD-Cer and C_5-DMB-Cer localization in the presence or absence of BFA in oligodendrocytes, which probably determine the subsequent metabolism and transport of these sphingolipids, are shown in Fig. 35.

The BFA-induced redistribution of tubulin in oligodendrocytes has not been observed in other cell types and it is not clear whether it is linked to the redistribution of the Golgi. The data suggest that BFA causes a rearrangement of the cellular cytoskeleton. Microtubules are particularly abundant in the cytoskeleton of mature oligodendrocytes, both in vivo (Wood and Bunge, 1984) and in vitro (Wilson and Brophy, 1989). Microtubules interact with a variety of proteins including those that mediate their linkage with the Golgi, such as the 110 kDa protein (crosslinking the Golgi with MAP2 in a variety of nonneuronal cell types, Allan and Kreis, 1986) and the 58 kDa protein (Bloom and Brashear, 1989). Additionally, microtubules interact with multiple coat proteins, each of which may be involved in a single transport step (Pelham, 1991) as well as with GTP-binding proteins that may mediate the association of Golgi membranes with coat proteins and could be the sites of BFA action (Kreis et al., 1992). Microtubules may also associate with cell-specific proteins and/or lipids, such as MBP and GalC in oligodendrocytes (Wilson and Brophy, 1989; Dyer and Benjamins, 1989b, respectively). Therefore, the effect of BFA on tubulin may also be cell specific and detected only in cells lacking intermediate filaments and abundant microfilaments in the cell body.

Receptor-mediated recycling of Tf in oligodendrocytes was unaffected in the presence of BFA, despite the dramatic changes in the organelles of the secretory pathway and the corresponding modifications on lipid metabolism. Since iron delivery is also unaffected by BFA in other cell types (Lippincott-Schwartz et al., 1991a), the effects of BFA may be specific to certain cellular functions.

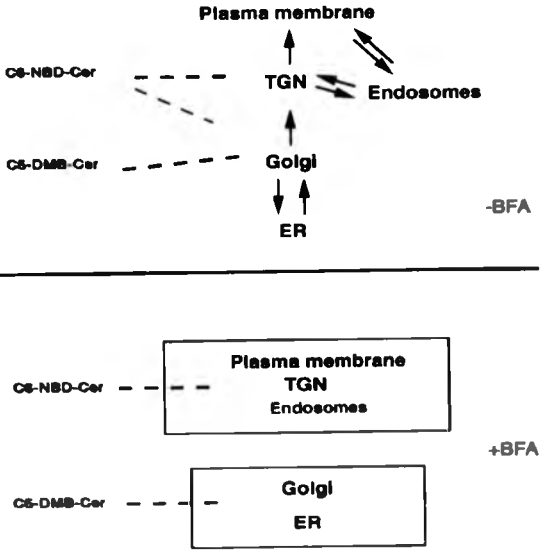

Fig. 35 The localization of C_6-NBD-Cer and C_5-DMB-Cer in BFA-treated oligodendrocytes. In the absence of BFA, C_6-NBD-Cer and C_5-DMB-Cer localize in different, interconnected Golgi compartments via the recognition of specific lipids. BFA causes the segregation of the Golgi from the TGN which leads to the formation of two different recycling compartments: the plasma membrane/TGN/endosomal and the Golgi/ER compartment, which determine the localization and subsequent metabolism of C_6-NBD-Cer and C_5-DMB-Cer.

The association of sphingolipids with cytoskeletons

6.1 Introduction

The association of myelin-specific sphingolipids with the cytoskeletons of glial cells and myelin was examined by immunocytochemistry, lipid analysis and by following the fate of fluorescent sphingolipid precursors.

Establishing the presence of sphingolipids in the cytoskeletons of oligodendrocytes was of particular interest, since Wilson and Brophy, (1989) proposed that lipid-protein interactions in the cytoskeleton may play dynamic and/or regulatory roles during development. GalC may associate with MBP and microtubules (Dyer and Benjamins, 1988, 1989b) and sphingolipids are enriched in the cytoskeleton of myelin (Gillespie et al., 1989). Lipid-protein interactions in the cytoskeletons of oligodendrocytes may matter during the extension of myelin, since the cytoskeleton is known to control cell shape and motility (Niggli and Burger, 1987). Interactions of lipids with the cytoskeleton are also thought to be a prerequisite for vesicular transport (Mateoni and Kreis, 1987; Vale and Hotani, 1988; Steinert and Roop, 1988), and such interactions may be involved in membrane flow in oligodendrocytes.

In a series of initial experiments, immature and mature oligodendrocytes were extracted with Triton X-100. The presence of the major myelin sphingolipid GalC in the cytoskeletons of oligodendrocytes was established immunocytochemically and its distribution was compared with those of microfilaments and microtubules, since microfilaments are found in the extremities of extending processes in immature cells, whereas microtubules are found at the cell body and the major processes throughout development (Wilson and Brophy, 1989). The presence of specific lipid classes in the cytoskeletons of oligodendrocytes was confirmed by lipid analysis.

Another series of experiments attempted to assess whether the specific association and enrichment of sphingolipids in the cytoskeleton of CNS myelin (Gillespie et al., 1989) also occurred in PNS myelin. It was also important to compare the fatty acid (FA) compositions of cytoskeletally associated lipids with those in the intact membrane, since such an analysis might provide clues about the role of FA chain composition during the interaction of specific lipid classes with the cytoskeleton.

In order to visualize the possible interaction of sphingolipids with the cytoskeleton, it was decided to examine if C_6-NBD-Cer and C_6-DMB-Cer or their respective -Cb and -SM

metabolites might be incorporated into the cytoskeleton. If so, a comparison between the compositions of fluorescent and endogenous sphingolipids associating with the cytoskeleton might provide information about structural features that could be important for such associations.

GalC associates with the cytoskeletons of oligodendrocytes

GalC is present in the cytoskeletons of immature and mature oligodendrocytes and the patterns of cytoskeletally-associated GalC fluorescence are strikingly different during development (Fig. 36). Punctate-vesicular and flat sheet-like fluorescence are seen in the cytoskeletons from young and mature oligodendrocytes, respectively. In immature cells, anti-GalC decorates peripheral microfilaments, whereas little GalC colocalizes with microtubules. In these cultures mature oligodendrocytes contain few microfilaments (data not shown; Wilson and Brophy, 1989) and GalC codistributes with tubulin in the cytoskeleton. Mature oligodendrocyte cytoskeletons are more extensive and contain more GalC than their immature counterparts.

The association of GalC with the cytoskeleton of younger oligodendrocytes might be transient and related to microfilament-mediated transport to myelinating processes, whereas some GalC might associate permanently with microtubules in mature cells. The microfilament-rich processes of immature oligodendrocyte cytoskeletons contain CNP (Wilson and Brophy, 1989) and it is possible that GalC, microfilaments and CNP may interact in the peripheral cytoskeleton of these cells. However, since MBP colocalizes with microtubules in the processes of mature oligodendrocytes (Wilson and Brophy, 1989), it is possible that in these cells GalC might interact with MBP and tubulin. It therefore appears that although GalC interacts with the cytoskeleton at all times, GalC associates with different cytoskeletal elements during development. The studies of Dyer and Benjamins, (1989b) suggested that a linking between GalC, MBP and microtubules may exist in the cytoskeletons of oligodendrocytes and Fig. 36 indicates that GalC, MBP and tubulin may interact in the cytoskeletons of mature but not immature cells.

The lipid compositions of oligodendrocyte and myelin cytoskeletons.

The lipid to protein ratio in the cytoskeletons of oligodendrocytes was smaller by comparison with intact cells (Table 4), and a lower ratio is also found in the cytoskeleton of CNS myelin by comparison with the intact membrane (Gillespie et al., 1989; Table 5). Cholesterol is a

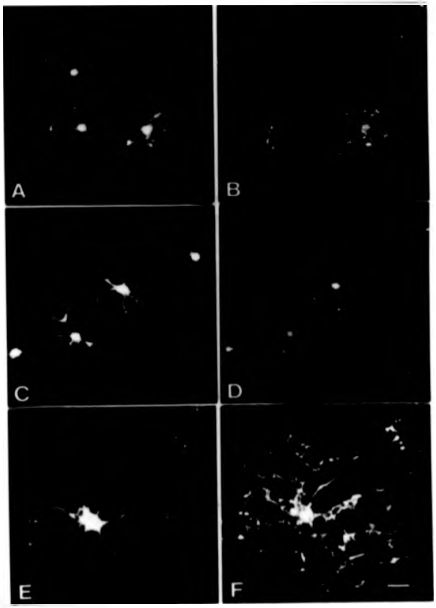

Fig. 36. The association of GalC with the cytoskeletons of oligodendrocytes

Oligodendrocyte progenitors differentiated for 3 d (*A,B,C* and *D*) or 6 d (*E* and *F*), were then extracted with Triton X-100 and examined by double indirect immunofluorescence. *A*: actin (TRITC); *C* and *E*: tubulin (TRITC); *B, D* and *F*: GalC (FITC). The microfilament-rich peripheral processes of immature oligodendrocyte cytoskeletons (*A*) were decorated with anti-GalC in a punctate/vesicular fashion and anti-GalC staining was also present in some cell bodies (*B*). By contrast, microtubules were mainly present in the cell body and major processes of immature oligodendrocyte cytoskeletons (*C*), and did not colocalize with GalC to a great extent (*D*). Microtubules were found in the cell body and major processes in cytoskeletons from mature oligodendrocytes (*E*), where they colocalized with GalC (*F*). Compared to younger cells, the cytoskeletons from mature oligodendrocytes contained more GalC-associated fluorescence. Bar: 10μm.

Table 4 The lipid compositions of cultured rat brain oligodendrocytes and their cytoskeletons.

O-2A progenitors that had differentiated to oligodendrocytes for 4-5 d after the removal of bFGF from the medium, were extracted with a buffer containing Triton X-100 (Wilson and Brophy, 1989). Lipids from unextracted cells or cytoskeletons (CSKs) were separated by TLC, visualized by charring and quantified by densitometry. All values are means of measurements from at least three different experiments, with SD≤10% of each mean value. The values in brackets are for oligodendrocytes cultured for 34 d, recalculated from Fressinaud et al., (1990) for comparison.

	CELLS	CSK
Lipid / protein (μg/μg)	1.92	0.53
Lipid class (weight %)		
Cholesterol	45 (N/A)	57
Cerebroside	3 (8)	5
% Class		
GalC-non-OH	53	46
GalC-OH	43	51
GlcC	4	3
Sulfatide	1 (4)	1
Phospholipid	51 (41)	37
% Class		
PE	43 (48)	45
PC	34 (20)	38
PS	15 (17)	6
PI	2 (10)	2
SM	6 (5)	9

Table 5. Lipid composition of the myelin associated cytoskeleton.

Lipids were extracted from either 3-4 week old rat CNS myelin or its detergent-insoluble cytoskeleton (CSK) and analyzed as described in Materials and Methods. All values were the means of duplicate measurements made on at least three different experiments. The standard deviations were in all cases <15% of each mean value. Values in brackets refer to trigeminal nerve (PNS) myelin and its CSK.

COMPOSITION

COMPONENT	MYELIN	MYELIN CSK
Lipid / protein (μmol/mg)	4.5 (3.4)	2.2 (3.3)
Lipid class (mol%)		
Cholesterol	39 (34)	41 (40)
Cerebroside	11 (12)	35 (27)
% Class		
GalC non-OH	33 (50)	40 (48)
GalC-OH	63 (45)	59 (51)
GlcC	4 (5)	1 (1)
Sulfatide	4 (8)	1 (2)
Phospholipid	46 (46)	23 (31)
% Class		
PE	40 (37)	18 (4)
PC	37 (18)	34 (34)
PS	12 (13)	3 (5)
PI	4 (2)	2 (2)
SM	7 (30)	43 (45)

major lipid component in oligodendrocytes (Podusio et al., 1990; Table 4) and the predominant lipid in their cytoskeletons. Although these immature cells contain little Cb (mainly GalC), this lipid is somewhat enriched in their cytoskeletons, as was also found in CNS myelin (Gillespie et al., 1989). The proportions of individual GalC classes in the cytoskeleton were the inverse of those in intact cells, with GalC-Non-OH and GalC-OH predominating in intact cells and cytoskeletons, respectively. The low GalC-OH/GalC-Non-OH ratio in intact oligodendrocytes may be another indication of their immaturity, since GalC-OH predominates in mature CNS myelin and its associated cytoskeleton (Norton and Cammer, 1984; Gillespie et al., 1989, respectively). GalC-OH, the main Cb in CNS myelin (Norton and Cammer, 1984) displays a high affinity for the cytoskeletons of oligodendrocytes and CNS myelin by comparison to GalC-Non-OH (Gillespie et al., 1989; Tables 4 and 5), therefore the enrichment of GalC-OH in myelin may be due to its strong interaction with the cytoskeletons of oligodendrocytes and myelin throughout development.

The increased proportion of cholesterol in the cytoskeleton of oligodendrocytes is mainly accounted for by a complementary decrease in phospholipids (Table 4). The phospholipid composition in the cytoskeleton is different from that in intact cells, in that SM is increased in the cytoskeleton with a concomitant decrease in PS. SM is also increased and PS decreased in the cytoskeleton of CNS myelin, but the increase in SM is much greater and mostly accounted for by a concomitant decrease in PE (Gillespie et al., 1989; Table 5). This suggests that not only GalC but also SM, another sphingolipid, displays a strong affinity for the cytoskeleton of myelin and oligodendrocytes.

The strong affinity of various sphingolipids for cellular cytoskeletons has been known for some time (Sakakibara et al., 1981; Gillespie et al., 1989; Packham et al., 1991; Gillard et al., 1991, 1992), and at least one protein is thought to be sorted through the Golgi via an interaction of its GPI-anchor with glycosphingolipids (Brown and Rose, 1992). Many GPI-anchored proteins are insoluble in Triton-X-100 (Low, 1989), leading to speculation that sphingolipids may mediate contact between cytoskeletal elements and membrane proteins containing covalently attached lipids. However, covalently attached lipids may also be involved in interactions other than with the cytoskeleton, since PLP contains at least two molecules of palmitate per polypeptide chain (Bizzozero and Lees, 1986) but either does not

interact at all with the cytoskeleton in rat CNS myelin (Gillespie et al., 1989) or to a very small extent in rabbit CNS myelin (Pereyra et al., 1988).

The cytoskeleton of CNS myelin contains less lipid per mg protein than the intact membrane (Table 5; Gillespie et al., 1989). By contrast, the lipid/protein ratios in PNS myelin and its associated cytoskeleton are very similar (Table 5).

Although cholesterol is enriched in the cytoskeleton of myelin (mainly PNS) (Table 5), the major differences between myelin and its associated cytoskeleton are in the sphingolipids and phospholipids. The Cbs are proportionately enriched and the total phospholipids depleted in the cytoskeleton. The relative proportions of individual Cb classes do not vary significantly between myelin and its cytoskeleton. PE is significantly reduced, while SM is the most abundant phospholipid in the cytoskeleton. The differences in lipid composition between CNS myelin and its associated cytoskeleton are analogous to the ones found by Gillespie et al., (1989) and comparison with PNS myelin shows that the strong affinity of sphingolipids for the cytoskeleton is not restricted to CNS myelin and oligodendrocytes. Sphingolipids are the only lipids that show a consistent proportionate increase in the cytoskeletons of CNS, PNS myelin and oligodendrocytes.

Lipids of the cytoskeleton are enriched in saturated fatty acids.

Since the lipid compositions of myelin and its associated cytoskeleton are markedly different (Table 5), a comparison of their FA compositions might help understand why specific lipid classes display a preferential association with the cytoskeleton. This analysis was only performed on CNS tissue, since the differences in lipid composition between CNS and PNS myelin and their respective cytoskeletons are comparable (Table 5).

Myelin and cytoskeletal lipids differ in their FA compositions and these differences are predominantly accounted for by PE, PC and SM (Table 6).

24:0 and 24:1 are the main FAs in myelin GalC (Norton and Cammer, 1984). The FA compositions of cytoskeletally-associated Cbs are almost identical to those in myelin (Table 6). Therefore, although Cbs are enriched in the cytoskeleton, association of Cbs with the cytoskeleton may not have a specific FA composition requirement.

Table 6: The main differences between the fatty acid classes of lipids found in CNS myelin and its associated cytoskeleton. The results are the means of at least two different duplicate experiments. Only significant differences are shown and the Student's *t* - test P-values were always <0.05.
M: Myelin, C: Cytoskeleton. DMA: Dimethylacetal, a plasmalogen derivative. ND: Not detected.

LIPID CLASS

	CER		SULF		PE		PI		PS		PC		SM	
FATTY ACID	M	C	M	C	M	C	M	C	M	C	M	C	M	C
14:0			2.4	9.0										
16:0			6.3	9.7							31.8	54.4	30.2	41.6
18:0							39.3	20.8						
Total Sats	54.8	55.6	48.0	62.8	15.2	23.5	45.3	33.9	53.9	54.7	56.7	77.5	59.6	75.9
14:1			2.4	4.9										
18:1							8.3	12.7	26.0	21.9	32.3	16.4		
20:1					4.6	8.8								
24:1			13.6	7.7									22.3	16.7
Tot. Monoenes	36.2	35.3	33.0	23.1	24.1	31.4	11.0	15.0	33.5	37.0	36.2	18.5	27.7	20.2
18:1 DMA					11	5.1								
Total DMA					31.2	27.0								
20:4 (n-6)					7.7	3.9	25.4	3.5	2.2	.9	1.9	.4		
22:2 (n-6)													2.6	.7
22:4 (n-6)					5.7	2.7					1.6	1.0		
Total (n-6) PUFA	4.0	2.9	4.8	2.5	15.3	8.4	30.5	8.5	5.1	1.9	5.3	1.6	2.6	.7
22:6 (n-3)							5.4	11.6						
Total (n-3) PUFA	ND	ND	1.4	ND	12.3	5.6	5.8	14.6	3.2	2.5	1.2	1.2	ND	ND

Cytoskeletally-associated sulfatides are enriched in saturated FAs (mainly 14:0 and 16:0), while the monoenes (mainly 18:1 and 24:1) are approximately halved and PUFAs are either depleted or not detected in the cytoskeleton, with the exception of 20:4(n-6) and 22:4(n-6), whose proportions do not change.

The proportions of all the saturated FAs and monoenes are increased in cytoskeletally-associated PE; this increase is primarily due to the approximate doubling of the 20:1 species. Total plasmalogens (see Table 6 under dimethylacetals: DMA) are proportionately decreased in the cytoskeleton and this is due to a halving in the amount of 18:1, the main plasmalogen in myelin PE (Norton and Cammer, 1984). Total PUFAs are also decreased to approximately half in the cytoskeleton, which is principally reflected in the 20:4(n-6), 22:4(n-6) and 22:6(n-3) species.

The decrease in cytoskeletally-associated PI is mainly due to an almost halving in the proportion of 18:0 by comparison with myelin; 18:0 is the major FA in myelin PI, representing approximately 40% of the total FA (Table 6). The proportions of the 20:1 monoenes are approximately quadrupled in the cytoskeleton and the 20:4(n-6) PUFAs, the major PUFAs in myelin PI, can account for the major decrease of total (n-6) PUFAs in cytoskeletally-associated PI. Uniquely, the (n-3) PUFAs of PI are the only cytoskeletally-associated PUFAs that are proportionately enriched.

Only small differences are noted in the FA compositions of myelin and cytoskeletally-associated PS; the main difference is in the proportion of 24:1, which is depleted in the cytoskeleton.

The predominant FA in myelin PC is 16:0 (Norton and Cammer, 1984); the proportion of this FA is increased in the cytoskeleton, making up more than 50% of the cytoskeletally-associated FA in PC (Table 6). By contrast, the proportion of 18:1, the main monoene in PC, is approximately halved in the cytoskeleton, leading to a corresponding halving in the total cytoskeletally-associated monoenes. The (n-6) PUFAs are also decreased in cytoskeletally-associated PC.

In SM, saturated FAs account for approximately 55 and 75% of the total FAs in myelin and the cytoskeleton, respectively (Table 6). These differences are mainly due to a proportionate increase in cytoskeletally-associated 18:0, the major FA in myelin SM. The major differences

in the monoenes and PUFA content of cytoskeletal SM are decreases in 24:1 and 22:2(n-6) in the cytoskeleton.

In summary, FA analysis of individual myelin and cytoskeletal lipid classes, which was also confirmed by total FA analysis (data not shown), suggested that the cytoskeletally-associated lipid of myelin is enriched in all classes of saturated FAs and depleted in monoenes, (n-6) and (n-3) polyunsaturated FAs (PUFAs) and plasmalogens by comparison with myelin lipid. 16:0 and to a lesser extent 20:0 and 24:0 are proportionately enriched in the cytoskeleton and monoenes (with the exception of 24:1) are depleted, the PUFAs are reduced to approximately 25% and the plasmalogens to 50% of their proportions in total myelin lipid. However, all the FAs present in myelin are also found in the cytoskeleton, indicating that Triton X-100 does not preferentially solubilize lipids that contain a specific FA chain.

Marieri and Low, (1989) have shown that Band 3, a transmembrane ion transport protein in red blood cells, copurifies with phospholipids containing long chain saturated FAs after non-ionic detergent treatment; their work has suggested that the tight association of Band 3 with long chain saturated FAs is necessary for stabilization of Band 3, and it is possible that the enrichment of saturated FAs in the cytoskeleton of myelin may have a similar role.

C_5-DMB-lipids associate with the cytoskeletons of oligodendrocytes after overnight incubation.

Although small amounts of C_5-DMB-lipids associate with the cytoskeletons of oligodendrocytes after 2 and 5 h of incubation at 37°C, overnight incubation is necessary for these lipids to accumulate in the cytoskeleton; however, the relative amounts of metabolic products of C_5-DMB-Cer remain constant after 2 h of incubation (data not shown). Cytoskeletally-associated C_5-DMB-lipids are mainly seen in a perinuclear location and some fluorescence is also present along the major processes (Fig. 37). By contrast, C_5-NBD-Cer and its -SM and -Cb metabolites (Lipsky and Pagano, 1983) do not associate with the cytoskeletons of oligodendrocytes under these conditions.

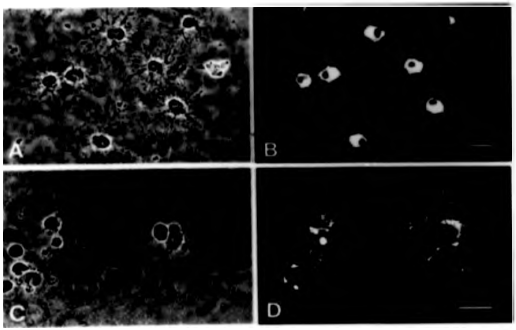

Fig. 37 Colocalization of C_5-DMB lipids with the cytoskeletons of oligodendrocytes.

Oligodendrocytes at 4 d of differentiation were incubated with C_5-DMB-Cer/DF-BSA for 10 min at 37°C, washed and incubated at 37°C overnight. Whole cells (*A*), or cytoskeletons resulting from extraction with Triton X-100 (*C*), were fixed and examined by indirect immunofluorescence. In unextracted cells, C_5-DMB-lipid fluorescence (red channel) was mainly in the cell body, with some fluorescence along the major processes (*B*). C_5-DMB-lipids were also associated with the cytoskeletons of oligodendrocytes, where the fluorescence was present in a perinuclear location and at the processes (*D*). Bars: 10μm

C_6-NBD- and C_5-DMB-Cer are very different as regards their spectral properties, metabolic fates and abilities to label intracellular compartments; this is thought to be a consequence of their fatty-acyl chain compositions (Pagano et al., 1991). The NBD group (see Section 1, Fig. 8) is polar and tends to loop back to the polar region of the membrane (Chattopadhyay and London, 1987, 1988), making the sphingosine backbone the only portion of the molecule with a potential for embedding in the membrane. The limited interaction of C_6-NBD-lipids with the hydrophobic core of the lipid bilayer may account for the total extraction of these lipids with non-ionic detergent. Since the DMB group is mainly non-polar and bulkier than the NBD group, DMB probably remains associated with the non-polar region of the membrane, which may account for the ability of DMB-lipids to interact with the cytoskeleton. However, since overnight incubation was necessary in order to detect sufficient C_5-DMB-lipids (mainly C_5-DMB-SM) in the cytoskeletons of oligodendrocytes, it is possible that equilibration with cellular lipids and/or proteins may also be of importance for interaction with the cytoskeleton. C_5-DMB-lipids are found in a perinuclear location and along the major processes of oligodendrocyte cytoskeletons, where microtubules are also located (Wilson and Brophy, 1989; Fig. 3B). Since microtubules are involved in vesicular transport (Pearse and Robinson, 1990; Vallee and Shpetner, 1990; Pelham, 1991) and microtubules are the major cytoskeletal structure in oligodendrocytes, both in vivo (Wood and Bunge, 1984) and in culture (Wilson and Brophy, 1989), these data suggest that C_5-DMB-lipids may continuously cycle in transport vesicles that move along microtubules and slowly become concentrated on the tubulin cytoskeleton.

Table 7 shows that following overnight incubation, the ratios of cellular to cytoskeletally-associated endogenous lipids (control cells) and unextracted to cytoskeletally-associated C_5-DMB-lipids are rather similar, implying that C_5-DMB-lipids may behave in a manner similar to endogenous lipids. Although C_6-DMB-SM is the predominant cellular and cytoskeletally-associated metabolite of C_5-DMB-Cer, C_5-DMB-Cbs (approximately 95% C_5-DMB-GlcC) are enriched in the cytoskeletons of oligodendrocytes after overnight incubation. This is consistent with the enrichment of endogenous Cbs in oligodendrocytic cytoskeletons (Table 4) and the enrichment of Cbs in the cytoskeletons of CNS and PNS myelin (Gillespie et al., 1989; Table 5).

Table 7: The association of N-[5(5,7-dimethyl borondipyrromethene difluoride)-1-pentanoyl] ceramide (C_5-DMB-Cer) and its cerebroside (Cb) and sphingomyelin (SM) metabolites with the cytoskeletons of oligodendrocytes.

Oligodendrocytes at differentiation stage 4-5 d after the removal of bFGF were incubated overnight in the absence (control cells) or presence of C_5-DMB-Cer. Cellular lipids (control cells) and C_5-DMB-lipids from either unextracted cells or cytoskeletons (CSKs) were quantitated as described in Materials and Methods.

LIPID / PROTEIN RATIO

	Cells	CSK	Cells/CSK
Controls			
(μg lipid/μg protein)	1.92	0.53	3.62
C_5-DMB-Cer-treated			
(pmol lipid/μg protein)			
a) Total lipid	3.68	1.27	2.90
b) Lipid Class			
Cer	0.26	0.06	4.3
SM	3.08	1.01	3.0
Cb	0.34	0.20	1.7

Sphingolipids associate with the cytoskeleton of Schwann cells

The presence of GalC (Fig. 38, *B*) and C_5-DMB-lipids (Fig. 38, *D*) in the cytoskeletons of Schwann cells shows that association of these lipids with the cytoskeleton is not limited to oligodendrocytes. Since in oligodendrocytes most of the C_5-DMB-lipid is C_5-DMB-SM after overnight incubation (Table 7), C_5-DMB-SM may also associate with the cytoskeletons of Schwann cells.

Cytoskeletally-associated GalC colocalizes with peripheral microfilaments in immature oligodendrocytes and with the cell body and process-associated microtubules in mature oligodendrocytes (Fig. 38), which does not reflect the perinuclear distribution of GalC in Schwann cell cytoskeletons (Fig. 38). Although oligodendrocytes and Schwann cells perform the same function in vivo, their morphologies and modes of myelination are very different, and it is possible that cytoskeletally-associated GalC in Schwann cells may have a different role to that in oligodendrocytes.

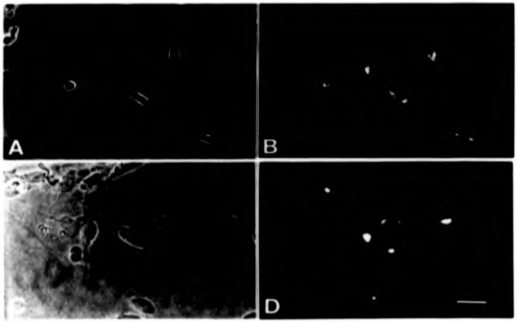

Fig. 38 Sphingolipids associate with the cytoskeletons of Schwann cells.

Schwann cells were incubated at 37°C for 10 min in the absence (*A*) or presence (*C*) of C_5-DMB-Cer/DF-BSA complexes, washed and incubated at 37°C overnight. After extraction with Triton X-100 and fixation, the cytoskeletons from cells incubated in the absence of C_5-DMB-Cer were processed for indirect immunofluorescence using anti-GalC (TRITC) (*B*). Cytoskeletally-associated GalC was seen in a perinuclear location and in structures that resembled vesicles (*B*), whereas the cytoskeletons from cells incubated with C_5-DMB-Cer retained fluorescence in a perinuclear location only (*D*). Bar: 10μm.

6.3 Discussion

Immunocytochemistry showed that GalC associates with the cytoskeletons of oligodendrocytes and Schwann cells, and in oligodendrocytes this was confirmed by lipid analysis. Lipid analysis also showed that by comparison with total oligodendrocyte and myelin membrane lipids, cytoskeletally-associated lipids are enriched in sphingolipids.

Since sphingolipids are also enriched in the cytoskeletons of both CNS and PNS myelin, these lipids may have analogous roles in both systems and their cytoskeletal association may be a prerequisite for myelin function. Much information is currently available about the roles of gangliosides as modulators for transmembrane signals and mediators of cellular interactions (for review see Hakomori, 1990), the role of sphingomyelin in such interactions is beginning to emerge (Kolesnick, 1991) and Dyer and Benjamins, (1992) suggested that GalC and sulfatide may independently mediate Ca^{2+} responses in oligodendrocytes. G_{M3} colocalizes with intermediate filaments in human umbilical vein endothelial cells (HUVEC) (Gillard et al., 1991), but the possible association of gangliosides with the cytoskeleton has not yet been investigated in myelin and myelinating cells. Sphingolipid association with the cytoskeleton may therefore mediate axonal communication and intracellular signaling in myelinating cells and myelin.

It is possible that cytoskeletally-associated GalC and perhaps other sphingolipids may mediate events between the plasma membrane and the cytoskeleton via linker proteins. On the surface of lymphocytes, GM1 ganglioside undergoes lateral redistribution and forms patches after binding cholera toxin, suggesting that GM1-toxin complexes may be indirectly associated with the cytoskeleton via a transmembrane component (Sahyoun et al., 1981); based on similar morphological changes on oligodendrocytes after anti-GalC treatment, Dyer and Benjamins (1989b) proposed that GalC may be important in transmitting transmembrane signals and regulate oligodendrocyte membrane sheet morphology by indirectly associating with microtubules via MBP.

Although GalC associates with the cytoskeletons of oligodendrocytes throughout development, more GalC is seen in the cytoskeletons of mature cells, suggesting that as oligodendrocytes mature GalC accumulates in the cytoskeleton. In young cell cytoskeletons

GalC is linked to microfilaments, that also contain CNP (Wilson and Brophy, 1989); however, in mature cell cytoskeletons GalC colocalizes with microtubules, that contain MBP (Wilson and Brophy, 1989). Therefore, the proposition of Dyer and Benjamins, (1989b) for a possible tubulin/MBP/GalC linkage in the cytoskeleton appears justified in the case of mature cells.

Cytoskeletally-associated GalC may also be involved in the delivery of molecules to myelin via its interaction with CNP and microfilaments in young oligodendrocytes, whereas in mature cells GalC may participate in vesicular transport and/or stabilization of the tubulin cytoskeleton via its interaction with MBP. Thus, the interaction of GalC with the cytoskeletons of oligodendrocytes and CNS myelin may have a role in myelinogenesis (as originally proposed by Gillespie et al., 1989) and in the mature sheath. Cytoskeletally-associated GalC may have similar but not identical functions in Schwann cells since, unlike in oligodendrocytes, Schwann cell development is under axonal control (for review see Jessen and Mirsky, 1991) and the cytoskeleton of Schwann cells contains abundant intermediate filaments (Kelly et al., 1992).

Saturated FAs (primarily 16:0) are enriched and all other FA classes are depleted in the cytoskeleton of CNS myelin, with PE, PC and SM accounting for the major differences. Diacylglycerol and palmitic acid (16:0) form supramolecular complexes and are linked to the actin cytoskeleton via α-actinin (Burn and Burger, 1985). The affinity of saturated FAs for cytoskeletons and their possible involvement in aggregation was exemplified by Packham et al., (1991), who showed that when platelets are induced to aggregate with thrombin ^{3}H-labeled saturated FAs and in particular palmitic acid are rapidly incorporated in PC, whereas ^{3}H-labeled unsaturated FAs are excluded. Therefore, it seems that preferential association of saturated FAs with cytoskeletons, and in particular palmitic acid which is also enriched in cytoskeletally-associated myelin PC and SM, may not be unique to myelin and myelinating cells but might be a general mechanism promoting the strong and rapid association of lipids with cytoskeletons.

The observation that C_5-DMB- but not C_6-NBD-lipids have the potential to associate with the cytoskeleton of oligodendrocytes and Schwann cells also indicates that acyl chain composition may preferentially determine the association of lipids with cytoskeletons, while the association of C_6-DMB-SM and -Cb with the cytoskeletons of oligodendrocytes

reinforces the view that SM and Cbs have a strong tendency to incorporate in the cytoskeletons of myelin and myelinating cells.

The association of myelin proteins with the cytoskeleton during development

7.1 Introduction

The cytoskeleton is involved in a variety of functions via lateral or end-on linkages to other cellular components, including molecules in the plasma membrane (for review see Niggli and Burger, 1987). Immunologically-related proteins that associate with the cytoskeleton can have different functions in different cell types: spectrin in brush border microvilli (densely packed specilizations of intestinal epithelial cells) acts as a microfilament cross-linker, whereas in synaptosomes spectrin appears to control the function of the glutamate receptor (Siman et al., 1985). The myelin-specific proteins MBP and CNP associate with the cytoskeleton of mature CNS myelin (Pereyra et al., 1988; Gillespie et al., 1989). Dyer and Benjamins, (1989a) have speculated that microfilaments may be linked with microtubules and with CNP in cultured oligodendrocytes. In these cells CNP interacts with microfilaments during process extension, whereas MBP interacts with microtubules throughout development (Wilson and Brophy, 1989). MAG also interacts with the cytoskeleton in myelin (Pereyra et al., 1988), and Trapp et al., (1989a) have proposed that since oligodendrocytic MAG is found in multivesicular bodies (MVBs), this protein may be associated with an endocytic pathway that originates in the periaxonal membrane of CNS myelin internodes and terminates in the perinuclear cytoplasm.

These data suggest that the compositions of myelin and oligodendrocyte cytoskeletons change during development and that such changes could be important in myelination. Therefore, initial experiments were aimed at examining which myelin-specific proteins associate with the cytoskeleton at the onset (postnatal day 9, P9) and during active myelination (P15). An examination of the protein composition of the myelin cytoskeleton during development might provide clues about the roles of individual components of the cytoskeleton during myelination. Therefore, rat CNS myelin from these developmental stages was extracted with Triton X-100 in the manner described by Gillespie et al., (1989) and the presence of myelin-specific proteins in the cytoskeleton was established by Western blotting. Additionally, it was hoped that deglycosylation of detergent-soluble and -insoluble myelin fractions followed by immunoblotting would indicate which MAG isoforms associate with the cytoskeleton during development.

The localization of MAG in young and mature oligodendrocytes and its possible association

with the cytoskeleton was examined by immunocytochemistry and Western blotting. Double labeling with anti-MAG and either phalloidin (recognizing F-actin) or anti-tubulin might reveal whether MAG colocalizes with microtubules or microfilaments in intact oligodendrocytes and oligodendrocyte cytoskeletons during development; comparison of these data with those of Wilson and Brophy, (1989) might also indicate whether MAG colocalizes and perhaps interacts with either CNP or MBP during development.

7.2 Results

The protein composition of the cytoskeleton of rat CNS myelin increases in complexity during development.

The myelin extraction buffer system was tested on adult rat CNS myelin by essentially repeating the immunoblotting experiments of Gillespie et al., (1989) with identical results (data not shown).

The myelin cytoskeleton from P9 animals contains approximately half the tubulin and half the 21.5, 18.5 and 17.0 kDa MBPs but very little actin and no CNP (Fig. 39). The association of the MBPs and tubulin in the myelin cytoskeleton before active myelination may be important in establishing a foundation upon which the myelin sheath will eventually be built. Approximately half the actin, all the tubulin and most of the MBP and CNP polypeptides are found in the cytoskeleton at P15. These results show that the association of the 21.5, 18.5 and 17.0 kDa MBPs with the myelin cytoskeleton precedes that of actin and CNP; the association of CNP and F-actin with the cytoskeleton at P15 may mean that these proteins are important during active myelination. The distribution of CNP between the detergent-soluble fraction and the cytoskeleton resembles that of actin at P9 and P15, respectively. All the CNP is detergent-soluble at P9 and most of the smaller polypeptide (CNP1) and all the CNP2 are associated with the cytoskeleton at P15. The finding of CNP and F-actin in the myelin cytoskeleton at P15 may indicate that F-actin is involved in the delivery of CNP to myelin and supports the earlier proposal that cytoskeletally-associated CNP and F-actin interact in the peripheral processes of immature oligodendrocytes (Wilson and Brophy, 1989).

At P9 the 21.5 kDa MBP is enriched in the cytoskeleton; this MBP polypeptide is totally associated with the cytoskeleton at P15 and the studies of Pereyra et al., (1988) and Gillespie et al., (1989) have shown that the 21.5 kDa MBP is exclusively associated with the cytoskeleton in mature myelin. These data suggest that either post-transcriptional modification may influence the extent of interaction of the 21.5 kDa MBP with the cytoskeleton and the form that displays strong affinity for the cytoskeleton predominates during active myelination and in adult myelin, or that the presence of microfilaments (which are essentially absent from P9 myelin) may be necessary for all the 21.5 kDa MBP to

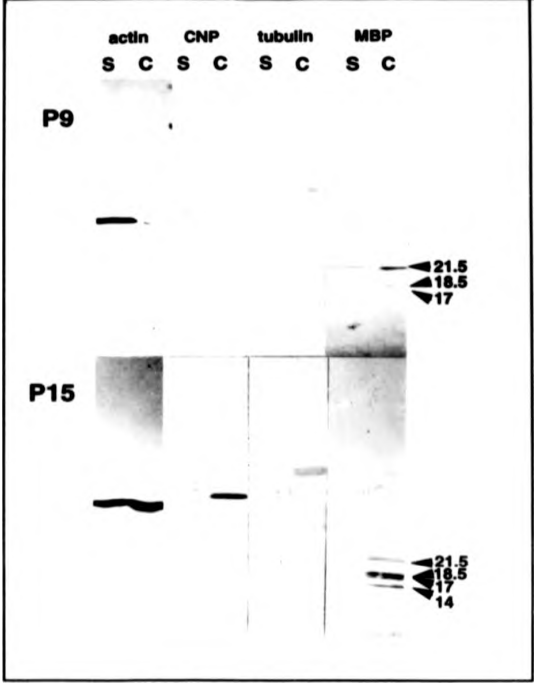

Fig. 39 The distribution of rat CNS myelin proteins between the Triton X-100-soluble (S) and -insoluble cytoskeleton (C) fractions during development.

Rat brain myelin from postnatal days 9 and 15 (P9 and P15) was extracted with Triton X-100 as described in Materials and Methods. The distribution of proteins between the detergent-soluble and cytoskeleton fractions was demonstrated by Western blotting. CNP co-distributed with actin and the distribution of the 21.5, 18.5 and 17.0 kDa MBPs resembled that of tubulin at P9 and P15, respectively. The 14.0 kDa MBP, which was not detected at P9, distributed like actin at P15.

associate with the cytoskeleton.

Approximately half of the 18.5 and 17.0 kDa MBPs are found in the myelin cytoskeleton at P9 and these MBPs are totally associated with the cytoskeleton at P15. The distributions of the 21.5, 18.5 and 17.0 kDa MBPs between the detergent-soluble fraction and the cytoskeleton of myelin, reflect those of tubulin at P9 and P15, respectively, suggesting a structural relationship between these proteins during development. Since approximately half the 18.5 and 17.0 kDa MBPs from mature rat CNS myelin are detergent-soluble (Gillespie et al., 1989) while at P9 these proteins are associated with the myelin cytoskeleton, it is possible that total association with the cytoskeleton is only necessary during the period of active myelination.

The 14.0 kDa MBP is not detected in myelin at P9 but is present at P15, when it distributes almost equally between the detergent-soluble and -insoluble fractions. This data and those of others (Barbarese et al., 1978; Morell et al., 1984) indicate that the 14.0 kDa MBP appears later than the other MBPs and persists in adult myelin. The finding that the 14.0 kDa MBP, CNP and microfilaments associate with the myelin cytoskeleton at approximately the same time, and data showing that this association persists in adult myelin (Gillespie et al., 1989; Pereyra et al., 1988) suggests that the 14.0 kDa MBP, CNP and F-actin might interact during active myelination and in mature myelin.

All the PLP and DM20 are detergent-soluble, both at P9 and P15 (data not shown), as was previously demonstrated for mature rat CNS myelin (Gillespie et al., 1989).

The distributions of actin, CNP and tubulin between the detergent-soluble fraction and the cytoskeleton at P15 are very similar to those found by Gillespie et al., (1989) and Pereyra et al., (1988) for mature myelin, indicating that their pattern of association proteins with the myelin cytoskeleton may have already been established by P15. By contrast, the pattern of association of MBP with the cytoskeleton changes throughout development and may only become established in mature myelin.

MAG associates with the myelin cytoskeleton during myelination

Western blotting indicates that MAG associates with the cytoskeleton of CNS myelin at P9 and P15 (Fig. 40). Most of the S-MAG associates with the cytoskeleton at P9 and this may

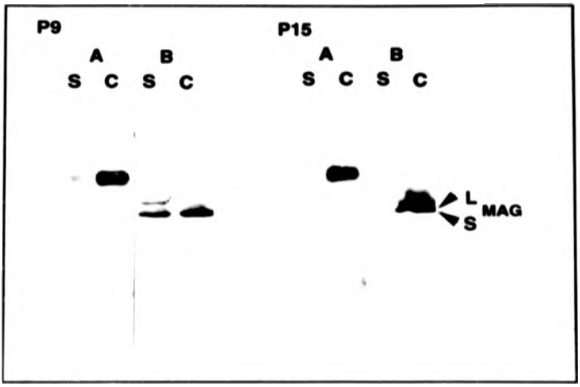

Fig. 40 The association of MAG with the myelin cytoskeleton during development

Rat CNS myelin from postnatal days 9 and 15 (P9 and P15) was extracted with Triton X-100. Equal volumes of detergent-soluble (S) and -insoluble cytoskeleton (C) fractions were incubated in the absence (*A*) or presence (*B*) of endoglycosidase-F and the distribution of MAG was shown by Western blotting. MAG was predominantly (P9) or exclusively (P15) associated with the cytoskeleton. Significant amounts of the small (S-) and large (L-)MAG polypeptides were detergent-soluble at P9 only.

mean that S-MAG and the 21.5 kDa MBP (Fig. 39) are the first myelin-specific proteins that associate with the cytoskeleton of CNS myelin. The strong association of MAG with the cytoskeleton persists at P15 (Fig. 40) and MAG is enriched in the cytoskeletons of CNS and PNS myelin from 4-6 week old animals (data not shown).

A small but significant amount of S-MAG and all of the L-MAG are detergent-soluble at P9 (Fig. 40, Panel *B*), whereas at P15 both of the MAG polypeptides are cytoskeletally-associated (P15, Panel *B*). The distribution of MAG between the detergent-soluble fraction and the cytoskeleton at P9 and P15 resembles that of tubulin and the 21.5, 18.5 and 17.0 kDa MBPs, but not that of actin and CNP (compare Figs. 39 and 40).

In CNS and PNS myelin from 4-6 week old rat, S-MAG partitions mainly and L-MAG totally with the cytoskeleton (results not shown). At this age, the distribution of MAG between the detergent-soluble and cytoskeletal fractions resembles the distributions of tubulin and the 21.5, 18.5 and 17.0 kDa MBPs (Gillespie et al., 1989); this may indicate that the interaction of MAG, tubulin and the MBPs with the cytoskeleton of myelin is important for the stabilization of adult myelin.

MAG-cytoskeleton interactions in oligodendrocytes.

Oligodendrocytes at 4 d of differentiation (Fig. 41, *A*) have smaller cell bodies and less extensive processes in comparison with their more mature 14 d counterparts (Fig. 41, *D*). In immature oligodendrocytes, microfilaments are restricted to peripheral processes (Fig. 41, *B*), whereas MAG is found at the cell body and in the cell periphery where it colocalizes with microfilaments (Fig. 41, *C*). In support of this association, Trapp et al., (1989b) have shown that MAG colocalizes with actin in Schwann cells. Extraction with Triton X-100 indicates that MAG does not associate with the cytoskeleton in immature oligodendrocytes (data not shown). Wilson and Brophy, (1989) demonstrated that F-actin and CNP colocalize in the periphery of immature oligodendrocytes and their cytoskeletons. Since MAG, CNP and microfilaments are found in the peripheral processes of immature oligodendrocytes where MAG does not associate with the cytoskeleton, it is possible that weak interactions between MAG and either microfilaments or CNP may be involved in the transport of MAG to myelin.

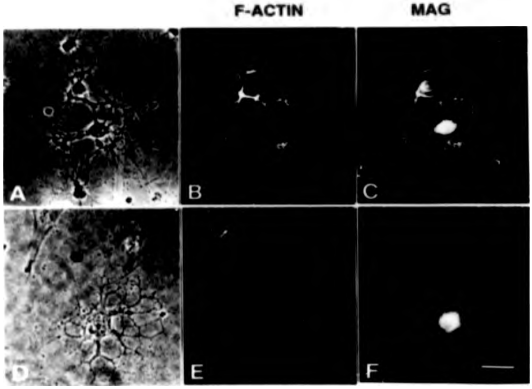

Fig. 41 MAG colocalizes with microfilaments in the elongating processes of immature oligodendrocytes.

O-2A progenitors were permitted to differentiate to oligodendrocytes for 4 d (*A*, *B* and *C*) or 14 d (*D*, *E* and *F*), respectively, in defined medium/1% FCS. The cells were fixed and processed for fluorescence microscopy using phalloidin-TRITC (a stain for microfilaments) (*B* and *E*) and anti-MAG (FITC) (*C* and *F*). MAG and microfilaments colocalized in the processes of oligodendrocytes at 4 d of differentiation, whereas MAG was restricted to the cell body of mature oligodendrocytes that are devoid of microfilaments. An astrocyte that does contain microfilaments is seen in the top left corner in *D* and *E*. Bar: 10 mm.

Mature oligodendrocytes do not contain intermediate filaments and the absence of microfilaments was shown by Wilson and Brophy, (1989) and confirmed by these experiments (Fig. 41, *E*). In these cells, MAG is found predominantly but not exclusively at the cell body (Fig. 41, *F*). I speculated that if MAG does associate with the cytoskeleton of mature oligodendrocytes, it may do so with microtubules. The data show that oligodendrocyte cytoskeletons prepared from cells at 14 d of differentiation (Fig. 42 *D*) contain MAG, that decorates microtubules at the cell body and cellular processes (Fig. 42, *E* and *F*), all the MAG is cytoskeletally-associated at this developmental stage in culture (Fig. 43). The distribution pattern of MAG in the cytoskeleton resembles that of MAG in oligodendrocytes on sections from brain and spinal cord (Sternberger et al., 1979). These results suggest that MAG and tubulin probably interact in the cytoskeletons of mature oligodendrocytes and CNS myelin (Fig. 40).

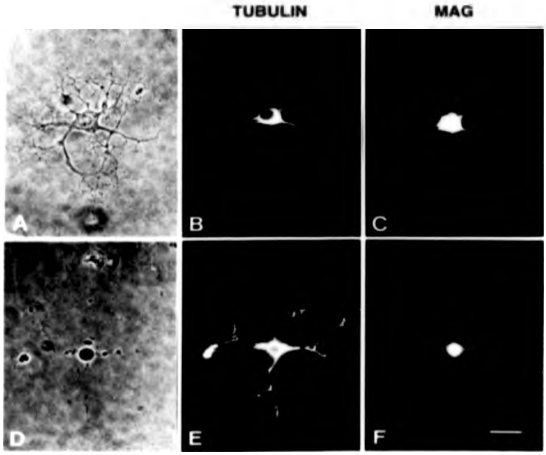

Fig. 42 MAG colocalizes with tubulin in the cytoskeleton of mature oligodendrocytes.

Oligodendrocytes at 14 d of differentiation (*A*, *B* and *C*) or their cytoskeletons (*D*, *E* and *F*) were fixed and processed for double indirect immunofluorescence using anti-tubulin (TRITC) (*B* and *E*) and anti-MAG (FITC) (*C* and *F*). MAG codistributed with tubulin in the cell bodies and in the major processes of mature oligodendrocytes (*B* and *C*) and their cytoskeletons (*E* and *F*). Bar 10mm

Fig. 43 MAG is totally associated with the cytoskeletons of 14-d old oligodendrocytes

Oligodendrocytes at 14 d of differentiation were extracted with Triton X-100. The detergent-soluble (S) and -insoluble cytoskeleton (C) fractions and CNS myelin (MY) from P14 rat were immunoblotted for MAG.

7.3 Discussion

Interactions between the cellular cytoskeleton and the plasma membrane have been implicated in the control of cell shape and movement in a variety of cell types (for review see Carraway and Carothers, 1989) and the extension of myelinating processes from an oligodendrocyte requires a drastic change in cell morphology that probably involves the cellular cytoskeleton (Wilson and Brophy, 1989). The association of myelin-specific proteins with the cytoskeletons of CNS myelin (Pereyra et al., 1988; Gillespie et al., 1989) and oligodendrocytes (Wilson and Brophy, 1989) indicated that specific associations may exist between either MBP and tubulin or CNP and actin in myelin and in oligodendrocytes. The present data show that the cytoskeletons of myelin and oligodendrocytes increase in complexity during active myelination. PLP and DM20 from mature rat brain myelin are solubilized totally by detergent (Gillespie et al., 1989, respectively) as are PLP and DM20 from P9 and P15 rat brain myelin, suggesting that these proteins do not interact with the cytoskeleton of rat CNS myelin.

The late appearance of the 14.0 kDa MBP in myelin (also shown by Rousel and Nussbaum, 1981) suggests that this MBP may have a specific role during the late stages of myelination. Since the 14.0 kDa MBP is the only MBP polypeptide that co-distributes with actin, CNP and tubulin at all times during development, it is possible that the 14.0 kDa MBP may be involved in linking CNP/microfilament with MBP/microtubule complexes. This notion is supported by the Triton X-100 solubilization of both CNP and actin in P9 myelin when the 14.0 kDa MBP is not yet expressed, and by experiments where specific disruption of oligodendrocyte microfilaments results in the simultaneous disruption of microtubules (Dyer and Benjamins, 1989a). Therefore, owing to the late developmental expression of the 14.0 kDa MBP, macromolecular CNP/microfilament/MBP/microtubule complexes may only start forming during the period of active myelination and persist in mature myelin.

The enrichment of the 21.5 kDa MBP in early myelin and its strong association with the cytoskeleton throughout development is in support of a formative and/or stabilizing role for this MBP in myelin, as was previously proposed by Gillespie et al., (1989).

CNP2 is not associated with the myelin cytoskeleton at P9 but is found in the cytoskeletons of P15 and 4-6 week old myelin. Since CNP2 is the only known myelin protein that is

phosphorylated in a cAMP-dependent manner (Bradbury and Thompson, 1984), it is possible that cAMP-dependent phosphorylation of CNP2 may only involve the cytoskeleton during active myelination and in mature myelin. However, since the experiments of Bradbury and Thompson (1984) were performed with myelin from adult animals, it is not known whether cAMP-dependent phosphorylation of CNP2 may also occur during early and active myelination, when phosphorylation may be related to association with the cytoskeleton.

Although radioactive fucose labeling of rat brain at different ages indicates that there may be a change in the MW of MAG during development (Quarles et al., 1983/84), it was not possible to ascertain whether this change occurs in the polypeptide or carbohydrate portion of MAG. In rat and mouse, the mRNA coding for L-MAG is the dominant MAG mRNA at P15, while the mRNA coding for S-MAG dominates at P62 (Frail and Brown, 1984); however, it has never been conclusively shown that the relative levels of deglycosylated L- and S-MAG polypeptides follow the same developmental shift as their respective mRNAs. The finding that in P9, P15 and 4-6 week old rat CNS myelin, S-MAG is the predominant MAG polypeptide, suggests that posttranscriptional regulation and not the relative levels of MAG mRNA may be responsible for the amounts of L- and S-MAG polypeptides in myelin. Such regulation of myelin (and other) proteins is common and was also found in PLP and DM20, when at early ages the relative levels of their respective mRNAs do not correspond to the relative levels of PLP and DM20 (LeVine et al., 1990). The association of MAG with the cytoskeleton of myelin was shown previously (Pereyra et al., 1986); however, these are the first data to show which and how much of each MAG polypeptide associates with the cytoskeleton during development and that MAG only associates with the cytoskeleton of terminally differentiated oligodendrocytes.

MAG is thought to create and maintain the axon/myelin apposition (Quarles, 1983/84) and S-MAG, the deglycosylated form of which primarily partitions with the myelin cytoskeleton throughout development, may be involved in retrograde transport in oligodendrocytes (Trapp et al., 1989a). Since retrograde transport involves microtubules (for review see Turner and Tartakoff, 1989), the possibility that MAG may be involved in such transport is supported further by the colocalization of MAG and microtubules in the cytoskeletons of myelin and mature oligodendrocytes. The particularly specific link between MAG and tubulin is

exemplified in P14 myelin as well as in cultured oligodendrocytes at 14 d of differentiation, where Western blotting shows that all the MAG is found in the cytoskeletal fraction. Trapp et al. (1989a) showed that MAG is present in multivesicular bodies (MVBs) in oligodendrocytes in vivo, and MVBs are similar in structure to the MAG-enriched vesicles that Sternberger et al. (1979) observed in oligodendrocytes stained with anti-MAG on thin sections. It is therefore attractive to hypothesize that the punctate pattern of MAG staining that is observed in the processes of oligodendrocyte cytoskeletons may represent MAG-enriched MVBs in strong association with microtubules during retrograde transport.

Phosphorylation of cytoskeletally-associated proteins in myelin

8.1 Introduction

The phosphorylation state of proteins represents a dynamic balance between the activities of phosphatases and kinases. Phosphorylation/dephosphorylation events lead to changes in the structure of myelin proteins (Ramwani and Moscarello, 1990) and differences in the phosphorylation state of myelin-specific proteins may determine the flexibility with which they interact in vivo. Myelin membrane flexibility may thus be determined by protein phosphorylation at different residues on the polypeptide backbone, which would depend on small differences in protein sequence and the specificities of enzymes available at different loci.

Phosphorylation may control the interaction of cytoskeletal proteins with one another and/or other cellular proteins, since disruption of phosphorylation results in an aberrant organization of the cytoskeleton in retinal ganglion neurons (Nixon et al., 1987). Pathogenic accumulation of abnormally phosphorylated cytoskeletal proteins is characteristic of several neurodegenerative conditions, such as Alzheimer's disease, Pick's disease, amyotropic lateral sclerosis and Parkinsons disease (Johnson and Jope, 1988). Gillespie et al., (1989) showed that the cytoskeleton of CNS myelin is strongly associated with specific proteins and they speculated that the reversible phosphorylation and dephosphorylation of these proteins might regulate interactions between the membrane and the cytoskeleton. Therefore, this initial study aimed to assess

a) if cytoskeletally-associated myelin-specific proteins are a distinct subset, as distinguished by the extent of their in vitro phosphorylation and

b) the possible effect of phosphorylation on the degree of association of proteins with the cytoskeleton.

In order to answer these questions, rat CNS and PNS myelin was phosphorylated with [γ-^{32}P]ATP, extracted with Triton X-100 and the proteins of the detergent-soluble fraction and the cytoskeleton were analyzed by immunoblotting and autoradiography. This study permitted a direct comparison between the amounts of myelin proteins that were either associated with the cytoskeleton or extracted by detergent and the relative extents of their in vitro phosphorylation.

8.2 Results

MBPs that associate with the cytoskeleton are phosphorylated less heavily than Triton X-100-extractable MBPs.

The partitioning of myelin-specific proteins between the soluble and cytoskeleton fractions was independent of *in vitro* phosphorylation and/or the presence of cAMP (data not shown). Gillespie et al., (1989) showed identical protein distributions for non-phosphorylated 4-6 week old rat CNS myelin. Since the extent of myelin protein association with the cytoskeleton is not controlled by *in vitro* phosphorylation, amino acid residues at, or in proximity to, the contact sites with the cytoskeleton might not be phosphorylated.

The MBPs are the major group of phosphorylated myelin proteins in the soluble fraction (Fig. 44, Panel *A2* and *B2*). Of the four MBP variants (21.5, 18.5, 17.0 and 14.0 kDa) found in rat CNS and PNS myelin, the 21.5 kDa MBPs are exclusively and the 17.0 kDa MBPs predominantly associated with the cytoskeleton (Panel *A3* and *B3*). Although the 18.5 and the 17.0 kDa MBPs from both CNS and PNS myelin are enriched in the cytoskeleton, these proteins are more heavily phosphorylated in the soluble fraction. In contrast, the extent of phosphorylation of the 14.0 kDa MBP reflects its relative abundance in the soluble and cytoskeletal fractions, both in CNS and PNS myelin. As a general rule, the MBPs which are enriched in the soluble fraction are phosphorylated to a greater extent than their cytoskeletally-associated counterparts.

PLP and DM20 are not phosphorylated in CNS myelin and detergent-soluble Po is phosphorylated to a greater extent than cytoskeletally-associated Po.

When phosphorylated or non-phosphorylated rat CNS myelin is extracted with Triton X-100, PLP and DM20 are completely solubilized, as was also previously shown by Gillespie et al., (1989) for non-phosphorylated myelin. PLP and DM20 are not phosphorylated by [γ-^{32}P]ATP *in vitro* (Fig. 45, Panel *A2*).

Although Po, the major protein in PNS myelin, is enriched in the cytoskeleton (Fig. 45, Panel *B1* and *B3*), detergent-soluble Po is phosphorylated to a greater extent (Fig 45, Panel *B2*).

In summary, the predominant CNS and PNS myelin proteins that were phosphorylated

Fig. 44: The distribution of phosphorylated MBPs between the Triton X-100-soluble (S) an insoluble cytoskeleton (C) fractions of CNS and PNS myelin.

Rat CNS (*A*) and PNS (*B*) myelin was phosphorylated with [γ-^{32}P]ATP in vitro. The distributi of proteins between the detergent-soluble (S) and cytoskeleton (C) fractions was analyzed SDS-PAGE, Western blotting and autoradiography.

Panel *A1* and *B1*: nitrocellulose transfers of soluble and cytoskeletal fractions stain with 0.1% (w/v) Amido Black, Panel *A2* and *B2*: autoradiograms of the transfers shown in Pa *1*. Panel *A3* and *B3*: Western blots showing the distribution of MBPs between the soluble a cytoskeletal fractions. Detergent-soluble MBPs incorporated more [γ-^{32}P] label than th cytoskeletally-associated counterparts.

A

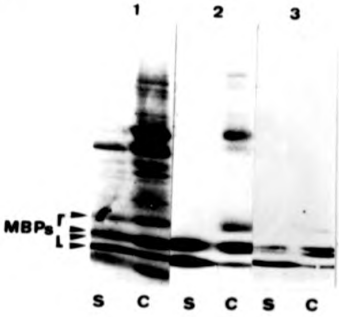

B

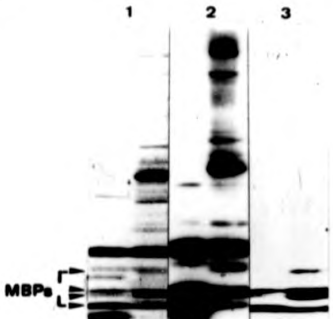

Fig. 45: The distribution of PLP and DM20 (CNS myelin) and Po (PNS myelin) between the detergent-soluble (S) and -insoluble cytoskeleton (C) fractions is independent of in vitro phosphorylation.

Rat CNS (*A*) or PNS (*B*) myelin was phosphorylated in vitro with [γ-^{32}P]ATP and the distribution of proteins between the soluble and cytoskeleton fractions was analyzed by Western blotting and autoradiography.

Panel *A1* and *B1*: nitrocellulose transfers of soluble and cytoskeleton fractions stained with 0.1% Amido Black. Panel *A2* and *B2*: autoradiograms of the transfers in Panel 1. Panel *A3* and *B3*: Western blots showing the distributions of PLP and DM20 (*A*) and Po (*B*) between the soluble and cytoskeletal fractions. PLP and DM20 were totally extracted by Triton X-100 (Panel *A3*) and were not phosphorylated (Panel *A2*). Although Po was enriched in the cytoskeletal fraction (Panel *B3*), more [γ-^{32}P] label was incorporated in soluble Po (Panel *B2*).

A

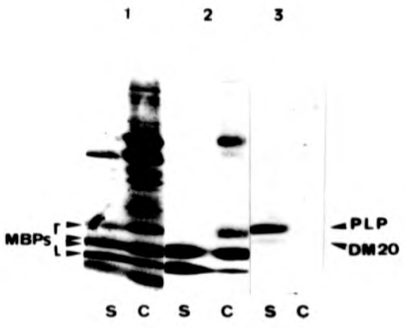

B

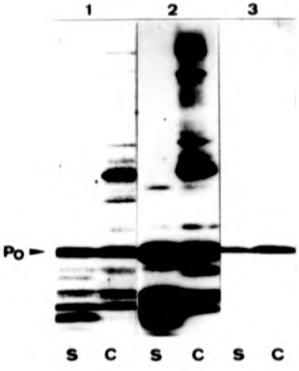

in vitro (the MBPs and Po) also associated with the cytoskeleton, and the detergent-soluble proteins were phosphorylated more heavily.

The cytoskeletal association of phosphorylated CNP2 in the presence of cAMP.

The 46.0 kDa (CNP1) and 48.0 kDa (CNP2) polypeptides of phosphorylated CNS and PNS myelin do not associate with the cytoskeleton to the same extent (Fig. 46, Panels *A4* and *B4*); identical results were obtained for non-phosphorylated myelin (data not shown). CNP1 partitions equally between the soluble fraction and the cytoskeleton, whereas CNP2 is enriched in the cytoskeleton, both in CNS and PNS myelin; analogous distributions were shown for the CNPs of rat and rabbit CNS myelin (Gillespie et al., 1989; Pereyra et al., 1998, respectively). Fig. 46 (Panels *A1* and *B1*, *A2* and *B2*; *A3* and *B3*) shows that CNP2 from CNS myelin is the main myelin protein that can be phosphorylated in a cAMP-dependent manner in vitro, and that in CNS and PNS myelin CNP2 is the major phosphorylated form of CNP. Although some stimulation of CNP2 phosphorylation by cAMP is observed in PNS myelin (Fig. 46, Panel *B3*), this effect is much less pronounced than the corresponding one in CNS myelin (Fig. 46, Panel *A3*). Remarkably, the enrichment of phosphorylated CNP2 in the detergent-soluble fraction of PNS myelin does not reflect the enrichment of this polypeptide in the cytoskeletal fraction (Fig. 46, Panel *B4*). These results show that in the presence of cAMP, CNP2 from CNS myelin incorporates much more [γ^{32}P] label than CNP2 from PNS myelin. The CNP2 polypeptides from CNS and PNS myelin also differ in that the main phosphorylated species associates with the cytoskeleton in CNS but is detergent-soluble in PNS myelin.

Fig. 46 Phosphorylation of myelin in the presence of cAMP and the distribution of CNP between the detergent-soluble (S) and -insoluble cytoskeleton (C) fractions.

Rat CNS (*A*) and PNS (*B*) myelin was phosphorylated in vitro with [γ-^{32}P]ATP in the presence (+) or absence (-) of cAMP then extracted with Triton X-100. The distribution of proteins between the soluble (S) and cytoskeletal (C) fractions was analyzed by immunoblotting and autoradiography.

Panels *A1* and *B1* are autoradiograms of myelin proteins resolved by SDS-PAGE after phosphorylation. cAMP predominantly stimulated the phosphorylation of CNP2 from CNS myelin. The distribution of phosphorylated CNPs between the soluble and cytoskeletal fractions in the absence or presence of cAMP is shown in Panel *A2* and *B2*, and *A3* and *B3*, respectively. Western blotting (Panels *A4* and *B4*) shows that in both CNS and PNS myelin, CNP1 distributes equally between the soluble and cytoskeleton fractions while CNP2 is enriched in the cytoskeleton

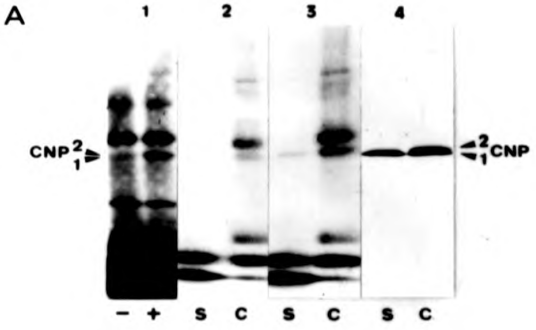
A
1
2
3
4
CNP 2 1
2 1 CNP
– + S C S C S C

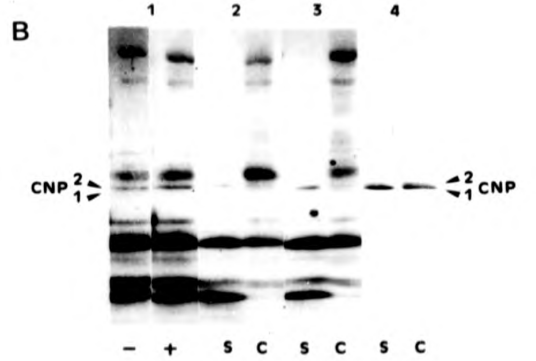
B
1
2
3
4
CNP 2 1
2 1 CNP
– + S C S C S C

8.3 Discussion

This study showed that most myelin-specific proteins, with the notable exceptions of PLP and DM20, are phosphorylated in vitro, in agreement with the consensus of previously published data (Agrawal et al., 1982, 1990; Martenson et al., 1983; Ulmer et al., 1987; Vartanian et al., 1986; Deibler et al., 1990; Ramwani and Moscarello, 1990; Wiggins and Morell, 1980; Bradbury et al., 1984).

With the exception of CNP2, phosphorylated myelin-specific proteins partitioned between the detergent-soluble fraction and the cytoskeleton. Since the proteins in the soluble fraction were phosphorylated to a greater extent and their degree of association with the cytoskeleton was independent of phosphorylation, contact with the cytoskeleton may inhibit phosphorylation for steric reasons. Alternatively, or perhaps additionally, different charge isomers of proteins such as the MBPs (Martenson et al., 1969) that are phosphorylated on different amino acid residues (Ramwani and Moscarello, 1990), may have conformations that either permit or forbid association with the cytoskeleton. In support of the involvement of phosphorylation in conformational changes in MBPs, Deibler et al., (1990) have shown that when component 3 of the 18.5 kDa bovine MBP is monophosphorylated on threonine 97 in vitro, its CD spectrum changes to a 13% more structured conformation involving 17 amino acid residues in β-structures. Gillespie et al., (1989) have shown that a specific subset of sphingolipids also associates with the myelin cytoskeleton, therefore the availability of a complex mixture of MBPs with an inherent high degree of conformational adaptability controlled by phosphorylation, could be a distinct advantage during the interaction of the MBPs with various combinations of proteins and lipids in the bilayer. Therefore, associations that may involve phosphorylation in control of dynamic interactions in the cytoskeleton may also contribute in myelin flexibility.

The CNPs are phosphorylated in vivo by protein kinase A in the PNS and by protein kinase C in the CNS (Agrawal et al., 1990). In contrast to CNP1, CNP2 in CNS myelin has multiple phosphorylation sites and its cAMP-dependent phosphorylation in vitro is exclusively by an intrinsic Type I kinase (Bradbury et al, 1984). CNPs primarily associate with single or loosely wrapped ATP-rich membranes in contact with Schwann cells or oligodendrocyte cytoplasm (Trapp et al., 1988), which makes these proteins ideal

phosphorylation/dephosphorylation targets by resident kinases and phosphatases. Phosphorylation of CNP may therefore be important in regulating cell-cell interactions by causing reorganization of the myelin membrane via the cytoskeleton. cAMP-dependent phosphorylation for CNP2 may be a specific CNS requirement, enabling the oligodendrocyte to respond to cyclic nucleotide signals sent from various axonal contacts by selectively altering its cytoskeleton. Phosphorylation of CNP might affect all the types of cytoskeletal elements, since Dyer and Benjamins, (1989a) have shown that CNP, microtubules, microfilaments and MBP may be linked in oligodendrocytes. Phosphorylation of CNP may also be involved in the regulation of microfilament-dependent process extension and the delivery of components from young oligodendrocytes to myelin, since Wilson and Brophy, (1989) have shown that CNP reacts strongly with microfilaments in the extremities of elongating myelin-like processes.

PLP and DM20 are not phosphorylated in vitro and do not partition with the myelin cytoskeleton in rat, lending further support to the proposal that phosphorylation may be a mechanism responsible for controlling dynamic processes between the cellular membrane and the cytoskeleton. By contrast, the major PNS myelin transmembrane glycoprotein Po, which was previously implicated in homotypic cell-cell interactions in transfected HeLa cells (D'Urso et al., 1990) is phosphorylated in vitro and a significant portion of Po partitions with the cytoskeleton; these results suggest that the cytoskeleton of PNS myelin and possibly Schwann cells might be involved in myelin-axon interactions via the reversible phosphorylation of Po.

Since protein cycling between the membrane and the cytoskeleton may also be important for myelin function, phosphorylation might additionally represent a simple way for myelinating cells to partition solely membrane from cytoskeletally-associated proteins.

Phosphorylation of myelin-specific proteins can now be considered in terms of their association with the cytoskeleton, and it is possible that phosphorylation may be a general mechanism in control of specialized and/or dynamic functions for cytoskeletally-associated proteins in most cells.

Myelin and its associated cytoskeleton: a comparative study of the protein and lipid compositions in wild type (wt) and rumpshaker (*rsh*) mouse

9.1 Introduction

The rumpshaker (*rsh*) mouse was recently recognized as a CNS myelin mutant with an X-linked inheritable defect in PLP gene expression (Griffiths et al., 1990). Although other X-linked PLP mutants are noted for severe lesions, in heterozygote *rsh* females no major CNS hypomyelinated or amyelinated areas exist, with the exception of hypomyelinated fibers in the spinal cord (Fanarraga et al., 1991). This mutant is unusual in that healthy oligodendrocytes with well preserved secretory pathway organelles are increased in number but do not elaborate normal myelin in brain. A comparative study of the optic nerve and spinal cord in *rsh* showed that the myelin sheath in the spinal cord is abnormally thin, probably due to an unusually large axon diameter. Immunostaining intensity was reduced for PLP and MBP but increased for GFAP, both in the optic nerve and spinal cord (Fanarraga et al., 1992). This myelin mutant is unusual in that the animal displays normal longevity and breeding and produces substantial amounts of myelin.

This study undertook to define biochemical differences between wild type (wt) and *rsh* mouse myelin. The lipids and proteins of brain myelin and myelin cytoskeletons were quantitated and their compositions compared in order to ascertain the presence of particular species. These analyses might help explain how the extent of protein and lipid association with the cytoskeleton contributes in making *rsh* such an unusual myelin mutant and further our understanding into the roles of specific molecules that associate with the myelin cytoskeleton.

9.2 Results

The lipid compositions of myelin and myelin-associated cytoskeletons in wt and *rsh* are very different

The protein and lipid measurements indicate that on a weight basis, the brain of P40 *rsh* contains a lot less myelin (protein and lipid) compared to that of wt mouse of the same age (Table 8A). The myelin compositions of *rsh* and wt mouse must also differ, since the lipid/protein ratio in *rsh* is approximately twice that in wt. Myelin from wt mouse contains a higher proportion of cytoskeletal protein/g brain and the ratios of cytoskeletal lipid/g brain are very similar in wt and *rsh*. However, the myelin cytoskeleton of *rsh* has a very high lipid/protein ratio, as is also evident in *rsh* myelin. Overall, although the brain from *rsh* is depleted in myelin by comparison with wt mouse, the myelin and myelin cytoskeleton from *rsh* have a higher proportion of lipid and are depleted in protein.

Lipid class analysis shows that the major lipid composition differences between wt and *rsh* mouse myelin are in cholesterol, Cb and sulfatide (Table 8B). Although cholesterol is the predominant lipid in wt and *rsh* myelin, the proportion of this lipid is greatly increased in *rsh*. Such an increase is unusual, since cholesterol is present in analogous proportions in wt rat and mouse CNS myelin (Section 6 and Table 8B).

In contrast to the increase in cholesterol, the proportions of Cb and sulfatide are decreased in *rsh* myelin by comparison to wt mouse myelin (Table 8B). However, the proportions of individual Cb classes are very similar in wt and *rsh* mouse myelin. Total phospholipid is also very similar in wt and *rsh* mouse myelin, with PE and PC accounting for most; however, while PE is the major phospholipid class in wt mouse, PC predominates in *rsh* (Table 8B). In wt rat the proportion of myelin galactolipids and the PE/PC ratio (~1.2, both at P15 and P20) (Norton and Cammer, 1984) increase with age. Since a low proportion of Cbs and a low PE/PC ratio (~0.9) is also found in *rsh* myelin, the lipid composition of *rsh* myelin appears to resemble that in immature rather than mature wt animals. The amount and proportions of sphingolipids and phospholipids in *rsh* myelin suggests that this might be an animal where the synthesis of myelin-specific lipids has been arrested at an early stage of myelination.

Table 8A: The lipid and protein content of CNS myelin and myelin-associated cytoskeleton (CSK) of wild type (wt) and rumpshaker (*rsh*)

	MYELIN		CSK	
	wt	*rsh*	wt	*rsh*
Yield				
mg protein/g brain	5.8	0.7	0.9	0.1
mg lipid/g brain	12.2	3.4	0.6	0.5
Lipid / Protein ratio				
(mg/mg)	2.1	4.9	0.7	5.0

Table 8B: Lipid analysis of myelin and its associated cytoskeleton (CSK) in wild type (wt) and rumpshaker (*rsh*)

	MYELIN		CSK	
Lipid class (Mol %)	wt	*rsh*	wt	*rsh*
Cholesterol	38.0	46.0	34.0	56.0
Cerebroside	25.0	18.0	33.0	10.0
% Class				
GalC-non-OH	28	24	38	42
GalC-OH	69	72	62	58
GlcC	3	4	ND	ND
Sulfatide	4.0	2.0	6.0	3.0
Phospholipid	33.0	34.0	27.0	31.0
% Class				
PE	46	35	42	38
PC	33	40	35	39
PS	13	15	9	9
PI	3	4	3	3
SM	5	6	11	11

Comparison of the lipid compositions of wt myelin and wt myelin cytoskeleton in mouse (Table 8B) shows that cholesterol and total phospholipid are decreased and Cb and sulfatide increased in the cytoskeleton. Cb is also increased and phospholipid decreased in the cytoskeleton of wt rat CNS myelin (Gillespie et al., 1989; Section 6). However, although SM is increased in the cytoskeleton of wt rat and mouse (Section 6, Table 8B), SM represents a higher proportion of the cytoskeletal phospholipid in rat.

The differences in cytoskeletal lipid composition between wt and *rsh* mouse are even more pronounced than the corresponding differences in myelin (Table 8B). Cholesterol makes up more than half of the cytoskeletal lipid in *rsh*, whereas Cb accounts for only 10% and sulfatide for 3%. Total phospholipid is slightly increased in the cytoskeleton of *rsh*, where PE and PC are in approximately equal proportions (Table 8B). By contrast, PE is the major phospholipid in the cytoskeleton of wt mouse, rat and bovine CNS myelin (Table 8B, Gillespie et al., 1989; Norton and Cammer, 1984, respectively). Galactolipids are also reduced in *jp*, *jp^{msd}*, *qk*, and *shi* but to date no other studies of cytoskeletally-associated lipid compositions are available for myelin mutants.

Protein association with the cytoskeleton

Immunoblotting showed that actin, tubulin, MAG and CNP are present in similar proportions in wt and *rsh* myelin (Fig. 47); the distribution of these proteins between the detergent-soluble and cytoskeletal fractions is very similar in wt and *rsh*. The proportion of PLP is higher in wt than in *rsh*. PLP appears during active myelination and later than other myelin proteins in the CNS (Gardiner and Macklin, 1988; LeVine et al., 1990; van Dorsselaer et al., 1987), and in cultured oligodendrocytes PLP is detected after MAG but before MBP (Dubois-Dalcq et al., 1986). Although some PLP was detected in the myelin cytoskeleton of wt, the majority of PLP was extracted by Triton X-100 both in wt and *rsh* myelin. Western blotting suggests that the difference in the relative amounts of PLP between wt and *rsh* can probably be accounted for by the portion of PLP that associates with the cytoskeleton in wt.

The total amounts of the 18.5 and 17.0 kDa MBPs and the distributions of these proteins between the detergent-soluble fraction and the cytoskeleton were very similar in wt and *rsh*. All the 21.5 kDa MBP partitioned with the cytoskeleton, both in wt and *rsh*, and

Fig. 47. The association of proteins with the myelin cytoskeleton in wild type (wt) and rumpshaker (*rsh*) mouse.

Myelin postnatal day 40 (P40) from wt and *rsh* mouse was extracted with Triton X-100 and equal volumes of the detergent -soluble (S) and -insoluble cytoskeleton (C) fractions were electrophoresed and transferred to nitrocellulose. Western blotting with antibodies against actin (ACT), tubulin (TUB), myelin-associated glycoprotein (MAG), 2',3'-cyclic nucleotide 3'-phosphohydrolase (CNP), proteolipid protein (PLP) and myelin basic protein (MBP) shows that the relative amounts of actin, tubulin and MAG in myelin and their respective distributions between the detergent-soluble and -insoluble fractions are not affected. There is a higher proportion of PLP in wt, where PLP is enriched in the soluble fraction; by contrast, *rsh* PLP is found exclusively in the soluble fraction. The 21.5 kDa MBP is increased relative to the other MBPs in *rsh* myelin and this MBP is found in the cytoskeletal fraction, both in wt and *rsh*. The 14.0 kDa MBP is depleted in *rsh* myelin but the distribution of this MBP between the detergent-soluble and -insoluble fractions is similar in wt and *rsh*.

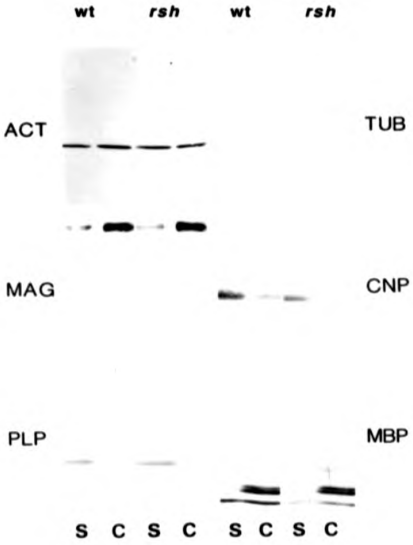
wt
rsh
wt
rsh
ACT
TUB
MAG
CNP
PLP
MBP
S C S C S C S C

there was a small proportionate increase of this MBP in *rsh*. Although there was a smaller proportion of the 14.0 kDa MBP in *rsh* myelin, this protein distributed similarly between the detergent-soluble fraction and the cytoskeleton in wt and *rsh*.

PLP is reduced in *jp*, *qk* and *shi*, MBP in *jp*, *qk*, *shi* and *tw*, whereas there is a small increase of CNP in *shi* and the activity of this enzyme is reduced in *jp* and *qk* (Hogan and Greenfield, 1984). The relative decreases of myelin-specific lipids and PLP in *rsh*, coupled with the proportionate increase of the 21.5 kDa and decrease of the 14.0 kDa MBPs, which are known to be characteristics of immature myelin (Barbarese et al., 1978; Carson et al., 1983), indicate that in the brain of *rsh*, myelination arrest probably occurs at an early stage. Although this stage has not been defined as yet, these data suggest that the myelination arrest in *rsh* might occur after MAG and CNP but before PLP and MBP have established their pattern of association with the cytoskeleton.

9.3 Discussion

This analysis shows that *rsh* has greatly reduced amounts of myelin compared to the normal animal, thus confirming the morphological and morphometric studies of Griffiths et al., (1990); however, *rsh* has considerably more myelin than other X-linked PLP mutants (for review see Skoff and Knapp, 1992). Since a high lipid/protein ratio in myelin is thought to be a function of normal development (Norton and Cammer, 1984), the presence of substantial amounts of lipid in *rsh* myelin may aid axonal conduction.

Myelination in *rsh* is thought to be halted during early development (Skoff and Knapp, 1992; Hudson and Nadon, 1992). This contention is supported by the finding that in comparison with wt animals *rsh* has a low content of sphingolipids, PLP (also see Griffiths et al., 1990) and 14.0 kDa MBP, but relatively high amounts of PE, PC and the 21.5 kDa MBP which are characteristic of immature myelin.

The PLP gene is also found in astrocytes, where it encodes a mRNA that is different from the PLP mRNA in oligodendrocytes (Macklin, 1988), and the previous explanation that a defect in PLP is the cause for dysmyelination in *jp*, *gk* and *jp*^{msd} (i.e. no PLP - no myelin) is no longer viable (Skoff and Knapp, 1992). It is now thought that defects in the PLP gene influence the early differentiation of both astrocytes and oligodendrocytes in the mutants, and that defective astrocytes may be partly responsible for the absence of oligodendrocyte-specific differentiation signals. PLP and DM20 are also thought to promote oligodendrocyte differentiation independently and provide the structural underpinning of the myelin sheath by maintaining the correct spacing between apposed bilayers in the intraperiod zone (Hudson and Nadon, 1992). Although PLP is not associated with the CNS myelin cytoskeleton in rat (Gillespie et al., 1989), a small amount of PLP (≤10%) is found in the cytoskeleton of rabbit CNS myelin (Pereyra et al., 1988), indicating that the association of PLP with the cytoskeleton of myelin may be species-specific. It was therefore of interest that some PLP was found in the myelin cytoskeleton of wt but not *rsh* mouse, where the amount of cytoskeletally associated PLP might represent the difference in the relative amounts of PLP in wt and *rsh* myelin. However, the possible function of cytoskeletally associated PLP is unknown.

Although myelin-specific proteins (with the exception of PLP) associate to approximately the same extent with the myelin cytoskeletons both in wt and *rsh*, there are very pronounced differences in the relative quantities and classes of lipids that associate with the cytoskeleton. The predominant differences in *rsh* are in the Cbs which are drastically reduced and in cholesterol which is increased in the cytoskeleton. Although a great reduction in Cbs is a universal feature amongst myelin mutants, this is the first demonstration that the Cbs are also drastically reduced in the cytoskeleton of such a mutant by comparison with myelin; in contrast, in wt mouse the Cbs are greatly enriched in the cytoskeleton. Sphingolipids associate with the cytoskeleton of CNS myelin and oligodendrocytes (Gillespie et al., 1989; Dyer and Benjamins, 1989b, respectively) and such lipids are thought to be involved in cell-cell communication and the modulation of transmembrane signals in a many normal and transformed cell types (Hakomori, 1989, 1990; Kolesnick, 1991; Dyer and Benjamins, 1985, 1989, 1992). Axonal and intracellular communication may therefore involve the interaction of sphingolipids with the cytoskeleton in myelin and myelinating cells. Gillespie et al., (1989) have proposed that sphingolipids in association with the cytoskeleton may also have roles in myelinogenesis. Therefore, loss of sphingolipids from myelin and its associated cytoskeleton might not only affect myelinating cells but the CNS as a whole.

Conclusions and future directions

10.1 Culture systems for glial cells

The establishment and characterization of a rat CNS primary glial culture system where large numbers of O-2A progenitors differentiated to oligodendrocytes in a sequential and predictable manner, permitted immunocytochemical and biochemical experiments to be carried out in parallel on cells from the same cultures during different developmental stages.

Fluorescent activated cell sorting (FACS) (Behar et al., 1988), the combined use of mitogenic factors such as bFGF and PDGF (Bögler et al., 1990; Louis et al., 1992) and perhaps different defined media (e.g. Bottenstein and Sato, 1979) may in future permit the isolation of large, highly purified populations of O-2A progenitors with the potential to differentiate to oligodendrocytes, possibly under the influence of (uncharacterized as yet) differentiation factors (Levi et al., 1987, 1991, Agresti et al., 1991). Such cultures should permit even more accurate immunocytochemical and biochemical investigations, in the total absence of other cell types.

It will also be important to establish the possible presence of O-2A^{adult} progenitors in brain and spinal cord (only shown in the optic nerve by Wren et al., 1992), such progenitors are bipotential and divide asymmetrically, thus generating differentiated progeny (oligodendrocytes) and their own replenishment throughout adult life. Studies on brain O-2A^{adult} progenitors, preoligodendrocytes (O4$^+$,GalC$^-$) (Gard and Pfeiffer, 1989, 1990), and oligodendrocytes which may also generate new oligodendrocytes (Wood and Bunge, 1991) should increase our understanding of cellular regeneration in adult animals in general and remyelination in particular. Such studies should complement transplantation technology (Harvey et al., 1991, Bunge, 1991; Blakemmore and Franklin, 1991) and could be of potential use in curing demyelinating diseases of the CNS.

10.2 MAP1B in the CNS.

Microtubule associated proteins such as MAP1B, that probably crosslinks microtubules in neurons (Noble et al., 1989; Sato-Yoshitake et al., 1989) and may have a role in neurite extension and the development of polarity (Tucker et al., 1988a, b; Matus, 1988, 1989) are thought to play important roles during the development of the CNS. Since MAP1B is also

expressed in glia (Diaz and Avila, 1989) including oligodendrocytes (Fisher et al., 1990), but its function in these cells is unknown, it was attempted to identify the developmental point when MAP1B is first expressed in glia of the O-2A lineage and its possible function in oligodendrocytes (Section 4). Immunocytochemistry showed that although MAP1B is absent from O-2A progenitors, vigorous MAP1B expression coincides with the time when preoligodendrocytes begin to extend numerous long, pre-myelin-like processes; this suggested that MAP1B might be first expressed when myelin processes begin to enlarge. One function of MAP1B might be to crosslink (and possibly stabilize) microtubules during processes extension by preoligodendrocytes and early oligodendrocytes, which would be similar to its proposed role in neurite extension.

The presence of MAP1B in terminally differentiated oligodendrocytes (albeit at lower levels of expression than in preoligodendrocytes) and their cytoskeletons suggests that MAP1B might have the additional specialized function of stabilizing microtubules in the processes; this idea was supported by the antisense experiments. Since microtubules are the predominant filamentous structure in mature oligodendrocytes both in vivo (Wood and Bunge, 1984) and in vitro (Wilson and Brophy, 1989; Section 7), it is possible that in these cells MAP1B may stabilize microtubules by direct crosslinking instead of via indirect association with actin and or CNP, as was suggested by Fisher et al., (1990). However, since MAP1B is absent from CNS myelin, stabilization of microtubules in myelin may be via microfilaments, CNP, MBP and/or lipids that associate with the cytoskeleton (Gillespie et al., 1989; Sections 6 and 7).

The hypothesis that MAP1B could be involved in process extension and the stabilization of microtubules in young and mature oligodendrocytes respectively, could be tested by inducing MAP1B expression in O-2A progenitors and abolishing MAP1B expression in more developmentally advanced cells. This could be accomplished by transfecting of O-2A progenitors with either sense or antisense MAP1B cDNA and then switching the expression of MAP1B on or off during development. In situ hybridization analysis, both at the light and electron microscope levels, might additionally reveal possible inter-relationships between MAP1B synthesis and the cytoskeleton.

A recent report (Mansfield et al., 1992) has shown that only the phosphorylated form of

MAP1B is present in neuronal growth cones, where some MAP1B associates with the cytoskeleton; this study suggested that the interaction of phosphorylated MAP1B with the cytoskeleton might be of importance during neurite extension. It would be therefore important to assess whether phosphorylated forms of MAP1B exist in preoligodendrocytes, mature oligodendrocytes and their respective cytoskeletons, since this might indicate the possible role(s) of MAP1B phosphorylation in cells of the oligodendrocyte lineage.

The relationship between cytoskeletal reorganization and morphological differentiation involving MAPs is of great general interest. When embryonal carcinoma cells are induced to differentiate in the presence of retinoic acid, they express MAP2 and they withdraw from the cell cycle (Dinsmore and Solomon, 1991). If the expression of MAP2 protein is inhibited by antisense RNA during induction, these cells express other differentiation-specific markers but they do not differentiate morphologically nor do they stop dividing (Dinsmore and Solomon, 1991). It appears that there is a fundamental interrelationship between expression of MAP2, developmentally-regulated changes in cell morphology and the prevention of cell division. The induction of MAP1B expression may have a similar function in oligodendrocytes since it precedes their terminal differentiation. Support for this view comes from studies on axonal MAP1B. Axons that grow out from newly-committed neurons contain MAP1B but axons that regrow from axotomized, terminally-differentiated neurons do not (Viereck et al., 1989; Woodhams et al., 1989). An analysis of the interactions between MAP1B and microtubules should assist our understanding of the molecular mechanisms that regulate the transition of cells of the O-2A lineage from proliferative progenitor to myelinating oligodendrocyte.

10.3 Sphingolipid metabolism and transport

The membranes of eukaryotic cells contain numerous classes of sphingolipids, which differ in the composition of their long chain base. The distribution of sphingolipids is not random, since some are enriched in the membranes of certain organelles, while asymmetric distribution occurs across lipid bilayers such as the plasma membrane. Since no intracellular membrane system can synthesize all its own sphingolipids de novo, the study of biosynthesis, translocation and sorting of sphingolipids relates to membrane biogenesis and homeostasis. The metabolism and transport of these lipids may also relate to the

biosynthesis and translocation of secretory proteins, since both processes are thought to occur through similar intracellular compartments (Simons and van Meer, 1988; Simons and Wandinger-Ness, 1990; Rosenwald et al., 1992; Kok et al., 1989). Additionally, forward transport from the ER through the Golgi to the plasma membrane may take place via bulk flow, proceeding by default without the need for a special signal, both for secretory proteins and endogenous sphingolipids (Wieland et al., 1987; Young et al., 1992, respectively). Although sphingolipids appear to utilize the secretory pathway, the transport of certain phospholipids may involve carrier proteins since in BFA-treated rat hepatocytes ER to plasma membrane traffic of PE continues normally when vesicle-mediated protein traffic is negligible (Vance et al., 1991; Vance, 1992). A better understanding of protein synthesis through the secretory pathway, possibly by approaches such as the use of viral membrane proteins to follow biosynthetic traffic (for a review see Griffiths and Sodeik, 1992) may enhance our understanding of lipid metabolism and transport.

The present study (Section 5) examined the biosynthesis and transport of sphingolipids in oligodendrocytes, since GalC is a differentiation marker (Raff et al., 1978; Bansal and Pfeiffer, 1985; Gard and Pfeiffer, 1989) that probably interacts with the oligodendrocyte cytoskeleton (Dyer and Benjamins, 1989a). In addition GalC is characteristic of CNS myelin (Norton and Cammer, 1984), and GalC and SM are enriched in the cytoskeleton of CNS myelin where they may interact with myelin-specific proteins (Gillespie et al., 1989).

Of the fluorescent Cer analogues that were used, C_6-NBD-Cer appears to be an excellent substrate for metabolic studies (Lipsky and Pagano, 1983; Pagano et al., 1990), but only inserts partly in biological membranes (Chattopadhyay and London, 1987, 1988) and is subject to photobleaching, while C_5-DMB-Cer has high fluorescent yields but is not representative of endogenous Cer metabolism in vitro (Pagano et al., 1991). The present study suggests that using C_6-NBD-Cer and C_5-DMB-Cer in parallel may be advantageous, since the metabolic and transport properties of different intracellular compartments can be examined on a comparative basis.

Fluorescent Cer analogues were used in combination with the O-2A lineage primary culture system and a stage of "active" metabolism to fluorescent GalC was identified, which coincided with the expression of oligodendrocyte-specific markers by the majority of the cells.

Cultures at this stage were used to study the metabolism and transport of C_6-NBD-Cer, C_5-DMB-Cer and their metabolites in the presence or absence of BFA. In the absence of BFA C_6-NBD-Cer localized in the *trans*-Golgi and the TGN, while C_5-DMB-Cer localized in Golgi compartments other than the TGN before any significant metabolism had occurred. C_6-NBD-lipids were found in *trans*-most Golgi cisternae and in early endosomes when the maximum conversion of C_6-NBD-Cer had occurred and these lipids localized in late endosomes upon further incubation. By contrast, C_5-DMB-lipids were predominantly in the ER and at the plasma membrane upon maximum conversion of C_5-DMB-Cer and in Golgi compartments and Golgi-derived vesicles after 5 h of incubation. Although this study was not aimed at discovering the exact sites of fluorescent Cer metabolism in oligodendrocytes, the results suggest that significant amounts of Cer may be converted to SM in the Golgi and the plasma membrane (as suggested by Koval and Pagano, 1991 for non-glial cells), whereas a significant amount of GalC biosynthesis may take place at the plasma membrane and the TGN. Therefore these data are in broad agreement with immunocytochemical (Roussel et al., 1987) and fractionation studies (Nescovic et al., 1973; Constantino-Ceccarini and Suzuki, 1975; Koul and Jungalwala, 1981).

While the initial localization of Cers probably depends on specific interactions between their acyl chains and Golgi compartment-specific lipids, the metabolism and transport of Cers may be determined by the intracellular compartment where they initially localize. This view might be justified, since when *trans*-Golgi to TGN traffic was disrupted and two separate compartments were formed, C_6-NBD-Cer colocalized with the TGN/plasma membrane/endosomal compartment and its metabolism to fluorescent GalC reflected our predicted localization of UDP-galactose ceramide galactosyltransferase. In similarly treated cells the metabolism of C_5-DMB-Cer was unaffected, indicating that this lipid was probably metabolized in the ER/*cis*-/*medial*-/*trans*-Golgi compartment; in support, the major part of SM biosynthesis is thought to occur in the *cis*- and *medial*-Golgi (Koval and Pagano, 1991; Futerman et al., 1990; Jeckel et al., 1990) and normal lipid recycling takes place between the Golgi (excluding the TGN) and the ER (Pagano, 1990; Lippincott-Schwartz et al., 1990).

In addition to causing profound changes in organelles of the secretory pathway, BFA also affected the distribution of tubulin in oligodendrocytes, the effect on tubulin might be

mediated through the cytoskeleton and requires further investigation. Since the uptake and recycling of iron was not altered in these (and other) cells, the effects of BFA might be specific to certain cell functions only. The BFA-induced changes were reversible and the TGN recovered faster than the rest of the Golgi, indicating that organelle reassembly might occur at different rates. The return of the TGN and tubulin to their original distributions required considerable time of recovery (hours rather than minutes) and depended on the time of exposure to BFA.

These data add to the wealth of literature regarding sphingolipid biosynthesis and transport and indicate some possibly unique features of oligodendrocytes as regards the biosynthesis of GalC and the structure of the cytoskeleton. These cells will be excellent candidates for studies addressing how sphingolipids and proteins are cotransported during their biosynthesis through the Golgi, since at least at least one major oligodendrocyte protein (PLP) is synthesized and transported through the Golgi (Townsend et al., 1984), its transport in *jp* is arrested at the Golgi (Roussel et al., 1987b) and inhibition of glycosphingolipid biosynthesis affects the translocation of PLP to myelin membrane (Pasquini et al., 1989). Future studies should additionally employ truncated Cer analogues such as C_8C_8-Cer (Karrenbauer et al., 1990; Brüning et al., 1992) and perhaps radioactive Cers with long chain fatty acids that may resemble endogenous Cer precursors to a greater extent.

The biosynthesis, transport and roles of sphingolipids such as GalC might also be investigated by molecular genetics, in an analogous way to the study of PE in *E. coli* (Dowhan, 1992); a possible approach might be to change the structure of key enzymes such as UDP-galactose-4'-epimerase or UDP-galactose:galactosyltransferase and either stimulate or downregulate the biosynthesis of GalC at key points in development. GalC production could be monitored via the conversion of C_6-NBD-Cer to -GalC and the possible changes (in morphology, function of the secretory pathway, expression of differentiation-specific markers, etc.) related to GalC biosynthesis and transport.

Past studies using fluorescent sphingolipid analogues have not examined gangliosides, possibly due to the small amounts and great variety of these glucosphingolipids in cells. The design of novel, highly fluorescent Cers that can be preferentially converted to the GlcC analogue by inserting into the appropriate intracellular compartment(s) may add an extra

dimension to the study of ganglioside biosynthesis and transport.

10.4 Sphingolipids in association with cytoskeletons

Cell surface glycosphingolipids are very immunogenic and are useful markers of differentiation and malignant transformation (Hakomori and Kanagi, 1983; Ralff, 1989; Hakomori, 1989, 1990; Gillard et al., 1992). Such lipids modulate the activities of membrane-associated kinases and epidermal growth factor (EGF) (Hanai et al., 1988; Igahashi et al., 1989), while the carbohydrates moieties of glycolipids in neutrophils, platelets and T-lymphocytes mediate adhesive reactions to endothelium (Phillips et al., 1990; Larsen et al., 1990).

Although it has been known for sometime that sphingolipids associate with cytoskeletons (Sakakibara, 1981; Burn and Burger, 1985), the possible importance of such interactions is only beginning to emerge (Packham et al., 1991; Gillard et al., 1991, 1992; Mateoni and Kreis, 1987; Vale and Hotani, 1988; Steinert and Roop, 1988; Dyer and Benjamins, 1989b; Gillespie et al., 1989). The cytoskeleton of CNS myelin is enriched in GalC by comparison with the intact membrane (Gillespie et al., 1989). Although GalC was proposed to have direct links with the oligodendrocytic cytoskeleton (Dyer and Benjamins, 1989b) and anti-GalC causes an influx of calcium in oligodendrocytes implicating the cytoskeleton in transmembrane signaling (Dyer and Benjamins, 1990), the association of GalC with the cytoskeleton had not been shown in a conclusive way prior to this study, possibly due to lack of sufficient material. GalC is enriched in oligodendrocyte cytoskeletons and this sphingolipid may be associated with microfilaments and/or CNP in young cells and with microtubules and/or MBP in mature cells; such associations imply that different, specific interactions may exist between GalC and the cytoskeletons of actively myelinating and mature cells, respectively. Cytoskeletally-associated GalC may therefore have a variety of roles in oligodendrocytes and myelin during development, which should be examined at specific stages of differentiation in culture. The possible importance of cytoskeletally-associated GalC in myelination is further underlined by the presence of GalC in the cytoskeletons of both PNS myelin and Schwann cells; however, studies with pure Schwann cell populations in culture are hindered at present, since these cells specifically require axons or perhaps

axonally-derived signals in order to differentiate (Jessen and Mirsky, 1991).

Although the association of GalC and its possible role in the cytoskeleton are under investigation and might be further elucidated by molecular genetics (see under sphingolipid metabolism and transport), little or no attention has been paid to cytoskeletal sulfatide, SM and possibly gangliosides. Gillespie et al., (1989) have shown the presence of both sulfatide and SM (and the enrichment of SM) in the cytoskeleton of CNS myelin, and the present study suggests that these sphingolipids are present in the cytoskeletons of oligodendrocytes. The association of SM with cellular and membraneous cytoskeletons may modulate a variety of cellular interactions, since membrane proteins associate with cytoskeletal phospholipids (Moss and White, 1992) and at least two products of SM metabolism (diacylglycerol and sphingoid bases) have been implicated as biological effectors (Nishizuka, 1988; Rando, 1988; Hannun and Bell, 1989; Merrill and Stevens, 1989). The role of cytoskeletally-associated sulfatide is not clear, but it may be similar to GalC. Gangliosides have unique functions in several cell types (Gonatas et al., 1984; Bremer et al., 1984; Wiegandt, 1982; Sung et al., 1991); the gangliosides recognized by A2B5 and anti-G_{D3} are present in O-2A progenitors (Raff, 1989; LeVine and Goldman, 1988a, b) but not in mature oligodendrocytes, while gangliosides are true constituents of CNS myelin (Norton and Cammer, 1984). Gangliosides may therefore be transported to myelin immediately after O-2A progenitors begin to differentiate to oligodendrocytes. Future studies should investigate whether gangliosides interact with the cytoskeletons of O-2A progenitors and myelin and assess the possible functions of such associations.

Phospholipids containing saturated FAs are enriched in the cytoskeleton of CNS myelin, and significant amounts of C_6-DMB- but not C_6-NBD-lipids accumulate into the cytoskeletons of myelinating cells after overnight incubation. These findings suggest that the preferential association of sphingolipids with the cytoskeleton may depend on acyl chain composition in specialized membranes (such as myelin), and on continuous recycling as well as acyl chain composition in cells. The possibility that fluorescent lipid molecules may preferentially associate with specific proteins of the cytoskeleton could be further explored by using probes such as 5-[^{125}I] iodonaphthyl-1-azide (INA) (Bercovici and Gitler, 1978) that can be photoactivated in the presence of fluorescent lipids with UV light (Rosenwald et al.,

1991). Extraction with non-ionic detergent prior to photoactivation might indicate which cytoskeletal proteins are in close proximity to fluorescent lipids. Additionally, since INA is membrane-permeant, photoactivation in intact cells may show which intracellular, compartment-specific proteins, are involved in sphingolipid metabolism and transport.

10.5 The association of proteins with cytoskeletons during development

Linker proteins have been implicated in mediating cytoskeletally-driven movements in animal cells (for a review see Bray and White, 1988). Such proteins have been identified by their association with Triton X-100 insoluble residues in several cell types (Fulton et al., 1980; Apgar et al., 1986; Bennet, 1985; Jesaitus et al., 1984; Fox et al., 1988; Wilson and Brophy, 1989; Mansfield et al., 1992) and in specialized membranes such as CNS myelin (Pereyra et al., 1988; Gillespie et al., 1989). The extension of oligodendrocyte processes and that of neurites have strong similarities as regards their cytoskeletal elements: while microtubules are abundant in the growing axons of *Aplysia*, growth cones are devoid of microtubules but rich in microfilaments (Forscher and Smith, 1988); CNP-associated microfilaments are enriched in the termini of myelin-like processes in young oligodendrocytes, while MBP-associated microtubules are found in the processes of mature cells (Wilson and Brophy, 1989). Oligodendrocytes and neurons may be derived from a common progenitor cell (for a review see Cameron and Pakic, 1991) and may therefore have similar mechanisms for process extension, however oligodendrocytes may utilize their own specialized cytoskeletally-associated proteins and possibly lipids. Additionally, oligodendrocytes may have evolved specialized mechanisms whereby isoprenylated proteins (such as CNP) may have roles in signal transduction and the regulation of the cell cycle via the cytoskeleton.

The association of specialized linker proteins with the cytoskeleton may be even more complex in mature CNS myelin, where microtubules, microfilaments, CNP, MBP and MAG associate with the Triton X-100-insoluble residue that also contains GalC and SM (Gillespie et al., 1989). Examination of the cytoskeleton during development reveals a possible association between microtubules, early MBPs and S-MAG in early myelin, with microfilaments, CNP, L-MAG and the 14.0 kDa (late) MBP added to the cytoskeleton during active myelination. Such a developmental rearrangement of the cytoskeleton would conform

with the idea of myelin membrane sheets forming as MBPs accumulate and microfilaments depolymerize in the cell processes (proposed by Wilson and Brophy, 1989), this would permit the attachment of loose (immature) myelin to axons during early myelination, when microfilaments together with microtubules would determine the shape and, possibly via linker proteins, flexibility of compacting and compact myelin. Future experiments could address these possibilities by specifically inhibiting or promoting the expression of myelin-specific (proposed linker) proteins in culture, and also perhaps in mutants where the expression of such proteins is normally inhibited (such as *shi*, an MBP mutant); the possible observed changes would be related to the extent of protein expression and cytoskeletal association. Such investigations should also examine which lipids may associate with the cytoskeleton of myelin and myelinating cells during development, since sphingolipids in particular may have directive roles relating to process extension via the cytoskeleton. Although such studies are possible and certainly worthwhile, their results may only be suggestive at best due to the inherent complexity of cellular and specialized membrane interactions. The identification of specific lipid-protein interactions that involve the cytoskeleton during myelination in brain and also perhaps of a host of specific lipid-protein interactions in other tissues, will most probably be achieved by analysis of simple reconstituted systems such as the ones that have been used to identify the dynamics and specificity of lipid interactions with either PLP or MBP (for review see Brophy, 1992). Candidate molecules for studying such interactions should include GalC, SM, gangliosides, CNP and MAG.

10.6 Protein phosphorylation and association with cytoskeletons

Phosphorylation has been long known to alter the biological functions of various proteins, probably by introducing changes in their conformation. This idea is supported by studies on the molecular basis of phosphorylation reactions in a number of enzyme and/or receptor systems, showing that the reactions or responses are controlled, at least partly, by attainment of required conformations in enzymes or protein substrates (Kandekar and Jacobson, 1969; Holt and Sawyer, 1968; Perlman et al., 1969; Hanson et al., 1969). Certain myelin-specific proteins may act as linkers and their phosphorylation (Bradbury et al., 1964; Ulmer et al., 1987; Vartanian et al., 1988; Deibler et al., 1990; Ramwani and Moscarello,

1990, Agrawal et al., 1982, 1990; Martenson et al., 1983; Wiggins and Morell, 1980) may mediate interactions between the membrane and its associated cytoskeleton. These proteins interact with the myelin cytoskeleton (Pereyra et al., 1988; Gillespie et al., 1989) and phosphorylation causes extensive conformational changes in at least one (MBP) isoform (Deibler et al., 1990). Since analogous linker proteins were found in a variety of animal cells (Mansfield et al., 1992; Fulton et al., 1980; Apgar et al., 1986; Bray and White, 1988; Bennet, 1985; Jesaitus et al., 1984; Fox et al., 1988), the study of phosphorylation as a possible mechanism for controlling cytoskeleton-membrane interactions should be of universal interest in cell biology.

Protein phosphorylation can determine association with the cytoskeleton as well as preferential association with membranes; phosphorylation of band 4.1 reduces its ability to bind spectrin (Eder et al., 1986) and promotes spectrin binding to microfilaments (Ling et al., 1988), while phosphorylation of tubulin with calmodulin-dependent kinase exposes hydrophobic domains that enable the phosphorylated protein to interact with membranes (Hargreaves et al., 1986). Reversible phosphorylation of myelin proteins may alter their conformation such that association with membranes is favored, while association with the cytoskeleton is hindered. This scenario might explain why cytoskeletally-associated myelin proteins are phosphorylated less heavily than detergent-extractable forms in vitro, although it does not explain why the relative degree of protein association with the cytoskeleton is not influenced by phosphorylation. Such issues might be resolved and this study furthered if phosphorylation was to be additionally carried out in culture and in vivo; since in the MBPs at least phosphorylation is short-lived (DesJardins and Morell, 1983), a time course of label incorporation may be necessary during each experiment. Such studies might also show whether cytoskeletally-associated myelin proteins are a truly underphosphorylated subset (as was shown by the in vitro phosphorylation of myelin) and whether association with the cytoskeleton may only be characteristic of some isoforms. The possibility that some MBP charge isoforms (Martenson et al., 1989) may preferentially associate with the cytoskeleton can be examined by subjecting detergent-soluble and -insoluble myelin fractions to two-dimensional gel electrophoresis.

Amongst CNS myelin proteins, only the phosphorylation of CNP2 is stimulated by cAMP in

vitro (Bradbury et al., 1984; Section 8). cAMP however inhibits MBP phosphorylation in cultured oligodendrocytes (Ulmer et al., 1987) via galactosylsphingosine, a potential catabolite of GalC, interfering with the release of diacylglycerol from phosphatidylinositol thus affecting protein kinase C (Vartanian et al., 1989). Therefore, future phosphorylation experiments involving cultured cells should include cAMP, and might additionally investigate the possible link between the induction of GalC biosynthesis during development and cytoskeletal changes that might be caused by cAMP.

Phosphorylation/dephosphorylation of myelin-specific proteins should also be considered in terms of the locations of specific enzymes, since preferential modification of myelin proteins could be due to the topology of such enzymes in the membrane. The presence and localizations of phosphorylation-related enzymes can be established by immunocytochemistry. Disruption of the functions of such enzymes might indicate how they affect the association of myelin proteins with the cytoskeleton.

10.7 Myelin mutants and the cytoskeleton

Mutations affecting myelination in the nervous system have been discovered in a number of species, with the extent of dysmyelination and its effect on lifespan varying considerably amongst mutants. Such animals are particularly suitable for biochemical investigations, since they provide sufficiently homogeneous material and the defect is usually in a single gene locus.

The most severe cases of dysmyelination are found amongst the X-linked recessive disorders, which only appear to affect the CNS. Such mutations with the exception of *rsh* are lethal, which makes the study of *rsh* unique. The present results show that in addition to the defect in PLP expression in *rsh* (Griffiths et al., 1990), cytoskeletally-associated PLP is absent and there is a small increase in the 21.5 kDa MBP and a considerable decrease in the 14.0 kDa MBP, thus indicating a possible arrest during early myelination. Such an arrest is also indicated by the decrease in the PE/PC ratio and the decrease of Cbs in myelin. Further studies, possibly using CNS myelin from wt animals during early myelination (P7-P9) should indicate how the Cbs in the myelin cytoskeleton of *rsh* compare with those in wt.

Such studies would also be interesting from the developmental point of view, since they might indicate the amounts and classes of lipids that associate with the early CNS myelin cytoskeleton (made up of microtubules, early MBPs and S-MAG, see Section 7).

Cytoskeletally-associated PLP may have a role in mouse and rabbit but not rat myelin. The PLP gene is highly conserved (for a review see Macklin, 1992), therefore the possibility that species-specific posttranslational modifications may determine the partial association of PLP with the cytoskeleton needs to be examined. Such modifications may be substituted in rat myelin PLP and their absence may affect myelination in *rsh* mouse. The possible defect in MBP gene expression in *rsh* certainly requires further investigation, since such a study may ultimately lead to the discovery of the molecular basis for the alternative splicing of the primary MBP transcript; considering the complex structure and regulation of the MBP gene (for a review see Kamholz and Wrabetz, 1992), such a study should also be of great general interest in molecular biology. In addition, the relative amounts of the mRNAs coding for L- and S-MAG, the amounts of the respective protein isoforms and their degree of association with the cytoskeleton must be assessed in *rsh* myelin, since such a study might further our knowledge on the developmental regulation of MAG and its role in the cytoskeleton.

References

Afar, Deh, Salzer, J. L., Roder, J., Braun, P. E. and Bell, J. C. (1990) J. Neurochem. 55, 1418-1426

Agrawal, H. C. and Agrawal, D. (1991) Neurochem. Res. 16, 855-858

Agrawal, H. C., Agrawal, D. and Jenkins, R. P. (1986) Neurochem. Res. 11, 375-382

Agrawal, H.C., Norohna, A.B., Agrawal, D. and Quarles, R.H. (1990) Bioc. Biop. Res Comm. 169(3):953-958

Agrawal, H.C., O'Connel, K., Randl, C.L. and Agrawal, D. (1982) Biochem.J. 201:39-47

Agrawal, H.C., Sprinkle, T.J. and Agrawal D. (1990a) J. Biol. Chem. 265, 11849-11853

Agrawal, H.C., Sprinkle, T.J. and Agrawal D. (1990b) Bioch. Biop. Res. Comm. 170(2):817-823

Agresti, C., Aloisi, F. & Levi, G. (1991) Developmental Biology 114: 16-29

Alcade, J., Bonay, P., Roa, A., Vilaro, S. and Sandoval, I. V. (1992) J. Cell Biol. 116, 69-83

Allan, D. and Walkin, C. M. (1988) Biochim. Biophys. Acta 938, 403-410

Allan, V. J. and Kreis, T. E. (1986) J. Cell Biol. 103, 2229-2239

Aloisi, F., Agresti, C. D'Urso and D.Levi, G. (1988) Proc. Natl. Acad. Sci. USA 85, 6167-6171

Amzel, L. M. and Poljack, R. J. (1979) Annu. Rev. Biochem. 48, 961-997

Anderson, D.J. (1989) TINS. 3:83-85

Apgar, J.R. & Mesher, M.F. (1986). In: "Membrane Skeletons and Cytoskeletal-Membrane Associations (Bennett, V., Cohen, C.M., Lux, S.E. & Palek, J., eds.), pp.293-305, Alan R. Liss, New York.

Arganoff B.W. (1989) In: Basic Neurochemistry" Molecular and Medical Aspects, 4th ed. (Siegel G.J ed.) pp 91-107 Raven Press, New York

Armstrong, R., Friedrich Jr., V., Holmes, K.V. and Dubois-Dalcq, M. (1990) J. Cell Biol. 111: 1183-1195

Arvinte, T. and Hildenbrand, K. (1984) Biochim. Biophys. Acta 775, 86-94

Ash, J.F., Louvard, D. and Singers, S.J. (1977) J. Cell Biol. 74, 5584-5588

Bass, P. W. and Black, M. M. (1990) J. Cell Biol., 111,495-509.

Balakrishnan, K. Hsu, F. J. Cooper, A. D. and McConnel, H. M. (1982) J. Biol. Chem. 257, 6427-6433

Bansal, R., Warrington, A.E., Gard, A.L., Ranchit, B. and Pfeiffer, S.E. (1990) In "Annals of

the New York Academy of Sciences" 605:409-411

Bansal, R., Warrington A. E., Gard, A. L., B. Ranscht, and S. E. Pfeiffer (1989) J. Neurosci. Res. 24, 548-557

Bansal, R. and Pfeiffer , S. E. (1985) J. Neurosci. Res. 14, 21-34

Barbarese, E., Braun, P. E. and Carson, J. H. (1977) Proc. Natl. Acad. Sci. U.S.A.74, 3306-3364

Barbarese, E., Carlson, J. H. and Braun, P. E. (1978) J. Neurochem., 31,. 779-782

Behar, T., F. A. McMorris, E. A. Novotny, J. L. Barker, and M. Dubois-Dalcq (1988) J. Neurosci. Res. 21, 168-180.

Bell, M.V., Simpson, C.M.F. and Sargent, J.R. (1983) Lipids 18, 720-726

Ben-Ze'ev, A. (1986). Trends Biochem. Sci. 11, 478-481

Benjamins, J. A., Calahan, R. E., Montgomery, I. E. and Studzinsky, D. M. (1987) J. Neuroimmunol. 14, 325-338

Bennet, V. (1985) Ann. Rev. Biochem. 54:273-304

Bercovici, T. and Gitler, C. (1987) Biochemistry, 17 1484-1489

Bernier, L., Alvarez, F. Norgard, E. M., Raible, D. W., Mentanberry, A., Schembri, J. G., Sabbatini, D. D. and Colman, D. R. (1987) J. Neurosci. 7, 2703-2710.

Besnard, F., Perraud, F., Sensenbenner, M. and Labourdette G. (1989) Int. J. Dev. Neurosci. 7 401-409.

Birchmeier, W., (1984) TIBS 9,192-195

Bird, T. D., Farrel, D. F. and Sumi, S. M. (1978) J. Neurochem. 31, 387-395

Birkett, D. J., Price, N. C., Radda, G. K. and Salmon, A. G. (1970) FEBS Lett. 6, 346-348

Bizzozero, O. A. and Lees, M. B. (1986) J. Neurochem. 46, 630-636

Blackenmore, W. F. and Franklin, R. J. M. (1991) TINS 14, 323-327

Bligh, E. G. and Dyer, W. J. (1959) Can. J. Biochem. 37, 911-917

Blobel, G. and Dobberstein, B. (1975) J. Cell Biol. 104, 749-760

Bloom, G. S. and Brashear, D. A. (1989) J. Biol. Chem. 264, 16083-16092

Bloom, G. S., Luca, F. C. and Vallee, R. B. (1985) Proc. Natl. Acad. Sci. USA 82:5404-5408.

Bögler, O., Wren, D., Barnett, S.C. Land, H. & Noble, M. (1990) Proc. Natl. Acad. Sci. USA 87: 6368-6372

Bologa L., Aizenman, Y., Chiapelli, F. and de Vellis, J. (1986) J. Neurosci. Res. 15, 521-528

Bottenstein, J.E. and Sato, G.H. (1979) Proc. Natl. Acad. Sci. USA 76, 514-517

Boyer, E. D. (ed.) In: "Enzymes" (1983), Ch. 10, pp. 358-407

Bradbury, J. M. and Thompson, R. J. (1964) Biochem. J. 221, 361-368

Bradbury, J. M., Campbell, R. S. and Thompson, R.J. (1964) Biochem. J. 221, 351-359

Brammer, M. J. (1984) J. Neurochem. 42, 135-141

Braskus, T. A., Dahiya, R. and Dudeja, P. K. (1988) Biochim. and Biophysica Acta, 958, 218-216

Braun P. E (1984) In: "Myelin" 2nd ed (Morell, P., ed.). Plenum Press, New York

Braun, P. E., De Angelis, D., Shtybel, W. W. and Bernier, L. (1991) J. Neurosci. Res. 30, 540-544

Bray, D. and White, J. G. (1988) Science 239, 883-889

Breitfield, P.P., McKinnon, W.C. and Mostov, K. E. (1990) J. Cell Biol. 111, 2365-2373

Bremer, E. G., Hakomori, S., Bowen-Pope, D. F., Raines, E. and Ross, R. (1984) J. Biol. Chem. 259, 6818-6825

Brenner, S. L. and Brinkley, B. R. (1981) Cold Spring Harbor Symp. Quant. Biol. 46, 241-256

Brophy, P. J. (1992) In Myelin: Biology and Chemistry, (Martenson, R. E, ed) pp197-212 CRC Press Inc.

Brown, D. A. and Rose, J. K. (1992) Cell, 68, 533-544

Brown, S. Levinson, W. and Spudich, J.A. (1976) J. Supramol. Struct. 5, 119-130

Brüning, A., Karrenbauer, A., Schnabel, E. and Wieland, F. T. (1992) J. Biol. Chem. 267, 5052-5055

Bunge, M. B., Bunge, R. P. and Ris, H. (1961) J. Biophys. Biochem. Cytol. 10, 67-94

Bunge, P. P. (1991) In "Annals of the New York Academy of Sciences", (Duncan, I. D., Skoff, R. P. and Colman, D., eds.) 605, 229-233

Burgess, T.L., Skoufias, D. A. and Wilson, L. (1991) Cell motility and the Cytoskeleton 20, 289-300

Burke, B. and Warren, G. (1984) Cell 36, 847-856

Burn, P. and Burger, M. M. (1985) Experimentia 41, 779

Burn, P., Rothman, A., Meyer, R. K. and Burger, M. M. (1988) Nature 314, 469-472

Caceres, A., and Kosik K. S. (1990) Nature 343, 461-463.

Cambi F., Lees, M. B., Williams, R. and Maclin, W. (1983) Ann. Neurol. 13, 303-308

Cameron, R. S. and Paluc, P. (1991) GLIA 4: 124-137

Campagnoni, A. T. (1988) J. Neurochem. 51, 1-14

Carraway, K. L. and Carothers, C. A. (1989) Biochim. Biophys. Acta 988, 147-157

Carson, J. H., Nielson, M. L. and Barbarese, E. (1983) Dev. Biol. 98, 485-492

Chandekar, L. P., Paik, W. K. and Kim, S. (1986) Biochem. J. 240, 471-479

Chang, P. C., Yang, J. C., Fujitaki, J. M., Chiu, K. C. and Smith, R. A. (1986) Biochemistry, 25, 2682-2686

Chattopadhay, A. and London, E. (1988) Biochim. Biophys. Acta 938, 24-34

Chattopadhyay A. and London, E. (1987) Biochemistry 26, 39-45

Chattopadhyay, A. (1990) Chem. Phys. Lipids. 53, 1-15

Christie W.W. (1982). Lipid analysis, 2nd Edition, pp52-53. Pergamon Press, Oxford, U.K.

Christie, W. W. (1973) Lipid analysis, 2nd edn., pp 197-201

Colman, D. R., Kreibich, G., Frey, A. B. and Sabatini, D. (1982) J. Cell Biol. 95, 598-608

Connolly, J. A. and Kalnins, V. I. (1980) Exp. Cell Res. 127, 341-350

Connor, J. R. and Fine, R. E. (1986) Brain Res. 368, 319-328

Constantino-Ceccarini E. and Suzuki, K. (1978) J. Biol. Chem. 253, 340-342

Constantino-Ceccarini, E. and Suzuki, K. (1975) Brain Res. 93, 358-362

Crang, A. J. and Jackobsen, W. (1983) J. Neurochem. 39, 244-247

Cunningham, B.A., Hemperly, J.J., Murray, B.A., Prediger, E.A., Brackenberry, R. and Eddelman, G.M. (1987) Science 236, 799-806

de Ferra, F., Engh, H., Hudson, L., Kamholz, J., Puckel, C., Molineaux, S. and Lazzarini, R. A. (1985) Cell 43, 721-727

de Nechaud B., Wolff, A., Jeantet, C. and Bourre, J-M. (1983) J. Neurochem. 41, 1538-1544

de Nechaud, B., Wolff, A., Jeantet, C. and Bourre J. M. (1983) J.Neurochem. 41, 1538-1544

Deibler, G. E., Stone, A. L. and Kies, M. W. (1990) Proteins: Structure, Function and Genetics 7, 32-40

Del Rio Hortega, P. (1919) Bol. Soc. Esp. Biol. (Madrid) 9, 69-120

Des Jardins, K. C. and Morell, P. (1983) J. Cell Biol. 97, 436-446

Di Biase, A., Argiolas, L., Contaloni, A. and Salvati, S. (1991) Neurochem. Res. 16, 551-554

Diaz, N. J., and Avila, J. (1989) J. Cell Sci. 92, 607-620

Diehl, H.-J., Schaich, M., Budzinsky, R.-M. and Stoffel, W. (1986) Proc. Natl. Acad. Sci. U.S.A. 83, 9807-9811

Dinsmore, J. H., and Solomon, F. (1991) Cell 64, 817-826

Dorns, R. W., Russ, G. and Yewdell, J. W. (1989) J. Cell Biol. 109, 61-72

Donaldson, J. G., Lippincott-Schwartz, J., Bloom, G. S., Kreis, T. E. and Klausner, R. D. (1990) J. Cell Biol. 111, 2295-2306

Dowhan, W. (1992) In Dynamics of membrane assembly (Jos A. F. den Camp, ed.) NATO ASI series H: Cell Biology vol. 63, pp11-32

Dubois-Dalcq, M. E. and Armstrong, R. C. (1991) In "Myelin: Biology and Biochemistry" (Martenson, R. E., ed.) pp. 81-122, CRC Press Inc.

Dubois-Dalcq, M. E., Behar, T., Hudson, L. and Lazzarini, R. A.(1986) J. Cell Biol. 102, 384-392

Duncan, J. R. and Cornfeld, S. (1988) J. Cell Biol. 106, 617-628

Dyer, C. A. and Benjamins, J. A. (1989a) J.Neuroscience Res. 24, 201-212

Dyer, C. A. and Benjamins, J. A. (1989b) J.Neuroscience Res. 24, 213-221

Dyer, C. A. and Benjamins, J. A. (1990) J. Cell Biol. (111, 625-633)

Dyer, C. A. and Benjamins, J. A. (1992) J. Neurosci. Res. 30, 699-711

D'Urso, D, Brophy, P. J. , Stugaitis, S. M. Gillespie, S. C., Frey, A. B., Stempak, J. G. and Coleman, D. R. (1990) Neuron 2, 449-460

Edelman, G.M. (1984) Ann. Rev. Neurosci. 7, 339-377

Eder, P. S., Soong, C.-J. and Tao, M. (1988) Biochemistry 25, 1764-1770

Edwards, M. A., Braun, P.E. and Bell, C. J. (1989) J. Neurochem. 52, 317-320

Eisenbarth, G. S., Walsh, F. S. and Nirenberg, M. (1979) Proc. Natl. Acad. Sci. USA 76, 4913-4917

Eng., L. F. and Noble, E. P. (1968) Lipids 3, 157-162

Espinosa de los Monteros, A. and Foucaud, B. (1987) Dev. Brain Res. 35, 123-130

Everly, J. L., Brady, R. O. and Quarles, R. H. (1973) J. Neurochem. 21, 329-334

Eylar, J. (1972) In "Functional and Structural Proteins of the Nervous System" (Davison, A.,

Mandel, P. and Morgan, I., eds.) 215-240, Plenum Press, New York

Fanarraga, M. L., Griffiths, I. R., McCulloch, M. C., Barrie, J. A., Cattanach, B. M., Brophy, P. J. and Kennedy, P. G. E. (1991) Neuropathol. and Applied Neurobiol. 17, 323-334

Fannarraga, M. L., Griffiths, I. R., McCulloch, M. C., Barrie, J. A., Kennedy, P. G. E. and Brophy, P. J. (1992) GLIA 5, 161-170

Federoff, S. (1985) in "Molecular Bases of Neurol Development" (Edelman, G. M., Gall, E. D. and Cowan, W. M., eds.) pp. 91-117, Wiley, New York

Fernandez-Moran, H. (1950) Exp. Cell Ress. 1, 143-149)

ffrench-Constant, C., Miller, R. H., Kruse, J., Schachner, M. and Raff, M. C. (1986) J. Cell Biol. 102, 844-853

Figlewicz, D. A., Nolan, C. E. and Jungalwala, F. B. (1985) Trans. Am. Soc. Neurochem. 16, 130-139

Filbin, M. T., Walsh, F. S., Trapp, B. D., Pizzey, J. A. and Tennekoon, G. I. (1990) Nature 344, 871-872

Fischer, I., Konola, J. and Cochary, E. (1990) J. Neurosci. Res. 27, 112-124

Folch J. and Lees, M B. (1951) J. Biol. Chem. 191, 807-817

Forscher, P. and Smith, S. J. (1988) J. Cell Biol. 102, 384-392

Fox, J. E. B., Boyles, J.K., Berndt, M.C. Steffen, P.K. and Anderson, L. K. (1988) J.Cell Biol 106, 1525-1538

Frail, D. E. and Brown, P. E. (1984) J. Biol. Chem. 259, 14857-14862

Fressinaud, C., Vallat, J.M., Rigaud, M., Cassagne, C., La Bourdette, G. and Sarlieve, L.L. (1990) Neurochem. Int. 16, 27-39

Fujishiro, M., Koshaka, S., Nagaike, K. and Tsukada, Y. (1986) J. Neurochem. 47, 191-195

Fujiwara, T., Oda, K. Yokota, S. Takatsuki, A and Ikehara, Y. (1988) J. Biol. Chem. 263, 18545-18552

Fulton A. B., Wan, K. M. and Penman, S. (1980) Cell 20, 849-857

Futerman A. H., Steiger, B., Hubbard, A. L. and Pagano, R. E. (1990) J. Biol. Chem. 265, 8650-8657

Futerman, A. H. and Pagano, R. E. (1991) Biochem. J. 280, 295-302

Gall, C. and Gall, D. R. C. (1968) Nature 220, 165-173

Ganser, A. R. and Kirshner, D. A. (1980) In "Neurological Functions Affecting Myelination" (N. Baumann, ed.) Amsterdam: Elsevier pp. 171-176

Gard, A. L., and Pfeiffer, S. E. (1989) Development 106, 119-132

Gard, A. L., and Pfeiffer, S. E. (1990) Neuron 5, 615-625

Gardam, M. A., Ilovich, J. J. and Silvius, J. R. (1989) Biochemistry, 28, 884-893

Gardiner, M.V and Macklin, W.B. (1988) J. Neurochem. 51, 360-371

Geren, B. B. and Smith, F. O. (1954) In "Fine Structure of Cells" Symposium, Leiden, pp. 251-260

Geuze, H. S. and Morré, J.D. (1991) J. Elec. Mic. Techniques 17, 24-34

Ghosh P. B. and Whitehouse, M. W. (1968) Biochem. J. 108, 155-156

Gilard, B. K., Heath, J. P., Thurmon, L. T. and Marcus, D. M. (1991) Exp. Cell Res. 192, 433-444

Gilard, B. K., Thurmon, L. T. and Marcus, D. M. (1992) Cell Motility and the Cytoskeleton 21, 255-271

Gillespie, C. S., Bernier, L. , Brophy, P. J. and Colman, D. R. (1990b) J. Neurochem. 54, 656-661

Gillespie, C. S., Trapp, B. D., Colman, D. R. and Brophy, P. J. (1990a) J. Neurochem. 54, 1556-1561

Gillespie, C.S., Wilson R., Davidson, A. and Brophy P.J. (1989) Biochem J. 260, 689-696

Godfraind, C., Friedrich, V. L., Holmes, K. V. and Dubois-Dalcq, M. (1989) J. Cell Biol. 109, 2405-2419

Gonatas, N. K., Stieber, A., Gonatas, J., Mommoi, T. and Fishman, P. H. (1983) Molecular and Cellular Biology 3, 91-101

Gonzalez, A.-M., Buscaglia, M., Ong, M. and Baird, A. (1990) J. Cell Biol. 110, 753-765

Gould, R. M., Jessen, K. R., Mirsky, R. and Tennekoon, G. (1992) In " Myelin: Biology and Chemistry" (Martenson, R. E., ed.) pp 123-171, CRC Press Inc.

Griffith, L. M. and Pollard, T. D. (1982) J. Biol. Chem. 257, 9143-9151

Griffiths, G. and Sodeik, B. (1992) In: Dynamics of membrane assembly (Jos A. F. den Camp, ed.) NATO ASI, series H: Cell Biology vol. 63, pp33-38

Griffiths, I. R. and Simons, K. (1986) Science 234, 438-443

Griffiths, I. R., Scott, I., McCulloch, M. C., Barrie, J. A., McPhilemy, K. and Cattanach, B. M. J. (1990) Neurocytol. 19, 273-283

Hakomori, S. (1989) Adv. Cancer Res. 91, 157-331

Hakomori, S. (1990) J. Biol. Chem. 265, 18713-18716

Hakomori, S. and Kanagi, R. (1983) J. N. C. I 71, 141-151

Hanai, N., Nores, G. A., MacLeod, C. and Torre-Mendez, L. (1988) J. Biol. Chem. 263, 10915-10921

Hannun, Y. A. and Bell, R. M. (1989) Science 243, 500-507

Hanson, T., Stagsted, J., Pedersen, L., Roth, R. A., Goldstein, A. and Olsson, L. (1989) Proc. Natl. Acad. Sci. USA 86, 3123-3126

Hardy, M., Reddy, U. R. and Pleasure, D. (1992) J. Neurosci. Res. 31, 254-262

Hardy, R. and Reynolds, R. (1991) Development 111, 1061-1080

Hargreaves, A.J., Wandosell, F. and Avila, P. (1986) Nature 323, 827-828

Harri, E., Loeffler, W., Sigg, H. P., Stahelin, H. and Tamm, H. (1963) Helv. Chem. Acta 46, 1235-1243)

Harrow, E. & Lane, D. (1988) In: "Antibodies: A laboratory manual" Cold Spring Harbor Laboratory pp 258-259

Harvey, A. R., Chen, M. and Dyson, S. E. (1991) In "Annals of the New York Academy of Sciences". (Duncan, I. D., Skoff, R. P. and Colman, D., eds.) 605, 573-576

Hirano, A., (1968) J Cell Biol. 38: 367-373

Ho, W. C., Allan, J., Von Meer, G, Berger, E. G. and Kreis, T. E. (1989) J. Cell Biol. 48, 250-263

Hoekstra, D. (1982) Biochemistry 21, 2833-2840

Hogan, E. L. and Greenfield, S. In: "Myelin" (1984) (Morell, P. ed.) pp 489-534, Plenum Press, New York

Holt, C. and Sawyer, L. (1988) Protein Eng. 2, 251-259

Hopkins, C. R. (1992) TIBS 17, 27-31

Huber, G., and Matus, A. (1984) J. Neurosci. 4, 151-160

Hudson, L. D. and Nadon, N. L (1992) In: "Myelin: Biology and Chemistry" (Martenson, R. E. ed.) pp677-702 CRC Press Inc.

Hudson, L. D., Friedrich, Jr., V. L., Behar, T., Dubois-Dalcq, M. and Lazzarini, R. A. (1989) J. Cell Biol. 109, 717-723

Hudson, L., Ono, K., Friedrich, V., Benecke, J., Dubois, Dalcq M. and Lazzarini, R. A. (1987) J. Neurosci. Res. 18, 322-334

Hunkapiller, T. and Hood, L. E. (1986) Nature 323, 15-16

Hunziker, W., Whitney., J. A. and Mellman, I. (1991) Cell 6, 568-579

Igahashi, Y., Hakomori, S., Toyokuni, T., Dean, B., Fujita, S., Sugimoto, M., Ogawa, T., El-Ghendy, K. and Racker, E. (1989) Biochemistry 28, 6796-6800

Igarashi, M. and Suzuki, K. (1977) J. Neurochem. 28, 729-738

Ikenaka, K., Kagawa, T. and Mikoshiba, K. (1992) J. Neurochem. 58, 2248-2253

Imamoto, K., Paterson, J. A. and Leblond, C. P. (1978) J. Comp. Neurol. 180-115-138

Jeckel, D., Karrenbauer, A., Birk, R., Schmidt, R. R. and Wieland, F. (1990) FEBS Lett. 261, 255-157

Jeckel, D., Karrenbauer, A., Burger, K. N. J., van Meer, G. and Wieland, F. (1992) J. Cell Biol. 117, 259-267

Jesaitus, A. J., Naemura, J. R., Sklar, L. A., Cochrane, C.G. and Painter, R. G. (1984) J. Cell Biol. 98, 1376-1387

Jessen, K. R. and Mirsky, R. (1991) GLIA 4, 185-194

Jessen, K. R., Morgan, L., Brammer, M. and Mirsky, R. (1985) J. Cell Biol. 101, 1135-1143

Johanson, L. B.-A., Molotkovsky, J. G. and Bergelson, L. D. (1990) Chemistry and Physics of Lipids 53, 185-189

Johnson , G. V. W. and Jope, R. S. (1988) Brain Research, 456, 95-103

Johnson, P. W., Abramov-Newerly, W., Seilheimer, B., Sadoul, R., Tropak, M. B. Arquint, M., Dunn, R. J., Schachner, M. and roder, J. (1989) Neuron 3, 377-385

Kamholz, J. and Wrabetz, L. (1992) in Myelin: Biology and Chemistry, (Martenson, R. E, ed) pp367-385 CRC Press Inc.

Kandekar, S. S. and Jacobson, G. R. (1989) J. Cell Biochem. 39, 207-216

Kang, H. C., Fisher, P. J., Prendergast, F. G. and Haughland, R. P. (1988) J. Cell Biol. 107, 34a

Kaplan, M. S. and Hinds, J. W. (1980) J. Comp. Neurol. 193, 711-727

Karin N. J. and Waehneldt T. V. (1985) Neurochem. Res. 10, 897-907

Karrenbauer, A., Jeckel, D., Just, W., Birk, R., Schmidt, R. R., Rothman, J. E. and Wieland, F. T. (1990) Cell, 63, 259-267

Kasurinen, J. and Somerharju, P. (1992) In: Dynamics of membrane assembly (Jos A. F. den Camp, ed.) NATO ASI series H: Cell Biology vol. 63, pp127-14

Kean, E. C. (1968) J. Lipid Res. 9, 319-327

Keenan, T. W., Morré, D. J. and Basu, S. (1974) J. Biol. Chem. 249, 310-315

Kelly, B.M., Gillespie, C.S., Sherman D.L. and Brophy, P.J. (1992) J. Cell Biol. 118, 397-410

Kendler, A. and Dawson, G. (1992) J. Neurosci. Res. 31, 205-211

Kishimoto, Y. (1983), In the "Enzymes", vol. XVI (Boyer, P.D., ed) pp 358-407, Academic Press, New York

Kishimoto, Y. and Kawamura, N. (1979) Mol. Cell. Bioch. 23, 17-25

Kitten, G. T. and Nigg, E. A. (1991) J. Cell Biol. 113, 13-23

Klausner, R. D., Donaldson, J. G. and Lippincott-Schwartz, J. (1992) J. Cell Biol. 116, 1071-1080

Klein, D., Leinekugel, P., Pohlentz, G., Schwarzmann, G. and Sandhoff, K. (1988) In "Trends in Ganglioside Research: Neurochemical and Neurogenerative Aspects", (Ledeen, R. W., Hogan, E. L., Tettamanti, G., Yates, A. J. and Ku, R. K. eds.) pp. 247-258 Padova, Liviana

Kobayashi, T. (1984) FEBS Lett. 169, 224-228

Kobayashi, T. and Pagano, R. E. (1989) J. Biol. Chem. 264, 5966-5973

Kobayashi, T. and Pagano, R. E. (1988) Cell 55, 797-805

Kofler, A., Gratzer, W.B., Clarke, G.D. and Hales, A. (1983) J. Cell Sci. 61, 191-216

Kok, J. W., Eskelinen, S., Hoekstra, K. and Hoekstra, D. (1989) Proc. Natl. Acad. Sci. USA 86, 9869-9900

Kolesnick, R. N. (1991) Prog. Lip. Res. 30, 1-38

Koul, O. and Jungalwala, F. B. (1981) Biochem. J. 194, 633-637

Koul, O. and Jungalwala, F. B. (1986) Neurochem. Res. 11, 231-239

Koul, O., Chou, K. H. and Jungalwala, F. B. (1980) Biochem. J. 186, 959-969

Koul, O., Singh, I. and Jungalwala, F. B. (1988) J. Neurochem. 50, 580-586

Koval, M. and Pagano, R. E. (1989) J. Cell Biol. 108, 2169-2181

Koval, M. and Pagano, R. E. (1990) J. Cell Biol. 111, 429-442

Koval, M. and Pagano, R. E. (1991) Biochimica and Biophysica Acta 1062, 113-125

Koval, M. and Pagano, R. E. (1991). Biochim. Biophys. Acta 1062: 113-125

Kreibich, G. and Sabatini, D. D. (1974) J. Cell Biol. 61, 789-807

Kreis, T. E. (1990) Cell Motil. Cytoskeleton 15, 67-70

Kronquist, K. E., Crandall, B. and F. Macklin, W. B. and Campagnoni, A. T. (1987) J. Neurosci. Res. 18, 395-401

Ktistakis, N. T., Linder, M. E. and Roth, M. G. (1992) Nature 356, 344-346

Kurishita T. and Ledeen, R. W. (1984) J. Neurochem. 42, 326-333

Kurishita, T., Vaswani, K. K., Morrow, C. R., Novak, G. P. and Ledeen, R. W. (1987) J. Neurochem. 48, 1-7

Kurihara, T. and Takahashi, Y. (1973) J. Biol. Chem. 262, 3256-3261

Kurihara, T., Fowler, A. V. and Takahashi, Y. (1987) J. Biol. Chem. 262, 3256-3261

Kurihara, T., Takahashi, Y., Nishiyama, A. and Kumanishi, T. (1988) Bioch. Biop. Res. Comm. 152, 837-842

Laemmli, U. K. (1970) Nature 227, 680-682

Lai, C., Brow, M. A., Nave, K-A., Norohna, A. G., Quarles, R. H., Bloom, F.E., Milner, R. J. and Sutcliffe, J. G. (1987) Proc. Natl. Acad. Sci. USA 84, 4337-4341

Larsen E., Palabrica, T., Sajer, S., Gilbert, G. E., Wagner, D. D., Furie, B. C. and Furie, B. (1990) Cell 63, 467-474

Laursen R. A., Sammiulah, M. and Lees. M. B. (1984) Proc. Natl. Acad. Sci. U.S.A. 81, 2912-2916

Le Duarin, N., Dulac, C., Dupin, E. and Cameron-Dury, P. (1991) GLIA 4: 175-184

Ledeen, R. W., Fong, J. W. and Brostoff, S. W. (1975) Trans. Am. Soc. Neurochem. 6, 149

Lees, M. B. and Brostoff, S. W. (1984) In: "Myelin", 2nd ed., (Morell, P. ed.), pp. 197-224, Plenum Press, New York

Lemke, G. (1988) Trends in Neurosciences 9, 266-270

Lemke, G. (1988) Neuron, 1, 535-543

Lemke, G. and Axel, R. (1985) Cell 40, 501-508

Lemke, G., Lamar, E. and Patterson, E. (1988) Neuron, 1, 73-83

Lerner, P., Campagnoni, A. G. and Sampugna, J. (1974) J. Neurochem. 22, 163-172

Letterier, J. F., Liem, R. K. H. and Shelanski, M. L. (1982) J. Cell Biol. 95, 982-986

Levi, G., Agresti, C., D'Urso, D. and Aloisi, F. (1991) Neurosci. Lett. 128, 37-41

Levi, G., Aloisi, F. and Wilkin, G. P. (1987) J. Neurosci. Res. 18, 407-417.

LeVine S.M., Wong, D. and Macklin, W. B. (1990) Dev. Neurosci. 12, 235-250

LeVine, S. M. (1989) Neuron 3, 103-112

LeVine, S. M. and Goldman, J. E. (1988a) J. Neurosci. 8, 3992-4001

LeVine, S. M. and Goldman, J. E. (1988b) J. Comp. Neurol. 277, 441-449

Linardic, C. M., Jayadev, S. and Hannun, Y. A. (1992a) Clinical Res. 40, 323-334

Linardic, C. M., Jayadev, S. and Hannun, Y. A. (1992b) J. Biol. Chem. 267, 14909-14911

Lippincott-Schwartz J., Yuan, L., Tipper, C., Amherdt, M., Orci, L. and Klausner, R. D. (1991a) Cell, 67601-616

Lippincott-Schwartz, J., Donaldson, J. G., Schweizer, A., Berger, E. G., Hauri, H.-P., Yuan, L. C. and Klausner, R. D. (1990) Cell 60, 821-836

Lippincott-Schwartz, J., Glickman, J., Donaldson, J. G., Robbins, J., Kreis, E., Seamon, K. B., Sheetz, M. P. and Klausner, R. D. (1991b) J. Cell Biol. 112, 567-577

Lipsky, N. G. and Pagano, R. E. (1983) Proc. Natl. Acad. Sci. USA 80, 2608-2612

Lipsky, N. G. and Pagano, R. E. (1985a) J. Cell Biol. 100, 27-34

Lipsky, N. G. and Pagano, R. E. (1985b) Science 228, 745-747

Lisak, R. P., Pleasure, D., Silderberg, D. H., Manning, M. and Saida, T. (1981) Brain Res 223, 107-122)

Lobel, P., Fujimoto, K., Ye, R. D., Griffiths, G. and Kornfeld, S. (1989) Cell 57, 787-796

Louis, J. C., Magal, E., Muir, D., Manthorpe, M. and Varon, S. J. Neurosci. Res. 31, 193-204

Low, M. (1992) Biochim. Biophys. Acta 988, 427-454

Lowry, O. H., Rosenbrough, N. J., Farr, A. L. and Randall, R. J. (1951) J. Biol. Chem. 193, 265-268

Lucocq, J. and Warren, G. (1987) EMBO J. 6, 3239-3246

Luzio, J. P., Brake, B., Banting, G., Howell, K. E., Braghetta, P. and Stanley, K. K. (1990) Biochem. J. 270, 97-102.

Macala, L. J., Yu, R.K. and Ando, S. (1983) J. Lip. Res. 24, 1243-1250

Macklin W. B. (1988) Trans. Am. Soc. Neurochem. 19, 132-143

Macklin W. B., Weill, C. L. and Deininger, P. L. (1986) J. Neurosci. Res. 16, 203-217

Macklin, W. B. (1992) In Myelin: Biology and Chemistry, (Martenson, R. E, ed) pp257-276 CRC Press Inc.

Malgat, M., Maurice, A. and Baraud, J. (1986) J. Lip. Res. 27, 251-260

Manieri L. R. and Low, P. S. (1989) Biochem. Biophys. Res. Commun. 159, 1012-1019

Mansfield, S. G., Diaz-Nido, J., Gordon-Weeks, P. R. and Avila, J. (1992) J. Neurocytology 21, 1007-1022

Martenson, R. E., Law, M. J. and Diebler, G. E. (1983) J. Biol. Chem. 258, 930-937

Martenson, R.E., Deibler, G.E. and Kies, M. W. (1969). Proc. Natl. Acad. Sci. (U.S.A.) 63, 4962-4966

Mateoni, R. and Kreis, T. E. (1987) J. Cell Biol. 105, 1253-1256

Matthieu, J. M., Everly, J. L., Brady, R. O. and Quarles, R. H. (1975) Biochim. Biophys. Acta 392, 167-174

Matthieu, J.-M., Constantino-Ceccarini E., Bény, M. and Reigner, J. (1980) J. Neurochem. 35, 1345-1350

Maturana, R. H. (1960) J. Biophys. Biochem. Cytol. 7, 107-120

Matus, A. (1988) Annu. Rev. Neurosci. 11, 29-44

Matus, A. (1990) J. Physiol. Paris. 84, 134-137

Maurice, A. , Malgat, M. and Baraud, J. (1989) Biochimie 71, 373-378

Mc Keehan, W. (1984) In: "Cell culture methods for molecular and cell biology", (Barnes, W., Sirbasku, D.A., Sato, G.H., eds) Vol.1, pp209-213 Alan R. Liss Inc., N.Y.

McCarthy, K. and de Vellis, J. (1980) J. Cell Biol. 85, 890-902;

McCarthy, K. D., and DeVellis, J. (1980) J. Cell Biol. 85, 890-902

McGarry, R.C., Helfand, S. L., Quarles, R.H. and Roder, J. C. (1983) Nature 306, 376-378

McKinnon, R. D., Matsui, T., Dubois-Dalcq, D. M. and Aaronson, S. A. (1990) Neuron 5, 603-614

McMorris, F. A. and Dubois-Dalcq, D. M. (1988) J. Neurosci. Res. 21, 199-209

McMorris, F. a., Furlanetto, F. W., Dubois-Dalcq, M., Mozell, R. L., Carson, M. J. and Raible, D. W. (1990) In: "Differentiation and functions of glial cells" (Levi, G. ed.) pp61-78 Alan R.

Liss, New York

Meir, H. and MacPike, A. D. (1970) Exp. Brain Res. 10, 502-509

Mentaberry, A., Adasnik, M., Atchinson, M., Norgard, E. M., Alvarez, F., Sabatini, D. D. and Colman, D. R.(1986) Proc. Natl. Acad. Sci. USA. 83, 1111-1114

Merrill, A. H. Jr. and Stevens, V. L. (1989) Biochim. Biophys. Acta 1010, 131-139

Miller, R. H., David, S., Patel, R., Abney, E. R. and Raff, M. C. (1985) Dev. Biol. 111, 35-41

Miller-Prodzara, H. and Fishman, P. H. (1982) Biochemistry 21, 3265-3270

Miller-Prodzara, H. and Fishman, P. H. (1984) Biochim. Biophys. Acta 804, 44-51

Milner R.J., Lai, C., Nave, K. A., Lenoir, D., Ogata, J. and Sutcliffe, J. G. (1985b) Cell 42, 931-939

Modesti, N. M. and Barra, H. S. (1986) Biochem. Biophys. Res. Comm. 136,482-489

Moore, P. L., Guzikowski, A. P., Kang, H. C. and Haughland, R. P. (1988) J. Cell Biol. 107, 34a

Morell P. and Radin, N. S. (1969) Biochemistry 8, 506-512 Raven Press, New York

Morell P., Quarles R. H. and Norton W. T. (1989) In: "Basic Neurochemistry: Molecular and Medical Aspects" 4th ed. (Siegel G.J ed) , pp 109-135

Morell, P. and Toews, A. D. (1984) In: "Oligodendroglia" (Norton, W. T. ed.) pp. 47-86. Plenum Press, New York

Moscarello, M.A. (1990) In: Dynamic Interactions of Myelin Proteins", pp 25-48. Allan R. Leiss, Inc

Moss, D. J. and White, C. A. (1992) Eur. J. Cell Biol. 57, 59-65

Murasoka, S. and Takahashi, T. (1989) Dev. Brain Res. 49, 63-74

Murray N and Sleck, A.J. (1984) Lancet 1, 711-713

Naismith, A.L., Hoffman-Chudzik, E., Taul, L-C and Riordan, J. R. (1985) Nucleic Acids Res. 13, 7413-7425

Nave, K.-A., Lai, C., Bloom, F. E. and Milner, R. J. (1987) Proc. Natl. Acad. Sci. (USA) 84, 5665-5669

Nescovic, N. M., Salvieve, L. L. and Mandel, P. (1973) J. Neurochem. 20, 1419-1430

Newman, S., Kitamura, K. and Campagnoni, A. T. (1987) Proc. Natl. Acad. Sci. U.S.A. 84, 886-890

Nicols, J. W. (1985) Biochemistry 24, 6390-6398

Nicols, J. W. and Pagano, R. E. (1981) Biochemistry 20, 2783-2789

Nicols, J. W. and Pagano, R. E. (1982) Biochemistry 21, 1720-1726

Niggli, V. and Burger, M. M. (1987) J. Membrane Biol. 100, 97-121

Nishizuka, Y. (1988) Nature (London) 334, 661-665

Nixon, R. A., Lewis, S. E. and Marotta, C. A. (1987) J. Neurosci. 7, 1145-1158

Noble, M. (1991) GLIA 4, 157-164

Noble, M., Barnett, S. C., Bogler, O., Land, H., Wolswijk, G. and Wren, D. (1990) In: "Proto-oncogenes in cell development" Wiley, Chichester (Ciba Foundation Symposium 150) p227-249

Noble, M., Lewis, S. A. and Cowan, N. J. (1989) J. Cell Biol. 109, 3367-3376

Noble, M., Murray, K., Stroobant, P., Waterfield, M. D. and Riddle, P. (1988) Nature 333, 560-562

Norton, W. T. (1981) In: "Basic Neurochemistry" (Siegias G J, Alberts R. W., Arganoff B W, Kutzman, eds) R. Boston pp83-92 Little Brown,

Norton, W. T. and Cammer, W., (1984) In: "Myelin" 2nd ed (Morell P, ed) pp147-195 Plenum Press, New York

Norton, W. T. and Farooq, M. (1989) J. Neurosci. 9, 769-773

Norton, W. T. and Poduslo, S. E. (1973) J.Neurochem. 21, 759-766

Norton, W. T.(1977) In: "Myelin" 1st ed. (Morell, P. ed.) pp. 161- 199 Plenum Press, New York

Nussbaum, J. and Mandel, P. (1973) Brain Res. 61, 295-306

Omanand, K., Singh, I. and Jungalwala, F. B. (1988) J. Neurochem., 50, 580-588

Orci, L., Tagaya, M., Amherdt, M., Perrelet, A., Donaldson, J., Lippincott-Schwartz, J., Klausner, R. D. and Rothman, J. E. (1991) Cell 64, 1183-1195

Owens, G. C. and Bunge, R. P. (1991) Neuron 7, 565-575

Packham, M. A., Guccione, M. A., Bryant, N. L. and Livne, A. (1991) Lipids 26, 485-491

Pagano, R. E. (1988) TIBS, 13, 202-206

Pagano, R. E. (1990) Curr. Opinion in Cell Biol. 2, 662-663

Pagano, R. E. and Martin, O. C. (1988) Biochemistry 27, 4439-4445

Pagano, R. E. and Sleight, R. G. (1985a) Trends Biochem. Sci. 10, 421-425

Pagano, R. E. and Sleight, R. G. (1985b) Science 229, 1051-1057

Pagano, R. E., Sepanski, M. A. and Martin, O. (1989) J. Cell Biol. 109, 2067-2079

Pagano, R. E., Sepanski, M. and Martin, O. (1989) J. Cell Biol. 109, 2067-2079

Pagano, R.E., Martin, O.C., Kang, H.C. and Haughland, R. P. (1991) J. Cell Biol. 113(6): 1267-1279

Pasquini, J. M., Guarna, M. M., Besiomoreno, M. A., Iturequi, M. T., Oteiza, P. I. and Soto, E. F. (1989) J. Neurosci. Res. 22, 289-296

Paterson, J. A. (1983) Anat. Anz. 153, 149-168

Patton, S. (1970) J. Theor. Biol. 29, 489-491

Pearse, B. M. F. and Robinson, M. S. (1990) Annu. Rev. Cell Biol. 6, 151-171

Pedraza, L., Owens, G. C., Green, L. A. D. and Salzer, J. L. (1990) J. Cell Biol. 111, 2651-2661

Pelham, H. R. B. (1991) Cell 67, 449-451

Pereyra, P. M., Horvath, E. and Brown, P. E. (1988) .Neurochem. Res. 143, 583-595

Perlman, R., Bottaro, D. P., White, M. F. and Kahn, C. R. (1989) J. Biol. Chem. 264, 8946-8950

Peters, A. (1960) J. Biophys. Biochem. Cytol. 7, 121-126)

Phillips, M. L., Nudelman, E., Gaeta, F. C. A., Singhal, A. K., Hakomori, S. and Paulson, J. C. (1990) Science 250, 1130-1132

Poduslo, J. F. and Brown, P. E. (1975). J. Biol. Chem. 250, 1099-1105

Poduslo, S. E., Miller, K. and Pak, C. H. (1990) Neurochemical Research 15, 739-742

Polak, M., Heymaker, W., Johnson, J. E. Jnr and D'Amelio, F. (1982) In "Histology and Histopathology of the Nervous System" (Haymaker, W. and Adams, R. D. eds.) pp. 363-480. Charles C. Thomas Springfield

Poltorak, M., Sadoul, R., Keilhauer, G.Landa, C.Fahrig, T. and Schachner, M. (1987) . J. Cell Biol. 105, 1893-1899

Price, J. (1987) Development 101, 409-419

Price, N. C., Cohn, M. and Schirmer, R. H. (1978) J. Biol. Chem. 250, 644-652

Quarles R.H., Everly, J.L. and Brady, R.O. (1972) Biochem. Biophys. Res. Comm. 66, 491-

Quarles, R. H. (1983/84) Dev. Neurosci. 6, 285-303

Quarles, R. H., Barbarash, G. R., Figlewitz, D. A. and McIntyre, L. J. (1983) Biochim. Biophys. Acta 757, 140-143

Raff, M. C., Mirsky, R., Fields, K. L., Lisak, R. P., Dorfman, S. H., Silderberg, D. H., Gregson N. A., Liebowitz, S., Kennedy, M. C. (1978) Nature, 274, 813-16

Raff, M. C. (1989) Science 243, 1450-1455

Raff, M. C., Aney, E., Brockes, J. P. and Hornby-Smith, A. (1978) Cell 15, 813-822

Raff, M. C., Lillien, L. E., Richardson, W. D., Burne, J. F. and Noble, M. D. (1988) Nature 333, 562-565.

Raff, M. C., Miller, R. H. and Noble, M. D. (1983) Nature 303, 390-396

Raff, M. C., Williams, B. P. and Miller, R. H. (1984) EMBO J. 5, 1857-1864

Raine, C. S. (1984) in "Myelin", 2nd ed., (Morell, P. ed.) pp. 259-310, Plenum Press, New York

Ramon y Cajal, S. (1934) In: "Degeneration and regeneration of the nervous system" vol 2, pp 485-921, Oxford University Press, London, 1958

Ramwani, J. and Moscarello, M. A. (1990) J. Neurochem. 55, 1703-1710

Ramwani, J. and Moscarello, M. A. (1990) J. Neurochem. 55, 1703-1710

Rancht, B., Clapshaw, P. A., Price, J., Noble, M. and Seifert, W. (1982) Proc. Natl. Acad. Sci. USA 79, 2709-2713

Rando, R. R. (1988) FASEB J. 2, 2348-2355

Ranvier, L. (1871) C. R. Acad. Sci. 73, 1168

Reaves, R. and Banting, G. (1992) J. Cell Biol. 116, 85-94

Richardson, W. D., Pringle, N., Mosley, M. J., Westermark, B. and Dubois-Dalcq, M. (1988) Cell 53, 309-319.

Rogalski, A. A., Bergman, J. E. and Singer, S. J. (1984) J. Cell Biol. 99, 1101-1109

Rome, L. H., Bullock, P. N., Chiappelli, F., Cardwell, M., Adinolfi, A. M. and Swanson, D. (1986) J. Neurosci. Res. 15, 49-65

Rosenwald, A. G., Pagano, R. E. and Raviv, Y. (1991) J. Biol. Chem. 266, 9614-9621

Rothman, J. E. (1987) Cell 50, 521-522

Rothman, J. E. and Orci, L. (1990) FASEB J. 4, 1460-1468

Roussel, G. and Nussbaum, J. L. (1981) Histochem. J. 13, 1029-1047

Roussel, G., Nussbaum, J. L., Espinosa de los Monteros, A. and Nesovic, N. M. (1987) J. Neurocytol. 16, 85-92

Saavedra, R. A., Fors, L., Seal, S. N. and Markus, A. (1989) J. Mol. Evol. 29, 149-156

Sahyoun, N., Shatila, T., LeVine, H. and Cuatrecasas, P. (1981) Biochem. Biophys. Res. Comm. 102, 1216-1222

Saito, M., Saito, M. and Rosenberg, A. (1984) Biochemistry 23, 1043-1046

Sakakibara, K., Momoi, T., Uchida, T. and Nagai, Y. (1981) Nature 293, 76-79

Salzer J.L., Holmes, W. P. and Colman, D. R. (1987) J. Cell Biol. 104, 957-965

Sandel, J. H. and Mashland, R. H. (1988) J. Histochem. Cytochem. 36, 555-559

Sankaram, M. B., Brophy, P. J. and Marsh, D. (1989a) Biochemistry 9685-9691

Sankaram, M. B., Brophy, P. J. and Marsh, D. (1989b) Biochemistry 9691-9698

Sankaram, M. B., Brophy, P. J. and Marsh, D. (1989c) Biochemistry 9698-9707

Sato, C., Larocca, J. N., Pasquini, J. M. and Soto, E. F. (1986) Neurochem. Int. 8, 109-114

Sato-Yoshitake, R., Shiomura, Y., Miyasaka, H. and Hirokawa, N. (1989) Neuron 3, 229-236

Schachner, M., Kim, S. K. and Zehnle, R. (1981) Develop. Biol. 83, 328-333

Schmidt, M (1983) Curr. Top. Microbiol. Immunol. 102, 101-126

Schnabb, M. E. and Schnell, L. (1989) J. Neurocytology 18, 161-169.

Schroit, A. J. and Madsen, J. W. (1983) Biochemistry 22, 3617-3623

Schwann, T. (1839) *Microskopishe Untersuchungen über die Uebereinstimmung in der struktur und dem Wachtsum der Tiere und Pflanzen.* Sander, Berlin

Schwarzmann, G. and Sandhoff, K. (1990) Biochemistry, 29, 10865-10871

Schmitt, F. O. and Bear, R.S. (1939) Biol. Rev. 14, 27-50

Schmitt, F. O., Bear, R. S. and Clark, G. L. (1936) Radiology 25, 131-151;

Scolding, N. J., Frith, S., Linington, C., Morgan, B. P., Campbell, A. K. and Compston, D. A. S. (1989) J.Neuroimmunology 22, 169-176.

Seamon, K. B. and Daly, J. W. (1986) Adv. Cyclic Nucleotide Protein Phosphorylation Res. 20, 1-214

Shanker, G., Campagnoni, A. T. and Pieringer, R. A. (1987) J. Neurosci. Res. 17, 220-224

Shlesinger, M. J. (1992) In: Dynamics of membrane assembly (Jos A. F. den Camp, ed.) vol. 63, pp197-210 and 349-364,NATO ASI, series H:Cell Biology

Siman, R., Baudry, M. and Lynch, G. (1985) Nature 313, 225-228

Simons, K. and van Meer, G. (1988) Biochemistry 27, 6197-6202

Simons, K. and Wandinger-Ness, A. (1990) Cell 62, 207-210

Singh, I., Nolan, C. E., Figlewicz, D. and Jungalwala, F. B. (1986) Trans. Am. Soc. Neurochem. 17, 314-322

Sjöstrand, F. S. (1949) J. Cell Comp. Physiol. 33, 383-388

Skoff, R. P. and Knapp, P. E. (1992) In: "Myelin: Biology and Chemistry" (Martenson, R. E. ed) pp653-676. CRC Press Inc.

Skoff, R. P., Price, D. L. and Stocks, A. (1976) J. Comp. Neurol. 18, 291-312

Skoff, R.P. & Knapp, P.E. (1991) GLIA 4: 165-174

Sleight, R. G. and Pagano, R. E. (1985) J. Biol. Chem. 260, 1146-1154

Snider, M. D. and Rogers, O. C. (1985) J. Cell Biol. 100, 826-834

Sobue, G. and Pleasure, D. (1984) Science, 224, 72-74)

Sommer, I and Schachner, M. (1981) Dev. Biol. 83, 311-327

Sommer, I and Schachner, M. (1982) Neuroscience Letters 29, 183-188

Sossin, W. S., Fisher, J. M. and Scheller, R. H. (1990) J. Cell Biol. 110, 1-25

Sperry, W. M., Brand, F. C. (1943) J. Biol. Chem. 150, 315-324

Sprinkle, T. J., McMorris, F. A., Yoshino, J. and deVries, G.H. (1985) Neurochem. Res. 10, 919-931

Sprinkle, T.J, Wells, M.R., Garver, F.A. and Smith, S.B. (1980) J. Neurochem. 41, 1644-1671

Stein, O., Oette, K., Hollander, G., Dabach, Y., Ben-Naim, M. and Stein, Y. (1989) Biochim. Biophys. Acta 1003, 175-182

Steinert, P. M. and Roop, D. R. (1988) Annu. Rev. Biochem. 57, 593-625

Sternberger , N. H., Quarles, R. H., Itoyama, Y. and Webster, H. De F. (1979) Proc. Natl. Acad. Sci. USA 76, 1510-1514

Stoner, G. L. (1984) J. Neurochem 43, 433-447

Sturrock, R. R. (1982) J. Anat. 134, 771-793;

Sturrock, R. R. (1985) J. Anat. 141, 19-26

Sung, H. Y., Yavin, E., Hammer, J. A. and Quarles, R. H. (1991) J. Neurochem. 57, 2144-2147

Susan, J. M., Kabakoff, B., Fisher, P. A. and Lennarrz, W. J. (1992) In Dynamics of membrane assembly (Jos A. F. den Camp, ed.) NATO ASI series H:Cell Biology vol. 63, pp189-196,

Sutcliffe, J. G. (1987) Trends in Genetics 3, 73-78

Suzuki, M., Sakamoto, Y., Kitamura, K., Fukunara, K., Yamamoto, H., Miyamoto, H. and Uyemura, K. (1990) J. Neurochem. 55, 1899-1971

Tanaka Y. and Schrott A. J. (1983) J. Biol. Chem. 258, 11335-11343

Tartakoff, A. M. (1983) Cell 32, 1026-1028

Thompson, R.J., Bradbury, R.J. and Richardson , P.J. (1986) Biochem. Soc. Trans. 14, 351-352

Thyberg, J. and Moskalewski, S. (1985) Exp. Cell Res. 159, 1-16

Timsit, S. G., Bally-Cuif, L., Colman, D. R. and Zalc, B. (1992) J. Neurochem. 58, 1172-1175

Tirell, J. G. and Coffee, C.J. (1986) Comp. Biochem. Physiol. 83B, 867-873

Towbin, H., Staehlin, T. and Gordon, J. (1979) Proc. Natl. Acad. Sci. (USA) 76, 4350-4354

Townsend, L. E., Benjamins, J. A. and Skoff, R. P. (1984) J.Neurochem. 43, 139-145

Trapp, B. D., Itoyama, Y., Macintosh, T. D. and Quarles, R. H. (1983) J. Neurochem. 40, 47-54

Trapp, B. D., Bernier, L., Andrews, B. and Colman, D. R. (1988) J. Neurochem. 51, 859-868

Trapp, B. D., Hauer, P. and Lemke, G. (1988) J. Neurosci. 8, 3515-3521

Trapp, B. D., Itoyama, Y., Sternberger, N. H., Quarles, R. H. and Webster, H. DeF. (1981) J. Cell Biol. 90, 1-6

Trapp, B. D., Moench, T., Pulley, M., Barbosa, E., Tennekoon, G. and Griffin J. (1987) Proc. Natl. Acad. Sci. USA. 84, 7773-7777

Trapp, B. D., Quarles, R. H. and Suzuki, K. (1984) J. Cell biol. 99, 594-606

Trapp, B., Andrews, B., Cootsuco, C. and Quarles, R. (1989a) J. Cell Biol. 109, 2417-2426

Trapp, B.D., Andrews, B.S., Wong, A., O'Connel, M. and Griffin, J.W. (1989b) J. Neurocytol. 18: 47-60

Trinchera, M. and Ghidoni, R. (1989) J. Biol. Chem. 264, 15766-15769

Trotter, J. and Schachner, M. (1989) Dev. Brain. Res. 46, 115-122

Tucker, R. P. and Matus, A. I (1988a) Dev. Biol., 130, 423-434

Tucker, R. P., Binder, L. I. and Matus, A. I. (1988) J. Comp. Neurol. 271, 44-55

Tucker, R. P., Binder, L. I., Viereck, C., Hemmings, B. A. and Matus, A. I. (1988b) J. Neurosci. 8, 4503-4512

Turner, D. L., Snyder, E. Y. and Cepko, C. L. (1990) Neuron 4, 833-845

Turner, J. R. and Tartakoff, A. M. (1989) J. Cell Biol. 109, 2081-2088

Turner, R. S., Chou, C.-H., Mazzei, G. J., Dembure, P. and Kuo, J. F.(1984) J. Neurochem. 43, 1257-1246

Ulmer, J. B., Edwards, A. M., McMorris, F. A. and Braun, P. E. (1987) J. Biol. Chem. 262, 1748-1755

Uster, P. S. and Deamer, D. W. (1981) Arch. Biochem. Biophys. 209, 385-395

Vale, R. D. and Hotani, H. (1988) J. Cell Biol. 107, 2233-2241

Vallee, R. B. and Shpetner, H. S. (1990) Annu. Rev. Biochem. 59, 909-932

van Dorsselaer, A., Nebih, R., Sorokine, O., Schindler, P. and Lu, B. (1987) C. R. Acad. Sci. Paris 305, 555-560

van Echten, G., Iber, H., Stotz, H., Takatsuki, A. and Sandhoff, K. (1990) Eur. J. Cell Biol. 51, 135-139

van Echten, G. and Sandhoff, K. (1989) J. Neurochem. 52, 207-214

van Meer, G. (1989) Ann. Rev. Cell Biol. 5, 247-275

van Meer, G., Stelzer, E. H. K., Wijnaendts-van-Resandt, R. W. and Simons, K. (1987) J. Cell Biol. 105, 1623-1635

Vance, J. E. (1992) In: Dynamics of membrane assembly (Jos A. F. den Camp, ed.) NATO ASI series H Cell Biology vol. 63, pp103-126

Vance, J. E., Aasman, E. J. and Szarka, R. (1991) J. Biol. Chem. 266, 8241-8247

Vartanian, T., Dawson, G., Sollven, B., Nelson, D. J. and Schuzet, S. (1989) GLIA 2, 370-379

Vartanian, T., Szuchet, S., Dawson, G. and Campagnoni, A. T. (1986) Science 234, 1395-1398

Vaysse, P. J.-J., and Goldman, J. E. (1990) Neuron 5, 227-235.

Viereck, C., Tucker, R. P. and Matus, A. I. (1989) Neuroscience 9, 3547-3557

Virchow, R (1854) *Veber das ausgebreitete Vorkommen einer dem Nervenmark analogen Substanz in der tierichen Geweben*. Virchow's Arch. Path. Anat. 6, 562

Vlodavsky, I., Bar-Shavit, R., Ishai-Michaeli, R. Bashkin, P. and Fuks, Zvi (1991) TIBS 16, 268-271

Vogel, U. S. and Thompson, R. J. (1987) FEBS Lett. 218, 261-265

Waenheldt, T. V. and Malotka, J. (1980) Brain Res. 189, 582-587

Warner, F. D. and Mitchell, D. D. (1980) Int. Rev. Cytol. 66, 1-43

Warren, K. R., Mirsa, R. S., Arora, R. C. and Radin, N. S. (1976) J. Neurochem. 26, 1063-1072

Watt, F. M. (1986) Trends Biochem. Sci. 11, 482-485

Wells , M.R. and Sprinkle, T.J. (1981). J. Neurochem. 36, 633-639

Wiegandt, H. (1982) In "Advances in Neurochemistry" (Arganoff, B. W. and Aprison, M. H., eds.) vol. 4 pp 149-223, Plenum Press, New York

Wieland, F. T., Gleason, M. L., Serafini, T. A. and Rothman, J. E. (1987) Cell 50, 289-300

Wiggins, R. C. and Morell, P. (1980) J. Neurochem. 34, 627-634

Willard, H. F. and Riordan, J. R. (1985) Science 230, 940-942

Williams, A. F. (1987) Immunol. Today 8, 298-303

Williams, A. F. (1987) Today 8, 298-303

Williams, B. P., Read, J. and Price, J. (1991) Neuron 7, 685-693

Wilson, L. and Margolis, R. L. (1981) Cold Spring Harbor Symp. Quant. Biol. 16, 199-205

Wilson, R. and Brophy, P. J. (1989) J.Neuroscience Res. 22, 439-448

Wollgram, F. and Kotorii, K. (1968) J. Neurochem. 15, 1281-1290

Wolswijk, G., Riddle, P. N. and Noble, M. (1991) Glia 4, 495-503

Wolswijk, G. and Noble, M. (1989) Development 105, 387-400

Wood, P. and Bunge, R. P. (1984) In: "Oligodendroglia" (Norton, W. I., ed) vol. 5 pp 1-46 Plenum Press, New York

Wood, P. M. and Bunge, R. P. (1991) GLIA 4, 225-232

Wood, S. A., Park, J. E. and Brown, W. J. (1991) Cell 67, 616-629

Woodhams, P. L., Calvert, R. and Dunnett, S. B. (1989) Neuroscience 28, 49-59

Woodman, P. G. and Warren, G. (1989) In: "Methods in Cell Biology" vol. 31, pp 197-206

Wren, D., Wolswijk, G. and Noble, M. (1992) J. Cell Biol. 116, 167-176

Yang, S-D., Liu, J-S., Fong, Y-L., Yu, J-S. and Tzen, T-C. (1987) J. Neurochem. 48, 160-166)

Young Jr, W. W., Lutz, M. S., Mills, S. E. and Lecher-Osborn, S. (1990) Proc. Natl. Acad. Sci. USA 87, 6838-6842

Zeller N. K., Behar, T. N., Dubois-Dalcq, M E. and Lazzarini, R. A. (1985) J. Neurosci. 5, 2955-2962

Acknowledgments

I am truly grateful to the Science and Engineering Research Council (SERC), whose financial support enabled me to carry out this work.

My supervisor Dr. Peter J. Brophy is thanked for providing a stimulating work environment, top class supervision and vast amounts of help throughout the project.

I also thank my co-supervisor Professor J. R. Sargent and his team at the NERC Unit of Aquatic Biochemistry, in particular Drs. Jim Henderson and Mike Bell, for helpful advice and making use of their facilities.

Thanks to Drs R. Pagano, I. Sommer and R. McKinnon for offering advice and materials at key points of my project.

I acknowledge the goodwill of Dr. R. Wilson, who gave up precious time to teach me lipid analysis techniques.

I thank all the staff members in the Department of Biological and Molecular Sciences (DBMS), who helped in creating an atmosphere of goodwill thus making my work more enjoyable.

The members of our group Drs Bernadette Kelly and Stewart Gillespie, Ms Diane Sherman and Fiona McAllistair as well as Mr Robert McDermott are thanked for being tolerant co-workers and helpful friends. I feel privileged to have worked with them.

I also thank Mr L. Taylor for printing the photographs contained within this thesis.